

© 2022

Emily T. Slesinger

ALL RIGHTS RESERVED

**BLACK SEA BASS PHYSIOLOGY AND LIFE HISTORY IN THE CONTEXT OF
SEASONAL AND LONG-TERM CLIMATE CHANGE**

By

EMILY TESS SLESINGER

A dissertation submitted to the

School of Graduate Studies

Rutgers, The State University of New Jersey

In partial fulfillment of the requirements

For the degree of

Doctor of Philosophy

Graduate Program in Oceanography

Written under the direction of

Grace K. Saba

And approved by

New Brunswick, New Jersey

January, 2022

ABSTRACT OF THE DISSERTATION

Black sea bass physiology and life history in the context of seasonal and long-term

climate change

By EMILY TESS SLESINGER

Dissertation Director:

Grace K. Saba

The US Northeast Shelf (USNES) provides habitat for many economically and ecologically important fish species and is one of the most rapidly warming regions in the world. A common response from several fishes to warming has been poleward distribution shifts, potentially including the Northern stock of black sea bass (*Centropristis striata*). Black sea bass inhabit coastal waters along the USNES from (south to north) Cape Hatteras, NC to the Gulf of Maine during summer and migrate to the southern shelf-slope edge for the winter. Understanding the causes and implications of the distribution shift in black sea bass is important for fisheries management because state-specific quotas are based on regional biomass. Research on these impacts of ocean warming on fish species will help support proactiveness from fisheries management towards the changes in fish population dynamics and distributions, and avoiding future conflicts. Therefore, for my dissertation, I researched the impacts of ocean warming on black sea bass from the individual to population level with a focus on population dynamics and distribution extents as they relate to fisheries management.

Chapter 2 used laboratory-based physiological experiments to determine optimal temperatures by measuring metabolic rates and hypoxia tolerance at a range of temperatures. Black sea bass could not acclimate to 30°C, and while 24°C was technically the thermal optimum, measured as the temperature with highest aerobic scope, 24°C was suggested to be the maximum tolerable temperature. This decision was determined based on Metabolic Index values reaching limiting values near 24°C, which suggested this temperature may not be optimal. The southern portion of BSB range can warm to >24°C; therefore, temperature is likely a dominant driver of recent distribution shifts, at least in the southern extent of their distribution.

Chapter 3 investigated if black sea bass in the northern extent, that has currently been experiencing increasing biomass, utilized spawning strategies suitable for higher latitude regions with shorter summers. I measured black sea bass spawning timing and output, and found spawning duration was shortest in the northern range extent. This result was expected because summers are shorter at higher latitudes, and typically lead to fish populations with contracted spawning seasons. Under this premise, fish at higher latitudes should have higher reproductive output to account for the shorter spawning season. However, for black sea bass, reproductive output was lower compared to their southern range extent, and may lead to reduced recruitment in black sea bass at the northern in the future.

Chapter 4 examined the intraspecific differences in energy allocation throughout spawning across the whole distribution of black sea bass. To do this, lipid concentration, energy density and total energies of the liver, gonad and muscle were measured in fish collected from pre- to post-spawning. Male fish invested less energy into reproduction

than female fish and were more often similar across the distribution (i.e. similar energy usage throughout the distribution during spawning). Compared to the southern region, black sea bass in the northern portion of their range began spawning with lower energy reserves and lower gonad energy, potentially leading to the lower reproductive output observed in Chapter 3.

Chapter 5 investigated distribution shifts for black sea bass and four other US NES fish in relation to laboratory measurements of thermal limits. Metabolic Index was measured for each species across four seasons (winter, spring, summer, and fall) from 1970-2019. The limiting Metabolic Index value was lower for cold water species than warm water species. All seasons saw a decline in Metabolic Index over time, but the effects were most pronounced in summer and winter when the decline allowed some regions to reach limiting values or lower. Future habitat loss based on Metabolic Index critical limits was determined for each species. Warm water species will experience a loss of habitat in the inshore and southern portions of their distributions, while some of the cold water species, such as Atlantic cod, may lose additional habitat within the Georges Bank and Gulf of Maine portions of the USNES. The use of Metabolic Index allows for an analysis of just thermal habitat change without accounting for effects of distribution changes based on other factors such as previous fishing pressure. These values provide a modest account of what may happen into the future.

This dissertation fills research gaps for relevant questions the USNES fisheries face now and into the future. Ocean warming will continue to affect fish populations. Providing information about how fish populations will be affected will allow for

proactive management and early warning for flexibility in fishermen switching focal harvest species.

DEDICATION

From 2006 when I was exposed to our climate crisis by watching the film “An Inconvenient Truth” to the finalization of my PhD, about 20 years later, CO₂ levels rose ~30ppm from ~385ppm to ~415ppm. To put this in perspective, long-term climate fluctuations between glacial and interglacial periods are around 100ppm and occur on the order of *100,000 years*. So in 20 years, we have seen an increase of 30% of what usually occurs over 100,000 years. This past July (2021) was the warmest since 1880. Friends’, family, and neighbors’ houses have burned from wildfire, flooded from extreme weather events, and flattened from hurricane winds. This dissertation is dedicated to all those affected by climate change now and into the future. My research is only a small part in a large scientific arena, but together we can find solutions, prepare for the inevitable future, and make the world a better place for generations to come.

ACKNOWLEDGEMENTS

I would like to thank my advisor Dr. Grace Saba for being a wonderful mentor, friend, and scientific guide throughout this journey. Your unwavering support and patience were fundamental to the completion of this dissertation. But my thanks extend beyond what is typically given for an academic advisor. As your first graduate student, I watched you navigate your tenure track professorship and new lab while also being an excellent wife and mom. I have loved being a part of your lab and as people have joined and left, the lab has always been warm and welcoming, which is a testament to your leadership. Witnessing your success throughout my time at Rutgers, I now feel more confident in my own pursuits of a scientific career.

To my dissertation committee, Josh Kohut, Olaf, Jensen, and Brad Seibel, thank you for being wonderful sources of assistance through various chapters in this dissertation. I enjoyed each of your perspectives throughout my research, but also appreciated how you all worked together as a team, showing me how various research backgrounds can meld together for interdisciplinary research.

I would also like to thank the lab members of Dr. Saba's lab, Liza, Lauren, Ailey, Ted, Lori, and Jessica. Throughout my PhD, I always felt so lucky to be part of an amazing group of people who were scientific colleagues, but also became friends. Especially during COVID-19 when we were all remote, seeing all of your virtual faces weekly and catching up on each of our respective research projects gave me the normalcy and stability to get through this difficult time.

This research would not be possible without the help of undergraduate assistance. To Aviva Lerman, Anthony Renner, Sophia Berezin, Jillian Devita, Jacob Dale, Zakqary

Roy, Emma Huntzinger, Timothy Stolarz, Catherine McTighe, Gil Osofsky, Ailey Sheehan, Kiernan Bates, Karolina Zbaski, Mamadou Nbaye, Juan Osario, Kimberly Aldana, Shiyue Zhao, Maura Doscher, Kasey Walsh, Meridian Mathes, Luis Rodriguez-Mendoza, Shawn Hazlett, Grace Chung, and Rachael Young: thank you for your time and dedication to assist in various parts of this research. From fish dissections to late night stints during physiology experiments, all the good, fun, and frustrating parts of research were all taken in stride by each and every one of you.

I also conducted research across the East Coast, and was supported by local fisheries laboratories at University of Massachusetts Dartmouth and Virginia Institute of Marine Science (College of William and Mary). Thank you to Forrest Williams at UMass Dartmouth and Jim Gartland at VIMS for providing lab space. In addition, I was supported by fishermen and researchers at state fisheries departments for collection of fish, and am immensely grateful for their support.

Community is also incredibly important during a PhD, and I would like to thank all of the students within the Oceanography Graduate program. Schuyler, Liza, Jackie, Lauren, Vince, Cliff, Jonathan, Stan, Austin, Chris, Ryan, Quintin, Hailey, Joe, Jessica, Sam, and Heidi, thank you for making the graduate community welcoming and fun. From nights at Pino's to camping trips, I was able to find balance and camaraderie during these my PhD. And how unique it was to have a group of friends who were all going through the same exact things.

Much of the work that occurs underneath the curtains, such as finances, laboratory supply purchasing and technical support, would not be possible without many important people. Thank you to the "front office ladies" Sarah, Donna, Denise, Patty, Lucy, and

Lillian for what seems like always helping with silly things I could not figure out. And thank you to the IT team for helping me out, especially when in my first year I was really good at falling for phishing scams.

A big thank you to the faculty in the Oceanography department. Thank you to Oscar Schofield for being a great department chair and Yair Rosenthal for being a supportive Graduate Program Director. I always felt supported during my time at Rutgers. In the beginning of my PhD, I took many classes that would be later reassessed during my qualifying exams or used in knowledge I needed for my research. Thank you to Silke, Liz, John, Paul, Oscar, Grace, Bob, Gary, Diane and Travis for being great instructors and continuing to be colleagues and friends after classes were over.

I also want to thank my trail running community. Finding trail running was the perfect balance to the stresses of a PhD and I enjoyed the companionship and ability to talk about other things than science for a few hours in the woods.

And to my parents and family. There is no amount of gratitude that will ever be enough for all the support and love you have provided. Mom and Dad, I am so incredibly thankful for your support in high school and college. Having parents that understood academia was a blessing and I enjoyed navigating my PhD with many “well back in my day” anecdotes. I know how fortunate I am to pursue this passion and it really is only possible through your unyielding love and support. To my brother Tom (Tommy to me), it has been such a pleasure to transition from just siblings to best friends navigating our careers. I also come from quite the nerdy family. A huge thanks to my grandparents, uncles, aunts, and cousins for supporting me through this time with both thoughtful questions and help/jokes when I seemed stressed at holidays.

And finally, thank you to my partner Nick. Meeting you during my PhD was unexpected and one of the best things to come out of this experience. Having gone through this experience yourself, you have continued to be an excellent source of guidance and support. Thank you for helping edit fellowship applications and various writing pieces when I knew how busy you were. Thank you for literally buying champagne any time I did something “good” to celebrate. Thank you for being my rock during what is already a stressful experience, and only got much more stressful during COVID-19. Thank you for being the person I can come home to and continue to nerd out with (and vice versa). I’m excited for what the future has in store for us!

Funding: A big thank you to my funding sources throughout my PhD including internal Rutgers research funding (TA/GA Professional Development Fund, Off-Campus Dissertation Development Fund, and University and Louis Bevier Fellowship), external research funding (National Oceanic and Atmospheric Administration Office of Oceanic and Atmospheric Research Coastal and Ocean Climate Applications Program (NA150AR4310119), and George Burlew Scholarship), and travel funding for conferences (Center for Fisheries and Ocean Sustainability Student Conference Travel, and John E. Skinner Memorial Award).

TABLE OF CONTENTS

ABSTRACT OF THE DISSERTATION	ii
DEDICATION	vi
ACKNOWLEDGEMENTS	vii
TABLE OF CONTENTS	xi
LIST OF TABLES	xiv
LIST OF FIGURES	xvi
CHAPTER 1: Introduction	1
1.1 OCEAN WARMING AND THE U.S. NORTHEAST SHELF.....	1
1.2 FISH PHYSIOLOGY AND ENERGETICS	3
1.3 THE EFFECTS OF OCEAN WARMING ON FISH.....	6
1.4 US NES FISHERIES AND FISHERIES MANAGEMENT	8
1.5 BLACK SEA BASS (<i>CENTROPRISTIS STRIATA</i>)	12
1.6 DISSERTATION QUESTIONS	15
1.7 REFERENCES	16
CHAPTER 2: The Effect of Ocean Warming on Black Sea Bass (<i>Centropristis striata</i>) Aerobic Scope and Hypoxia Tolerance	22
2.1 ABSTRACT	22
2.2 INTRODUCTION	23
2.3 MATERIALS AND METHODS	28
2.3.1 Fish collection and husbandry	28
2.3.2 Experimental setup.....	29
2.3.4 Critical %O ₂ determinations.....	33
2.3.5 Ethics statement	34
2.3.6 Data analysis.....	35
2.4 RESULTS	38
2.4.1 Metabolic rates and aerobic scope	38
2.4.2 Critical %O ₂ and Metabolic Index	39
2.4.3 Chronic high temperature exposure	40
2.5 DISCUSSION	41
2.6 ACKNOWLEDGEMENTS	47
2.7 REFERENCES	47
2.8 TABLES.....	53
2.9 FIGURES	56
2.10 SUPPLEMENTAL MATERIAL	63

CHAPTER 3: Spawning phenology of a rapidly shifting marine species throughout its range	65
3.1 ABSTRACT	65
3.2 INTRODUCTION	66
3.3 MATERIALS AND METHODS	71
3.3.1 Fish Collection.....	71
3.3.2 Fish Processing	73
3.3.3 Statistical Analyses	74
3.4 RESULTS	78
3.4.2 General Seasonal and Regional Patterns.....	79
3.4.3 Spawning Phenology.....	80
3.4.4 Reproductive Output.....	82
3.4.5 Indirect Energy Indices	82
3.5 DISCUSSION	83
3.5.2 Julian Day and Temperature Effects on Spawning Phenology	84
3.5.3 Reproductive Output Across Spawning Locations.....	86
3.5.4 Energy Allocation Throughout Spawning.....	88
3.5.5 Trailing Edge of U.S. Northern Black Sea Bass Range Expansion.....	89
3.5.6 Study Limitations.....	91
3.5.7 Conclusions	92
3.6 ACKNOWLEDGEMENTS	93
3.7 REFERENCES.....	94
3.8 TABLES.....	100
3.9 FIGURES	103
3.10 SUPPLEMENTAL INFORMATION	110
CHAPTER 4: Regional differences in energy allocation of black sea bass (<i>Centropristis striata</i>) on the US Northeast Shelf (36°N - 42°N) throughout the spawning season	128
4.1 ABSTRACT	128
4.2 INTRODUCTION	129
4.3 METHODS	134
4.3.2 Ethics Statement	135
4.3.3 Lipid Extractions.....	135
4.3.4 Estimation of Energy Densities	136
4.3.5 Data Analysis.....	137
4.4 RESULTS	139
4.4.1 Tissue Specific Lipid and Energy.....	139
4.4.2 Seasonal Patterns	142
4.5 DISCUSSION	143

4.6 ACKNOWLEDGEMENTS	154
4.7 REFERENCES	154
4.8 TABLES.....	160
4.9 FIGURES	165
4.10 SUPPLEMENTAL INFORMATION	171
CHAPTER 5: Physiologically-based assessment of historical and future changes in metabolically available habitat for US Northeast Shelf species.....	175
5.1 ABSTRACT	175
5.2 INTRODUCTION	176
5.3 METHODS	180
5.3.1 Defining Strata and Regions.....	180
5.3.2 Compilation of Temperature and Oxygen Data	181
5.3.3 Incorporation of Fishery Data.....	184
5.3.4 Calculation of Species-Specific MI Parameters	184
5.3.5 Determining MI _{crit} , Minimum MI Dynamics, and MI Rate of Change Over Time.....	185
5.3.6 Prediction of Future MI and Habitat Loss.....	187
5.4 RESULTS	187
5.4.1 Species-Specific MI _{crit} and Minimum MI Dynamics.....	187
5.4.2 MI Rate of Change Over Time	190
5.4.3 Prediction of Future MI and Habitat Loss.....	191
5.5 DISCUSSION	192
5.5.2 Decreasing MI from 1970 – Present	194
5.5.3 Species-Specific Differences in Minimum MI and Future Habitat Loss	195
5.5.4 Case Study: Dissolved Oxygen in the NYB.....	202
5.5.5 Considerations When Using Metabolic Index.....	204
5.5.6 Conclusions	208
5.6 ACKNOWLEDGEMENTS	208
5.7 REFERENCES	208
5.8 TABLES.....	215
5.9 FIGURES	218
5.10 SUPPLEMENTAL INFORMATION	227
CHAPTER 6: Conclusions.....	241

LIST OF TABLES

CHAPTER 2

Table 2.1 ANCOVA results for metabolic rates and aerobic scope.....	53
Table 2.2 The MO_{2adj} mean \pm S.E. values for all metabolic rates, aerobic scope and hypoxia tolerance.	54
Table 2.3 Q_{10} values separated between each temperature increment.	55

Supplemental Information

Table S2.1 Duration of All Intermittent Cycles at Each Temperature.....	63
---	----

CHAPTER 3

Table 3.1 GLMs evaluated to explain probability of spawning capable fish	100
Table 3.2 Candidate GLMs evaluated to explain variation in gonadosomatic index	101
Table 3.3 Candidate GLMs evaluating the variation in Hepatosomatic Index.....	102

Supplemental Information

Table S3.1 Candidate models evaluating the variation in K_n	111
Table S3.2 Summary information for fish collections	112
Table S3.3 Summary of fish characteristics from each sampling location	113

CHAPTER 4

Table 4.1 Sample sizes of fish by region, sex, and maturity stage.	160
Table 4.2 BIC values used to compete the null and regional models.	161
Table 4.3 Model results for the regional GLMs.....	162
Table 4.4 GAM results for each model.	163
Table 4.5 Liver and gonad total energy (kJ) amounts cumulative and throughout spawning.	164

Supplemental Information

Table S4.1 The models used in analysis, their distribution family and link functions. ... 171

CHAPTER 5

Table 5.1 Species information used in this study..... 215

Table 5.2 Species-specific parameters. 216

Table 5.3 Comparison of species parameters between this study and Deutsch et al. 2020
..... 217

Supplemental Information

Table S5.1 Year when MI_{crit} is reached..... 227

LIST OF FIGURES

CHAPTER 2

Figure 2.1 Seasonal black sea bass distribution throughout their range on the U.S. Northeast Shelf.....	56
Figure 2.2 Temperature and body weight both affect standard metabolic rate in black sea bass.	57
Figure 2.3A and 2.3B Effect of temperature on standard metabolic rate and maximum metabolic rate measured with a chase and a swim-flume method.....	58
Figure 2.4A and 2.4B Effect of temperature on black sea bass aerobic scope.....	59
Figure 2.5 S_{crit} increases with increasing temperature.	60
Figure 2.6 S_{crit} dependence on standard metabolic rate.....	61
Figure 2.7 Factorial aerobic scope and metabolic index response to temperature.	62

Supplemental Information

Figure S2. 1 Normalized Fish Weights at Each Temperature Treatment.....	64
---	----

CHAPTER 3

Figure 3.1 Collection locations for black sea bass throughout the entire sampling period.	103
Figure 3.2 Summary of spawning characteristics for each region based on spawning stage and gonadosomatic index.	104
Figure 3.3 Spawning season start, end and duration for each region.....	105
Figure 3.4 Beginning and end of the spawning season GLM results.....	106
Figure 3.5 Gonadosomatic Index model results and raw data distribution for male and female fish across region.	108

Figure 3.6 HSI model results and raw distribution across region for male and female fish.	109
--	-----

Supplemental Information

Figure S3.1 Predicted versus residuals for the best fit Kn model.....	114
Figure S3.2 The results from the dominance analysis on Kn best fit GLM.....	115
Figure S3.3 Relative condition factor (Kn) for each region.....	116
Figure S3.4 Testing of proportion spawning capable levels to determine spawning season	117
Figure S3.5 Bottom temperature throughout sampling by region.....	118
Figure S3.6 Predicted versus residuals from the best fit model for the beginning of spawning model.....	119
Figure S3.7 Dominance analysis for beginning and end of spawning GLMS.....	120
Figure S3.8 Predicted versus residuals from the best fit model for the end of spawning model.....	121
Figure S3.9 Predicted versus residuals from the best fit model for GSI.....	122
Figure S3.10 Dominance analysis on GSI best fit GLM.....	123
Figure S3.11 Predicted versus residuals from the best fit model for HSI.....	124
Figure S3.12 Dominance analysis on HSI best fit GLM.....	125
Figure S3.13 Temperature differences between 2018 and 2019 across sampling locations.	126
Figure S3.14 Comparison of GSI in New Jersey fish from 2011-2013.....	127

CHAPTER 4

Figure 4.1 Compositional model results for muscle GLMs.	165
--	-----

Figure 4.2 Compositional model results for liver GLMs.	166
Figure 4.3 Compositional model results for gonad GLMs.	168
Figure 4.4 Seasonal GAM results.	170
<i>Supplemental Information</i>	
Figure S4.1 Linear trend of gonad % dry-weight and GED.	172
Figure S4.2 Linear trend of liver % dry-weight and LED.	173
Figure S4.3 Linear trend of muscle % dry-weight and MED.	174
CHAPTER 5	
Figure 5.1 Strata defined for this study.	218
Figure 5.2 Regression of $\ln(P_{crit})$ and inverse temperature for each species.	219
Figure 5.3 MI_{crit} values and evaluation for each species	220
Figure 5.4 Minimum MI trends in spring.	221
Figure 5.5 Minimum MI trends in fall.	222
Figure 5.6 MI trends over time per stratum.	224
Figure 5.7 MI_{crit} values for summer and fall.	226
<i>Supplemental Information</i>	
Figure S5.1 Defined regions across USNES.	229
Figure S5.2 Temperature throughout each season across USNES.	230
Figure S5.3 Temperature trends over time per stratum.	231
Figure S5.4 Mean oxygen (kPa) values per season.	232
Figure S5.5 Raw oxygen (kPa) values for each region and season.	235
Figure S5.6 Species presences across year, season, and stratum.	237
Figure S5.7 MI_{crit} values for winter and spring.	238

Figure S5.8 Case study of oxygen in NYB.....	239
Figure S5.9 Comparison of MI parameters with differing error in P_{crit}	240

CHAPTER 1: Introduction

1.1 OCEAN WARMING AND THE U.S. NORTHEAST SHELF

The ocean covers over 70% of the Earth providing habitat for a myriad of organisms, many of which may be vulnerable to ocean warming. The recent Intergovernmental Panel Climate Council 2021 confirmed human influence is a main driver of ocean warming and that under a low warming scenario, average ocean temperatures will still double in 2100 compared to 1971 values (IPCC, 2021). Ocean warming is primarily caused by the uptake of atmospheric heat as a result of global climate change (Gleckler *et al.*, 2016). Globally, warming can affect other ocean properties such as the amount of oxygen available in the water (Breitburg *et al.*, 2018) as well as affect the seasonality of temperate ecosystems (Burrows *et al.*, 2011). With respect to marine organisms, the global oceans can be divided into distinctive Large Marine Ecosystems (LMEs) that are delineated based off of their physical, chemical and biological characteristics. Out of the world's 63 LMEs, 61 of them have experienced warming since the 1970's (Belkin, 2009).

One LME, the U.S. Northeast Shelf (USNES), extends from Cape Hatteras, NC northward to the Gulf of Maine. The USNES is an important ecological region for the East Coast of the United States as it supports numerous fish and invertebrate species that are sought after in both recreational and commercial fisheries. Within the USNES, distinct subregions exist which include the Middle Atlantic Bight (Cape Hatteras, NC to Cape Cod, MA), Georges Bank, and the Gulf of Maine. These subregions are connected through the southward flow of the Labrador Current that distributes cold, fresh water

(Chapman and Beardsley, 1989), and the Gulf Stream that flows northward distributing warm and salty water (Gray and Cerame-Viuas, 1963). The USNES is also characterized by strong seasonality consisting of cold winters and hot summers, where the surface and bottom waters can fluctuate $\sim 20^{\circ}\text{C}$ and $\sim 7^{\circ}\text{C}$ throughout the year, respectively (Richaud *et al.*, 2016). Within this seasonal system, a unique oceanographic structure forms, known as the Cold Pool, over the New York Bight due to the southward advection of cold northern winter water at depth and stratification of the surface layer due to vernal heating (Houghton *et al.*, 1982; Castelao *et al.*, 2008). Biologically, the Cold Pool can serve as an important thermal refuge for marine organisms during the warm summer months (Sullivan *et al.*, 2005).

The USNES has been experiencing ocean warming since the 1970's. In some places, like the Gulf of Maine, ocean warming there has been occurring more rapidly than 99% of the world's oceans (Pershing *et al.*, 2015). While the warming trend is in part due to natural climate variability, about one-third of the warming has been attributed to anthropogenic climate change (Chen *et al.*, 2020). In addition to warming as a consequence of rising air temperatures, the USNES warming is occurring due to changing ocean circulation patterns. As aforementioned, the USNES is influenced by two major current systems, the Labrador Current flowing from the north bringing fresh cold water and the Gulf Stream originating from the south distributing salty warm water. Broadly, through large-scale ocean circulation changes, the Gulf Stream has shifted northward while the Labrador Current has weakened, allowing more warm water to flow across the USNES (Saba *et al.*, 2016; Caesar *et al.*, 2018). Not only is the shelf experiencing an overall change in temperature, but the phenology of the system has also

shifted including earlier spring transitions and later fall cooling (Friedland and Hare, 2007). Notably, the overall warming trend is projected to continue where under a doubling of CO₂ warming could increase by 3-4°C in the next 70 years (Saba *et al.*, 2016). As home to many economically and ecologically important marine species, current and future warming of the USNES is of major concern, and research is needed to understand the impacts warming will have on these species.

1.2 FISH PHYSIOLOGY AND ENERGETICS

Fish balance energy demands that can broadly be distributed between metabolism, growth, storage, and, for adult fish, reproduction. Understanding the relevance, role, and energy demand of the specific components to the energy budget allow for informed questions related to various aspects of a fish's life such as their larval or adult temperature sensitivity or lifetime reproductive output (an important metric for fisheries management – *see below*).

Fish metabolism is typically measured as oxygen consumption, a proxy for respiration rate, and laboratory studies often measure standard (SMR) and maximum metabolic rates (MMR) to encompass the full spectrum of aerobic metabolism. SMR is the minimum metabolic requirement to sustain basic organismal functions while MMR is the maximum metabolic rate reflective of maximal oxygen uptake (Bennett, 1978). The specific rates of SMR and MMR reflect trade-offs between fish species. High metabolic rates can be correlated with decreased growth (Álvarez and Nicieza, 2005), and typically seen as disadvantageous. Fish that can sustain faster swimming abilities typically can maintain high MMR and aerobic capacity (Claireaux *et al.*, 2006), but maintaining high

performing metabolic machinery requires higher SMR (Brill, 1996). A high SMR increases energy demands, which is associated with its own costs, such as increased foraging time increasing susceptibility to predation. Therefore, if high MMR and swimming capabilities are not needed, fish will tend to have lower SMR (Horodysky *et al.*, 2011). The relationship between MMR and SMR can also be described through aerobic scope which is the difference between the two values (MMR – SMR), and reflects the available scope for activities beyond what is needed for SMR (Fry and Hart, 1948). Reaching limiting levels of aerobic scope can be lethal, especially when fish can no longer feed or digest food (Chabot *et al.*, 2016). Altogether, fish metabolism supports daily requirements of fish and thus typically takes precedent for immediate usage of available energy, which can sometimes limit available energy toward growth and reproduction.

Growth and energy storage are important components of a fish's life. Fish have indeterminate growth and become reproductively active before they have reached their maximum size (Jennings *et al.*, 2001). Under this premise, older and larger individuals typically have higher fecundity because diverting energy towards growth becomes less important (Bunnell and Marschall, 2003; Hixon *et al.*, 2014). For fish that migrate, large size is an advantage because swimming efficiency increases with body size (Slotte, 1999). When growth conditions are not ideal year-round, fish can exhibit compensatory growth where growth is accelerated after a period of growth depression (Ali *et al.*, 2003). For juvenile fish living in temperate systems, growth and energy storage are vitally important as larger individuals increase their survival chances during the first winter (Conover, 1992). Even for adults, overwintering survival is related to lipid storage and

larger fish can typically store more lipids offering them an advantage in cold and food limited seasons (Schultz and Conover, 1997).

Additional energy beyond what is needed for metabolism and growth can be allocated towards reproductive development. As mentioned above, many fish continue to grow throughout their life while they are reproductively mature, which means there is always a tradeoff of where energy is allocated (growth vs reproduction). Reproduction is important for sustained population growth and survival, but adults also have to navigate trade-offs between adult survival and offspring viability. As such, the energetic condition of a fish can greatly affect its spawning behaviors and strategies (McBride *et al.*, 2015). In some cases, reproduction can be so costly that fish opt for semelparity so that all their energy is devoted towards spawning, as in the case of some salmonids (Kindsvater *et al.*, 2016). While not semelparous, some adult fish will still invest a large proportion of energy towards reproduction, promoting offspring over adult survival (Carscadden *et al.*, 1997). Ultimately, fish will evolve strategies that maximize their lifetime fitness and this can lead to variability in annual reproduction due to abiotic and biotic changes interannually.

Evolved reproductive strategies involve energetic tradeoffs, which can vary across time and life stages. Investigations of fish physiology and energetics is useful to empirically determine how environmental stressors may affect fish from the individual to population levels.

1.3 THE EFFECTS OF OCEAN WARMING ON FISH

Fish are ectotherms which means their body temperature is dependent on environmental temperature, and as such, an increase in ocean temperature will lead to an increase in body temperature and subsequently metabolic rates (Bennett, 1978; Clarke and Johnston, 1999). Within this framework, the oxygen- and capacity-limited thermal tolerance (OCLTT) theory was proposed to provide a link between climate change and its effects on whole animal metabolism. Briefly, warmer temperatures lead to reduced oxygen supply relative to increasing oxygen demand through various physiological mechanisms, limiting aerobic scope and the available energy for activities beyond SMR (Pörtner, 2010). Within the proposed framework, the temperature associated with highest aerobic scope is the thermal optimum and temperatures around the optimum provide a livable thermal window. These temperature windows can vary ontogenetically and based on species life histories (i.e. eurythermal vs stenothermal; Pörtner and Farrell, 2008). In some species, the OCLTT theory clearly shows the impacts of fish living outside of the thermal window. For example, for Pacific salmon in rivers that have warmed to temperatures beyond their thermal window, salmon experienced a reduction in aerobic scope, and subsequently premature death and reduced reproduction in the river passage (Eliason and Farrell, 2016).

While theoretically a useful tool to describe how fish physiology is affected by climate change and the subsequent performance effects, there are concerns about the utility and assumptions of the OCLTT theory as it oversimplifies metabolic processes (Schulte 2015). Some fish experience increasing aerobic scope with temperature up until a lethal temperature (Norin *et al.*, 2014), where in this case the highest aerobic scope is

not optimal for the fish. As such, another metric, the Metabolic Index, has also been introduced that similarly assess the oxygen supply of the environment to the oxygen demand of the fish based on temperature (Deutsch *et al.*, 2015). Unlike OCLTT, MI provides limiting values where fish are likely absent instead of providing temperature values that represent the physiological optimum for fish.

These physiological metrics of temperature effects on metabolism are useful when investigating how ocean warming may affect fish now and into the future. For example, some fish that inhabit a wide latitudinal distribution can exhibit regional thermal adaptations shedding light onto potential disparities within a population that could have geographic implications under ocean warming scenarios (Grabowski *et al.*, 2009). In other cases, fish that experience interannual temperature fluctuations show robustness towards increasing temperature (Collins *et al.*, 2013). Metabolism can be affected at either extreme cold or warm temperatures. Outside the native range, colder temperatures can lead to metabolic suppression (Costa *et al.*, 2013), while warmer temperatures can be detrimental for maximum metabolic performance and swimming speeds (Claireaux *et al.*, 2006). Importantly, some fish species can acclimate to high temperatures after chronic exposure (Sandblom *et al.*, 2014). Warmer temperatures can also affect tolerances to other environmental stressors. For example, under low-oxygen conditions, higher temperatures reduce hypoxia tolerance (Nilsson *et al.*, 2010; Capossela *et al.*, 2012) or can also lead to reduced aerobic scope under bacterial infections (Lapointe *et al.*, 2014). Therefore, ocean warming can lead to higher maintenance costs, relative to oxygen supply, reducing aerobic scope, which may ultimately limit available energy for the other important aspects of the fish life such as growth and reproduction.

While ocean warming can affect available energy for reproduction through the reduction in metabolic scope, warming can also affect reproduction from changes in behavioral responses to negative impacts on recruitment. In regions with harsh environmental conditions or under food limitation, adults can delay spawning for a year to increase their survival to the next spawning season, ultimately increasing their lifetime reproductive output (Finstad *et al.*, 2002; Beyer *et al.*, 2021). Another notable effect of ocean warming is changing phenology of the ocean seasons whereby the timing of warming or cooling has shifted. This can affect the timing of spawning migrations, (Dufour *et al.*, 2010; Anderson *et al.*, 2013), and the timing of peak spawning, which can affect recruitment (Carscadden *et al.*, 1997; Greve *et al.*, 2001; Jansen and Gislason, 2011). However, in some cases warming may be beneficial. For example, warming in areas that were historically cold can increase winter larval survival (Slotte, 1999) or reduce the need for larger body sizes for overwinter survival (Conover, 1992). How ocean warming affects reproduction and recruitment is nuanced, but energetic limitations related to metabolic changes and shifts in energy demand are an important element that must be considered.

1.4 US NES FISHERIES AND FISHERIES MANAGEMENT

The USNES supports many ecologically and economically important invertebrate and finfish species. In the New England region (Connecticut to Maine) and the Mid-Atlantic region (Virginian to New York), a diversity of finfish and invertebrates are targeted by both commercial and recreational fisheries. Throughout the entirety of the USNES, the commercial fishery provides 320,000 jobs and adds ~\$15 billion to GDP,

while 133,000 jobs and ~\$3 billion to GPD are added through domestic harvests. The recreational fishery brings in ~63,000 jobs and adds ~ \$5 billion to GPD (NMFS, 2019). Undoubtedly, the diverse array of harvestable species within the USNES supports local and regional economies through job opportunities and value added monetarily. Protecting and maintaining this significant economic source is vital and societally important and can be achieved through proper fisheries management.

The broad goals of fisheries management are to impose regulations that allow for the sustainable harvest of targeted species (Jennings *et al.*, 2001). Within the USNES region, fisheries are managed jointly through state and federal management. The federal government manages waters within the Exclusive Economic Zone 200 nautical miles offshore and inshore to 3 nautical miles; state management occurs 0-3 nautical miles from the shore. To provide continuity between state-managed fish species that inhabit waters across state lines, the Atlantic States Marine Fisheries Commission was founded in the 1940's through the Interstate Compact, which was voted on by the U.S. Congress. This commission provides management advice such as Fishery Management Plans for interstate species, which includes a majority of the harvested USNES species. These fish species are also managed by regional Fishery Management Councils that were created in 1976 through the Magnusen-Stevenson Act. The Mid Atlantic and the New England Fishery Management Councils manage species and collaborate on management plans for species that are shared between the two regions. State quotas are set by regional biomass of a targeted species so that fishing pressure across the USNES is proportional to the local fish biomass. While useful in principle, shared fisheries management is challenging and difficult to implement.

For USNES fish species, fishery management plans set harvest quota between recreational and commercial fisheries, minimum or slot size limits, and fishing seasons. These metrics are based upon stock assessments which assess the total spawning stock biomass and previous exploitation (Jennings *et al.*, 2001). Ultimately, the population biomass is affected by the addition of new individuals through reproduction and the loss of individuals through death. For the stock assessments, the total spawning biomass is a central focus because this is the portion of the population that can add new individuals through reproduction. Mortality is also a central focus as loss of individuals through death includes natural mortality and fishing mortality (Jennings *et al.*, 2001). In some stock assessments, the size of the fish is also a focus because of the effects disproportionate contribution large fish can have on fecundity and larval energetics (Jennings *et al.*, 2001). All of these aspects related to fisheries management, including growth, reproduction, and natural mortality, can also be affected by ocean warming, which creates the need for including impacts of climate change, namely ocean warming, in stock assessments to accurately provide fishery management plans that account for changes in mortality or reproduction related to ocean warming.

Ocean warming has led to vulnerability in approximately half of the USNES species (Hare *et al.*, 2016), and the dominant response of fish species to ocean warming has been distribution range shifts poleward (Kleisner *et al.*, 2017). The net shift in fish distributions has also occurred across distinct fish assemblages, indicating that the response to ocean warming is pervasive and not unique to a few species (Kleisner *et al.*, 2016). Notably, for some species, the distribution shift in their adult and juvenile populations has not tracked uniformly, indicating a mismatch in reproduction and

recruitment success (Walsh *et al.*, 2015). Warming has also led to phenology shifts in the seasonality of the USNES, leading to longer summers, which could also be contributing to range shifts (Henderson *et al.*, 2017). These shifts also can affect the lower trophic levels (Bi *et al.*, 2014), which in turn can lead to regime shifts in the fishery species (Perretti *et al.*, 2017). Specifically, ocean warming has contributed to the collapse and inability to rebuild the Atlantic cod stock (Pershing *et al.*, 2015) and has been documented as the driver for poleward range shifts in black sea bass and scup (Bell *et al.*, 2015).

Due to the dominant effects of ocean warming on fish species along the USNES and the management across multiple states for single stocks of species, understanding the effects of ocean warming, the extent of range shifts, drivers of warming, and overall effects is important for future management. This is notable because fishing pressure and the effects of ocean warming cannot be viewed as single entities. For example, in an assessment of USNES fish assemblages, due to ocean warming, returning fish stocks to historic levels may not be possible even with the reduction of fishing pressure (Lucey and Nye, 2010). Shifting fish distributions, and changes in reproduction and recruitment, will inevitably lead to conflict in both the reapportioning of state specific quotas (Pinsky *et al.*, 2018) and forcing fishermen to either adapt and fish for new species or finance longer fishing expeditions to reach the same population (Rheuban *et al.*, 2017). The future of fisheries management requires ample research on the effects of ocean warming on the individual to population level to provide pertinent information for management plans and providing proactive advice to fishery managers, fishermen, and consumers of fish.

1.5 BLACK SEA BASS (*CENTROPRISTIS STRIATA*)

Black sea bass (*Centropristis striata*) are a demersal reef fish that are found from the Gulf of Mexico and throughout the Atlantic coast from Florida to Maine. Across this range, black sea bass are separated into three distinctive management stocks: the Gulf of Mexico, the Southeastern, and the Northern (McCartney *et al.*, 2013). The Gulf of Mexico stock is separated by the panhandle of Florida, while the Southeastern and Northern stock of black sea bass are separated by a biological barrier at the tip of Cape Hatteras, NC. Here, the Gulf Stream, which flows northward along the coast of the Southeastern US, veers off at the tip of Cape Hatteras and flows northwest, providing a strong current system separating north and south of Cape Hatteras (Gray and Cerame-Viuas, 1963). These stocks are also genetically different (Bowen and Avise, 1990; Roy *et al.*, 2012), which can lead to differences in energetics and spawning (Wuenschel *et al.*, 2013). Due to physical differences in the environment and biological differences in reproduction, black sea bass are managed separately across the three stocks. While the focus of this dissertation is on the Northern stock of black sea bass, interpretation of results should include regional assessments as well as a wider scope across the entire range.

Black sea bass are protogynous hermaphrodites which means some female fish will transition to male during their lifetime. Protogynous hermaphrodites have social structures within their populations where the dominant large male will defend his territory and harem of female fish during the spawning season (Jennings *et al.*, 2001). When the dominant male dies, the next largest female transitions to male. Black sea bass typically transition after the spawning season (Provost *et al.*, 2017). However, this life

history trait does affect female fecundity. Typically, large female fish have the highest fecundity because they have reached near to maximum growth (Hixon *et al.*, 2014), but for black sea bass, fecundity peaks at an intermediate size, likely due to the potential for transition later in life (Klibansky and Scharf, 2017). Sex change makes management of black sea bass challenging. Fishing restrictions, such as minimum size limits, can indirectly skew the sex ratio when the size limit disproportionately targets one sex (large males in this case; McGovern and Olney, 1996). Also, the number of females within the population can change across time as female fish transition to male (Provost *et al.*, 2017), changing the female spawning stock biomass commonly used in stock assessments (Alonzo *et al.*, 2008).

Partially due to their territoriality, black sea bass typically associate with reefs during the spawning season because they provide shelter (Steimle and Figley, 1996). Reefs along the Mid Atlantic Bight can be natural rocks or artificially made through shipwrecks or intentional placement of foreign objects to create more reef habitat, while the reefs in southern New England are typically natural and from shellfish reefs (Steimle and Zetlin, 2000). Movement patterns around the reefs differ between male and female fish, where male fish typically have more movement likely due to defending territories or smaller male fish sneaking in to spawn (Fabrizio *et al.*, 2014). Differing reef habitat and the use of it by black sea bass is important to consider when viewing the population as a single stock, for management, and for understanding future regional impacts of climate change.

Black sea bass seasonally migrate along the USNES. During the summer months black sea bass distribute throughout the inshore portion of the shelf (Cape Hatteras, NC

to Gulf of Maine) for spawning, which occurs from about June through October (Mercer, 1978; Wilk *et al.*, 1990), and then migrate offshore to the southeastern portion of the USNES near the continental shelf edge to overwinter (Moser and Shepherd, 2008). Spawning occurs inshore so larval fish are hatched near estuaries, which are used as nurseries for both larval and juvenile black sea bass (Musick and Mercer, 1977; Moser and Shepherd, 2008). Where black sea bass spawn is important as it can affect larval dispersal and settlement (Edwards *et al.*, 2008). Contrastingly, black sea bass overwinter offshore because this region is more thermally stable than inshore while ocean temperatures plummet. Migration offshore is likely cued by changes in temperature and photoperiod (Fabrizio *et al.*, 2013), and potentially water column breakdown from fall storms (Secor *et al.*, 2019). Black sea bass exhibit site fidelity and as such, black sea bass spawning in the northern regions will likely return to the northern regions the following summer (Moser and Shepherd, 2008). Therefore, black sea bass migrating to the north will have a longer migration distance than those migrating to the south. Altogether, a broad spawning range and differing migration dynamics can lead to can downstream effects on reproduction and recruitment.

Historically black sea bass were overfished and have since rebounded (Shepherd and Nieland, 2010) but there are still management concerns because the stock is considered “data poor”. Like other USNES species, black sea bass is managed with state specific quotas within state waters and then federally in waters 3-200 nautical miles offshore. Partially due to ocean warming and effects of prior fisheries management, black sea bass has been expanding their center of biomass northward (Bell *et al.*, 2015). This range expansion has impacts for both management and the ecosystem. Recently for

management, black sea bass were suggested to be managed as two sub-groups split at the Hudson Canyon due to differences in biophysical conditions there (SAW/SARC, 2016), and the most recent Addendum through Atlantic States Marine Fisheries Commission issued new quota allocations to provide higher quotas in the north reflecting the shift in biomass (ASMFC, 2021). For the ecosystem, black sea bass are expanding into and successfully recruiting in the Gulf of Maine (McBride *et al.*, 2018) which has impacts on local fauna, such as the American lobster (McMahan and Grabowski, 2019), the most lucrative fishery in the US.

1.6 DISSERTATION QUESTIONS

Understanding the impacts of ocean warming on black sea bass is important for several reasons. First, it allows for predictions into the future based off of different warming scenarios. Chapter 2 focuses on the temperature effects on black sea bass physiology through laboratory experiments. Second, understanding holistically what a change in biomass means for the black sea bass population is important as there could be intraspecific differences in reproduction and recruitment, with lasting effects on management. For example, the black sea bass center of biomass currently is near Massachusetts, which may prompt an increase in regional quota there. However, the perceived boom in black sea bass may be due to a very successful 2011 cohort that is primarily comprised of northern fish. Since then, recruitment has not been as biased towards the north and the 2011 cohort abundance is quickly diminishing as they reach their maximum age. Therefore, high biomass of black sea bass in this region could be temporary and understanding how energetics and reproduction differ throughout the

range can help with predictions. Chapter 3 addresses the intraspecific differences in spawning and reproductive output and Chapter 4 investigates the differences in spawning energetics of black sea bass throughout their distribution. Finally, integrating physiological data into broad understandings of thermal habitat and how that may change into the future is a focus for black sea bass and other USNES species. Many recent studies showing the thermal preferences for specific fish are based on statistical correlation between fish distribution and temperature. Chapter 5 analyzes change in thermal habitat in the USNES for five species, including black sea bass, using a physiological metric instead of statistical correlation to temperature. This dissertation concludes in Chapter 6 with general conclusions and recommendations for future research needs.

1.7 REFERENCES

- Atlantic States Marine Fisheries Commission (ASMFC). 2021. Addendum XXXIII to the summer flounder, scup, and black sea bass fishery management plan. Black sea bass commercial allocation. 1–15 pp.
- Ali, M., Nicieza, A., and Wootton, R. J. 2003. Compensatory growth in fishes: A response to growth depression. *Fish and Fisheries*, 4: 147–190.
- Alonzo, S. H., Ish, T., Key, M., MacCall, A. D., and Mangel, M. 2008. The importance of incorporating protogynous sex change into stock assessments. *Bulletin of Marine Science*, 83: 163–179.
- Álvarez, D., and Nicieza, A. G. 2005. Is metabolic rate a reliable predictor of growth and survival of brown trout (*Salmo trutta*) in the wild? *Canadian Journal of Fisheries and Aquatic Sciences*, 62: 643–649.
- Anderson, J. J., Gurarie, E., Bracis, C., Burke, B. J., and Laidre, K. L. 2013. Modeling climate change impacts on phenology and population dynamics of migratory marine species. *Ecological Modelling*, 264: 83–97. Elsevier B.V.
- Belkin, I. M. 2009. Rapid warming of Large Marine Ecosystems. *Progress in Oceanography*, 81: 207–213.
- Bell, R. J., Richardson, D. E., Hare, J. A., Lynch, P. D., and Fratantoni, P. S. 2015. Disentangling the effects of climate, abundance, and size on the distribution of marine fish: an example based on four stocks from the Northeast US shelf. *ICES Journal of Marine Science*, 72: 1311–1322.

- Bennett, A. F. 1978. Activity metabolism of the lower vertebrates. *Annual Review of Physiology*, 400: 447–469.
- Beyer, S., Alonzo, S., and Sogard, S. 2021. Zero, one or more broods: reproductive plasticity in response to temperature, food, and body size in the live-bearing rosy rockfish *Sebastes rosaceus*. *Marine Ecology Progress Series*, 669: 151–173.
- Bi, H., Ji, R., Liu, H., Jo, Y. H., and Hare, J. A. 2014. Decadal changes in zooplankton of the Northeast U.S. continental shelf. *PLoS ONE*, 9: e87720.
- Bowen, B. W., and Avise, J. C. 1990. Genetic structure of Atlantic and Gulf of Mexico populations of sea bass, menhaden, and sturgeon: Influence of zoogeographic factors and life-history patterns. *Marine Biology*, 107: 371–381.
- Breitburg, D., Levin, L. A., Oschlies, A., Grégoire, M., Chavez, F. P., Conley, D. J., Garçon, V., *et al.* 2018. Declining oxygen in the global ocean and coastal waters. *Science*, 359: 1–11.
- Brill, R. W. 1996. Selective advantages conferred by the high performance physiology of tunas, billfishes, and dolphin fish. *Comparative Biochemistry and Physiology - A Physiology*, 113: 3–15.
- Bunnell, D. B., and Marschall, E. A. 2003. Optimal energy allocation to ovaries after spawning. *Evolutionary Ecology Research*, 5: 439–457.
- Burrows, M. T., Schoeman, D. S., Buckley, L. B., Moore, P., Poloczanska, E. S., Brander, K. M., Brown, C., *et al.* 2011. The pace of shifting climate in marine and terrestrial ecosystems. *Science*, 334: 652–655.
- Caesar, L., Rahmstorf, S., Robinson, A., Feulner, G., and Saba, V. 2018. Observed fingerprint of a weakening Atlantic Ocean overturning circulation. *Nature*, 556: 191–196.
- Capossela, K. M., Brill, R. W., Fabrizio, M. C., and Bushnell, P. G. 2012. Metabolic and cardiorespiratory responses of summer flounder *Paralichthys dentatus* to hypoxia at two temperatures. *Journal of Fish Biology*, 81: 1043–1058.
- Carscadden, J., Nakashima, B. S., and Frank, K. T. 1997. Effects of fish length and temperature on the timing of peak spawning in capelin (*Mallotus villosus*). *Canadian Journal of Fisheries and Aquatic Sciences*, 54: 781–787.
- Castelao, R., Glenn, S., Schofield, O., Chant, R., Wilkin, J., and Kohut, J. 2008. Seasonal evolution of hydrographic fields in the central Middle Atlantic Bight from glider observations. *Geophysical Research Letters*, 35: 6–11.
- Chabot, D., Koenker, R., and Farrell, A. P. 2016. The measurement of specific dynamic action in fishes. *Journal of Fish Biology*, 88: 152–172.
- Chapman, D. C., and Beardsley, R. C. 1989. On the origin of shelf water in the Middle Atlantic Bight. *American Meteorological Society*, 19: 384–391.
- Chen, Z., Kwon, Y. O., Chen, K., Fratantoni, P., Gawarkiewicz, G., and Joyce, T. M. 2020. Long-Term SST Variability on the Northwest Atlantic Continental Shelf and Slope. *Geophysical Research Letters*, 47: 1–11.
- Claireaux, G., Couturier, C., and Groison, A. 2006. Effect of temperature on maximum swimming speed and cost of transport in juvenile European sea bass (*Dicentrarchus labrax*). *Journal of Experimental Biology*, 209: 3420–3428.
- Clarke, A., and Johnston, N. 1999. Scaling of metabolic rate with body mass and temperature in teleost fish. *Journal of Animal Ecology*, 68: 893–905.
- Collins, G. M., Clark, T. D., Rummer, J. L., and Carton, A. G. 2013. Hypoxia tolerance is

- conserved across genetically distinct sub-populations of an iconic, tropical Australian teleost (*Lates calcarifer*). *Conservation Physiology*, 1: doi:10.1093/conphys/cot29.
- Conover, D. O. 1992. Seasonality and the scheduling of life history at different latitudes. *Journal of Fish Biology*, 41: 161–178.
- Costa, I. A. S. F., Driedzic, W. R., and Gamperl, A. K. 2013. Metabolic and Cardiac Responses of Cunner *Tautoglabrus adspersus* to Seasonal and Acute Changes in Temperature. *Physiological and Biochemical Zoology*, 86: 233–244.
- Deutsch, C., Ferrel, A., Seibel, B., Portner, H. O., and Huey, R. B. 2015. Climate change tightens a metabolic constraint on marine habitats. *Science*, 348: 1132–1136.
- Dufour, F., Arrizabalaga, H., Irigoien, X., and Santiago, J. 2010. Climate impacts on albacore and bluefin tunas migrations phenology and spatial distribution. *Progress in Oceanography*, 86: 283–290.
- Edwards, K. P., Hare, J. A., and Werner, F. E. 2008. Dispersal of black sea bass (*Centropristis striata*) larvae on the southeast U.S. continental shelf: Results of a coupled vertical larval behavior - 3D circulation model. *Fisheries Oceanography*, 17: 299–315.
- Eliason, E. J., and Farrell, A. P. 2016. Oxygen uptake in Pacific salmon *Oncorhynchus* spp.: When ecology and physiology meet. *Journal of Fish Biology*, 88: 359–388.
- Fabrizio, M. C., Manderson, J. P., and Pessutti, J. P. 2013. Habitat associations and dispersal of black sea bass from a mid-Atlantic Bight reef. *Marine Ecology Progress Series*, 482: 241–253.
- Fabrizio, M. C., Manderson, J. P., and Pessutti, J. P. 2014. Home range and seasonal movements of Black Sea Bass (*Centropristis striata*) during their inshore residency at a reef in the mid-Atlantic Bight. *Fisheries Bulletin*, 112: 82–97.
- Finstad, A. G., Berg, O. K., Langeland, A., and Lohrmann, A. 2002. Reproductive investment and energy allocation in an alpine Arctic charr, *Salvelinus alpinus*, population. *Environmental Biology of Fishes*, 65: 63–70.
- Friedland, K. D., and Hare, J. A. 2007. Long-term trends and regime shifts in sea surface temperature on the continental shelf of the northeast United States. *Continental Shelf Research*, 27: 2313–2328.
- Fry, F. E. J., and Hart, J. S. 1948. The relation of temperature to oxygen consumption in the goldfish. *The Biological Bulletin*, 94: 66–77.
- Gleckler, P. J., Durack, P. J., Stouffer, R. J., Johnson, G. C., and Forest, C. E. 2016. Industrial-era global ocean heat uptake doubles in recent decades. *Nature Climate Change*, 6: 394–398.
- Grabowski, T. B., Young, S. P., Libungan, L. A., Steinarsson, A., and Marteinsdottir, G. 2009. Evidence of phenotypic plasticity and local adaptation in metabolic rates between components of the Icelandic cod (*Gadus morhua* L.) stock. *Environmental Biology of Fishes*, 86: 361–370.
- Gray, I. E., and Cerase-Viuas, M. J. 1963. The circulation of surface waters in Raleigh Bay, North Carolina. *Limnology and Oceanography*, 8: 330–337.
- Greve, W., Lange, U., Reiners, F., and Nast, J. 2001. Predicting the seasonality of North Sea zooplankton. *Senckenbergiana maritima*, 31: 263–268.
- Hare, J. A., Morrison, W. E., Nelson, M. W., Stachura, M. M., Teeters, E. J., Griffis, R. B., Alexander, M. A., *et al.* 2016. A vulnerability assessment of fish and

- invertebrates to climate change on the northeast u.s. continental shelf. PLoS ONE, 11: 1–30.
- Henderson, M. E., Mills, K. E., Thomas, A. C., Pershing, A. J., and Nye, J. A. 2017. Effects of spring onset and summer duration on fish species distribution and biomass along the Northeast United States continental shelf. *Reviews in Fish Biology and Fisheries*, 27: 411–424.
- Hixon, M. a, Johnson, D. W., and Sogard, S. M. 2014. Structure in Fishery Populations. *ICES Journal of Marine Science*, 71: 2171–2185.
- Horodysky, A. Z., Brill, R. W., Bushnell, P. G., Musick, J. A., and Latour, R. J. 2011. Comparative metabolic rates of common western North Atlantic Ocean sciaenid fishes. *Journal of Fish Biology*, 79: 235–255.
- Houghton, R. W., Schlitz, R., Beardsley, R. C., Butman, B., and Chamberlin, J. L. 1982. The Middle Atlantic Bight Cold Pool: Evolution of the Temperature Structure During Summer 1979.
- IPCC. 2021. Climate Change 2021: The physical science basis. Contribution to Working Group 1 to the Sixth Assessment Report of the Intergovernmental Panel on Climate Change. Masson-Delmotte, V Zhai, P Pirani, A Connors, S.L. pp.
- Jansen, T., and Gislason, H. 2011. Temperature affects the timing of spawning and migration of North Sea mackerel. *Continental Shelf Research*, 31: 64–72.
- Jennings, S., Kaiser, M. J., and Reynolds, J. D. 2001. *Marine Fisheries Ecology*. Blackwell Science Ltd., Malden, MA.
- Kindsvater, H. K., Braun, D. C., Otto, S. P., and Reynolds, J. D. 2016. Costs of reproduction can explain the correlated evolution of semelparity and egg size: Theory and a test with salmon. *Ecology Letters*, 19: 687–696.
- Kleisner, K. M., Fogarty, M. J., McGee, S., Barnett, A., Fratantoni, P., Greene, J., Hare, J. A., *et al.* 2016. The effects of sub-regional climate velocity on the distribution and spatial extent of marine species assemblages. PLoS ONE, 11: 1–21.
- Kleisner, K. M., Fogarty, M. J., McGee, S., Hare, J. A., Moret, S., Perretti, C. T., and Saba, V. S. 2017. Marine species distribution shifts on the U.S. Northeast Continental Shelf under continued ocean warming. *Progress in Oceanography*, 153: 24–36.
- Klibansky, N., and Scharf, F. S. 2017. Fecundity peaks prior to sex transition in a protogynous marine batch spawning fish, black sea bass (*Centropristis striata*). *ICES Journal of Marine Science*: doi:10.1093/icesjms/fsx219.
- Lapointe, D., Vogelbein, W. K., Fabrizio, M. C., Gauthier, D. T., and Brill, R. W. 2014. Temperature, hypoxia, and mycobacteriosis: Effects on adult striped bass *Morone saxatilis* metabolic performance. *Diseases of Aquatic Organisms*, 108: 113–127.
- Lucey, S. M., and Nye, J. A. 2010. Shifting species assemblages in the Northeast US Continental Shelf Large Marine Ecosystem. *Marine Ecology Progress Series*, 415: 23–33.
- McBride, R. S., Somarakis, S., Fitzhugh, G. R., Albert, A., Yaragina, N. A., Wuenschel, M. J., Alonso-Fernández, A., *et al.* 2015. Energy acquisition and allocation to egg production in relation to fish reproductive strategies. *Fish and Fisheries*, 16: 23–57.
- McBride, R. S., Tweedie, M. K., and Oliveira, K. 2018. Reproduction, first-year growth, and expansion of spawning and nursery grounds of black sea bass (*Centropristis striata*) into a warming Gulf of Maine. *Fishery Bulletin*, 116: 323–336.

- McCartney, M. A., Burton, M. L., and Lima, T. G. 2013. Mitochondrial DNA differentiation between populations of black sea bass (*Centropristis striata*) across Cape Hatteras, North Carolina (USA). *Journal of Biogeography*, 40: 1386–1398.
- McGovern, J. C., and Olney, J. E. 1996. Factors affecting survival of early life stages and subsequent recruitment of striped bass on the Pamunkey River, Virginia. *Canadian Journal of Fisheries and Aquatic Sciences*, 53: 1713–1726.
- McMahan, M. D., and Grabowski, J. H. 2019. Nonconsumptive effects of a range-expanding predator on juvenile lobster (*Homarus americanus*) population dynamics. *Ecosphere*, 10: e02867.
- Mercer, L. P. 1978. The reproductive biology and population dynamics of black sea bass, *Centropristis striata*. Dissertation, College of William and Mary, Virginia pp.
- Moser, J., and Shepherd, G. R. 2008. Seasonal distribution and movement of black sea bass (*Centropristis striata*) in the Northwest Atlantic as determined from a mark-recapture experiment. *Journal of Northwest Atlantic Fishery Science*, 40: 17–28.
- Musick, J. A., and Mercer, L. P. 1977. Seasonal distribution of Black Sea Bass, *Centropristis striata*, in the Mid-Atlantic Bight with comments on ecology and fisheries of the species. *Trans. Amer. Fish. Soc.*, 106: 12–25.
- Nilsson, G. E., Östlund-Nilsson, S., and Munday, P. L. 2010. Effects of elevated temperature on coral reef fishes: Loss of hypoxia tolerance and inability to acclimate. *Comparative Biochemistry and Physiology - A Molecular and Integrative Physiology*, 156: 389–393.
- NMFS. 2019. National Observer Program FY 2017 Annual Report. NOAA Technical Memorandum, NMFS-F/SPO. www.fisheries.noaa.gov.
- Norin, T., Malte, H., and Clark, T. D. 2014. Aerobic scope does not predict the performance of a tropical eurythermal fish at elevated temperatures. *The Journal of Experimental Biology*, 217: 244–251.
- Perretti, C. T., Fogarty, M. J., Friedland, K. D., Hare, J. A., Lucey, S. M., McBride, R. S., Miller, T. J., *et al.* 2017. Regime shifts in fish recruitment on the Northeast US Continental Shelf. *Marine Ecology Progress Series*, 574: 1–11.
- Pershing, A. J., Alexander, M. A., Hernandez, C. M., Kerr, L. A., Le Bris, A., Mills, K. E., Nye, J. A., *et al.* 2015. Slow adaptation in the face of rapid warming leads to collapse of the Gulf of Maine cod fishery. *Science*, 350: 809–812.
- Pinsky, M. L., Reygondeau, G., Caddell, R., Palacios-Abrantes, J., Spijkers, J., and Cheung, W. W. L. 2018. Preparing ocean governance for species on the move. *Science*, 360: 1189–1192.
- Pörtner, H. O., and Farrell, A. P. 2008. Physiology and Climate Change. *Science*, 322: 690–692.
- Pörtner, H. O. 2010. Oxygen- and capacity-limitation of thermal tolerance: a matrix for integrating climate-related stressor effects in marine ecosystems. *Journal of Experimental Biology*, 213: 881–893.
- Provost, M. M., Jensen, O. P., and Berlinsky, D. L. 2017. Influence of size, age, and spawning season on sex change in black sea bass. *Marine and Coastal Fisheries*, 9: 126–138.
- Rheuban, J. E., Kavanaugh, M. T., and Doney, S. C. 2017. Implications of future Northwest Atlantic bottom temperatures on the American lobster (*Homarus americanus*) fishery. *Journal of Geophysical Research: Oceans*, 122: 1–12.

- Richaud, B., Kwon, Y. O., Joyce, T. M., Fratantoni, P. S., and Lentz, S. J. 2016. Surface and bottom temperature and salinity climatology along the continental shelf off the Canadian and U.S. East Coasts. *Continental Shelf Research*, 124: 165–181. Elsevier.
- Roy, E. M., Quattro, J. M., and Greig, T. W. 2012. Genetic management of black sea bass: Influence of biogeographic barriers on population structure. *Marine and Coastal Fisheries*, 4: 391–402.
- Saba, V. S., Griffies, S. M., Anderson, W. G., Winton, M., Alexander, M. A., Delworth, T. L., Hare, J. A., *et al.* 2016. Enhanced warming of the Northwest Atlantic Ocean under climate change. *Journal of Geophysical Research: Oceans*, 120: 1–15.
- Sandblom, E., Gräns, A., Axelsson, M., and Seth, H. 2014. Temperature acclimation rate of aerobic scope and feeding metabolism in fishes: implications in a thermally extreme future. *Proceedings of Royal Society of Biology*, 281: 20141490.
- SAW/SARC: Black sea bass working group. 2016. Black sea bass benchmark stock assessment review: Proposed partitioning of northern black sea bass stock for purposes of developing spatial stock assessment models. 1–40 pp.
- Schultz, E. T., and Conover, D. O. 1997. Latitudinal differences in somatic energy storage: Adaptive responses to seasonality in an estuarine fish (Atherinidae: Menidia menidia). *Oecologia*, 109: 516–529.
- Secor, D. H., Zhang, F., O'Brien, M. H. P., and Li, M. 2019. Ocean destratification and fish evacuation caused by a Mid-Atlantic tropical storm. *ICES Journal of Marine Science*, 76: 573–584.
- Shepherd, G. R., and Nieland, J. 2010. Black Sea Bass 2010 Stock Assessment Update. *Fisheries Science*: 1–25.
- Slotte, A. 1999. Effects of fish length and condition on spawning migration in Norwegian spring spawning herring (*Clupea harengus* L. Sarsia, 84: 111–127.
- Steimle, F. W., and Figley, W. 1996. The Importance of Artificial Reef Epifauna to Black Sea Bass Diets in the Middle Atlantic Bight. *North American Journal of Fisheries Management*, 16: 433–439.
- Steimle, F. W., and Zetlin, C. 2000. Reef habitats in the Middle Atlantic Bight: abundance, distribution, associated biological communities, and fishery resource use. *Marine Fisheries Review*, 62: 24–42.
- Sullivan, M. C., Cowen, R. K., and Steves, B. P. 2005. Evidence for atmosphere-ocean forcing of yellowtail flounder (*Limanda ferruginea*) recruitment in the Middle Atlantic Bight. *Fisheries Oceanography*, 14: 386–399.
- Walsh, H. J., Richardson, D. E., Marancik, K. E., and Hare, J. A. 2015. Long-term changes in the distributions of larval and adult fish in the northeast U.S. shelf ecosystem. *PLoS ONE*, 10: 1–31.
- Wilk, S. J., Morse, W. W., and Stehlik, L. L. 1990. Annual cycles of gonad-somatic indices as indicators of spawning activity for selected species of finfish collected from the New York Bight. *Fishery Bulletin*, 88: 775–786.
- Wuenschel, M. J., McBride, R. S., and Fitzhugh, G. R. 2013. Relations between total gonad energy and physiological measures of condition in the period leading up to spawning: Results of a laboratory experiment on black sea bass (*Centropristis striata*). *Fisheries Research*, 138: 110–119.

CHAPTER 2: The Effect of Ocean Warming on Black Sea Bass (*Centropristis striata*) Aerobic Scope and Hypoxia Tolerance

This chapter has been published as:

Slesinger, E., Andres, A., Young, R., Seibel, B., Saba, V., Phelan, B., Rosendale, J., Wiczorek, D., and Saba, G. 2019. The effect of ocean warming on black sea bass (*Centropristis striata*) aerobic scope and hypoxia tolerance. PLoS ONE 14(6): e0218930.

2.1 ABSTRACT

Over the last decade, ocean temperature on the U.S. Northeast Continental Shelf (U.S. NES) has warmed faster than the global average and is associated with observed distribution changes of the northern stock of black sea bass (*Centropristis striata*). Mechanistic models based on physiological responses to environmental conditions can improve future habitat suitability projections. We measured maximum, standard metabolic rate, and hypoxia tolerance (S_{crit}) of the northern adult black sea bass stock to assess performance across the known temperature range of the species. Two methods, chase and swim-flume, were employed to obtain maximum metabolic rate to examine whether the methods varied, and if so, the impact on absolute aerobic scope. A subset of individuals was held at 30°C for one month (30_{chronic}°C) prior to experiments to test acclimation potential. Absolute aerobic scope (maximum – standard metabolic rate) reached a maximum of 367.21 mgO₂ kg⁻¹ hr⁻¹ at 24.4°C while S_{crit} continued to increase in proportion to standard metabolic rate up to 30°C. The 30_{chronic}°C group exhibited a significantly lower maximum metabolic rate and absolute aerobic scope in relation to the short-term acclimated group, but standard metabolic rate or S_{crit} were not affected. This suggests a decline in performance of oxygen demand processes (e.g. muscle contraction) beyond 24°C despite maintenance of oxygen supply. The Metabolic Index, calculated from S_{crit} as an estimate of potential aerobic scope, closely matched the measured

factorial aerobic scope (maximum / standard metabolic rate) and declined with increasing temperature to a minimum below 3. This may represent a critical threshold value for the species. With temperatures on the U.S. NES projected to increase above 24°C in the next 80-years in the southern portion of the northern stock's range, it is likely black sea bass range will continue to shift poleward as the ocean continues to warm.

2.2 INTRODUCTION

Marine environments are progressively warming as a consequence of climate change (Belkin, 2009). Along the U.S. Northeast Shelf (U.S. NES), annual ocean temperature is rising faster than the global average (Pershing *et al.*, 2015; Caesar *et al.*, 2018) resulting in rapid temperature increases (Friedland and Hare, 2007; Kavanaugh *et al.*, 2017) with a strong warming signal prominent during spring, summer and fall (Friedland and Hare, 2007). Over the next 80-years, sea surface and bottom temperatures on the U.S. NES are projected to rise an additional 4.1°C and 5.0°C, respectively (Saba *et al.*, 2016; Kleisner *et al.*, 2017). Contemporary ocean warming on the U.S. NES has been associated with distribution shifts of many economically and ecologically important fish species both in latitude and/or depth (Nye *et al.*, 2009; Bell *et al.*, 2015; Kleisner *et al.*, 2016, 2017; Morley *et al.*, 2018), associated with tracking local climate velocities (Pinsky *et al.*, 2013). Understanding and projecting shifts in fish distribution will be important for characterizing potential ecological and economic impacts and anticipating and resolving fishery management conflicts (Pinsky *et al.*, 2018).

Temperature directly affects metabolic rates of marine ectotherms (Clarke and Johnston, 1999; Verberk *et al.*, 2016) and is believed to set the boundaries of species

ranges (Pörtner and Farrell, 2008; Deutsch *et al.*, 2015; Payne *et al.*, 2016). One explanation for the effects of temperature on ectothermic species' physiology is the oxygen and capacity-limited thermal tolerance hypothesis (OCLTT; Fry and Hart, 1948; Pörtner, 2010) that postulates thermal limitation occurs due to a mismatch in oxygen demand and supply at sub-optimal temperatures, and can ultimately determine metabolically suitable habitat (Pörtner and Knust, 2007). In this framework, the thermal optimum occurs where absolute aerobic scope (AAS), the difference between maximum (MMR) and standard metabolic rate (SMR; Schulte, 2015), is highest. SMR is the cost of maintenance for an organism and increases exponentially with temperature (Clarke and Johnston, 1999). MMR initially increases with temperature but may respond differently at high temperatures due to impaired oxygen supply or utilization. Importantly, MMR measurements can vary substantially depending on the method employed, typically an exhaustive chase or a swim-flume method (Norin and Clark, 2016; Rummer *et al.*, 2016). Varying MMR measurements can affect the AAS measurement, and thus the interpretation of temperature effects on AAS. The decrease in AAS beyond the thermal optimum is associated with the differing thermal sensitivities of MMR and SMR (Farrell, 2016) and suggests that these temperatures are suboptimal. AAS is thought to represent the capacity for oxygen uptake, beyond what supports maintenance metabolism, that can be utilized for activities that promote individual fitness (e.g. growth, reproduction, predator avoidance; (Pörtner and Peck, 2010). However, it should be noted that there are exemptions to this hypothesis found in other fish species (Healy and Schulte, 2012; Grans *et al.*, 2014; Norin *et al.*, 2014), including our own experiments, and this discrepancy is further discussed in Jutfelt *et al.* (2018). Nonetheless, the adaptive benefit of living at

suitable temperatures to maintain aerobic scope may provide a mechanistic explanation for fish distribution patterns.

The general distribution of fishes is broadly confined by thermal preferences. Oxygen availability can further constrain metabolically suitable habitat within thermal boundaries because environmental oxygen solubility decreases with warmer temperatures (Libes 1992, but see Verberk *et al.*, 2011). Simultaneously, warmer temperatures can increase fish oxygen demand (Del Toro Silva *et al.*, 2008; Capossela *et al.*, 2012), which can potentially reduce hypoxia tolerance from both a decrease in oxygen solubility and an increase in fish oxygen demand (Collins *et al.*, 2013; McDonnell and Chapman, 2015). The hypoxia tolerance of a fish can be estimated as the critical oxygen saturation level (S_{crit}), which is the % O₂ air-saturation (%O₂) below which oxygen supply cannot match the demands of maintenance metabolism. Further reductions in %O₂ cause a proportional decrease in SMR (Schurmann and Steffensen, 1997). Below the S_{crit} , ATP production relies on unsustainable anaerobic pathways that can lead to a host of biochemical challenges including a buildup of anaerobic end products and acid-base chemistry changes (Nilsson and Renshaw, 2004; Seibel, 2011), contributing to time-limited survival if the fish remains in water with oxygen levels below S_{crit} . Generally, a fish with a low S_{crit} is thought to be more tolerant of lower sustained oxygen levels (Claireaux and Chabot, 2016). Additionally, the S_{crit} further provides a means of calibrating the Metabolic Index (MI). Deutsch *et al.* (2015) proposed the MI as the ratio of environmental oxygen supply to animal oxygen demand, which is effectively an estimate of a species' time-averaged factorial aerobic scope. By definition, the MI is equal to 1 when the environmental %O₂ is equal to S_{crit} . The MI also contains a temperature

dependency term (E_o), which is calibrated by the S_{crit} at a given temperature, and takes into account temperature effects on the ratio of oxygen supply to fish demand. A minimum MI of 2-5 indicates the environmental capacity to supply oxygen at 2-5x the rate required to support metabolic needs at rest and is considered supportive of a population. This has delineated the equatorward distribution limit for a diverse group of marine fishes and invertebrates [reviewed in Deutsch *et al.* 2015]. The measurement of S_{crit} and subsequent calculation of a thermally sensitive MI have proven useful in predicting habitat suitability.

The northern stock of black sea bass (*Centropristis striata*) on the U.S. NES extends from Cape Hatteras to the Gulf of Maine and is centered in the Mid-Atlantic Bight (MAB; Roy *et al.*, 2012). These fish seasonally migrate from the continental shelf edge in cooler months to inshore depths (5-50m) in warmer months (Musick and Mercer, 1977; Moser and Shepherd, 2008; Fig 2.1). Seasonally migrating black sea bass thus experience a wide range of temperatures throughout the year, ranging from 6°C during winter and up to 27°C during summer/early fall months (Steimle *et al.*, 1999). While these are average seasonal temperatures, this region experiences large interannual variations in surface and bottom temperatures (Bigelow, 1933; Houghton *et al.*, 1982). In addition, under a predicted doubling of anthropogenic atmospheric CO₂ in the next 80 years, summer bottom temperature could reach 30°C in the southern portion of black sea bass range (Saba *et al.*, 2016). This could potentially limit the southern inshore extent of black sea bass habitat. Off the coast of New Jersey, periodic hypoxic events (e.g. O₂ concentration < 2.2 mg L⁻¹ at 14°C) can occur during the summer as a result of high biological activity (Schofield *et al.*, 2012) fueled by upwelling of nutrient rich waters

(Glenn *et al.*, 2004). Therefore, during the warm summer months oxygen limitation in hypoxic regions along the U.S. NES may also reduce metabolically available habitat for black sea bass.

The northern stock of black sea bass may already be exhibiting poleward shifts, likely due to ocean warming (Hare *et al.*, 2016; Kleisner *et al.*, 2017). Evidence for current black sea bass distribution shifts comes primarily from bottom trawl survey data (Hare *et al.*, 2016). Laboratory-based process studies focused on the physiology of an organism provide detailed mechanistic relationships between the environment and the animal (Wikelski and Cooke, 2006). Results from these physiological studies are useful for modeling metabolically suitable habitat based on environmental parameters (Lefevre *et al.*, 2017) and could be used to model current black sea bass distributions (e.g., Manderson *et al.*, 2011; Deutsch *et al.*, 2015) and project future distribution shifts with continued ocean warming.

There were three aims for this study. First, we measured AAS and S_{crit} (for MI calculation) for the northern stock of adult black sea bass over a range of temperatures experienced inshore to compare, if present, thermal optima. These parameters can potentially be used in future habitat suitability modeling and assessing future shifts in black sea bass distribution. Second, we tested the ability of black sea bass to acclimate to an extreme warm temperature (30°C) given the high likelihood such temperatures will become increasingly common under future climate change projections. A subset of black sea bass were acclimated to 30°C for one month and their aerobic performance was compared to those fish tested under short-term acclimations. And finally, we compared

two different MMR measurement methods, chase and swim-flume methods, to investigate which method performed better for black sea bass.

2.3 MATERIALS AND METHODS

2.3.1 Fish collection and husbandry

Adult black sea bass (*Centropristis striata*) from the northern stock (length = 221-398mm; weight = 193.7-700.4g) were collected off the coast of New Jersey, USA at depths of 15-20m in early June from Sea Girt Reef (40°7'07"N, 73°58'42"W) by fish traps (June 14 – 21 2016), and from local reefs off Sandy Hook (40°28'46"N, 73°57'47"W) by hook-and-line (June 28 – July 5 2017). Once captured, fish were housed in the NOAA James J. Howard Marine Laboratory, held at ambient temperature ($22 \pm 1^\circ\text{C}$) and salinity (26ppt), maintained at a natural photoperiod for New Jersey summer (14h:10h light:dark), and fed daily to satiation on a diet of sand lance and silversides for the duration of the respirometry experiments. Water temperature and salinity was monitored daily using a YSI (Pro-30; Yellow Springs, Ohio, USA), and water chemistry remained at suitable levels (< 20 μM nitrate, undetectable nitrite, < 0.05 μM ammonia, pH range of 7.98-8.04). Fish were acclimated to captive conditions for a minimum of two weeks prior to the trials, after which all experimental fish ate regularly and were in good condition. The time from fish collection to experiment trials ranged from two to four weeks. After acclimation, fish were measured for length (TL mm), weight (g), and tagged with individually numbered T-bar Floy tags inserted underneath the dorsal rays. For each temperature treatment, fish were acclimated at a rate of 2°C day^{-1} to reach experimental temperature, then held at the target treatment temperature for at least 48hr

prior to the start of experiments. We defined this, and refer to this process throughout, as a short-term acclimation. Fish were starved 48hr prior to the start of each experiment to eliminate effects of specific dynamic action (Chabot *et al.*, 2016a). A total of 152 experimental fish were used during 2016 and 2017 (S1 Dataset).

2.3.2 Experimental setup

Experimental tanks (1,200L) were filled with treated seawater from Sandy Hook Bay that continuously circulated through a closed system. Circulating seawater was treated using filters (sand and biological) and UV-light, and salinity was adjusted to mimic average summertime inshore NJ bottom water (32 ± 1 ppt). Experimental temperatures were achieved using in-line chillers (Aqua Logic Delta Star; San Diego, California, USA) and/or titanium exchanger heaters (Innovative Heat Concepts, Homestead, Florida, USA), and maintained at $\pm 1^\circ\text{C}$ from target temperature.

Metabolic rates were measured using intermittent respirometry under the protocols outlined in Clark *et al.* (2013) and Svendsen *et al.* (2016). Flow-through respirometers (13.5L; 23[H]x26[W]x37[L] cm plexiglass) were placed into the two experimental tanks (two respirometers per tank; four respirometers per trial). Flush pumps (Eheim Universal 600 l/h; Deizisau, Germany) connected to the respirometer were used to pull water from the surrounding temperature bath to replenish dissolved oxygen and eliminate metabolic waste buildup within the respirometer. The duration and timing of flushes set the intermittent cycles, which were controlled through a pre-determined time sequence using a DAQ-M instrument (Loligo Systems; Viborg, Denmark), and were determined based on the trial temperature so that % O₂ air-saturation

(%O₂) remained above below 75% (Svendsen *et al.*, 2016b). See Table S2.1 for list of intermittent flushes at each temperature. For each closed measure period (when flush pumps were off), the rate of decline in dissolved oxygen concentration within the sealed respirometer was used to calculate a mass specific rate of oxygen consumption, a proxy for metabolic rate. A closed recirculation loop connected with a smaller pump (Eheim Universal 300 l/h; Deizisau, Germany) was also utilized to uniformly disperse dissolved oxygen within the respirometer and provide waterflow across the oxygen dipping probe optical mini sensor (PreSens Pst3; Regensburg, Germany). Oxygen probes were calibrated in accordance with the supplier's manual (Oxygen dipping probe PSt3, PreSens GmbH, Regensburg, Germany) and checked with a YSI (ProSolo ODO; Yellow Springs, Ohio, USA) that was calibrated in 100 and 0 %O₂ sample waters. Autoresp computer software (Loligo Systems; Viborg, Denmark) and a Witrox-4 instrument (Loligo Systems; Viborg, Denmark) were used to continuously monitor dissolved oxygen and temperature within the respirometer over the course of the experiment.

Intermittent respirometry was also used in hypoxia experiments to control for CO₂ and metabolite build up within the respirometer (Rogers *et al.*, 2016). In this set up, each respirometer flush pump was connected to a separate external water reservoir containing the same system water. Within the external water reservoir, a pump (Eheim Universal 1200 l/h; Deizisau, Germany) was utilized to provide uniform mixing and to provide flow across an oxygen optode to monitor source %O₂ and served as a mixing device. Four small microdiffusers were connected to a N₂ gas canister (Schurmann and Steffensen, 1997) and utilized for diffusion of nitrogen gas, and a subsequent displacement of O₂, within the external bath. N₂ was manually released using a nitrogen purge regulator

(Randor SR5B-580 Airgas; Paris, France) allowing for monitoring of PSI within the canister and being released into the external water reservoir. For fine scale tuning of the %O₂ in the external water bath, system water was periodically pumped into the external reservoir and was used to replenish water supply. All changes in the %O₂ levels were performed during a closed measure period when the experimental respirometers were closed to external water flow to avoid fluctuations in the %O₂ level within the individual respirometers.

Experiments were conducted at a range of temperatures (12, 17, 22, 24, 27 and 30°C). For both 2016 and 2017 experiments, we conducted a short-term acclimation on black sea bass before the start of each aerobic scope trial (*see Fish Collection and Husbandry*). In addition to short-term acclimation trials at each temperature, we also included a temperature treatment with chronic exposure (one month) to 30°C (30_{chronic}°C) because projections of ocean warming within the next century predict summer bottom temperatures as high as 30°C in the southern portion of black sea bass range (Saba *et al.*, 2016). This allowed for testing of current black sea bass acclimation potential by assessing the effects of long-term exposure to 30°C on aerobic scope and hypoxia tolerance. Sample sizes for all temperature treatments are in the S1 Dataset.

We used two different methods in an attempt to elicit maximum metabolic rate (MMR): exhaustive-chase and swim-flume. MMR was tested using two different methods as the method used can affect the resulting metabolic rates and thus AAS (Roche *et al.*, 2013; Norin and Clark, 2016; Rummer *et al.*, 2016). Therefore, a comparison of AAS resulting from the “chase” and “swim-flume” methods was conducted. For the chase method, individual black sea bass were placed in a 4ft-diameter chase tank filled

with water from the experimental tanks. Fish were chased to exhaustion via tactile stimulation on the caudal fin. Exhaustion was determined as the point where fish became unresponsive to further tactile stimulation and air exposure. Fish were then immediately transferred and sealed within individual respirometers within ~1 minute from the end of the chase. Fish remained within respirometers for ~23hr allowing for recovery and subsequent standard metabolic rate (SMR) measurement (Chabot *et al.*, 2016b). Sixteen fish were used in each temperature treatment. In the 30_{chronic}°C temperature treatment, the sample size was nine fish due to the removal of five fish in poor condition before and two fish during experiments. At the end of SMR measurements, the first twelve fish rested for at least 24hr and then exercised in a swim-flume. The last four fish of each temperature treatment remained in the respirometer for hypoxia testing (see below). For the swim-flume, individual fish were exercised in an acrylic Brett-style flume respirometer (Loligo Systems 90L; Viborg, Denmark). Fish were placed within the working section of the flume (20[H] x 20[W] x 70[L] cm) and sealed within the flume for the duration of the experiment. A motor driven propeller, housed within the flume and separate from the working section, was utilized for both manual speed changes to allow for measurements across different activity levels and for continuous uniform mixing of water (and O₂) throughout the chamber. The flume was fully submerged within an external water bath (71[H] x 35[W] x 188[L] cm), to maintain consistent temperature throughout the trial. A pump (Eheim Universal 1200 l/h; Deizisau, Germany) was utilized for intermittent flushing of new system water into the flume chamber after measure periods and to supply system water to the external bath during measure periods. Fish were exercised using a sprint protocol. First, the fish was allowed to adjust to the

swim flume for 10 minutes with minimal flow to provide mixing. Then, the flow was slowly increased to a swimming speed of 0.95 BL s^{-1} , the lowest speed black sea bass began to swim, over a five-minute period. The fish adjusted to this speed for ~ 10 minutes. After the adjustment period, the speed was incrementally increased over a period of five minutes until the fish was sprinting (designated as >10 bursts utilizing the caudal fin during 30s intervals and an inability to maintain position in the working section without burst swimming). Once the fish reached their sprinting speed, the flush pump was turned off and the flume was sealed to allow measurement of metabolic rate. Fish were held at their sprint speed for a period of 10 minutes or until failure, determined when the fish rested at the backgate for >10 s.

Background respiration was measured by taking background MO_2 ($\text{MO}_{2\text{br}}$) pre- and post-trial in empty respirometers for ~ 1.5 hr. A linear regression between pre- and post- $\text{MO}_{2\text{br}}$ was used to apply a correction factor to each MO_2 value recorded throughout an experiment.

2.3.4 Critical %O₂ determinations

Hypoxia (S_{crit}) experiments were conducted on the last four fish of each temperature treatment trial. This allowed for reliable use of fish that were already acclimated to the respirometers and had reached SMR overnight. S_{crit} was measured by incrementally decreasing the %O₂ in the respirometers (Schurmann and Steffensen, 1997). We measured ~ 10 %O₂ bins. The number of bins was temperature dependent based on where S_{crit} occurred. The experiment started at 100 %O₂ and incrementally decreased by 10 %O₂ (100, 90, 80, 70%, etc.) until S_{crit} was reliably reached, indicated by

a significant decrease in metabolic rate and deviation in SMR. Consequently, as hypoxia tolerance decreased at higher temperatures, the number of %O₂ bins in the experiment decreased as well. At each %O₂ bin there were three intermittent (flush, wait, measure) cycles measured which collectively took ~30 minutes depending on the temperature. If a fish lost equilibrium or exhibited signs of distress, the experiment was immediately ended for that individual..

2.3.5 Ethics statement

Husbandry and experiments were conducted according to relevant national and international guidelines. Fish were collected under permits #1610 & #1717 issued by the New Jersey Department of Environmental Protection. No endangered or protected species were involved. Protocols for the treatment and euthanasia procedure of all animals reported here was approved by the Rutgers University Institutional Animal Care and Use Committee protocol number 15-054. All efforts were made to ensure minimal pain and suffering. Fish behavior, feeding, and condition were monitored daily. Any fish exhibiting apparent health issues or excessive stress (i.e. lack of appetite, difficulties with buoyancy or orientation) were not used in experiments. Fish that could not recover apparent health issues and exhibited extreme distress were euthanized with an overdose of MS-222 (250 mgL⁻¹). Between 2016 and 2017, 152 of 164 fish were used for experiments. Ten fish were in poor condition and two fish continued to experience symptoms of barotrauma (i.e. exophthalmia) prior to experiments and were not used. Three fish showed signs of distress during an experiment and were immediately removed and monitored. When condition did not improve, the fish were euthanized. All of these

mortalities were associated with the 30_{chronic}°C and 30°C temperature treatments. All experimental animals were euthanized at the end of the experiment with MS-222 (250 mgL⁻¹) to obtain a final sex of the fish and to prevent any potential spread of pathogens or infectious disease to natural populations that may have resulted from prolonged captivity in the laboratory (~2 months) and gone undetected.

2.3.6 Data analysis

Fish MO₂ is presented as mass-specific (MO₂: mgO₂ kg⁻¹ hr⁻¹) and was calculated from the slope of oxygen saturation decline during each closed measure period using the equation:

$$MO_2 = ([O_2]_{t_0} - [O_2]_{t_1}) \cdot \frac{V}{t} \cdot \frac{1}{BW}$$

where MO₂ is mass-specific metabolic rate (in mgO₂ kg⁻¹ hr⁻¹), [O₂]_{t0} is oxygen concentration (mgO₂/L) at time t=0, [O₂]_{t1} is the oxygen concentration at time t=1, V is the respirometer volume (L) without the fish volume, t is t₁-t₀ (hr) referring to one measure period, and BW is the body weight (kg) of the fish. The MO₂ was automatically calculated after each measurement period in the AutoResp program during the experiment. This calculation was used for both MO₂ measurements in the respirometers and in the swim-flume. Validation of each MO₂ value was conducted using R² values from each measure period. MO₂ measurements with R² values < 0.9 were not used.

Standard metabolic rate was calculated from a truncated dataset excluding the hours of elevated MO₂ values following exercise and by using the 20th quantile of the SMR data in the *calcSMR* package in R (Chabot *et al.*, 2016b). All fish SMR was measured for at least 15 hours in the truncated datasets. Briefly, a frequency distribution

of MO_2 values from the truncated data set was created and the value at the 20th quantile was taken as SMR. The use of the 20th quantile over other methods (i.e. lowest 10%, average of lowest 10 values) is preferred because MO_2 values naturally fluctuate above and below SMR and avoids potential underestimations of SMR (Chabot *et al.*, 2016b). MMR in the chase and swim-flume protocols was defined as the highest MO_2 measurement recorded during the respective trials. The difference between MMR methods was analyzed using a Welch two sample *t*-test because sample sizes were unequal. Aerobic scope was calculated from both MMR methods in absolute (AAS = MMR-SMR) and factorial terms (FAS = MMR/SMR). In 2016, fish testing was restricted to three temperatures (24, 27, and 30°C) due to difficulties in maintaining temperatures, and some individuals were tested at more than one temperature due to a limited number of fish obtained for testing. Only fish that were used once were ultimately included in 2016 data analysis to maintain data independence. There was a significant effect of mass on MO_2 ($F_{1,117} = 4.651$; $P < 0.05$; Fig. 2.2). Therefore, the effect of temperature on MO_2 was analyzed using a one-way ANCOVA with weight as a covariate. A Tukey's HSD *post hoc* test was used to determine significant pair-wise comparisons between temperatures. MO_2 was adjusted to the mean fish weight (346.9g) using the estimated marginal means from the ANCOVA. The estimated marginal means provides weight-adjusted MO_2 ($\text{MO}_{2\text{adj}}$) mean and standard errors for each temperature treatment. These values were used to report results and in graphs where weight had a significant effect on MO_2 . Curves for aerobic scope were modeled using a 3rd degree polynomial fit and were used to estimate a thermal optimum (temperature at the highest AS).

Q_{10} values were calculated for MO_{2adj} between temperature increments, and between the range of temperatures using the formula:

$$Q_{10} = \frac{R_2^{10/(T_2-T_1)}}{R_1}$$

where Q_{10} is the temperature coefficient for MO_2 , R_1 is the MO_2 at T_1 and R_2 is the MO_2 at T_2 .

S_{crit} was determined by using a broken-stick regression which fits two regression lines through the data: one through the region where MO_2 remained stable as % O_2 decreased and one through the portion where MO_2 decreased linearly with a decrease in % O_2 . The intersection of the two regression lines is the critical point used for S_{crit} (Yeager and Ultsch, 1989). This was analyzed using R code in the *calcO2crit* package from (Claireaux and Chabot, 2016). Because we had a sample size of four fish per temperature treatment, a power analysis was run to determine the statistical power of this small sample size. The effect of weight on S_{crit} was not significant ($P > 0.05$) so a one-way ANOVA was used to assess the effect of temperature on S_{crit} and a Tukey's HSD *post hoc* test was used to determine significant pair-wise comparisons between temperatures. The Metabolic Index (MI) was calculated using the equation from Deutsch *et al.* (2015):

$$\Phi = A_o B^n \frac{PO_2}{\exp\left(-\frac{E_o}{k_B T}\right)}$$

where Φ is the Metabolic Index, A_o is the ratio of rate coefficients, B^n is the body mass scaling, PO_2 is ambient O_2 pressure, E_o is the temperature dependence of baseline metabolic rate, k_B is the Boltzmann's constant, and T is temperature. Here, the S_{crit} data from each temperature treatment is used to determine the E_o and A_o parameters for the equation.

All statistical analyses were performed in R 3.4.3 (R Core Team, 2017). Data were checked for assumptions of normality by the visual Q-Q norm plot and statistically with the Shapiro-Wilk test where $P > 0.05$ indicate normally distributed data. Homogeneity was assessed using the Levene's test where a $P > 0.05$ indicates homogeneity. Data that did not fit assumptions of normality were log-transformed prior to further statistical analysis. Data are presented as mean \pm SE and results from statistical analyses are defined as significant at $P < 0.05$.

2.4 RESULTS

2.4.1 Metabolic rates and aerobic scope

SMR increased significantly with temperature (Figs 2.2A and 2.2B) and there was a significant effect of weight and temperature*weight interaction on SMR ($P < 0.05$; Table 2.1). SMR values obtained from the 20th quantile were within one standard deviation from the truncated dataset mean for each fish. While the results for the two MMR methods differed significantly ($P < 0.05$ for all temperatures), temperature, weight and temperature*weight interaction all had a significant effect on MMR using either method ($P < 0.05$; Table 2.1). The chase MMR increased continuously with temperature, while the swim-flume MMR increased with temperature up to $\sim 27^{\circ}\text{C}$ (Fig 2.3A & 2.3B). The MMR values from the swim-flume were consistently higher across the temperature range than from the chase method, indicating that the metabolic rate reached during the chase likely was not the maximum possible for this species.

While the chase method did not achieve MMR, it still provided an estimate of submaximal exercise performance across a temperature range. The MMR achieved using

the chase method increased continuously with temperature and reached a maximum adjusted value of $396.65 \pm 11.48 \text{ mg O}_2 \text{ kg}^{-1} \text{ hr}^{-1}$ at 30.0°C (the highest temperature measured; Table 2.2; Fig 2.3A). The MMR measured using the swim-flume reached a maximum of $497.96 \pm 21.92 \text{ mgO}_2 \text{ kg}^{-1} \text{ hr}^{-1}$ at 27°C (Table 2.2; Fig 2.3B). The AAS using the swim-flume method reached a maximum, typically referred to as “ T_{opt} ” at $\sim 24.4^\circ\text{C}$ (Fig. 2.3B). There was a significant effect of temperature, weight, and the temperature*weight interaction on AAS ($P < 0.05$) calculated individually from both MMR methods (Table 2.1). Using different MMR methods resulted in differences in the shape of the AAS curve (Fig 2.4A & 2.4B) and the estimated thermal optimum with consequences for its interpretation. The 24°C treatment was slightly overestimated and had larger standard error for AAS and MMR when normalized to a mean fish weight of 346.9g because the average fish weight for this temperature treatment was 253.9g (see Fig S2.1 for normalized weights at each temperature). However, the 24°C temperature treatment only used the chase method, which we determined did not provide an accurate estimate of MMR and therefore this overestimation does not impact our conclusions. All SMR, MMR and AAS weight-adjusted values, and S_{crit} values, are reported in Table 2.2. Q_{10} values are reported in Table 2.3.

2.4.2 Critical %O₂ and Metabolic Index

The power analysis determined that a sample size of four was adequate for statistical testing ($Power = 1$ with $n = 4, f = 1.71$ and $sig. level = 0.05$). This indicates that there was enough statistical power with a sample size of four fish since the variability between groups was larger than among groups. The critical %O₂ (S_{crit})

increased significantly with increasing temperature (Fig 2.5; $F_{5,18} = 14.023$, $P < 0.05$) and significantly increased with SMR (Fig 2.6; $F_{1,22} = 107.6$, $P < 0.001$). There was no significant difference between 12°C (19.65 ± 1.72 %O₂), 17°C (21.325 ± 1.75 %O₂) and 22°C (21.80 ± 1.21 %O₂), but S_{crit} increased significantly at 27°C (31.60 ± 1.67 %O₂) and further at 30°C (37.875 ± 3.39 %O₂). However, non-significance between 12, 17 and 22°C could be due to low sample size. The MI decreased with increasing temperature (Fig 2.7) but a critical MI (<1) was not observed during this experiment, even under the extreme warm temperatures. A mean critical MI of 3.3 was reported for diverse marine species [17], consistent with the value found near the upper temperature limit ($\sim 24.4^\circ\text{C}$) found here for MMR as well (Fig 2.7). FAS and MI were of the same magnitude and followed the same decreasing trend with increasing temperatures (Fig 2.7) supporting the interpretation of MI as another measure of AS.

2.4.3 Chronic high temperature exposure

The 30_{chronic}°C group AAS using both MMR methods significantly decreased when compared to the short-term acclimated 30°C fish that were only held at this temperature for a week (Fig 2.4). Based on Tukey *post hoc* differences, SMR did not change significantly between the 30_{chronic}°C and short-term acclimated 30°C treatments but there was a significant decrease in MMR between the short-term acclimated 30°C and 30_{chronic}°C treatments (Fig 2.3). There was no significant difference in S_{crit} between short-term acclimated 30°C and 30_{chronic}°C treatments (Fig 2.5).

2.5 DISCUSSION

The primary objective of this study was to measure aerobic scope and hypoxia tolerance at a range of ecologically relevant temperatures to assess the potential physiological impacts of ocean warming on and to determine metabolically available habitat for the northern stock of black sea bass. We measured the oxygen consumption rate, a proxy for metabolic rate, following two different exercise protocols. The swim-flume yielded much higher metabolic rates, indicating that the chase method did not elicit MMR. Using the swim-flume MMR, we found that AAS peaked at 24.4°C. S_{crit} increased with increasing temperatures as is typical of most (but not all, Wishner *et al.*, 2018) animals, including fishes (Rogers *et al.*, 2016). The observation that S_{crit} increased with temperature in proportion to SMR, while MMR in the swim-flume did not, suggests that exposure to high temperature did not alter the capacity for oxygen uptake and transport. Chronic exposure to 30°C resulted no change in SMR or S_{crit} but a significant drop in AAS resultant of reductions in MMR (using both methods) implying no loss of oxygen supply capacity as estimated from S_{crit} . Instead, this suggests a decrement in muscle function limiting maximum performance with longer exposure to warm temperatures that is not limited by oxygen supply capacity.

Absolute AS typically increases with temperature up to a point, often termed “thermal optima”, and then declines at higher temperatures resulting in a roughly bell-shaped curve. This curve has been identified in fishes that include, but is not limited to, juvenile European sea bass *Dicentrarchus labrax* (Claireaux *et al.*, 2006), turbot *Scophthalmus maximus* (Mallekh and Lagardere, 2002), coho salmon *Oncorhynchus kisutch* (Raby *et al.*, 2016), and sockeye salmon *Oncorhynchus nerka* (Farrell *et al.*,

2008). However, some studies have found left- or right-skewed curves (e.g. Healy and Schulte, 2012) while others find that AAS continues to increase up to the critical (lethal) temperature for the species (i.e. no temperature optimum for AAS is identifiable; e.g. Norin *et al.*, 2014; Lefevre, 2016). In our study, the black sea bass AAS curve was more bell-shaped with an estimated optimal temperature of 24.4°C. With this finding, the southern portion of the black sea bass range should be considered thermally optimal because bottom temperature is typically 24-26°C during the summer (Houghton *et al.*, 1982; Castelao *et al.*, 2008; from U.S. East Coast Regional ESPreSSO model, Wilkin and Hunter, 2013). However, if the loss in AAS at higher temperatures is due to a failure in muscular performance rather than potential oxygen supply, then 24°C may represent a maximum tolerable temperature rather than a temperature that allows optimal performance. In support of this interpretation, the MI (which closely matches FAS) declines with increasing temperature toward levels (~3 at 27°C in black sea bass) known to limit the geographic range of some species (Deutsch *et al.*, 2015). While the average bottom temperature in the southern portion of the northern stock of black sea bass is near 24°C during the summer months, there has still been a consistent expansion of their range northward into lower temperatures (NEFSC, 2017) further suggesting that the temperature eliciting maximum AAS is not, in fact, optimal. It is important to note that AAS is only a measured capacity to supply oxygen under maximum sustained exercise (Farrell, 2016). The required scope for other metabolic expenses (i.e. feeding, digestion; Holt and Jørgensen, 2015) change with temperature in unknown ways and metabolic needs can change seasonally and with ontogeny (Clark *et al.*, 2013). Thus, AAS may in this case be an inappropriate predictor of fitness, and does not appear to pinpoint an

optimum temperature or correlate with black sea bass distribution. When AAS is measured in the laboratory, important but non-basal energetic requirements (i.e. digestion, reproduction, growth) are removed to provide measurements of SMR. Future studies could benefit from investigating how aerobic capacity changes as other energetic parameters are included in experiments. Finally, the MI, which can be used to predict FAS, can indicate an upper tolerable temperature limit in black sea bass and better explains the northward expansion of these fish. This metric may be more relevant for determining metabolically suitable black sea bass habitat.

Black sea bass in the 30_{chronic}°C treatment did not acclimate, indicated by no change in SMR or S_{crit} and a significant decrease in their MMR and AS. Norin *et al.* (2014) similarly found that MMR and AAS in juvenile barramundi decreased significantly following 5 weeks at the highest study temperature (38°C). However, unlike black sea bass in our study, the juvenile barramundi SMR also decreased after the 5-week exposure. This same response has also been found for short-horn sculpin (*Myoxocephalus scorpius*) whose SMR was restored after being held at 16°C for 8 weeks to SMR values that were measured at 10°C (Sandblom *et al.*, 2014). The decrease in SMR can be a compensatory response to high temperatures by reducing energetic costs, but may be accompanied by a reduction in MMR. Importantly, black sea bass in the 30_{chronic}°C treatment may have suffered stress from long-term captivity, which could also reduce AAS; time did not permit for a control chronic trial at a cooler temperature (although all fish were held for at least 5 days). Understanding the acclimation potential of black sea bass would benefit from future studies focusing on effects of a chronic treatment at each temperature tested.

S_{crit} increased as temperature increased, most likely caused by rising SMR with higher temperatures, which has been shown in a majority of fish hypoxia studies (e.g. Schurmann and Steffensen, 1997; although see Wishner *et al.*, 2018). The 30_{chronic}°C group did not have a significant decrease in hypoxia tolerance compared to the short-term acclimation 30°C group, which agrees with no change in SMR between the two 30°C treatments. This suggests that the reduced MMR in 30_{chronic}°C fish resulted from reduced muscle function rather than from oxygen supply capacity issues. Black sea bass had lower S_{crit} than striped bass *Morone saxatilis* (Lapointe *et al.*, 2014) and summer flounder *Paralichthys dentatus* (Capossela *et al.*, 2012), two important species found throughout the MAB that periodically experience hypoxic water during the summer months. However, when compared with fish that frequently experience hypoxia, such as crucian carp (Yamanaka *et al.*, 2007), black sea bass were less hypoxia tolerant, especially in warmer water. Along these lines, black sea bass FAS and MI both decreased with increasing temperature (Fig. 2.6). During the summer months when bottom water temperature is warmest along the coastal MAB, periodic hypoxic events occur after large phytoplankton blooms in the surface waters. In the past, these hypoxic events decreased bottom water PO₂ below ~5.5kPa (26% air-saturation; 2.2 mg L⁻¹ at 14°C; Schofield *et al.*, 2012), providing a MI of ~1.3 at those temperatures for black sea bass. An MI of 1.3 confers very little aerobic scope for activities beyond basic maintenance costs, and likely does not allow for activities necessary for survival (i.e. foraging, predator evasion) and fitness (i.e. growth, reproduction). Thus, such environments can be tolerated for short periods but are not likely not supportive of a thriving population. At 30°C, even air-saturated water provides a MI of only 2.6 which is near the physiological limits of many

species (Deutsch *et al.*, 2015). Therefore, when determining the metabolically suitable habitat, both temperature and oxygen availability must be taken into consideration as both stressors might have synergistic effects on the physiology of this species.

The chase method did not elicit MMR in black sea bass since MMR from the swim-flume method was consistently higher. Which method, chase or swim-flume, provides a more reliable measure of MMR and AAS is debated (Norin and Clark, 2016; Killen *et al.*, 2017). Whether a maximum rate of oxygen uptake is achieved by either method could depend on the type of swimming the study fish species naturally exhibits in the wild. Norin *et al.* (2014) purposefully used a chase method for juvenile barramundi (*Lates calcarifer*), an ambush predator, that typically swims in quick bursts. In other cases, a fish will exhibit marked post-exercise oxygen consumption (EPOC; Plambech *et al.*, 2013), sometimes eliciting MMR minutes to hours after the cessation of exercise (Reidy *et al.*, 1995). The swim-flume method may be more ecologically relevant for endurance swimming exhibited by pelagic fish such as tunas (Killen *et al.*, 2017). Different MMR methods may promote a certain type of swimming which could cause a fish to fatigue before reaching MMR by depleting anaerobic stores, a noteworthy contributor to AAS (Ejbye-Ernst *et al.*, 2016). For this study, we employed a sprint protocol for the swim-flume, which prompted similar burst swimming as in the chase method. However, during the chase protocol, black sea bass switched almost immediately to burst swimming accompanied with quick turning/flipping movements, compared to a slower transition and continuously straight burst swimming in the swim-flume. The differences in MMR between the two methods could have been related to different

swimming types, durations and/or speeds which could recruit more anaerobic resources (Svendsen *et al.*, 2010) in the chase method, leading to exhaustion before reaching MMR.

In summary, the results from this study indicate that the northern stock of black sea bass reach a peak in AAS at $\sim 24^{\circ}\text{C}$, which is warmer than in the northern portion of their range in the U.S. NES. The MI of 3.8 in air-saturated water, calculated from S_{crit} at 24°C , suggests relatively limited scope for sustained activity at that temperature (Deutsch *et al.*, 2015). We suggest that, rather than an optimal temperature, the peak in MMR and AAS indicates the maximum tolerable temperature, beyond which black sea bass experience a failure in some subcellular or organ systems that contribute to muscle performance. Our study only used individuals from the northern stock that were collected during the summer off of the New Jersey coastline. Metabolic research on the southern stock (south of Cape Hatteras, NC) and/or individuals from the northern stock in waters outside of New Jersey could reveal variation in some of these physiological metrics. However, the distribution of the northern stock of black sea bass has shifted northward (Kleisner *et al.*, 2017) and this newly expanded habitat bottom temperature is almost 10°C colder than their apparent thermal optimum for AAS. We believe the preference for cooler waters reflects physiological limitation at higher temperatures, including possible limitation of oxygen supply relative to demand for growth and reproduction (reduced Metabolic Index) despite maintenance of oxygen supply capacity. However, many other factors, including food availability, additional energetic costs (e.g., evading predators, mating), or lower optimal temperatures for other critical processes may be important. This suggests AAS may not be the most appropriate predictor for habitat suitability in this species. Additionally, the northern stock of black sea bass

population size has been increasing in the last decade (Holt and Jørgensen, 2015), and this increase in biomass could be pushing part of the population northward. Regardless, the chronic exposure experiments presented here suggest little capacity for physiological adjustment to future temperatures. Black sea bass thermal habitat may shrink considerably in the southern region of the MAB as bottom water temperatures reach $>27^{\circ}\text{C}$ and continue to expand into the northern region of the MAB as ocean waters continue to warm, impacting fisheries in these two regions.

2.6 ACKNOWLEDGEMENTS

We thank Doug Zemeckis and Captain Chad Hacker (R/V Tagged Fish) for helping us collect black sea bass; Richard Brill and Andrij Horodysky for providing insight and suggestions for the study design; the students at the Marine and Science Technology Academy for their assistance in animal husbandry; and Laura Palamara Nazzaro for creating and providing black sea bass distribution maps. We also acknowledge the NOAA James J. Howard Laboratory personnel for their support and help throughout the study.

2.7 REFERENCES

- Belkin, I. M. 2009. Rapid warming of Large Marine Ecosystems. *Progress in Oceanography*, 81: 207–213.
- Bell, R. J., Richardson, D. E., Hare, J. A., Lynch, P. D., and Fratantoni, P. S. 2015. Disentangling the effects of climate, abundance, and size on the distribution of marine fish: an example based on four stocks from the Northeast US shelf. *ICES Journal of Marine Science*, 72: 1311–1322.
- Bigelow, H.B. 1993. Studies of the waters on the continental shelf, Cape Cod to Chesapeake Bay. I. The cycle of temperature. Massachusetts: Massachusetts Institute of Technology and Woods Hole Oceanographic Institution.
- Caesar, L., Rahmstorf, S., Robinson, A., Feulner, G., and Saba, V. 2018. Observed

- fingerprint of a weakening Atlantic Ocean overturning circulation. *Nature*, 556: 191–196.
- Capossela, K. M., Brill, R. W., Fabrizio, M. C., and Bushnell, P. G. 2012. Metabolic and cardiorespiratory responses of summer flounder *Paralichthys dentatus* to hypoxia at two temperatures. *Journal of Fish Biology*, 81: 1043–1058.
- Castelao, R., Glenn, S., Schofield, O., Chant, R., Wilkin, J., and Kohut, J. 2008. Seasonal evolution of hydrographic fields in the central Middle Atlantic Bight from glider observations. *Geophysical Research Letters*, 35: 6–11.
- Chabot, D., McKenzie, D. J., and Craig, J. F. 2016a. Metabolic rate in fishes: Definitions, methods and significance for conservation physiology. *Journal of Fish Biology*, 88: 1–9.
- Chabot, D., Steffensen, J. F., and Farrell, A. P. 2016b. The determination of standard metabolic rate in fishes. *Journal of Fish Biology*, 88: 81–121.
- Claireaux, G., Couturier, C., and Groison, A. 2006. Effect of temperature on maximum swimming speed and cost of transport in juvenile European sea bass (*Dicentrarchus labrax*). *Journal of Experimental Biology*, 209: 3420–3428.
- Claireaux, G., and Chabot, D. 2016. Responses by fishes to environmental hypoxia: Integration through Fry's concept of aerobic metabolic scope. *Journal of Fish Biology*, 88: 232–251.
- Clark, T. D., Sandblom, E., and Jutfelt, F. 2013. Aerobic scope measurements of fishes in an era of climate change: respirometry, relevance and recommendations. *Journal of Experimental Biology*, 216: 2771–2782.
- Clarke, A., and Johnston, N. 1999. Scaling of metabolic rate with body mass and temperature in teleost fish. *Journal of Animal Ecology*, 68: 893–905.
- Collins, G. M., Clark, T. D., Rummer, J. L., and Carton, A. G. 2013. Hypoxia tolerance is conserved across genetically distinct sub-populations of an iconic, tropical Australian teleost (*Lates calcarifer*). *Conservation Physiology*, 1: doi:10.1093/conphys/cot029.
- Del Toro Silva, F. M., Miller, J. M., Taylor, J. C., and Ellis, T. A. 2008. Influence of oxygen and temperature on growth and metabolic performance of *Paralichthys lethostigma* (Pleuronectiformes: Paralichthyidae). *Journal of Experimental Marine Biology and Ecology*, 358: 113–123.
- Deutsch, C., Ferrel, A., Seibel, B., Portner, H. O., and Huey, R. B. 2015. Climate change tightens a metabolic constraint on marine habitats. *Science*, 348: 1132–1136.
- Ejbye-Ernst, R., Michaelsen, T. Y., Tirsgaard, B., Wilson, J. M., Jensen, L. F., Steffensen, J. F., Pertoldi, C., *et al.* 2016. Partitioning the metabolic scope: The importance of anaerobic metabolism and implications for the oxygen- and capacity-limited thermal tolerance (OCLTT) hypothesis. *Conservation Physiology*, 4: 1–13.
- Farrell, A. P., Hinch, S. G., Cooke, S. J., Patterson, D. A., Crossin, G. T., Lapointe, M., and Mathes, M. T. 2008. Pacific Salmon in Hot Water: Applying Aerobic Scope Models and Biotelemetry to Predict the Success of Spawning Migrations. *Physiological and Biochemical Zoology*, 81: 697–709.
- Farrell, A. P. 2016. Pragmatic perspective on aerobic scope: Peaking, plummeting, pejus and apportioning. *Journal of Fish Biology*, 88: 322–343.
- Friedland, K. D., and Hare, J. A. 2007. Long-term trends and regime shifts in sea surface temperature on the continental shelf of the northeast United States. *Continental Shelf*

- Research, 27: 2313–2328.
- Fry, F. E. J., and Hart, J. S. 1948. The relation of temperature to oxygen consumption in the goldfish. *The Biological Bulletin*, 94: 66–77.
- Glenn, S., Arnone, R., Bergmann, T., Bissett, W. P., Crowley, M., Cullen, J., Gryzmski, J., *et al.* 2004. Biogeochemical impact of summertime coastal upwelling on the New Jersey Shelf. *Journal of Geophysical Research C: Oceans*, 109: 1–15.
- Grans, A., Jutfelt, F., Sandblom, E., Jonsson, E., Wiklander, K., Seth, H., Olsson, C., *et al.* 2014. Aerobic scope fails to explain the detrimental effects on growth resulting from warming and elevated CO₂ in Atlantic halibut. *Journal of Experimental Biology*, 217: 711–717.
- Hare, J. A., Morrison, W. E., Nelson, M. W., Stachura, M. M., Teeters, E. J., Griffis, R. B., Alexander, M. A., *et al.* 2016. A vulnerability assessment of fish and invertebrates to climate change on the northeast u.s. continental shelf. *PLoS ONE*, 11: 1–30.
- Healy, T. M., and Schulte, P. M. 2012. Thermal acclimation is not necessary to maintain a wide thermal breadth of aerobic scope in the common killifish (*Fundulus heteroclitus*). *Physiological and Biochemical Zoology*, 85: 107–119.
- Holt, R. E., and Jørgensen, C. 2015. Climate change in fish : effects of respiratory constraints on optimal life history and behaviour. *Biology Letters*, 11: 20141032.
- Houghton, R. W., Schlitz, R., Beardsley, R. C., Butman, B., and Chamberlin, J. L. 1982. The Middle Atlantic Bight Cold Pool: Evolution of the Temperature Structure During Summer 1979. *Journal of Physical Oceanography*, 12: 1019-1029.
- Jutfelt, F., Norin, T., Ern, R., Overgaard, J., Wang, T., McKenzie, D. J., Lefevre, S., *et al.* 2018. Oxygen- and capacity-limited thermal tolerance: blurring ecology and physiology. *The Journal of Experimental Biology*, 221: jeb169615.
- Kavanaugh, M. T., Rheuban, J. E., Luis, K. M. A., and Doney, S. C. 2017. Thirty-Three Years of Ocean Benthic Warming Along the U.S. Northeast Continental Shelf and Slope: Patterns, Drivers, and Ecological Consequences. *Journal of Geophysical Research: Oceans*: 1–16.
- Killen, S. S., Norin, T., and Halsey, L. G. 2017. Do method and species lifestyle affect measures of maximum metabolic rate in fishes? *Journal of Fish Biology*, 90: 1037–1046.
- Kleisner, K. M., Fogarty, M. J., McGee, S., Barnett, A., Fratantoni, P., Greene, J., Hare, J. A., *et al.* 2016. The effects of sub-regional climate velocity on the distribution and spatial extent of marine species assemblages. *PLoS ONE*, 11: 1–21.
- Kleisner, K. M., Fogarty, M. J., McGee, S., Hare, J. A., Moret, S., Perretti, C. T., and Saba, V. S. 2017. Marine species distribution shifts on the U.S. Northeast Continental Shelf under continued ocean warming. *Progress in Oceanography*, 153: 24–36.
- Lapointe, D., Vogelbein, W. K., Fabrizio, M. C., Gauthier, D. T., and Brill, R. W. 2014. Temperature, hypoxia, and mycobacteriosis: Effects on adult striped bass *Morone saxatilis* metabolic performance. *Diseases of Aquatic Organisms*, 108: 113–127.
- Lefevre, S. 2016. Are global warming and ocean acidification conspiring against marine ectotherms? A meta-analysis of the respiratory effects of elevated temperature, high CO₂ and their interaction. *Conservation Physiology*, 4: 1–31.
- Lefevre, S., McKenzie, D. J., and Nilsson, G. E. 2017. Models projecting the fate of fish

- populations under climate change need to be based on valid physiological mechanisms. *Global Change Biology*, 23: 3449–3459.
- Libes, S.M. 1992. *An Introduction to Marine Biogeochemistry*. New York: John Wiley & Sons, Inc.
- Mallekh, R., and Lagardere, J. P. 2002. Effect of temperature and dissolved oxygen concentration on the metabolic rate of the turbot and the relationship between metabolic scope and feeding demand. *Journal of Fish Biology*, 60: 1105–1115.
- Manderson, J., Palamara, L., Kohut, J., and Oliver, M. J. 2011. Ocean observatory data is useful for regional habitat modeling of species with different vertical habitat preferences. *Marine Ecology Progress Series*, 438: 1–17.
- McDonnell, L. H., and Chapman, L. J. 2015. At the edge of the thermal window: Effects of elevated temperature on the resting metabolism, hypoxia tolerance and upper critical thermal limit of a widespread African cichlid. *Conservation Physiology*, 3: 1–13.
- Morley, J. W., Selden, R. L., Latour, R. J., Frölicher, T. L., Seagraves, R. J., and Pinsky, M. L. 2018. Projecting shifts in thermal habitat for 686 species on the North American continental shelf. *PLoS ONE*, 13: 1–28.
- Moser, J., and Shepherd, G. R. 2008. Seasonal distribution and movement of black sea bass (*Centropristis striata*) in the Northwest Atlantic as determined from a mark-recapture experiment. *Journal of Northwest Atlantic Fishery Science*, 40: 17–28.
- Musick, J. A., and Mercer, L. P. 1977. Seasonal distribution of Black Sea Bass, *Centropristis striata*, in the Mid-Atlantic Bight with comments on ecology and fisheries of the species. *Trans. Amer. Fish. Soc.*, 106: 12–25.
- NEFSC (Northeast Fisheries Science Center). 2017. The 62nd northeast regional stock assessment workshop (62nd SAW). Ref. Doc. 17-03, NEFSC, Woods Hole, MA.
- Nilsson, G. E., and Renshaw, G. M. C. 2004. Hypoxic survival strategies in two fishes: extreme anoxia tolerance in the North European crucian carp and natural hypoxic preconditioning in a coral-reef shark. *The Journal of Experimental Biology*, 207: 3131–3139.
- Norin, T., Malte, H., and Clark, T. D. 2014. Aerobic scope does not predict the performance of a tropical eurythermal fish at elevated temperatures. *The Journal of Experimental Biology*, 217: 244–251.
- Norin, T., and Clark, T. D. 2016. Measurement and relevance of maximum metabolic rate in fishes. *Journal of Fish Biology*, 88: 122–151.
- Nye, J. A., Link, J. S., Hare, J. A., and Overholtz, W. J. 2009. Changing spatial distribution of fish stocks in relation to climate and population size on the Northeast United States continental shelf. *Marine Ecology Progress Series*, 393: 111–129.
- Payne, N. L., Smith, J. A., van der Meulen, D. E., Taylor, M. D., Watanabe, Y. Y., Takahashi, A., Marzullo, T. A., *et al.* 2016. Temperature dependence of fish performance in the wild: links with species biogeography and physiological thermal tolerance. *Functional Ecology*, 30: 903–912.
- Pershing, A. J., Alexander, M. A., Hernandez, C. M., Kerr, L. A., Le Bris, A., Mills, K. E., Nye, J. A., *et al.* 2015. Slow adaptation in the face of rapid warming leads to collapse of the Gulf of Maine cod fishery. *Science*, 350: 809–812.
- Pinsky, M. L., Worm, B., Fogarty, M. J., Sarmiento, J. L., and Levin, S. A. 2013. Marine taxa track local climate velocities. *Science*, 341: 1239–1242.

- Pinsky, M. L., Reygondeau, G., Caddell, R., Palacios-Abrantes, J., Spijkers, J., and Cheung, W. W. L. 2018. Preparing ocean governance for species on the move. *Science*, 360: 1189–1192.
- Plambech, M., Van Deurs, M., Steffensen, J. F., Tirsgaard, B., and Behrens, J. W. 2013. Excess post-hypoxic oxygen consumption in Atlantic cod *Gadus morhua*. *Journal of Fish Biology*, 83: 396–403.
- Pörtner, H. O., and Knust, R. 2007. Climate change affects marine fishes through the oxygen limitation of thermal tolerance. *Science*, 315: 95–97.
- Pörtner, H. O., and Farrell, A. P. 2008. Physiology and Climate Change. *Science*, 322: 690–692.
- Pörtner, H. O. 2010. Oxygen- and capacity-limitation of thermal tolerance: a matrix for integrating climate-related stressor effects in marine ecosystems. *Journal of Experimental Biology*, 213: 881–893.
- Pörtner, H. O., and Peck, M. A. 2010. Climate change effects on fishes and fisheries: Towards a cause-and-effect understanding. *Journal of Fish Biology*, 77: 1745–1779.
- R Core Team. 2019. R: A language and environment for statistical computing. R Foundation for Statistical Computing, Vienna, Austria. URL <https://www.R-project.org/>.
- Raby, G. D., Casselman, M. T., Cooke, S. J., Hinch, S. G., Farrell, A. P., and Clark, T. D. 2016. Aerobic scope increases throughout an ecologically relevant temperature range in coho salmon. *The Journal of Experimental Biology*, 219: 1922–1931.
- Reidy, S. P., Nelson, J. A., Tang, Y., and Kerr, S. R. 1995. Post-exercise metabolic rate in Atlantic cod and its dependence upon the methods of exhaustion. *Journal of Fish Biology*, 47: 377–386.
- Roche, D. G., Binning, S. a, Bosiger, Y., Johansen, J. L., and Rummer, J. L. 2013. Finding the best estimates of metabolic rates in a coral reef fish. *The Journal of Experimental Biology*, 216: 2103–2110.
- Rogers, N. J., Urbina, M. A., Reardon, E. E., Mckenzie, D. J., and Wilson, R. W. 2016. A new analysis of hypoxia tolerance in fishes using a database of critical oxygen level (P_{crit}). *Conservation Physiology*, 4: 1–19.
- Roy, E. M., Quattro, J. M., and Greig, T. W. 2012. Genetic management of black sea bass: Influence of biogeographic barriers on population structure. *Marine and Coastal Fisheries*, 4: 391–402.
- Rummer, J. L., Binning, S. A., Roche, D. G., and Johansen, J. L. 2016. Methods matter: Considering locomotory mode and respirometry technique when estimating metabolic rates of fishes. *Conservation Physiology*, 4: cow008.
- Saba, V. S., Griffies, S. M., Anderson, W. G., Winton, M., Alexander, M. A., Delworth, T. L., Hare, J. A., *et al.* 2016. Enhanced warming of the Northwest Atlantic Ocean under climate change. *Journal of Geophysical Research: Oceans*, 120: 1–15.
- Sandblom, E., Gräns, A., Axelsson, M., and Seth, H. 2014. Temperature acclimation rate of aerobic scope and feeding metabolism in fishes: implications in a thermally extreme future. *Proceedings of Royal Society of Biology*, 281: 20141490.
- Schofield, O., Roarty, H., Saba, G. K., Xu, Y., Kohut, J., Glenn, S., Manderson, J., *et al.* 2012. Phytoplankton dynamics and bottom water oxygen during a large bloom in the summer of 2011. *Oceans, 2012, IEEE*: 1–6.
- Schulte, P. M. 2015. The effects of temperature on aerobic metabolism: Towards a

- mechanistic understanding of the responses of ectotherms to a changing environment. *The Journal of Experimental Biology*, 218: 1856–1866.
- Schurmann, H., and Steffensen, J. F. 1997. Effects of temperature, hypoxia and activity on the metabolism of juvenile Atlantic cod. *Journal of Fish Biology*, 50: 1166–1180.
- Seibel, B. A. 2011. Critical oxygen levels and metabolic suppression in oceanic oxygen minimum zones. *The Journal of Experimental Biology*, 214: 326–336.
- Steimle, F., Zetlin, C., Berrien, P., Johnson, D., and Chang, S. 1999. Essential Fish Habitat Source Document: Scup, *Stenotomus chrysops*, Life History and Habitat Characteristics. NOAA Technical Memorandum: NMFS-NE-149.
- Svendsen, J. C., Tudorache, C., Jordan, A. D., Steffensen, J. F., Aarestrup, K., and Domenici, P. 2010. Partition of aerobic and anaerobic swimming costs related to gait transitions in a labriform swimmer. *Journal of Experimental Biology*, 213: 2177–2183.
- Svendsen, M. B. S., Bushnell, P. G., and Steffensen, J. F. 2016a. Design and setup of intermittent-flow respirometry system for aquatic organisms. *Journal of Fish Biology*, 88: 26–50.
- Svendsen, M. B. S., Bushnell, P. G., Christensen, E. A. F., and Steffensen, J. F. 2016b. Sources of variation in oxygen consumption of aquatic animals demonstrated by simulated constant oxygen consumption and respirometers of different sizes. *Journal of Fish Biology*, 88: 51–64.
- Verberk, W. C. E. P., Bilton, D. T., Calosi, P., and Spicer, J. I. 2011. Oxygen supply in aquatic ectotherms: Partial pressure and solubility together explain biodiversity and size patterns. *Ecology*, 92: 1565–1572.
- Verberk, W. C. E. P., Bartolini, F., Marshall, D. J., Portner, H. O., Terblanche, J. S., White, C. R., and Giomi, F. 2016. Can respiratory physiology predict thermal niches? *Annals of the New York Academy of Sciences*, 1365: 73–88.
- Wikelski, M., and Cooke, S. J. 2006. Conservation physiology. *Trends in Ecology and Evolution*, 21: 38–46.
- Wilkin, J. L., and Hunter, E. J. 2013. An assessment of the skill of real-time models of Mid-Atlantic Bight continental shelf circulation. *Journal of Geophysical Research: Oceans*, 118: 2919–2933.
- Wishner, K. F., Seibel, B. A., Roman, C., Deutsch, C., Outram, D., Shaw, C. T., Birk, M. A., *et al.* 2018. Ocean deoxygenation and zooplankton: very small oxygen differences matter. *Science Advances*, 4: eaau5180.
- Yamanaka, H., Kohmatsu, Y., and Yuma, M. 2007. Difference in the hypoxia tolerance of the round crucian carp and largemouth bass: Implications for physiological refugia in the macrophyte zone. *Ichthyological Research*, 54: 308–312.
- Yeager, G. R., and Ultsch, D. P. 1989. Physiological regulation and conformation : A BASIC program for the determination of critical points. *Physiological Zoology*, 62: 888–907.

2.8 TABLES

Table 2.1 ANCOVA results for metabolic rates and aerobic scope.

AAS = absolute aerobic scope, MMR = maximum metabolic rate, SMR = standard metabolic rate. ^a*P*-values calculated from ANCOVA; bolded values are significant.

Variable	Effect	DF	<i>F</i> -value	<i>P</i> -value ^a
AAS (chase)	Temperature	6, 105	13.877	< 0.001
	Weight	1, 105	2.082	> 0.05
	Temperature*weight	6, 105	2.106	0.0586
AAS (flume)	Temperature	5, 48	6.185	< 0.001
	Weight	1, 48	6.599	< 0.05
	Temperature*weight	5, 48	4.033	< 0.01
MMR (chase)	Temperature	6, 105	50.327	< 0.001
	Weight	1, 105	9.267	< 0.01
	Temperature*weight	6, 105	2.281	< 0.05
MMR (flume)	Temperature	5, 48	16.244	< 0.001
	Weight	1, 48	8.927	< 0.01
	Temperature*weight	5, 48	3.147	< 0.05
SMR	Temperature	6, 105	136.613	< 0.001
	Weight	1, 105	12.282	< 0.001
	Temperature*weight	6, 105	2.489	< 0.05

Table 2.2 The MO_{2adj} mean \pm S.E. values for all metabolic rates, aerobic scope and hypoxia tolerance.

SMR = standard metabolic rate, MMR = maximum metabolic rate, AAS = absolute aerobic scope, S_{crit} = critical %O₂ air saturation. ^aAdjusted MO_2 values for MMR and AAS at 24°C are overestimated due to the average weight of fish in the 24°C group to be smaller than the average weight for all study fish combined.

Temperature (°C)	SMR	Chase MMR	Flume MMR	Chase AAS	Flume AAS	S_{crit}
12	46.44±1.94	169.12±11.78	286.57±24.02	117.67±7.55	242.67±24.24	19.65
17	65.27±3.27	215.05±14.15	369.27±24.47	143.63±11.07	303.55±24.70	21.33
22	95.69±4.51	266.03±13.32	462.30±22.01	167.18±12.13	363.73±22.21	21.80
24	106.61±11.03	342.06±29.20 ^a	NA	230.39±36.65 ^a	NA	NA
27	140.55±4.48	357.44±8.99	497.96±21.92	208.96±10.24	351.65±22.12	31.60
30	173.36±7.05	396.65±11.48	479.88±25.29	213.20±13.33	310.20±25.52	37.88
30 _{chronic}	163.14±9.28	306.62±16.06	356.82±53.05	136.03±11.90	198.33±53.54	38.63

Table 2.3 Q₁₀ values separated between each temperature increment.

AAS = absolute aerobic scope, MMR = maximum metabolic rate, SMR = standard metabolic rate. ^aSlightly overestimated adjusted MO₂ for the 24°C fish is reflected in calculated Q₁₀ values.

	12-17°C	17-22°C	22-24°C	22-27°C	24-27°C	27-30°C	27-30°C
AS _{chase}	1.49	1.35	4.97 ^a	1.56	0.72 ^a	1.07	0.24
AS _{flume}	1.56	1.44	NA	0.93	NA	0.66	0.15
MMR _{chase}	1.62	1.53	3.51 ^a	1.81	1.16 ^a	1.41	0.60
MMR _{flume}	1.66	1.58	NA	1.16	NA	0.88	0.33
SMR	1.96	2.15	1.72	2.16	2.51	2.01	1.64

2.9 FIGURES

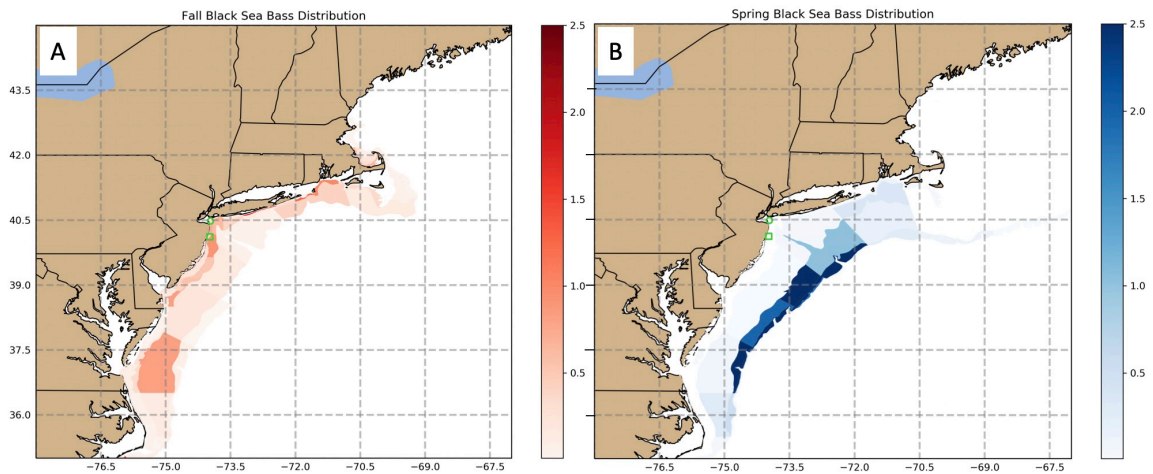


Figure 2.1 Seasonal black sea bass distribution throughout their range on the U.S. Northeast Shelf.

Black sea bass distribution is shown as mean strata CPUE (1980-2017) from the NOAA NMFS (National Marine Fisheries Service) bottom trawl survey (<https://www.nefsc.noaa.gov/femad/ecosurvey/mainpage/>). The color bars represent mean CPUE (kg tow⁻¹) where darker shades indicate a higher average CPUE. NMFS survey fall, typically September-November (A; red) and spring, typically February-April (B; blue), black sea bass distribution shows black sea bass inshore and offshore habitat, respectively. Green square = collection site in 2016; green circle = collection site in 2017.

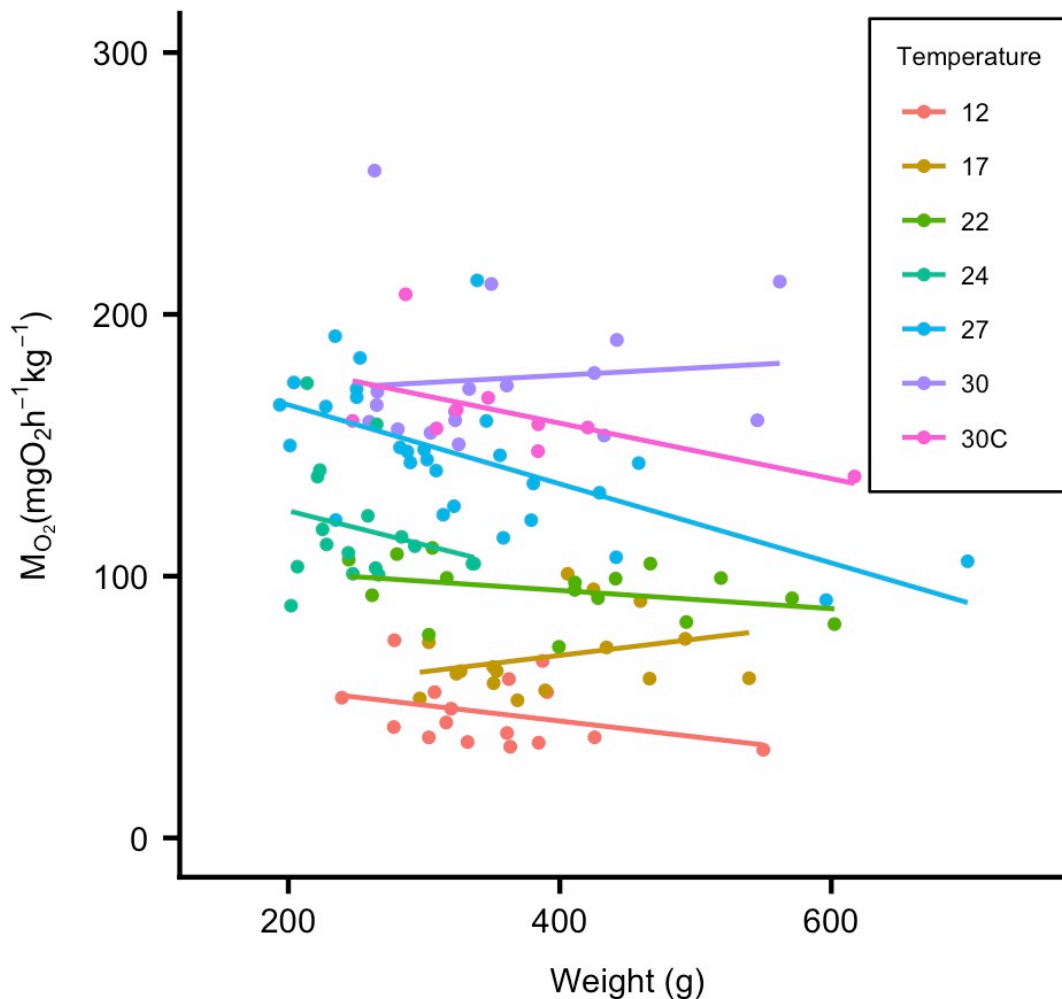


Figure 2.2 Temperature and body weight both affect standard metabolic rate in black sea bass.

SMR ($n=121$) for each temperature treatment is plotted against body weight (g). A fitted regression line demonstrates that in addition to the effect of temperature on SMR, body weight also has an effect ($P<0.05$). 30c = 30_{chronic} °C treatment.

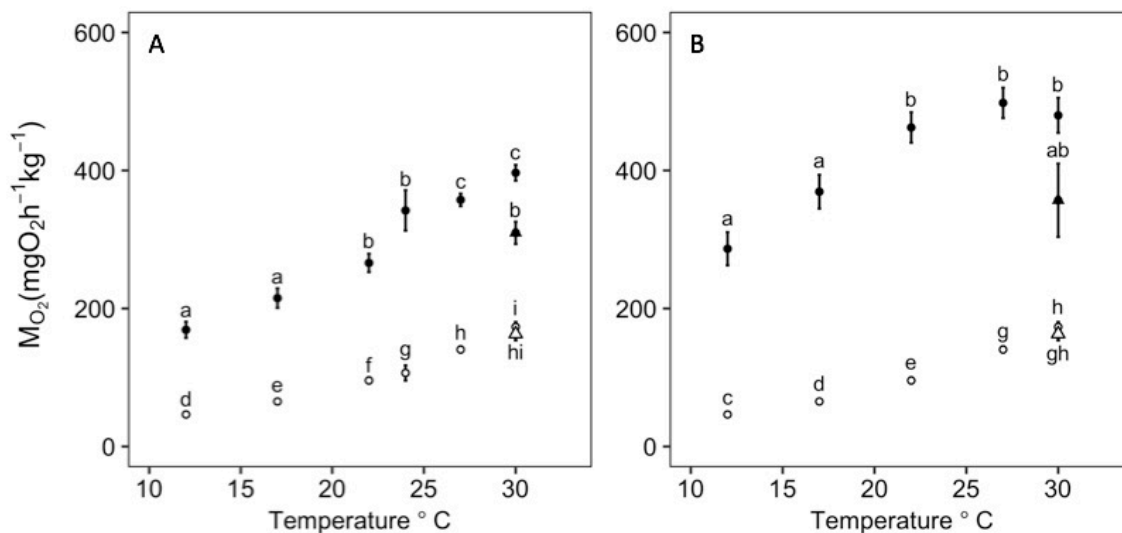


Figure 2.3A and 2.3B Effect of temperature on standard metabolic rate and maximum metabolic rate measured with a chase and a swim-flume method.

MMR (solid circles) and SMR (open circles) presented as mean \pm s.e. normalized to a mean weight of 346.9g for each temperature treatment for chase method MMR (A) and swim-flume method MMR (B). SMR is slightly different between (A) and (B) based on which fish were used for the respective MMR method. The 30_{chronic} °C group is denoted by triangles. Tukey *post hoc* significance between treatments is shown by letters where data points with different letters indicate a significant difference ($P < 0.05$).

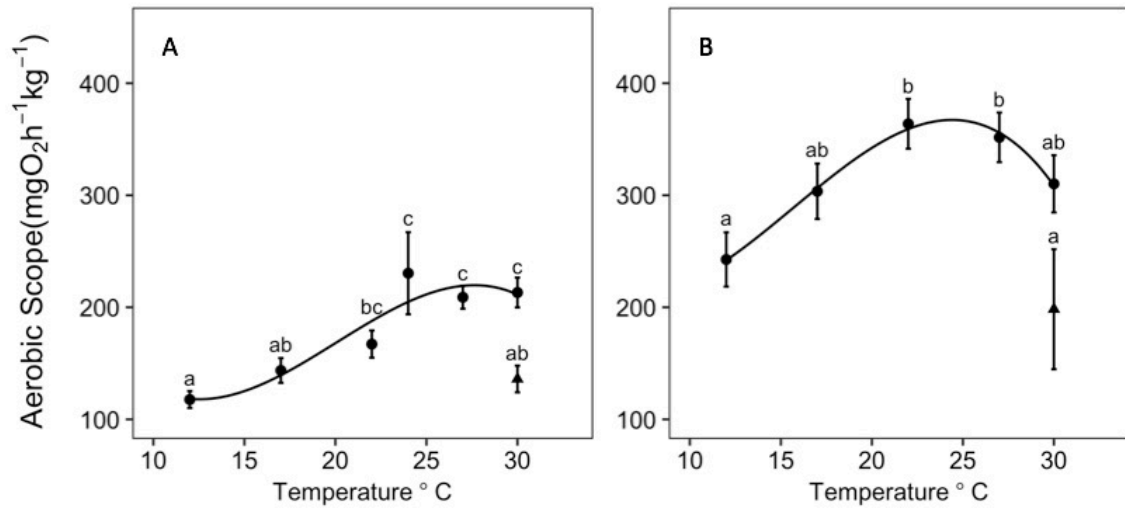


Figure 2.4A and 2.4B Effect of temperature on black sea bass aerobic scope.

Aerobic scope (mean \pm s.e.) of black sea bass normalized around a mean weight of 346.9g at each temperature treatment with the 30_{chronic}°C group denoted by the black triangle. Letters indicate Tukey *post hoc* significance between groups where data points sharing a letter are not significantly different ($P < 0.05$). Aerobic scope curves were generated from a) the chase MMR method ($y = 180.17 + 89.15x - 15.40x^2 - 21.55x^3$; $R^2 = 0.878$) and b) swim-flume MMR method ($y = 314.36 + 63.29x - 68.26x^2 - 19.65x^3$; $R^2 = 0.994$).

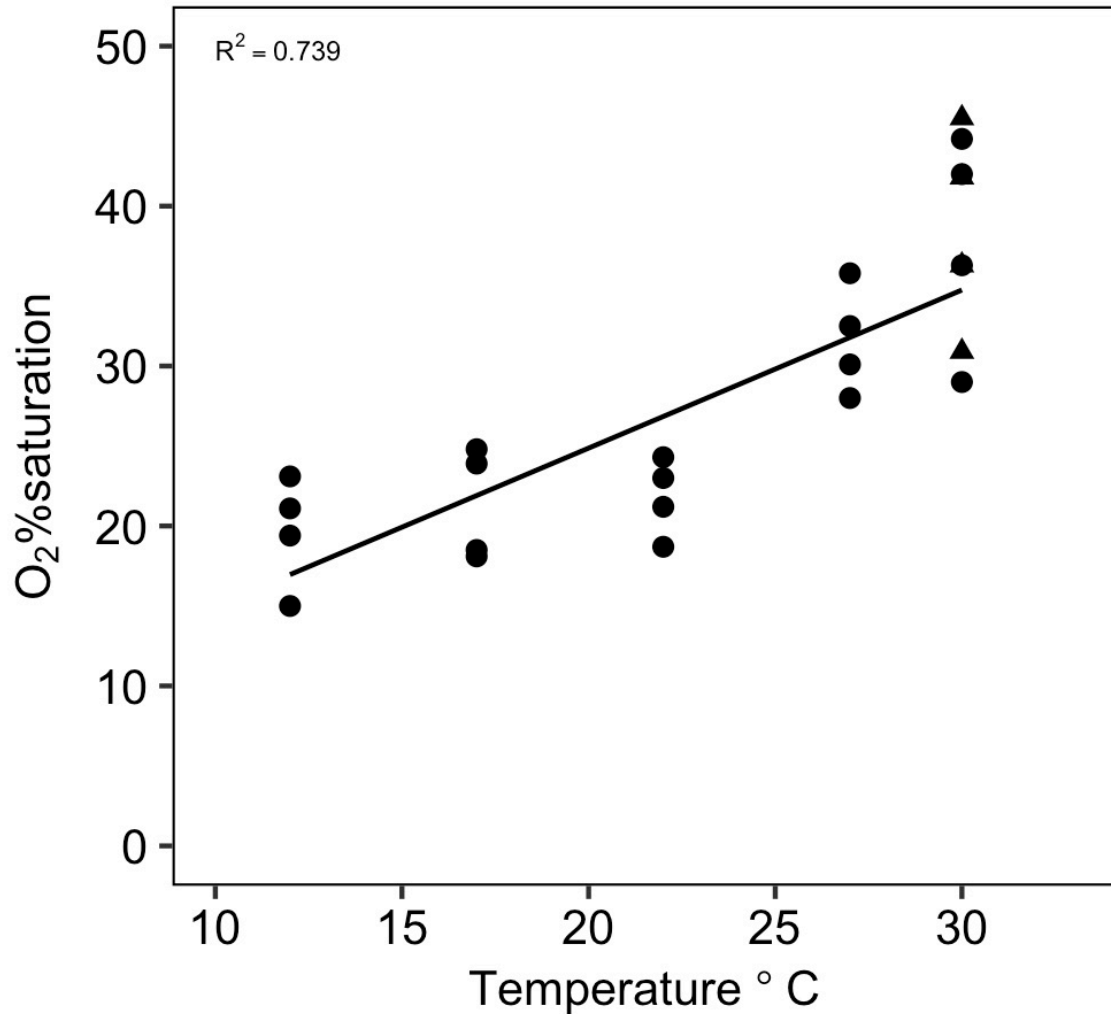


Figure 2.5 S_{crit} increases with increasing temperature.

S_{crit} presented as %O₂ for each temperature treatment. 30_{chronic}°C treatment is denoted by a triangle and there is no significant difference between the 30_{chronic}°C and short-term acclimated 30°C treatments. A linear-regression was fitted for these data points ($R^2 = 0.793$, $P < 0.001$) showing an increase in S_{crit} (e.g. a decrease in hypoxia tolerance) with increasing temperature.

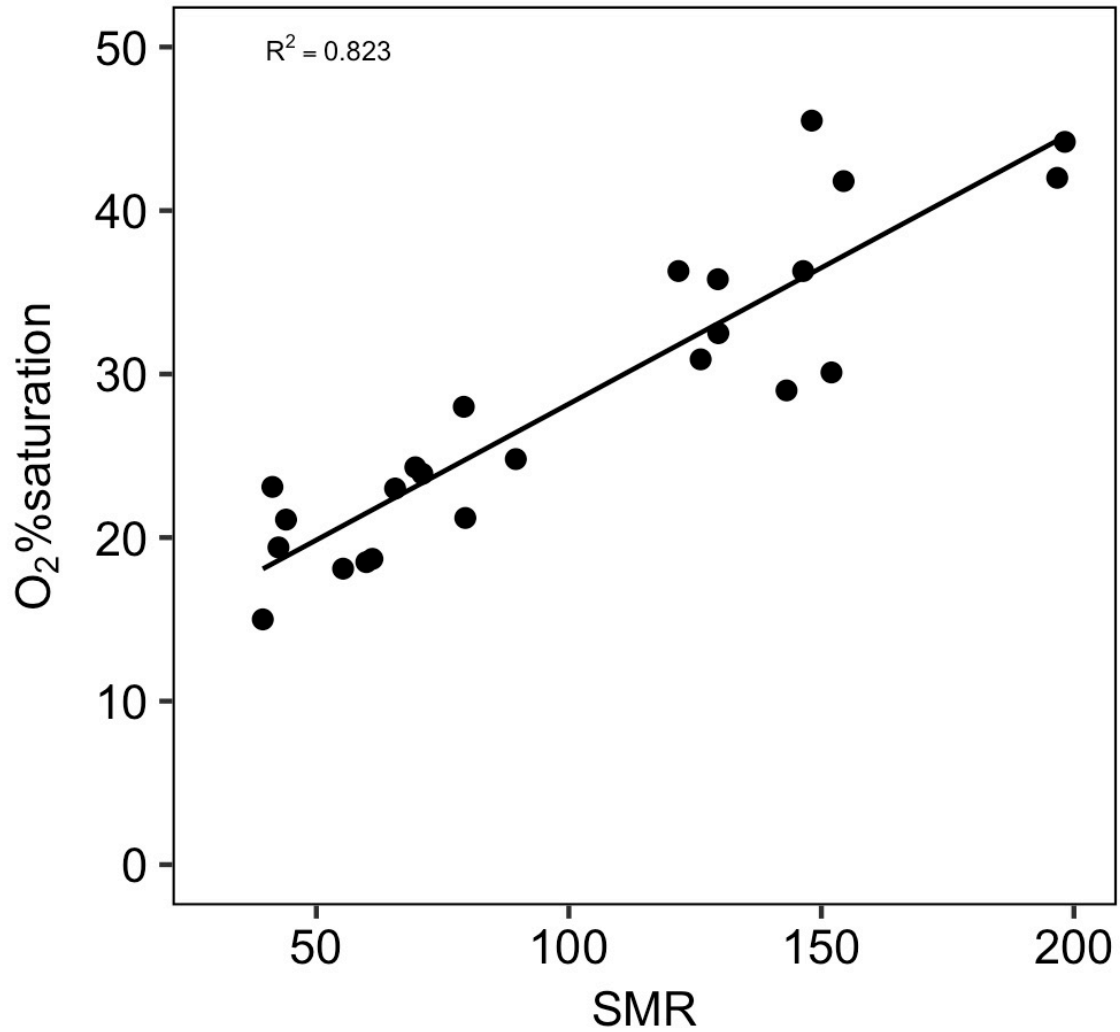


Figure 2.6 S_{crit} dependence on standard metabolic rate.

S_{crit} is plotted against standard metabolic rate measured during the hypoxia experiment. A linear-regression was fitted for these data points ($R_2 = 0.823$, $P < 0.001$) and shows an increase in S_{crit} as metabolic rates also rise.

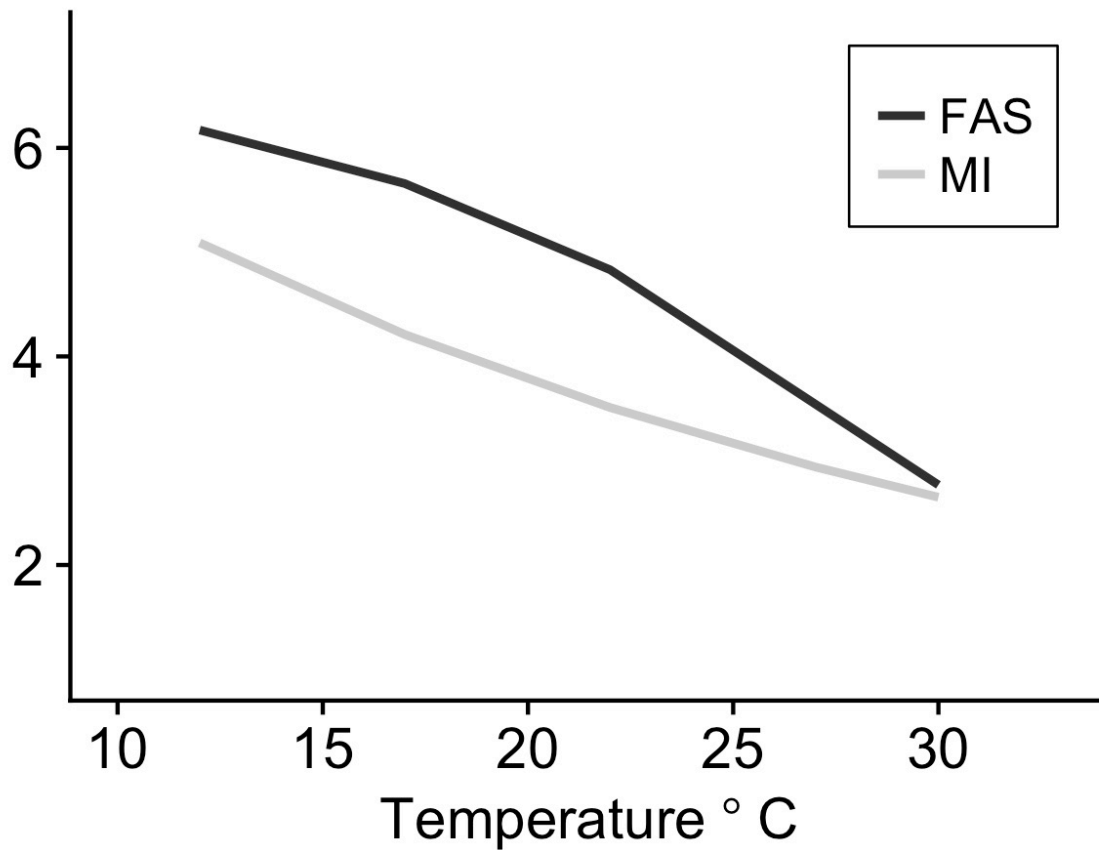


Figure 2.7 Factorial aerobic scope and metabolic index response to temperature.

Factorial aerobic scope (FAS) and metabolic index (MI) plotted against temperature.

Trends illustrate a decreasing trend in both measures as temperature increases. Both FAS and MI are unitless measures, but both measures scale similarly.

2.10 SUPPLEMENTAL MATERIAL

Table S2.1 Duration of All Intermittent Cycles at Each Temperature.

Each intermittent cycle comprises of a flush, wait and measure period (s). The amount of time set at each intermittent cycle component is listed for all temperature treatments.

Temperature (°C)	Flush (s)	Wait (s)	Measure (s)
12	360	45	600
17	270	45	480
22	360	45	360
24	600	45	360
27	360	45	360
30	360	45	300

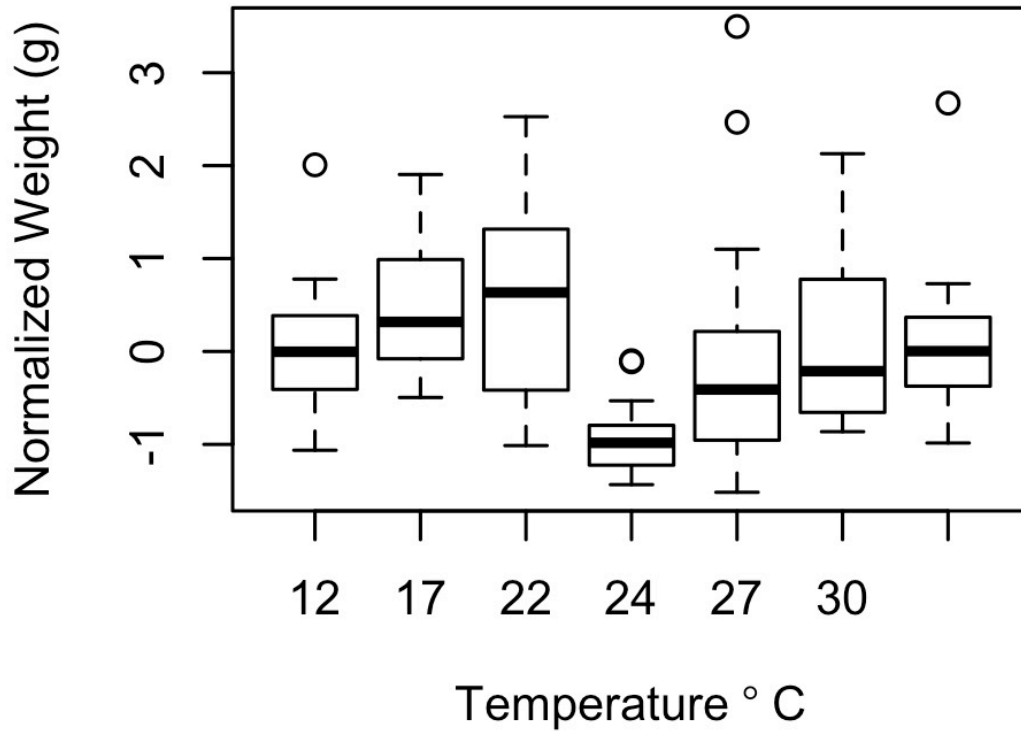


Figure S2. 1 Normalized Fish Weights at Each Temperature Treatment

Black sea bass weight (g) normalized to a mean of 0 and standard deviation of 1 for each temperature treatment. The 24°C temperature treatment group only consists of fish collected in 2016, and as seen by almost a difference of one standard deviation, were much smaller than the rest of the experimental fish.

CHAPTER 3: Spawning phenology of a rapidly shifting marine species throughout its range

This chapter is published as:

Slesinger, E., Jensen, O., and Saba, G. 2021. Spawning phenology of a rapidly shifting marine species throughout its range. *ICES Journal of Marine Science*, 78(3): 1010-1022.

3.1 ABSTRACT

Ocean warming is leading to poleward range shifts for many fish species, and while well described, potential life history phenology differences within fish populations along a gradient from their historic to current distributional range have not been studied. In a rapidly shifting fish population, the Northern stock of black sea bass (*Centropristis striata*), we investigated spawning phenology and output across the US Northeast Shelf to comprise locations in their historic and more recently occupied range near their northern range boundary. Spawning started later in the northern extreme of our study but also ended earlier, leading to decreased spawning duration from south to north. Spawning phenology was mostly driven by Julian day followed by temperature and latitude. Gonadosomatic index, a proxy for reproductive output, was lower in the northern region, indicating that black sea bass did not compensate for the shorter spawning season there. Hepatosomatic index was lower in the northern regions indicating lower pre-spawning liver energy reserves, potentially leading to lower re-productive output. These results suggest a potential for lower recruitment in the recently occupied range and should be further investigated to predict the impacts of ocean warming and for proactive fisheries management as black sea bass distributional range expands poleward.

3.2 INTRODUCTION

In temperate marine ecosystems, the rate and timing of seasonal warming and cooling sets the rhythm for biological activity, making these systems vulnerable to global climate change as it rapidly alters ocean thermal properties. Generally, the seasonality of mid- to high-latitude ocean temperatures is changing with spring warming advancing earlier and fall cooling occurring later. These phenological shifts are occurring more rapidly in the ocean than in terrestrial systems (Burrows *et al.*, 2011). Large-scale shifts in the timing of seasons in the physical ocean can affect the phenology, the timing of biological events, and distribution of marine organisms (Harley *et al.*, 2006; Richardson, 2008). For marine fish, responses to changing ocean *seasonality* can include earlier spawning migrations (e.g. Dufour *et al.*, 2010) and advanced spawning phenology (e.g. Rogers and Dougherty, 2019), whereas responses to ocean *warming* can include poleward range shifts (Kleisner *et al.*, 2016) and changes in population productivity (Free *et al.*, 2019).

Fish spawning phenology should theoretically be under strong selective pressure to promote successful reproduction and larval recruitment (De-Camino-Beck and Lewis, 2008). The timing of spawning balances reproducing in favorable conditions for adults and for larval hatching and growth. For adults, optimal breeding conditions can be influenced by temperature, habitat quality and local population density (Hendry *et al.*, 2001), and the presence or absence of such conditions can influence annual reproductive output for iteroparous adults (McBride *et al.*, 2015). For larvae, variation in survival is associated with the degree to which ontogenetic timing (e.g., hatching and first feeding) matches the timing of seasonal increases in their prey, a phenomenon demonstrated in

Atlantic cod (*Gadus morhua*; Kristiansen *et al.*, 2011) and haddock (*Melanogrammus aeglefinus*; Head *et al.*, 2005). When larval hatching does not overlap with high prey abundances, a mismatch can occur at a critical life stage and lead to low recruitment success for that year (Cushing, 1990).

Spawning phenology is also influenced by the degree of seasonality experienced from low to high latitudes. Shorter growing seasons at higher latitudes necessitate accurate timing of spawning to allow substantial larval growth before the onset of winter, increasing the probability of early life survival (Conover, 1992). Thus, temperature typically has an immediate physiological effect, and therefore is considered a proximal cue that sets the timing of reproductive development and spawning (Clark *et al.*, 2005). For fish that experience seasonality, daylength can also be a relevant cue (Bromage *et al.*, 2001), and can synergistically interact with temperature to set photothermal cue regimes for reproductive development (Pankhurst and Porter, 2003). Understanding the influences of seasonality on fish spawning is important because as fish distributions move to follow the direction and rate of local climate shifts (Pinsky *et al.*, 2013), they increasingly experience conditions where the relationships between temperature, daylength, and other seasonal cues differs from that in their historic range. Therefore, there is a need to investigate the interaction between shifting spawning phenology and distributional range shifts in marine species.

Marine fish with wide latitudinal spawning distributions will experience different environmental conditions depending on their spawning location, which can lead to intraspecific differences in spawning timing, duration, and reproductive output. In lower latitudes where growing seasons are longer, spawning duration is usually extended but

fecundity per spawning event can be lower (Vila-Gispert *et al.*, 2002). Conversely, in higher latitudes where growing seasons are shorter, spawning duration is truncated but fecundity per spawning event is higher and time between spawning events is shorter to garner total annual reproductive output comparable to the lower latitudes (Conover, 1992). For example, in a common reef fish (*Pomacentrus coelestis*), fish spawning at a higher latitude had both a shorter inter-spawning interval and higher clutch weight compared to their lower latitude counterparts (Kokita, 2004). Similarly, for largemouth bass (*Micropterus salmoides*), in a theoretical reciprocal transplant study, Garvey and Marschall (2003) found that the spawning strategies in the lower latitude fish were unsuccessful at higher latitudes, leading to significantly lower lifetime fitness. Thus, fish that are adapted to spawn across a wide latitudinal range will exhibit different spawning strategies to best optimize recruitment success throughout their entire range. However, for fish undergoing current poleward range shifts as a response to ocean warming (Fields *et al.*, 1993; Pinsky *et al.*, 2013), it is unknown if fish spawning at these new higher latitude regions will exhibit spawning strategies adapted for the shorter seasonal timeframe of acceptable spawning conditions at higher latitudes.

Lessons from ocean warming focused studies can help us understand how temperature differences across latitude may impact partitioning of energetic resources towards reproduction. This is particularly relevant because, although adult fish may have wide thermal windows making them resilient to climate change, actively spawning fish have a narrower thermal window and are significantly more sensitive to ocean warming (Dahlke *et al.*, 2020). As temperatures warm, fish energy demand increases to maintain higher metabolic rates (Pörtner and Farrell, 2008). Fish in warmer regions, if unable to

compensate through higher consumption, must compensate physiologically (Perry *et al.*, 2014) by allocating relatively more energy to metabolic maintenance than to reproduction and growth (Holt and Jørgensen, 2015). Energetic condition of a fish can be linked with reproductive output (Wuenschel *et al.*, 2013), and estimation of condition pre-, during and post-spawning can illuminate potential tradeoffs between metabolic demand and reproductive output.

The U.S. Northeast Shelf (US NES) is a broad continental shelf that extends from Cape Hatteras, NC to Georges Bank and provides habitat for a plethora of economically important fish species (Hare *et al.*, 2016). Climate change is affecting the shelf through rapid ocean warming (Chen *et al.*, 2020), including in the Gulf of Maine where temperatures have risen more rapidly than in 99% of the world's oceans (Pershing *et al.*, 2015), and shifting phenology to earlier spring warming and later fall cooling extending the duration of summer (Friedland and Hare, 2007; Henderson *et al.*, 2017). Ocean warming and shifting phenology of the US NES has already led to distributional range shifts for many important fish stocks (Bell *et al.*, 2015; Kleisner *et al.*, 2017). and higher fish abundance correlated to the lengthening of the summer season (Henderson *et al.*, 2017), respectively.

The U.S. Northern stock of black sea bass (*Centropristis striata*), a demersal reef fish, inhabits the US NES from Cape Hatteras, NC to the Gulf of Maine (Musick and Mercer, 1977; Roy *et al.*, 2012). Black sea bass are protogynous hermaphrodites and show female-biased sex ratios except at larger sizes and older ages (Mercer, 1978). Spawning occurs inshore throughout their entire distributional range during the late spring to early fall months (Moser and Shephard, 2008). Recently, there has been a

dramatic northward shift in the black sea bass population center of biomass (Bell *et al.*, 2015; Kleisner *et al.*, 2017) and successful spawning and recruitment in the Gulf of Maine, a region where they were once infrequent inhabitants (McBride *et al.*, 2018). These changes are attributed to recent ocean warming (Slesinger *et al.*, 2019). Together with a wide spawning distribution and range expansion, spawning conditions differ for black sea bass based upon latitude and temperature (Friedland and Hare, 2007; Richaud *et al.*, 2016). For example, during the beginning of the spawning season (~May), there can be a 6-10°C difference between bottom temperatures in the northern vs southern inshore spawning locations (Narváez *et al.*, 2015; Richaud *et al.*, 2016).

The recent black sea bass range expansion towards higher latitudes is important to study through the lens of phenology. Black sea bass, at multiple life stages, are voracious generalist feeders preying upon fish and epibenthic invertebrates (Drohan *et al.*, 2007); here, the timing of spawning and recruitment success in the newly expanded range could significantly alter existing ecosystems. For example, in the Gulf of Maine, juvenile lobsters are vulnerable to black sea bass predation, threatening the most valuable fishery in the U.S. (McMahan and Grabowski, 2019). Also, black sea bass are an important recreational and commercial fisheries species along the US NES (NEFSC, 2017), and proactive fisheries management could benefit from increased knowledge of black sea bass spawning timing and output as their biomass shifts northward. To assess the implications of range expansion and shifting phenology on spawning phenology and output, we collected black sea bass throughout their entire spawning season to encompass developing, spawning capable and post spawning fish as well as throughout their distributional range from locations spanning from Virginia to Massachusetts. Metrics

related to black sea bass spawning timing, reproductive output, and indirect energy indices were obtained for individual fish. We explored 1) the drivers of spawning season phenology and tested whether spawning season duration decreased with increasing latitude; 2) whether reproductive output was higher in the northern locations compared to the southern locations; and 3) differences in indirect energy indices throughout the spawning season and distributional range of black sea bass.

3.3 MATERIALS AND METHODS

3.3.1 Fish Collection

Fish collections targeted four inshore locations, representing almost the entire distributional range of the U.S. Northern stock of black sea bass, that included (from north to south) the U.S. states of Massachusetts (MA), New Jersey (NJ), Delaware (DE), and Virginia (VA). While the northern edge of the black sea bass range is now in the Gulf of Maine, collecting fish from this region was not attempted because of sampling challenges resulting from localized and patchy distributions (McMahan, 2017). In addition, fish collection occurred ~110km north of the southern edge of the U.S. Northern stock, Cape Hatteras, NC to eliminate the chance of unknowingly collecting fish from the U.S. Southern stock due to stock mixing in this region (Roy *et al.*, 2012). Time of collections specifically targeted black sea bass when they were first arriving inshore for spawning through the end of spawning when black sea bass are known to start offshore migrations for the winter. Collections in some regions were also constrained in time by the opening and closing of state mandated fishing seasons. Because the focus of this study was on spawning capable fish, only adults were kept and all fish <190mm TL were

returned to the water. In MA, fish were collected both from the Massachusetts Department of Marine Fisheries ventless trap survey and via hook-and-line sampling aboard a recreational charter boat. Sampling occurred in 2018 from the end of May to the end of August. In NJ, fish were collected both through a joint Rutgers University and New Jersey Department of Environmental Protection artificial reef trap survey and via hook-and-line sampling in conjunction with another ongoing black sea bass research project at Rutgers University at the time. Sampling occurred in 2018 from late April to the early November, but a gap in sampling during June occurred as an artifact of the sampling plan for the artificial reef trap survey. In DE, fish were collected through the Delaware Natural Resources and Environmental Control protected area trap survey in 2019 (end of May to the end of October). And in VA, fish were collected through hook-and-line sampling aboard a recreational charter boat in 2019 (end of May to mid-September). For all hook-and-line sampling, collections and euthanasia were performed by Slesinger and in accordance with Rutgers University IACUC Protocol (#PROTO201800054). Sampling duration, frequency, collection methods, and state or federal issued fishing permits are provided in Table S3.2.

Bottom temperature was measured during each sampling event. For collections using fish traps, each trap was fit with a bottom temperature logger (HOBO TidbiT v2 Water Temperature Data Logger, Onset Computer Corporation) to provide a single averaged temperature value for each sampling day. During hook-and-line sampling, a handheld profiling CTD device (SonTek CastAway-CTD, Xylem) was lowered to the bottom.

3.3.2 Fish Processing

Black sea bass were kept on ice and dissected in the laboratory no longer than 24 hours post capture. During dissections, length (mm TL) and weight (g) were measured, and the gonads and liver were removed and weighed to the nearest 0.01g. Black sea bass were sexed (male, female, transitional) and macroscopically assigned a maturity stage of either developing (DEV), spawning capable (SPC), or post-spawning (POST) following Brown-Peterson *et al.*, (2011). An ovarian mid-lobe cross-section was also removed, placed in a histology cassette, and fixed in 10% neutral-buffered formalin. After a minimum of one month in 10% neutral-buffered formalin, the histology cassettes were rinsed with deionized water and transferred to 70% ethanol for preservation. Ovarian cross-sections were processed for histology using a hematoxylin and eosin stain (Histology Consultants, Inc., Everson, WA). Histology was used to QA/QC the maturity stages assigned macroscopically to ensure proper classifications, especially during portions of the spawning season when black sea bass can transition from female to male and where macroscopic staging can become difficult due to the small size of the gonads (Klibansky and Scharf, 2015). Transitional status was assigned when male tissue was overgrowing the female tissue, there was significant atresia in residual oocytes, and male tissue comprised more than 5% of the gonadal cross-section (Klibansky and Scharf, 2015). Maturity stages were also used to estimate spawning season characteristics. For each region, a threshold of above 0.25 proportion SPC was set to estimate the active spawning season length, and a threshold of above 0.75 proportion SPC was used to estimate a range of peak spawning dates. Several other threshold values were tested, and threshold choice did not significantly alter the estimates of spawning season length (Fig

S3.4). Gonadosomatic index (GSI), calculated as $([\text{gonad weight}]/[\text{body weight}])*100$, can be used as a quick to measure proxy for reproductive output if maturity stages are known (Lowerre-Barbieri *et al.*, 2011) and was used in our study because estimating total annual or batch fecundities of black sea bass would have required more frequent sampling (Klibansky and Scharf, 2017). To eliminate biases related to oocyte size (Ganias *et al.*, 2014), only GSI measurements from SPC fish, where hydrated oocytes were present, were used.

Two indirect energy indices, relative condition factor (Kn) and hepatosomatic index (HSI) were calculated. These indices were chosen because Kn can fluctuate throughout the spawning season indicating energy usage for spawning or recovery in energy stores post-spawning (Slotte, 1999), and HSI can estimate liver energy reserves (Lambert and Dutil, 1997) used to determine pre-spawning energy as many fish recruit proteins and lipids from the liver for gonadal development (Brown and Murphy, 2004; Rosa *et al.*, 2020). Kn was calculated as the proportion of the measured fish weight to a predicted fish weight derived from a log-log length-weight relationship from all fish collected (Blackwell *et al.*, 2000). To remove the influence of reproduction on Kn, gonad weight was subtracted from both the final measured and predicted fish weights. HSI was calculated as $([\text{liver weight}]/[\text{body weight}])*100$.

3.3.3 Statistical Analyses

Generalized linear models (GLMs) were used to independently predict measures of spawning season phenology, reproductive output, and indirect energy indices. For each model, predictor variables were scaled to the mean of that predictor if they were included

in an interaction, and the variance inflation factor (VIF) was used to assess the impact of correlations among predictor variables where a VIF score >4 indicated collinearity between predictor variables (O'Brien 2007). For each model, the best fit models of spawning phenology, reproductive output, and indirect energy indices were determined using the second order Akaike's Information Criterion (AICc; Burnham and Anderson, 2002). For the reproductive output and spawning phenology models, collection method (trap vs. hook-and-line) was included as a factor to account for differing size and sex selectivity of the sampling methods (Provost 2013). If collection method was a significant predictor, results were scaled to a standardized collection method (hook-and-line). For predictor variables included in the best fit models, a dominance analysis, using the "dominanceanalysis" package in R (Navarrete, 2020), was used to compare the relative importance of each predictor in the model. The dominance analysis compares R^2 values (McFadden R^2 for GLMs) for each predictor across all subsets of the model to determine the relative contribution of one predictor over the other (Azen and Budescu, 2006). This analysis can be useful when all or most predictors are significant in the best fit model to further explore the ability of a predictor variable to explain the variance of the response variable. All analyses were performed using R (Version 4.0.1; R Core Team, 2019). GLMs were performed using the "glm" function, maps were made using the package "ggmap" (Kahle and Wickham, 2013) and GLM partial effects were visualized using the package "Jtools" (Long, 2020).

Spawning season phenology was investigated by fitting two separate candidate models with a binomial distribution that described the beginning and end of spawning separately. The beginning of spawning model included SPC and DEV fish, and the end of

spawning model included SPC and POST fish. To explore the effects of Julian day and daylength, two separate candidate models with either Julian day (Equation 1) or daylength (Equation 2) were fit to the beginning and the end of spawning models. Separate models were used due to collinearity between the two predictors, but both were assessed as they provided slightly different information. Julian day was constant across latitude and linearly increased throughout the spawning season, whereas daylength changed across latitude and responded non-linearly and non-monotonically with time as the spawning season overlapped with the summer solstice.

Equation 1

$$\begin{aligned} \log\left(\frac{\mu}{(1-\mu)}\right) = & \beta_0 + \beta_1 \text{Latitude} + \beta_2 \text{Temperature} + \beta_3 \text{Julian day} \\ & + \beta_4 \text{Collection method} + \beta_5 \text{Latitude} \times \text{Temperature} \\ & + \beta_6 \text{Latitude} \times \text{Julian day} + \varepsilon_i \end{aligned}$$

Equation 2

$$\begin{aligned} \log\left(\frac{\mu}{(1-\mu)}\right) = & \beta_0 + \beta_1 \text{Latitude} + \beta_2 \text{Temperature} + \beta_3 \text{Daylength} \\ & + \beta_4 \text{Collection method} + \beta_5 \text{Latitude} \times \text{Temperature} \\ & + \beta_6 \text{Latitude} \times \text{Daylength} + \varepsilon_i \end{aligned}$$

In both Equation 1 and Equation 2, μ = the probability of being SPC. Predictor variables were *latitude* (continuous), *temperature* (continuous), and *collection method* (categorical with two levels). The interaction term was *latitude x temperature*. In Equation 1, *Julian day* was included as a predictor variable and *Julian day x latitude* as an interaction term. In Equation 2, *daylength* was included as a predictor variable and *daylength x latitude* as an interaction term. The best fit models that included Julian day and daylength separately

were competed against each other using AICc to determine which metric, Julian day or daylength, best explained the variation in the data.

For reproductive output, a candidate model (Equation 3) was fit to GSI from SPC fish to allow analysis of reproductive output only during the time when fish were actively spawning.

Equation 3

$$\mu = \beta_0 + \beta_1 \text{Length} + \beta_2 \text{Sex} + \beta_3 \text{Location} + \beta_4 \text{Collection method} + \beta_5 \text{Length} \times \text{Sex} + \varepsilon_i$$

The response variable ($\mu = \text{GSI}$) was a non-negative ratio and modeled with a gamma distribution. Predictor variables were *length* (continuous), *sex* (categorical with two levels), *location* (categorical with four levels), and *collection method* (categorical with two levels). The interaction term was *sex x length* to account for sex-specific differences in size.

The change in indirect energy indices of black sea bass were investigated in reference to maturity stage (DEV, SPC, and POST) as well as collection location. Both HSI and Kn were modeled separately (Equation 4).

Equation 4

$$\mu = \beta_0 + \beta_1 \text{Length} + \beta_2 \text{Sex} + \beta_3 \text{Location} + \beta_4 \text{Maturity stage} + \beta_5 \text{Length} \times \text{Sex} + \varepsilon_i$$

Here, $\mu = \text{HSI}$ or Kn , to assess the indirect energy indices separately, but were both were non-negative ratios and modeled with a gamma distribution. For Equation 4, the predictor variables were *length* (continuous), *sex* (categorical with two levels), *location* (categorical with four levels), and *maturity stage* (categorical with three levels).

The interaction term was *sex x length* to include potential sex-specific differences between length and the indirect energy indices.

3.4 RESULTS

Throughout the spawning seasons of 2018 and 2019, a total of 898 black sea bass were collected in locations relevant to the current state of the black sea bass fishery and population, and spanning almost the entirety of the U.S. Northern stock distributional range (Fig 3.1). The total number of fish collected in each location can be found in SI Table 3.1. Because collections targeted black sea bass located inshore for spawning, most sampling occurred in relatively shallow inshore waters, except for in the southern locations (DE, VA). Both the DE state survey, which focused on protected reef areas, and the VA black sea bass fishery operates further offshore. Due to the apparent difficulty in obtaining adult black sea bass inshore, collections were not attempted inshore. These further offshore sampling sites led to deeper collections throughout the southern locations. Because of increasing depth at lower latitude collection sites, measured bottom temperature counterintuitively increased with higher latitudes. All locations experienced warming temperatures during late summer to early fall indicating the beginning of fall overturn as a result of increasing storm frequency (Rasmussen *et al.*, 2005; Fig 3S.5). We collected a broad range of sizes of adult black sea bass in each location (Table S3.3). On average, black sea bass in MA and VA were larger than in NJ and DE. While these size differences were likely attributed to the higher probability of collecting larger fish via hook-and-line sampling than in traps (Provost, 2013), they provide a representative size range of black sea bass throughout their entire range. Similarly, there were different

proportions of male-to-female fish in each location, which was likely an artifact of sampling and should not be taken as a population-wide sex proportion for black sea bass. Histology analysis agreed with the macroscopic evaluation of ovarian maturity stage in 97% of the samples and was able to determine misidentified fish that were either female fish early transitioning to male or female fish on the cusp of being spawning capable or spent. While we attempted to only collect sexually mature fish, there was one fish that was immature and was not used in analysis.

3.4.2 General Seasonal and Regional Patterns

Black sea bass spawning phenology differed both temporally and spatially (Fig 3.2). For each region, black sea bass reproduction followed representative patterns of asynchronous batch spawning fish whereby it was rare to collect 100% SPC fish on a single day during the active spawning season. Except for VA, the duration of sampling was sufficient to collect black sea bass pre- and post-spawning as seen by sampling days with 100% DEV or 100% POST fish, respectively (Fig 3.2). GSI closely followed female and male gonadal development with a peak when the proportion of SPC fish first reached a threshold of > 0.75 proportion SPC (Fig 3.2 & 3.3), and then decreased as fish began to enter post-spawning phases. This indicates higher reproductive output in the beginning of the spawning season, which is common for multiple batch spawners. The variation in GSI measurements from VA fish was likely attributed to the proportion SPC fluctuating throughout the spawning season (Fig 3.2). Altogether, this suggests that GSI was a good approximator of the spawning season and reproductive output proxy for black sea bass. By using the 0.25 proportion SPC threshold, the duration of the spawning season showed

an increasing trend with decreasing latitude (Fig 3.3). In addition, the regions where the spawning season was shorter, the duration of when black sea bass were >0.75 SPC was also shorter (Fig 3.3).

3.4.3 Spawning Phenology

Both the beginning and end of spawning phenology were analyzed separately and models using Julian day or daylength were competed against each other. For predicting both the beginning and end of spawning phenology best fit models, Julian day performed better when included in the model than when daylength was included (*beginning*: Julian day AICc = 492.94, daylength AICc = 669.53; *end*: Julian day AICc = 339.18, daylength AICc = 358.87). The model that explained the most variation in the probability SPC for the beginning of spawning included all main effects of latitude, Julian day, temperature, collection method, and a latitude by temperature and latitude by Julian day interaction. One other model had a Δ AICc < 6 (Richards, 2008; Table 3.1), however this model had a lower AICc weight and was not chosen (Burnham & Anderson, 2004). In the best fit model, all main effects and interactions were significant (p-value < 0.01 ; latitude|day p-value < 0.05) except for latitude (p-value > 0.05), which was still included because of the significant interaction between latitude and temperature and latitude and Julian day. Model residuals can be found in Fig S3.6. Overall, Julian day was the dominant predictor, followed by temperature, and a latitude by temperature interaction (Fig S3.7a). Specifically, the probability SPC during the beginning of spawning was higher in fish collected with hook-and-line than with traps (Fig 3.4a). The probability SPC increased with Julian day and was similar across all latitudes, with a slightly earlier start in the most

southern regions of the sampling locations (Fig 3.4b). The effect of temperature on probability SPC differed across latitude showing higher probability of SPC with lower temperatures in the southern latitudes and higher temperatures in the northern latitudes (Fig 3.4c). This is likely an effect of the sampling depths and associated temperatures within those regions.

The end of spawning probability SPC was best explained in a model with latitude, Julian day, temperature, collection method and a latitude by Julian day interaction. All main effects and interactions were significant (p -value < 0.01; temperature < 0.05). There were two other candidate models with a $\Delta\text{AICc} < 6$ (Richards, 2008), but the best fit model was chosen based on AICc weights (Burnham & Anderson, 2004). One model, which included all terms within the best fit model and a latitude by temperature interaction received only slightly less support ($\Delta\text{AICc} = 0.953$ and AIC weight of 0.331 vs 0.533 for the model without this interaction). All models with $\Delta\text{AICc} < 6$ are in Table 3.1 and model residuals can be found in Fig S3.8. The dominance analysis showed Julian day as the dominant predictor and followed by temperature (Fig S3.7b). For collection method, there was a higher probability of collecting SPC fish via traps than hook-and-line sampling (Fig 3.4d). The probability SPC decreased with increasing temperature (Fig 3.4e), indicating that the end of spawning was occurring when the fall temperatures were starting to increase associated with fall overturn in the region. The interaction between latitude and Julian day exhibited differing phenology across latitudes for the end of spawning with spawning ending on an earlier date in the northern regions and later in the southern regions (Fig 3.4f).

3.4.4 Reproductive Output

The reproductive output proxy, estimated from the GSI of SPC fish, showed regional and sex-specific differences (Table 3.2, Fig 3.5). The best fit model to explain variation in reproductive output included sex and location and both terms were significant (p -value < 0.01). Six alternative candidate models had a $\Delta AICc < 2$ that included additional terms and marginally improved the log likelihood. Therefore, the most parsimonious model was chosen (Arnold, 2010). All models with a $\Delta AICc < 6$ are reported in Table 3.2, and model residuals can be found in Fig 3S.9. The dominance analysis showed that location was the dominant predictor following the sex of the fish (Fig S3.10). From the best fit model, the sex of the fish had a negative coefficient value, indicating higher reproductive output in females than in males. For example, a male fish from DE was predicted to have an average GSI of 5.46 compared to a female fish from DE with a predicted average GSI of 6.71. Location for NJ, DE, and VA all had positive coefficient values with respect to MA indicating higher reproductive output when compared to MA (Fig 3.5). Here, a female fish from MA was predicted to have a GSI of 3.61 (compared to a female fish from DE with predicted average GSI of 6.71).

3.4.5 Indirect Energy Indices

The indirect energy index, HSI, varied throughout the spawning season and collection locations. The model that best explained variation in HSI included location, maturity stage, length, sex, and a length by sex interaction (Table 3.3), and all main effects and interactions were significant (p -value < 0.01), except for length, length|sex, and location between MA and NJ (p -value > 0.05). One other model, without the

interaction term, had a $\Delta AICc < 6$, but did not improve the log likelihood and had a lower AICc weight (Burnham & Anderson, 2004; Table 3.3). Model residuals can be found in Fig S3.11. The dominance analysis indicated that maturity stage was the dominant predictor (Fig S3.12). Specifically, for each region, as maturity stage advanced from DEV to SPC to POST, HSI decreased. HSI was higher in female than male fish and increased in southern locations (DE and VA; Fig 3.6). The length by sex interaction showed that HSI slightly increased with length for male fish but was relatively similar across sizes of females.

The relative condition factor (K_n) was largely uninformative for black sea bass and the values were relatively constant, remaining close to 1, throughout the spawning season and locations. As such, results for K_n can be found in the Supplementary Information (Table S3.1; Figs S3.1-3.3).

3.5 DISCUSSION

Our study demonstrates important intraspecific differences in spawning timing and output of the U.S. Northern stock of black sea bass, whereby spawning duration was shortest in the northern locations and longest in the southern locations. The beginning and end of spawning was mostly driven by Julian day and temperature. Reproductive output was lower in the northern locations and higher in the southern locations, which contrasts with previous studies that suggest reproductive output is highest in the higher latitudes to compensate for the shorter spawning duration. This result could be related to lower pre-spawning energy stores (e.g. HSI) in the northern fish when compared to the southern fish, potentially related to migration dynamics. These results suggest potential decreased

recruitment in the northern regions and further investigation is warranted as black sea bass continue to expand their range poleward.

3.5.2 Julian Day and Temperature Effects on Spawning Phenology

Black sea bass spawning duration decreased with increasing latitude, which corroborates well documented fish spawning patterns (Conover, 1992). The timing of the start and end of spawning was mostly driven by Julian day and temperature with interactive effects of latitude. In many fish spawning phenology studies, daylength and temperature are dominant drivers of the initiation and/or termination of spawning (e.g. Holt and Riley, 2001). However, in our models Julian day outperformed daylength, which is intriguing because daylength has been shown to affect the timing of reproduction in black sea bass (Howell *et al.*, 2003). This result could be an artifact of our statistical methodology and/or reproductive biology of black sea bass. The summer solstice (i.e., peak day length) occurred during a portion of the spawning season with high proportions of SPC fish, thus there was relatively little contrast in day length within our data. Along these lines, the daylength cue may have also been mediated through Julian day (with which it was highly correlated, $r^2 = 0.68$, $p\text{-value} < 0.001$) as some fish can use daylength as a cue to record time (Bromage *et al.*, 2001). Biologically, many studies that investigate effects of daylength on spawning phenology are focused on the timing of the initiation of vitellogenesis (e.g. Clark *et al.*, 2005). Our classification of the beginning of the active spawning season focused on when fish became SPC, or in other words, had initiated the oocyte hydration process which means these fish had already undergone vitellogenesis. For some fish, temperature can be used as a cue to synchronize

the final stages of maturation and initiate the transition into post-spawning phases (Van Der Kraak and Pankhurst, 1997), which is more aligned to the reproductive processes measured in our study. Moreover, daylength varied with latitude while Julian day was fixed across collection locations. The better performance of Julian day could indicate that population-wide timing of spawning may be more driven by internal biological clocks and/or proximal effects of temperature, a cue that did vary with latitude.

Temperature has also been shown to significantly influence spawning phenology for temperate fish species including mackerel (*Scomber scombrus*; Jansen and Gislason, 2011), walleye pollock (*Gadus chalcogrammus*; Rogers and Dougherty, 2019), and striped bass (*Morone saxatilis*; Clark *et al.*, 2005). While black sea bass spawning phenology was influenced by temperature, our results differed compared to these other species. It should be noted, however, that the VIF in the model predicting the start of spawning was moderately high (~ 4) – a reflection of the correlation ($r^2 = 0.51$) between latitude and temperature. The collinearity suggests that we cannot completely separate the effects of latitude and temperature on the start of spawning. Spawning began in cooler temperatures in the lower latitudes and warmer temperatures in the higher latitudes whereby the initiation of spawning at our northernmost site (MA) occurred at a bottom temperature of $\sim 15^\circ\text{C}$, while the equivalent temperature at our southernmost site (VA) was $\sim 10^\circ\text{C}$. This would indicate that across latitude the start of spawning was not as temperature sensitive. A lack of a strong relationship between temperature and spawning contrasts with other fish that will spawn earlier in warmer water (Lyons *et al.*, 2015). While apparent temperature insensitivity could make black sea bass resilient to climate change, it may disadvantage them if matching spawning to earlier warming would be

more adaptive. Spawning ended across each sampling location as fall bottom temperatures warmed such that across all sites there was an average warming of $7.25 \pm 4.19^\circ\text{C}$ from the beginning to end of the active spawning period. This fall warming is largely a destratification event-driven process and occurs as warm surface water mixes with the Cold Pool, a cold water mass below the mixed layer, due to the onset of fall storms (Rasmussen *et al.*, 2005). Fall mixing events have been shown to effect black sea bass behavior, whereby some fish began to migrate offshore (Secor *et al.*, 2019). Overall, the relationship between temperature and black sea bass spawning phenology is complex, and further research is needed to elucidate the different responses of the beginning and end of spawning to temperature.

3.5.3 Reproductive Output Across Spawning Locations

For black sea bass in this study, the reproductive output proxy, GSI, was consistently lower for male fish than for female fish (Fig 3.6). Sexual dimorphism in reproductive output have been found in other fishes (e.g. blackeye gobies (*Rhinogobiops nicholsii*); Yong & Grober, 2014) and showed higher female GSI than male GSI. Lower male reproductive output in this study is of interest for black sea bass because sperm limitation has been raised as a possible concern for hermaphroditic species that develop highly female skewed sex ratios (Provost & Jensen 2015). Across our sampling locations, there was lower GSI in the most northern location (MA; maximum GSI = 7.53) and higher GSI in the more southern collection locations (e.g. DE; maximum GSI = 14.53). GSI from black sea bass in the southern locations was also higher than in locations comprising their newly expanded range from Southern New England to Maine

(McMahan *et al.*, 2020). This contrasts with other studies which have found fish in the higher latitudes will compensate for a shorter spawning season through increases in higher reproductive output (Conover, 1992; Kokita, 2004). The lower reproductive output of individuals at the black sea bass northern range margin suggests that these fish may not be fully adapted to spawning at capacity at higher latitudes compared to individuals from their core historical range.

While no previous studies on black sea bass examined GSI across the entire distributional range of the Northern stock as we have done here, patterns within sub-regions or across studies generally contrast with our findings and suggest higher GSI in the more northern regions compared to the southern regions. For example, in Wuenschel *et al.*, (2011), black sea bass collected from Massachusetts and Rhode Island (i.e., the northern part of their range) from May to June had maximum GSI values ~10, while Wilk *et al.*, (1990) found black sea bass collected south of Rhode Island along the New York Bight (near the center of their range) to have maximum GSI values ~8 during July. In Rosa *et al.*, (2020), black sea bass from New Jersey in June had higher GSI than fish collected ~250km south off of the coast of Maryland during July and August. In all of these studies, the maximum GSI values from the different locations were measured during different months, thus confounding spatial comparisons of GSI. For example, comparing GSI from black sea bass caught in New Jersey in June to black sea bass caught in Maryland in August may lead to a comparison of GSI during peak spawning vs. towards the end of the active spawning season, respectively. Therefore, comparison across studies or at different time periods does not allow for a full assessment of regional differences in GSI. Our GSI comparisons were made across the entire duration of the

spawning season which allows for a more accurate comparison of estimated reproductive output amongst regions.

While the results for black sea bass indicate a reduction in reproductive output at higher latitudes, these results should also be considered alongside the use of GSI as a proxy for reproductive output. A female black sea bass with a higher GSI should have more oocytes (Mercer, 1978), but the oocyte stage can non-linearly affect the weight of the gonad (i.e. hydrated oocytes are disproportionately heavy; Ganas *et al.*, 2014). To account for this, we only analyzed GSI from a standardized maturity stage, where hydrated oocytes were present. There could be variation in the weight of the gonad if a female fish was in-between spawning batches and recently released hydrated eggs. However, because black sea bass are asynchronous spawners and should not all be within or between spawning batches at the same time, assessing the GSI from multiple fish caught on a single day should provide enough variation to use this proxy across collection dates.

3.5.4 Energy Allocation Throughout Spawning

Lower reproductive output at the northern regions of our sampling locations was unexpected but may be explained through the differences in energetic condition of black sea bass throughout spawning. HSI was lower in the northern region (MA) in developing fish when compared to the other sampling locations. However, post-spawning fish in MA had higher HSI than in the more southern regions, indicating a recovery in liver energy stores in this northern region. Fluctuations in HSI can be linked to reproductive output because the liver is a main energy storage depot (Brown and Murphy, 2004) and provides

hepatic vitellogenin to be used in developing oocytes at the beginning of ovarian development (Hiramatsu *et al.*, 2002). Thus, lower HSI in developing fish could lead to lower reproductive output. Although MA was our northernmost site, due to regional oceanographic patterns, this region warmed earlier and was the warmest during spawning compared to the other regions (Fig S3.5), potentially decreasing energy stores due to higher energy demand. Additionally, the patterns in HSI of MA black sea bass could be a product of migration distances. Black sea bass overwinter near the continental shelf edge off the coasts of Virginia to Maryland and migrate inshore for the summer to spawn leading to longer migration distances for the higher latitude fish (~100-200km for southern fish vs ~400-500km for northern fish; Moser and Shepherd, 2008). For MA fish, lower HSI before spawning could be related to lower energy reserves following migration, and relatively higher HSI in post-spawning fish (compared to other collection locations) could indicate increased feeding to prepare for a long migration to return to overwintering sites. While out of the scope of this study, future research is needed to focus on energy and lipid partitioning pre-, during, and post-spawning in black sea bass throughout their distributional range to disentangle the effects of migration and local oceanography on energetics and subsequent impacts on reproductive output.

3.5.5 Trailing Edge of U.S. Northern Black Sea Bass Range Expansion

Understanding the potential changes at the trailing edge of the U.S. Northern stock of black sea bass distributional range is important as this region is subject to ecosystem restructuring and thermal habitat loss (Kleisner *et al.*, 2017). While the spawning season in VA started earlier in the year and had the second longest spawning

duration after DE (Fig 3.3), GSI was high but variable due to fluctuations in the proportion of SPC fish towards the end of the spawning season (Fig 3.2d). Collecting adult black sea bass inshore was not attempted due to the fishery operating further offshore, which lead to the nearest inshore sampling site to be 35km from the coast. Black sea bass off of VA have historically been collected during the spawning season farther offshore (~35-50km; Mercer, 1978; Moser & Shephard, 2008), but in recent years, spawning black sea bass abundance has been low from inshore to mid-shelf (NorthEast Area Monitoring and Assessment Program survey data (<http://fluke.vims.edu/fishgis/faovims/index.htm>]; J. Gartland, pers. comm). In our study, black sea bass collections during the middle of the spawning season were made where there was a higher probability of catching fish, which led to sampling sites close to the shelf break (~100-140km from the coast). Altogether, the U.S. Northern stock of black sea bass distribution in the southern portion of their range has existed further offshore in the past, but increasing difficulty in obtaining black sea bass inshore may suggest a range contraction. This could be a result of ocean warming, where this region has experienced significant warming from 1977-2016 (Wallace *et al.*, 2018), but further research is required to understand the effects of warming at the trailing edge of U.S. Northern stock of black sea bass population.

It should be noted that our conclusions are not extended to the entire population of black sea bass. The U.S. Southern stock of black sea bass, which inhabits waters south of Cape Hatteras, NC to southern Florida, are considered genetically distinct and mostly reproductively isolated from each other (Drohan *et al.*, 2007; Roy *et al.*, 2012), and may have higher thermal tolerances (Atwood *et al.*, 2001). Spawning phenology and ocean

warming effects on the Southern stock of these fish and throughout their range are out of the scope of this study but would be valuable for further interpretation of the results for the U.S. Northern stock of black sea bass.

3.5.6 Study Limitations

Due to logistical constraints, black sea bass were collected across two separate years (2018 and 2019). While the dominant predictor of both the start and end of spawning was Julian day, suggesting these results are comparable across the two years, temperature did have a significant, yet more minor, effect on the timing of reproduction. Interannual temperature variability occurs across the US NES and has been shown to potentially impact interannual recruitment success of black sea bass (Miller *et al.*, 2016). Therefore, further investigation of spawning duration and reproductive output results across all regions was conducted. We assessed the difference in average monthly bottom temperatures for each spawning location between 2018 and 2019 using modeled bottom temperature from the Doppio Regional Ocean Model System model (Wilkin *et al.*, 2018) and found similar ($\sim\Delta 2-4^{\circ}\text{C}$) bottom temperatures between 2018 and 2019 in each collection location (Fig S3.13). Also, there was agreement on the timing of peak spawning between our study and previous studies. For example, Wilk *et al.*, (1990) found highest GSI during July of black sea bass collected from the New York Bight, which was similar timing for black sea bass in this study caught in a similar location (NJ). GSI data from fish collected off of the NJ coast from 2011 to 2013 also suggest peak spawning times around July (Fig S3.14; Provost *et al.*, 2017). While agreement in estimated peak spawning times for black sea bass is likely, reproductive output may differ interannually.

For the US Southern stock of black sea bass, significant interannual differences in proportions of spawning capable females and annual fecundity have been found (Klibansky and Scharf, 2017). While annual fecundity and GSI are linked, our GSI measurements likely provide a more conservative estimate of reproductive output and it is unknown the degree to which interannual variability in fecundity also leads to variability in GSI.

3.5.7 Conclusions

With ongoing climate change in the US NES region, both ocean warming and shifting phenology have been and will continue to affect many economically and ecologically important fish species. Our results showed that black sea bass do exhibit different spawning phenology across their latitudinal spawning gradient, yet their reproductive output did not compensate for a shorter spawning season in the northern regions. Black sea bass in state waters are managed with state-specific quotas that are based on regional biomass. As abundance increases in the north and reevaluations of state fishing quotas are suggested, there should be caution towards setting annual total allowable catch limits due to the potential variability in recruitment in these new regions and future impacts from ocean warming. This caution is also extended to the trailing edge of the U.S. Northern black sea bass distributional range where more data is required to investigate the potential impacts of ocean warming on adult energetics and productivity. The outcomes of this study, and potential impacts on recruitment and fishing quotas, are applicable globally to other range shifting species. Many mid- to high-latitude fish species are currently undergoing range shifts as a response to ocean warming and have

migratory behaviors related to spawning. As we found, even if a fish may be able to follow cues to shift the timing and duration of spawning, this does not ensure reproductive output will increase to compensate for new spawning phenology, leading to potentially lower recruitment in newly expanded ranges. While range shifts may be seen as adaptive for fish negatively impacted by ocean warming, these benefits may not be fully realized if there is reduced spawning output in these new regions.

3.6 ACKNOWLEDGEMENTS

We would like to thank Mark Wuenschel for guidance on this project and expert in histology; Douglas Zemeckis for providing initial insight into fish sampling designs; Laura Nazzaro for assisting with modeled bottom temperature; Ashley Trudeau and Zoe Kitchell for providing helpful discussion and insight on statistical methodology; the captains of the recreational fishing vessels including Eric Morrow, Skip Feller, and Mark Sterling; Steve Wilcox and Mike Trainor at the Massachusetts Department of Marine Fisheries, Peter Clarke at the New Jersey Department of Environmental Protection, and Scott Newlin at the Delaware Natural Resources and Environmental Control with Wes Townsend (commercial fisherman) for providing fish from trap surveys; and William Forrest Kennedy at the University of Massachusetts Dartmouth and Jim Gartland at the Virginia Institute of Marine Science for providing lab space and hospitality. Finally, we would like to acknowledge the undergraduates who assisted on dissections, including Kasey Walsh, Kiernan Bates, Karolina Zbaski, Timothy Stolarz, Maura Doscher, Juan Osario, Mamadou Nbaye, Shiyue Zhao, and Kimberly Aldana at Rutgers University, and Gil Osofsky at the Virginia Institute of Marine Science.

3.7 REFERENCES

- Arnold, T. W. 2010. Uninformative Parameters and Model Selection Using Akaike's Information Criterion. *Journal of Wildlife Management*, 74: 1175–1178.
- Atwood, H. L., Young, S. P., Tomasso, J. R., and Smith, T. I. J. 2001. Salinity and Temperature Tolerances of Black Sea Bass Juveniles. *North American Journal of Aquaculture*, 63: 285–288.
- Azen, R., and Budescu, D. V. 2006. Comparing Predictors in Multivariate Regression Models : An Extension of Dominance Analysis. *Journal of Educational Research Association and American Statistical Association*, 31: 157–180.
- Bell, R. J., Richardson, D. E., Hare, J. A., Lynch, P. D., and Fratantoni, P. S. 2015. Disentangling the effects of climate, abundance, and size on the distribution of marine fish: an example based on four stocks from the Northeast US shelf. *ICES Journal of Marine Science*, 72: 1311–1322.
- Blackwell, B. G., Brown, M. L., and Willis, D. W. 2000. Relative Weight (Wr) Status and Current Use in Fisheries Assessment and Management. *Reviews in Fisheries Science*, 8: 1–44.
- Bromage, N., Porter, M., and Randall, C. 2001. The environmental regulation of maturation in farmed finfish with special reference to the role of photoperiod and melatonin. *Aquaculture*, 197: 63–98.
- Brown-Peterson, N. J., Wyanski, D. M., Saborido-Rey, F., Macewicz, B. J., and Lowerre-Barbieri, S. K. 2011. A standardized terminology for describing reproductive development in fishes. *Marine and Coastal Fisheries*, 3: 52–70.
- Brown, M., and Murphy, B. R. 2004. Seasonal dynamics of direct and indirect condition indices in relation to energy allocation in largemouth bass *Micropterus salmoides* (Lacepede). *Ecology of Freshwater Fish*, 13: 23–36.
- Burnham, K. and Anderson, D. 2002. A practical information-theoretic approach. *In* Model selection and multimodal inference, pp. 2nd ed. Springer, New York.
- Burnham, K. and Anderson, D. 2004. Multimodel inference: Understanding AIC and BIC in model selection. *Sociological Methods and Research*, 33: 261-304.
- Burrows, M. T., Schoeman, D. S., Buckley, L. B., Moore, P., Poloczanska, E. S., Brander, K. M., Brown, C., *et al.* 2011. The pace of shifting climate in marine and terrestrial ecosystems. *Science*, 334: 652–655.
- Chellappa, S., Huntingford, F. A., Strang, R. H. C., and Thomson, R. Y. 1995. Condition factor and hepatic index as estimates of energy status in male three-spined stickleback. *Journal of Fish Biology*, 47: 775–787.
- Chen, Z., Kwon, Y. O., Chen, K., Fratantoni, P., Gawarkiewicz, G., and Joyce, T. M. 2020. Long-Term SST Variability on the Northwest Atlantic Continental Shelf and Slope. *Geophysical Research Letters*, 47: 1–11.
- Clark, R. W., Henderson-Arzapalo, A., and Sullivan, C. V. 2005. Disparate effects of constant and annually-cycling daylength and water temperature on reproductive maturation of striped bass (*Morone saxatilis*). *Aquaculture*, 249: 497–513.
- Conover, D. O. 1992. Seasonality and the scheduling of life history at different latitudes. *Journal of Fish Biology*, 41: 161–178.

- Cushing, D. H. 1990. Phytoplankton production and year-class strength in fish populations: an update of the match/mismatch hypothesis. *Advances in Marine Biology*, 26: 249–293.
- Dahlke, F., Wohlrab, S., Butzin, M., and Pörtner, H. 2020. Thermal bottlenecks in the lifecycle define climate vulnerability of fish. *Science*, In press: 65–70.
- De-Camino-Beck, T., and Lewis, M. A. 2008. On net reproductive rate and the timing of reproductive output. *American Naturalist*, 172: 128–139.
- Drohan, A. F., Manderson, J. P., and Packer, D. B. 2007. Essential Fish Habitat Source Document: Black Sea Bass, *Centropristis striata*, life history and habitat characteristics, 2nd edition. NOAA Tech Memo NMFS NE 200: 68 p.
- Dufour, F., Arrizabalaga, H., Irigoien, X., and Santiago, J. 2010. Climate impacts on albacore and bluefin tunas migrations phenology and spatial distribution. *Progress in Oceanography*, 86: 283–290.
- Fields, P. A., Graham, J., Rosenblatt, R., and Somero, G. N. 1993. Effects of expected climate change on marine faunas. *Trends in Ecology and Evolution*, 8: 361–367.
- Free, C.M., Thorson, J.T., Pinsky, M.L., Oken, K.L., Wiedenmann, J., and Jensen, O.P. 2019. Impacts of historical warming on marine fisheries production. *Science*, 363: 979-983.
- Friedland, K. D., and Hare, J. A. 2007. Long-term trends and regime shifts in sea surface temperature on the continental shelf of the northeast United States. *Continental Shelf Research*, 27: 2313–2328.
- Ganias, K., Murua, H., Glaramunt, G., Dominguez-Petit, R., Gonçalves, P., Juanes, F., Keneddy, J., *et al.* 2014. Chapter 4: Egg Production. *In Handbook of Applied Fisheries Reproductive Biology for Stock Assessment and Management*. Ed. by R. Domínguez-Petit, H. Murua, F. Saborido-Rey, and E. Trippel. Vigo, Spain. 109 pp.
- Garvey, J. E., and Marschall, E. A. 2003. Understanding latitudinal trends in fish body size through models of optimal seasonal energy allocation. *Canadian Journal of Fisheries and Aquatic Sciences*, 60: 938–948.
- Hare, J. A., Morrison, W. E., Nelson, M. W., Stachura, M. M., Teeters, E. J., Griffis, R. B., Alexander, M. A., *et al.* 2016. A vulnerability assessment of fish and invertebrates to climate change on the northeast u.s. continental shelf. *PLoS ONE*, 11: 1–30.
- Harley, C. D. G., Randall Hughes, A., Hultgren, K. M., Miner, B. G., Sorte, C. J. B., Thornber, C. S., Rodriguez, L. F., *et al.* 2006. The impacts of climate change in coastal marine systems. *Ecology Letters*, 9: 228–241.
- Head, E. J. H., Brickman, D., and Harris, L. R. 2005. An exceptional haddock year class and unusual environmental conditions on the Scotian Shelf in 1999. *Journal of Plankton Research*, 27: 597–602.
- Henderson, M. E., Mills, K. E., Thomas, A. C., Pershing, A. J., and Nye, J. A. 2017. Effects of spring onset and summer duration on fish species distribution and biomass along the Northeast United States continental shelf. *Reviews in Fish Biology and Fisheries*, 27: 411–424. Springer International Publishing.
- Hendry, A. P., Berg, O. K., and Quinn, T. P. 2001. Breeding location choice in salmon: Causes (habitat, competition, body size, energy stores) and consequences (life span, energy stores). *Oikos*, 93: 407–418.
- Hiramatsu, N., Matsubara, T., Weber, G. M., Sullivan, C. V., and Hara, A. 2002.

- Vitellogenesis in aquatic animals. *Fisheries*, 68: 694–699.
- Holt, G. J., and Riley, C. M. 2001. Laboratory spawning of coral reef fishes: effects of temperature and photoperiod. UJNR Technical Report No. 28: 33–38.
- Holt, R. E., and Jørgensen, C. 2015. Climate change in fish : effects of respiratory constraints on optimal life history and behaviour. *Biology Letters*, 11: 20141032.
- Howell, R. A., Berlinsky, D. L., and Bradley, T. M. 2003. The effects of photoperiod manipulation on the reproduction of black sea bass, *Centropristis striata*. *Aquaculture*, 218: 651–669.
- Jansen, T., and Gislason, H. 2011. Temperature affects the timing of spawning and migration of North Sea mackerel. *Continental Shelf Research*, 31: 64–72.
- Kahle, D., and Wickham, H. 2013. ggmap: Spatial Visualization with ggplot2. *The R Journal*, 5: 144–161.
- Kleisner, K. M., Fogarty, M. J., McGee, S., Barnett, A., Fratantoni, P., Greene, J., Hare, J. A., *et al.* 2016. The effects of sub-regional climate velocity on the distribution and spatial extent of marine species assemblages. *PLoS ONE*, 11: 1–21.
- Kleisner, K. M., Fogarty, M. J., McGee, S., Hare, J. A., Moret, S., Perretti, C. T., and Saba, V. S. 2017. Marine species distribution shifts on the U.S. Northeast Continental Shelf under continued ocean warming. *Progress in Oceanography*, 153: 24–36.
- Klibansky, N., and Scharf, F. S. 2015. Success and failure assessing gonad maturity in sequentially hermaphroditic fishes: Comparisons between macroscopic and microscopic methods. *Journal of Fish Biology*, 87: 930–957.
- Klibansky, N., and Scharf, F. S. 2017. Fecundity peaks prior to sex transition in a protogynous marine batch spawning fish, black sea bass (*Centropristis striata*). *ICES Journal of Marine Science*: doi:10.1093/icesjms/fsx219.
- Kokita, T. 2004. Latitudinal compensation in female reproductive rate of a geographically widespread reef fish. *Environmental Biology of Fishes*, 71: 213–224.
- Kristiansen, T., Drinkwater, K. F., Lough, R. G., and Sundby, S. 2011. Recruitment variability in North Atlantic cod and match-mismatch dynamics. *PLoS ONE*, 6: e17456.
- Lambert, Y., and Dutil, J. D. 1997. Can simple condition indices be used to monitor and quantify seasonal changes in the energy reserves of atlantic cod (*Gadus morhua*)? *Canadian Journal of Fisheries and Aquatic Sciences*, 54: 104–112.
- Long, J. A. 2020. jtools: Analysis and Presentation of Social Scientific Data. R package version 2.1.0.
- Lowerre-Barbieri, S.K., Ganas, K., Saborido-Rey, F., Murua, H., and Hunter, J.R. 2011. Reproductive timing in marine fishes: variability, temporal scales, and methods. *Marine and Coastal Fisheries*, 3: 71-91.
- Lyons, J., Rypel, A. L., Rasmussen, P. W., Burzynski, T. E., Eggold, B. T., Myers, J. T., Paoli, T. J., *et al.* 2015. Trends in the reproductive phenology of two great lakes fishes. *Transactions of the American Fisheries Society*, 144: 1263–1274.
- McBride, R. S., Somarakis, S., Fitzhugh, G. R., Albert, A., Yaragina, N. A., Wuenschel, M. J., Alonso-Fernández, A., *et al.* 2015. Energy acquisition and allocation to egg production in relation to fish reproductive strategies. *Fish and Fisheries*, 16: 23–57.
- McBride, R. S., Tweedie, M. K., and Oliveira, K. 2018. Reproduction, first-year growth, and expansion of spawning and nursery grounds of black sea bass (*Centropristis*

- striata*) into a warming Gulf of Maine. Fishery Bulletin, 116: 323–336.
- McMahan, M. D. 2017. Ecological and socioeconomic implications of a northern range expansion of black sea bass, *Centropristis striata*. Dissertation. Northeastern University, Boston, MA.
- McMahan, M. D., and Grabowski, J. H. 2019. Nonconsumptive effects of a range-expanding predator on juvenile lobster (*Homarus americanus*) population dynamics. Ecosphere, 10: e02867.
- McMahan, M.D., Sherwood, G.D., and Grabowski, J.H. 2020. Geographic variation in life-history traits of black sea bass (*Centropristis striata*) during a rapid range expansion. Frontiers in Marine Science, 7:567758.
- Mercer, L.P. 1978. The reproductive biology and population dynamics of black sea bass, *Centropristis striata*. Dissertation. College of William and Mary – Virginia Institute of Marine Science, Gloucester Point, VA.
- Miller, A. S., Shepherd, G. R., and Fratantoni, P. S. 2016. Offshore habitat preference of overwintering juvenile and adult black sea bass, *Centropristis striata*, and the relationship to year-class success. PLoS ONE, 11(1): e0147627
- Moser, J., and Shepherd, G. R. 2008. Seasonal distribution and movement of black sea bass (*Centropristis striata*) in the Northwest Atlantic as determined from a mark-recapture experiment. Journal of Northwest Atlantic Fishery Science, 40: 17–28.
- Musick, J. A., and Mercer, L. P. 1977. Seasonal distribution of Black Sea Bass, *Centropristis striata*, in the Mid-Atlantic Bight with comments on ecology and fisheries of the species. Trans. Amer. Fish. Soc., 106: 12–25.
- Narváez, D. A., Munroe, D. M., Hofmann, E. E., Klinck, J. M., Powell, E. N., Mann, R., and Curchitser, E. 2015. Long-term dynamics in Atlantic surfclam (*Spisula solidissima*) populations: The role of bottom water temperature. Journal of Marine Systems, 141: 136–148.
- Navarrete, C. B. 2020. dominanceanalysis: Dominance Analysis. R package version 1.3.0.
- NEFSC (Northeast Fisheries Science Center). 2017. The 62nd northeast regional stock assessment workshop (62nd SAW). Ref. Doc. 17-03, NEFSC, Woods Hole, MA.
- O'Brien, R.M. 2007. A caution regarding rules of thumb for variance inflation factors. Quality and Quantity, 41: 673-690.
- Ohshimo, S., Sato, T., Okochi, Y., Ishihara, Y., Tawa, A., Kawazu, M., Hiraoka, Y., *et al.* 2018. Long-term change in reproductive condition and evaluation of maternal effects in Pacific bluefin tuna, *Thunnus orientalis*, in the Sea of Japan. Fisheries Research, 204: 390-401.
- Pankhurst, N. W., and Porter, M. J. R. 2003. Cold and dark or warm and light: Variations on the theme of environmental control of reproduction. Fish Physiology and Biochemistry, 28: 385–389.
- Perry, A. L., Low, P. J. P. J., Ellis, J. R., and Reynolds, J. D. 2014. Climate Change and Distribution Shifts in Marine Fishes. Science, 308: 1912–1915.
- Pershing, A. J., Alexander, M. A., Hernandez, C. M., Kerr, L. A., Le Bris, A., Mills, K. E., Nye, J. A., *et al.* 2015. Slow adaptation in the face of rapid warming leads to collapse of the Gulf of Maine cod fishery. Science, 350: 809–812.
- Pinsky, M. L., Worm, B., Fogarty, M. J., Sarmiento, J. L., and Levin, S. A. 2013. Marine taxa track local climate velocities. Science, 341: 1239–1242.

- Pörtner, H. O., and Farrell, A. P. 2008. Physiology and Climate Change. *Science*, 322: 690–692.
- Provost, M. M. 2013. Understanding sex change in exploited fish populations: a review of east coast fish stocks and assessment of selectivity and sex change in black sea bass (*Centropristis striata*). Thesis. Rutgers University, New Brunswick, NJ.
- Provost, M.M. and Jensen, O.P. 2015. The impacts of fishing on hermaphroditic species and treatment of sex change in stock assessments. *Fisheries*, 40: 536-545.
- Provost, M. M., Jensen, O. P., and Berlinsky, D. L. 2017. Influence of size, age, and spawning season on sex change in black sea bass. *Marine and Coastal Fisheries*, 9: 126–138. Taylor & Francis.
- R Core Team. 2019. R: A language and environment for statistical computing. R Foundation for Statistical Computing, Vienna, Austria. URL <https://www.R-project.org/>.
- Rasmussen, L. L., Gawarkiewicz, G., Owens, W. B., and Lozier, M. S. 2005. Slope water, gulf stream, and seasonal influences on southern Mid-Atlantic Bight circulation during the fall-winter transition. *Journal of Geophysical Research C: Oceans*, 110: 1–16.
- Richards, S.A. 2008. Dealing with over dispersed count data in applied ecology. *Journal of Applied Ecology*, 45: 218-227.
- Richardson, A. J. 2008. In hot water: Zooplankton and climate change. *ICES Journal of Marine Science*, 65: 279–295.
- Richaud, B., Kwon, Y. O., Joyce, T. M., Fratantoni, P. S., and Lentz, S. J. 2016. Surface and bottom temperature and salinity climatology along the continental shelf off the Canadian and U.S. East Coasts. *Continental Shelf Research*, 124: 165–181.
- Rogers, L. A., and Dougherty, A. B. 2019. Effects of climate and demography on reproductive phenology of a harvested marine fish population. *Global Change Biology*, 25: 708–720.
- Rosa, G. A., Woodland, R. J., and Rowe, C. L. 2020. Carbon:nitrogen ratio as a proxy for tissue nonpolar lipid content and condition in black sea bass *Centropristis striata* along the Middle Atlantic Bight. *Marine Biology*, 167: 1–13.
- Roy, E. M., Quattro, J. M., and Greig, T. W. 2012. Genetic management of black sea bass: Influence of biogeographic barriers on population structure. *Marine and Coastal Fisheries*, 4: 391–402.
- Secor, D. H., Zhang, F., O'Brien, M. H. P., and Li, M. 2019. Ocean destratification and fish evacuation caused by a Mid-Atlantic tropical storm. *ICES Journal of Marine Science*, 76: 573–584.
- Slesinger, E., Andres, A., Young, R., Seibel, B., Saba, V., Phelan, B., Rosendale, J., *et al.* 2019. The effect of ocean warming on black sea bass (*Centropristis striata*) aerobic scope and hypoxia tolerance. *PLoS ONE*, 14(6): e0218390.
- Slotte, A. 1999. Effects of fish length and condition on spawning migration in Norwegian spring spawning herring (*Clupea harengus* L). *Sarsia*, 84: 111–127.
- Van Der Kraak, G. J., and Pankhurst, N. W. 1997. Temperature effects on the reproductive performance of fish. Cambridge University Press, Cambridge. 159–176 pp.
- Vila-Gispert, A., Moreno-Amich, R., and García-Berthou, E. 2002. Gradients of life-history variation: An intercontinental comparison of fishes. *Reviews in Fish Biology*

- and Fisheries, 12: 417–427.
- Wallace, E. J., Looney, L. B., and Gong, D. 2018. Multi-decadal trends and variability in temperature and salinity in the Mid-Atlantic Bight, Georges Bank, and Gulf of Maine. *Journal of Marine Research*, 76: 163–215.
- Wilk, S. J., Morse, W. W., and Stehlik, L. L. 1990. Annual cycles of gonad-somatic indices as indicators of spawning activity for selected species of finfish collected from the New York Bight. *Fishery Bulletin*, 88: 775–786.
- Wilkin, J., Levin, J., Lopez, A., Zavala-Garay, J., and Arango, H. 2018. A Coastal Ocean Forecast System for the U.S. Mid-Atlantic Bight and Gulf of Maine. *New Frontiers in Operational Oceanography*, 10.17125/g.
- Wuenschel, M. J., Shepherd, G. R., McBride, R. S., Jorgensen, R., Oliveira, K., Robillard, E., and Dayton, J. 2011. Sex and maturity of black sea bass collected in Massachusetts and Rhode Island waters; preliminary results based on macroscopic staging of gonads with comparison to survey data. Ref. Doc. 12, NEFSC, Woods Hole, MA.
- Wuenschel, M. J., McBride, R. S., and Fitzhugh, G. R. 2013. Relations between total gonad energy and physiological measures of condition in the period leading up to spawning: Results of a laboratory experiment on black sea bass (*Centropristis striata*). *Fisheries Research*, 138: 110–119.
- Yong, L. and Grober, M.S. 2014. Sex differences in the energetic content of reproductive tissues in the Blackeye Goby, *Rhinogobiops nicholsii*. *Environmental Biology of Fishes*, 97: 321–328.

3.8 TABLES

Table 3.1 GLMs evaluated to explain probability of spawning capable fish

Candidate models evaluated for their ability to explain the probability of spawning capable fish for the beginning and the end of spawning. Models were fit with a binomial distribution and a log-link function. Only candidate models with $\Delta\text{AICc} < 6$ are shown for both the beginning and end of spawning models. The relative likelihood of a model is represented by the AICc where an AICc = 1 represents the most likely. SPC = spawning capable, DEV = developing, and POST = post-spawning.

Response variable	Model	Df	LogLik	AICc	ΔAICc	AICc weight
Beginning of spawning SPC = 1; DEV = 0	Latitude + Julian Day + Temperature + Collection Method + Latitude Julian Day + Latitude Temperature	7	-239.375	492.935	0	0.747
	Latitude + Julian Day + Temperature + Collection Method + Latitude Temperature	6	-241.489	495.117	2.181	0.251
End of spawning SPC = 1; POST = 0	Latitude + Julian Day + Temperature + Collection Method + Latitude Julian Day	6	-163.522	339.175	0	0.533
	Latitude + Julian day + Temperature + Collection Method + Latitude Julian Day + Latitude Temperature	7	-162.977	340.128	0.953	0.331
	Latitude + Julian Day + Collection Method + Latitude Julian Day	5	-165.925	341.943	2.768	0.134

Table 3.2 Candidate GLMs evaluated to explain variation in gonadosomatic index

Candidate models evaluated for their ability to explain the variation in GSI from SPC fish. All models are fit with a gamma distribution and an identity link function. From all candidate models, only those with $\Delta\text{AICc} < 6$ are shown. The relative likelihood of a model is represented by the AICc where an AICc = 1 represents the most likely.

Model	Df	LogLik	AICc	ΔAICc	AICc weight
Sex + Location	6	-739.565	1491.364	0	0.273
Sex + Location + Length	7	-738.901	1492.114	0.750	0.187
Sex + Location + Collection Method	7	-739.091	1492.492	1.129	0.155
Sex + Location + Length + Collection Method	8	-738.081	1492.562	1.199	0.150
Sex + Location + Length + Length Sex	8	-738.180	1492.762	1.398	0.136
Sex + Location + Length + Collection Method + Length Sex	9	-737.438	1493.379	2.015	0.100

Table 3.3 Candidate GLMs evaluating the variation in Hepatosomatic Index

Candidate models evaluating the variation in the indirect energy index, HSI. Models were fit with a gamma distribution and an identity link function. Only models with $\Delta\text{AICc} < 6$. The relative likelihood of a model is represented by the AICc where an AICc = 1 represents the most likely. Stage = maturity stage.

Model	Df	LogLik	AICc	ΔAIC	AIC weight
Sex + Stage + Location + Length + Length Sex	10	-402.979	826.209	0	0.713
Sex + Stage + Location + Length	9	-405.004	828.214	2.005	0.262

3.9 FIGURES

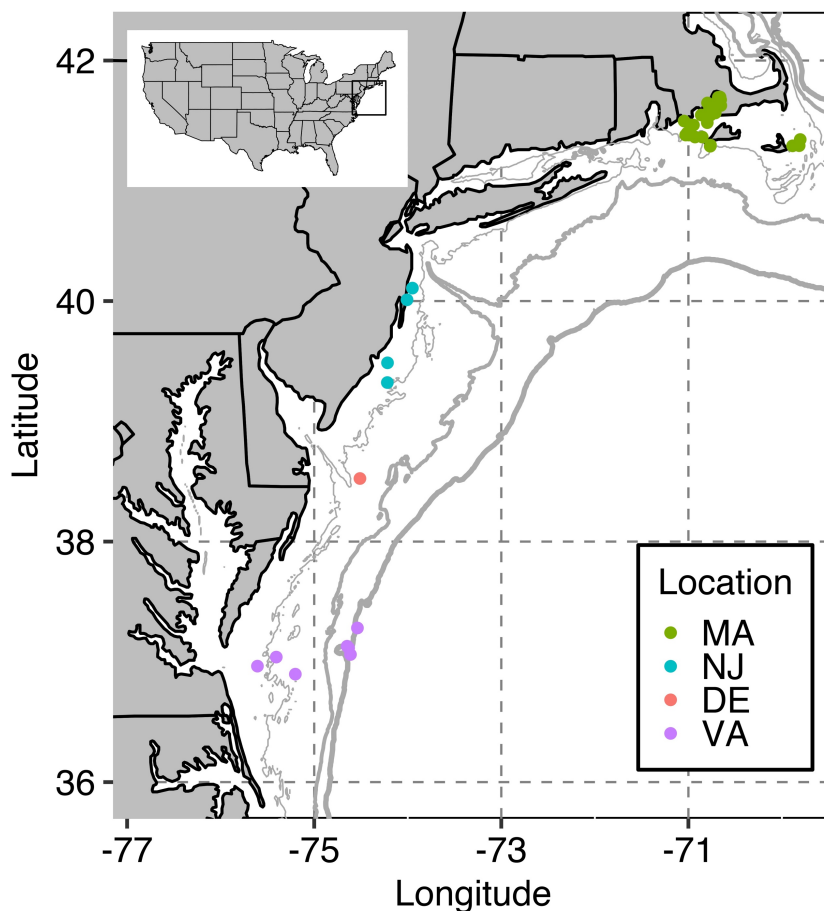


Figure 3.1 Collection locations for black sea bass throughout the entire sampling period.

Regional locations are designated as Virginia (purple), Delaware (red), New Jersey (blue), and Massachusetts (green). The grey lines from thinnest to thickest widths indicate the 25m, 50m, and 100m isobaths, respectively. The box within the inset map of the United States denotes the full study region. Note: where the 100m isobath occurs also approximates the shelf edge for the US NES.

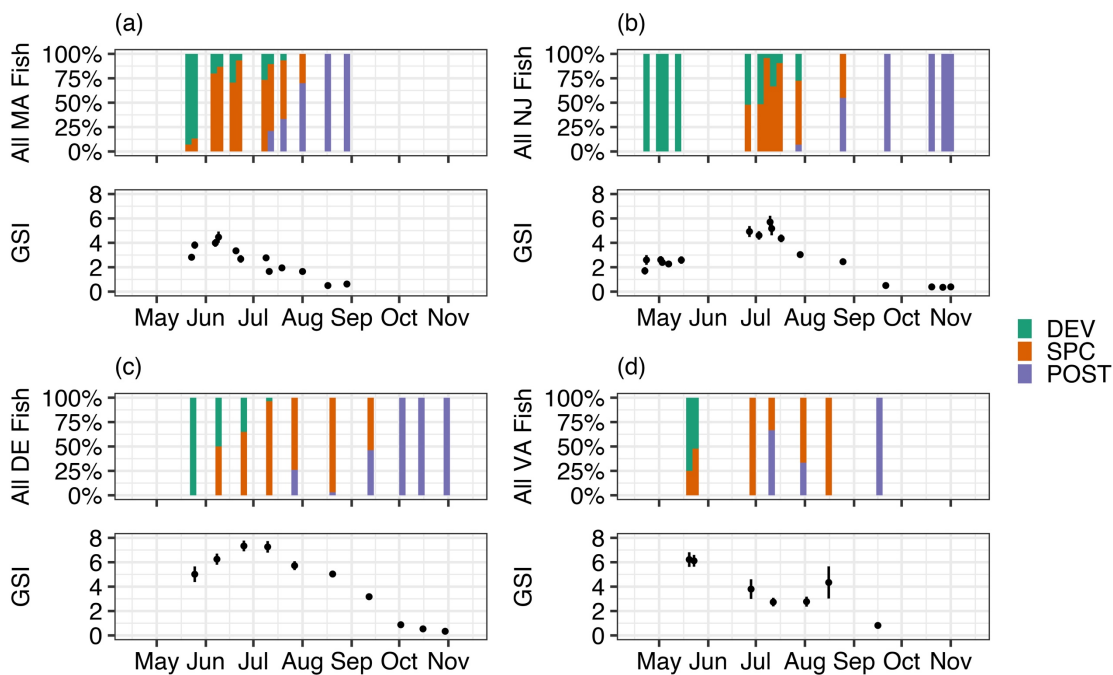


Figure 3.2 Summary of spawning characteristics for each region based on spawning stage and gonadosomatic index.

For (a) Massachusetts, (b) New Jersey, (c) Delaware, and (d) Virginia, the percent of fish in each maturity staging category are shown in the top panel, where the percent of fish for each sampling day is cumulative, and the GSI (mean \pm standard error) are shown in the bottom panel. For the maturity stages, DEV = developing fish, SPC = spawning capable fish, and POST = post-spawning fish.

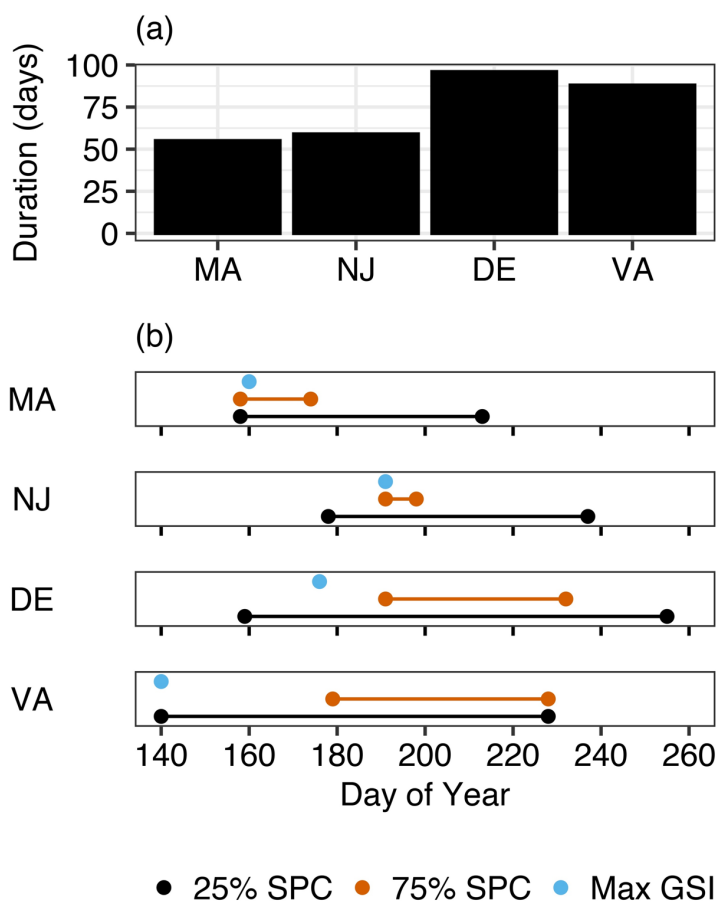


Figure 3.3 Spawning season start, end and duration for each region.

The spawning season characteristics are shown for each location in (a) the spawning duration (the Julian day difference between the beginning and end), and (b) the duration of the spawning season as designated by 25% of all fish SPC (black dot and lines), duration of when 75% of all fish were SPC (orange dot and lines), and the day when the mean GSI was highest (blue dot). For reference, Julian day 140 is May 20th and Julian day 260 is September 17th.

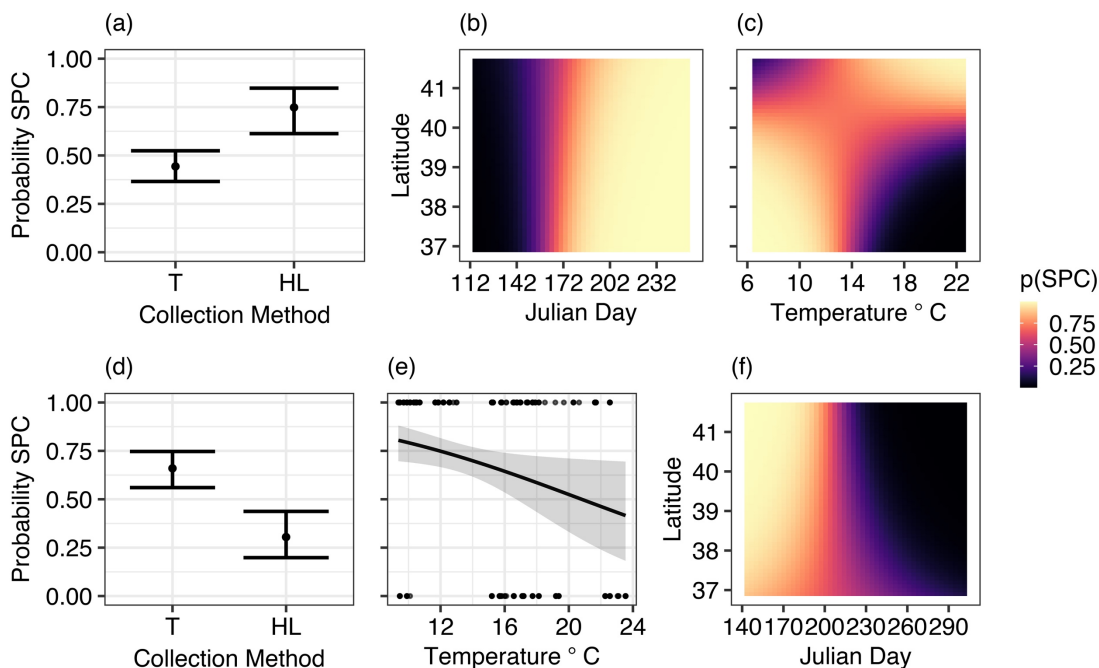


Figure 3.4 Beginning and end of the spawning season GLM results

Plotted partial fixed effects from the best fit model for the beginning of spawning (a, b, c) and end of spawning (e, d, f) GLM are shown. The beginning of spawning model best explains the probability of a fish being spawning capable (p(SPC)) over being developing based on (a) the single fixed partial effect for collection method, (b) the interaction between latitude and Julian day, and (c) the interaction between latitude and temperature. The end of spawning model best explains the probability of a fish being spawning capable (p(SPC)) over being post-spawning based on the single fixed partial effects for (d) collection method and (e) temperature, and (f) the interaction between latitude and Julian day. In (a) and (d), HL = hook and line and T = trap. For (b), (c), and (f), the predictor variables are plotted on the y- and x-axes and the estimated probability SPC is shown in the heat map with darker colors indicating lower probability and lighter colors indicating higher probability SPC. For each partial effect plot, a higher probability SPC

indicates that for (a), (b), and (c) a fish will have started spawning, and for (d), (e), and (f), a fish has not yet entered a post-spawning stage.

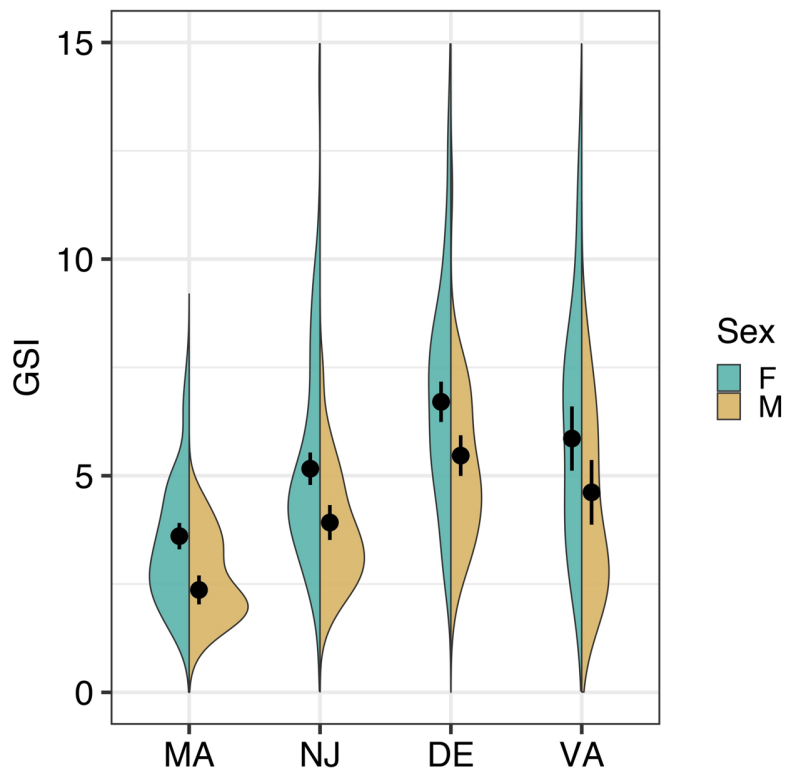


Figure 3.5 Gonadosomatic Index model results and raw data distribution for male and female fish across region.

The reproductive output estimated from GSI measurements from spawning capable fish (SPC), for each location, is shown with female and male fish separated (female = teal, male = yellow). The violin plots show both the distribution and structure of the raw GSI data. The points and associated error bars are estimated GSI and standard errors, respectively, from the best fit GLM model.

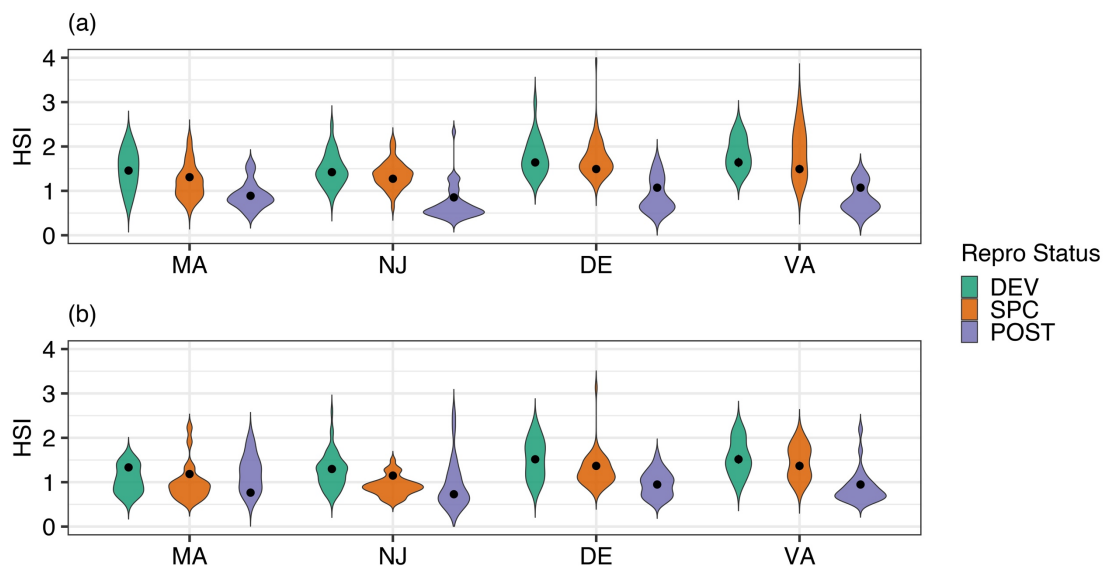


Figure 3.6 HSI model results and raw distribution across region for male and female fish.

HSI for each region is shown with (a) female and (b) male fish plotted separately. The violin plots show both the distribution and structure of the raw HSI data. The points and associated error bars are the estimated HSI and standard errors, respectively, from the best fit GLM model with the length of the fish kept constant to the mean length of all fish. For each region, HSI is separated by DEV = developing, SPC = spawning capable, and POST = post spawning fish.

3.10 SUPPLEMENTAL INFORMATION

Relative Condition Factor (Kn)

Results

The best fit model for Kn included location, maturity stage, and sex. Three other candidate model had a $\Delta AICc < 6$. Two of these models had fewer terms as in the best fit model but had substantially lower AICc weights (Burnham & Anderson, 2004; S3.1 Table), and model residuals can be found in Fig S3.1. From the best fit model, all main effects were significant (p-value < 0.01 ; difference between maturity stage DEV-SPC and location MA-VA p-value < 0.05) except for the difference between maturity stage of DEV-POST (p-value > 0.05). The dominance analysis showed that sex and location were equally dominant over maturity stage (Fig S3.2), but weakly correlated. These results indicate that Kn was higher in females, and that Kn decreased from developing to SPC fish, but recovered to developing levels in post spawning fish (Fig S3.3).

Table S3.1 Candidate models evaluating the variation in Kn.

Models were fit with a gamma distribution and an identity link function. Only models with $\Delta\text{AICc} < 6$. The relative likelihood of a model is represented by the AICc where an AICc = 1 represents the most likely. Stage = maturity stage.

Model	Df	LogLik	AICc	ΔAICc	AICc weight
Sex + Stage + Location	8	530.552	-1044.720	0	0.546
Sex + Stage + Location + Length + Length Sex	10	531.501	-1042.751	1.969	0.204
Sex + Stage + Location + Length	9	530.459	-1042.713	2.008	0.200
Sex + Location	6	525.500	-1038.906	5.815	0.030

Table S3.2 Summary information for fish collections

Details for each sample location including the start and end date, number of sampling days and fish caught, and collection methods with associated permits.

Region	Start Date	End Date	# Sampling Days	# of Fish Caught	Collection Methods Used	Collection Permits
Massachusetts (MA)	5/22/2018	8/28/2018	12	193	Fish Trap	N/A (collected by MA Department of Marine Fisheries)
					Hook and Line	MADMF #176184
New Jersey (NJ)	4/22/2018	11/1/2018	17	319	Fish Trap Hook and Line	NJDEP #SCP-1810
Delaware (DE)	5/23/2019	10/30/2019	10	285	Fish Trap	N/A (collected by DE Natural Resources and Environmental Control)
Virginia (VA)	5/19/2019	9/15/2019	7	101	Hook and Line	VAMRC #19-035 & NOAA EFP #19026

Table S3.3 Summary of fish characteristics from each sampling location

Within this table, length and weight (mean \pm standard deviation), and the number of fish per sex. F = female, M = male, T = transitional.

Region	Length (mean \pm S.D.)	Weight (mean \pm S.D.)	# of Fish by Sex	
Massachusetts (MA)	304.09 \pm 61.02	421.96 \pm 233.87	F	135
			M	58
New Jersey (NJ)	263.16 \pm 46.16	267.18 \pm 141.37	F	195
			M	121
			T	3
Delaware (DE)	271.96 \pm 43.35	281.73 \pm 125.85	F	140
			M	143
			T	2
Virginia (VA)	285.96 \pm 41.81	334.63 \pm 137.02	F	51
			M	50

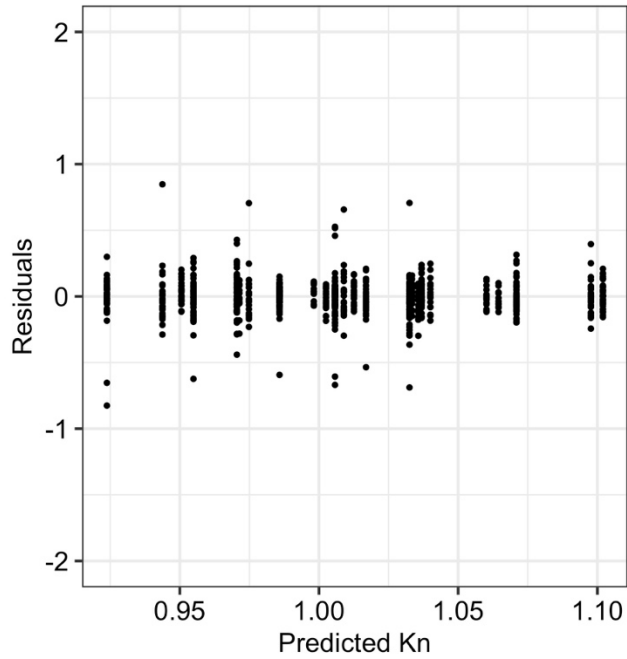


Figure S3.1 Predicted versus residuals for the best fit Kn model.

Predicted values lie within -1 to 1 and exhibit no observable pattern.

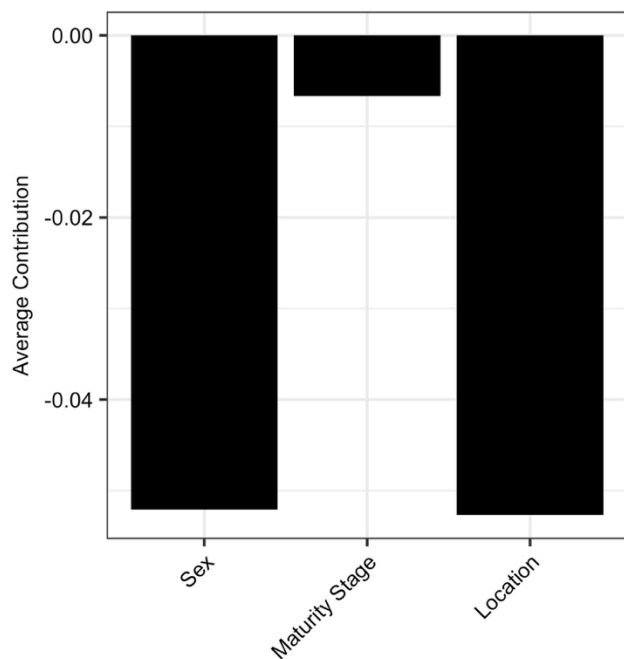


Figure S3.2 The results from the dominance analysis on Kn best fit GLM.

The average contribution is derived from the McFadden R^2 values in the analysis where a higher average contribution indicates dominance over the other predictor variables. Here, negative average contributions denote that the correlation between the predictor variables and Kn is negative.

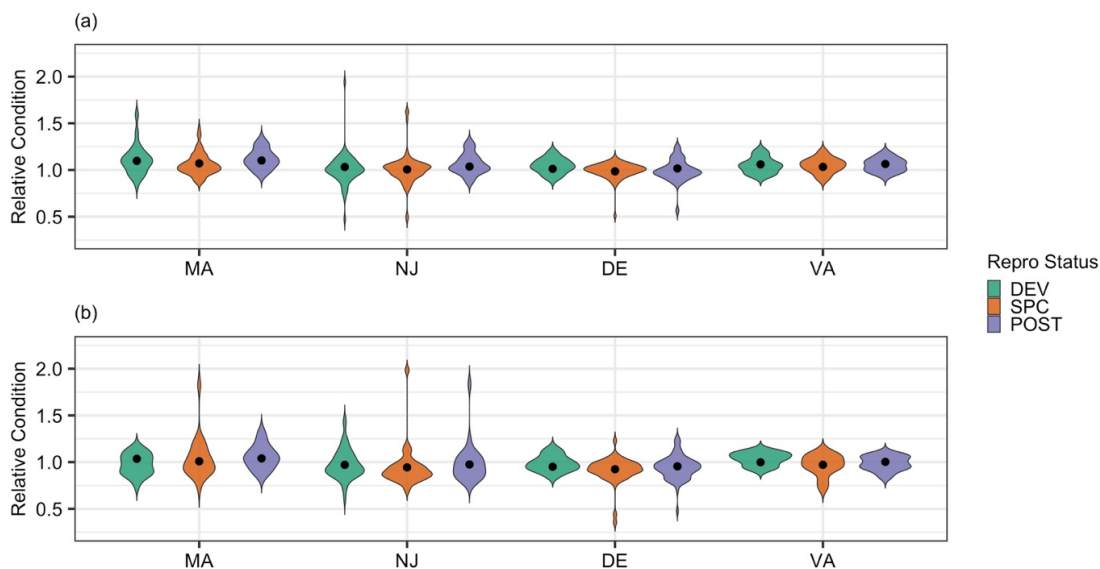


Figure S3.3 Relative condition factor (K_n) for each region

Relative condition factor (K_n) for each region is shown with (a) female and (b) male fish plotted separately. The violin plots show both the distribution and structure of the raw K_n data. The points and associated error bars are the estimated K_n and standard errors from the best fit GLM model. For each region, K_n is separated by DEV = developing, SPC = spawning capable, and POST = post spawning fish.

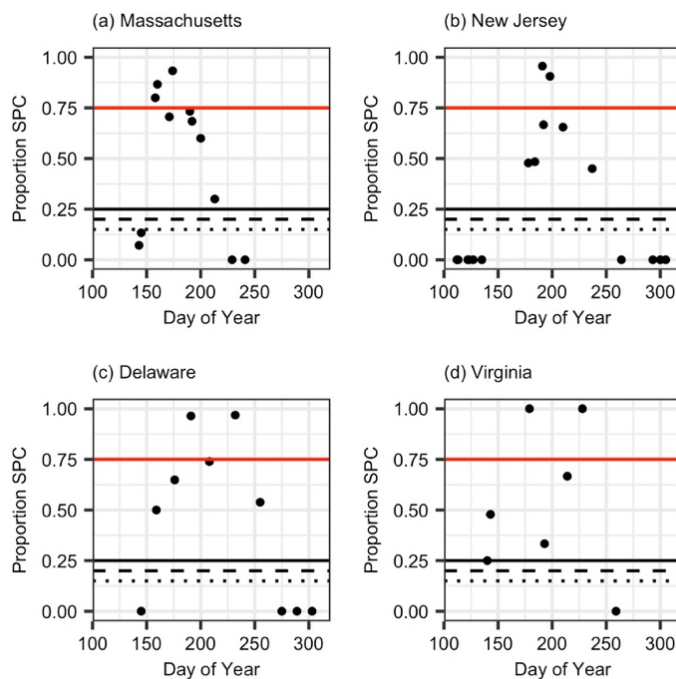


Figure S3.4 Testing of proportion spawning capable levels to determine spawning season

For (a) Massachusetts, (b) New Jersey, (c), Delaware, and (d) Virginia, the different threshold values of proportion spawning capable (SPC) to determine the start and end of the spawning season are provided to show the tested levels of 0.25 (solid black line), 0.20 (dashed black line), and 0.15 (dotted black line). For reference, the 75% SPC threshold used in Fig 3.3 is shown in red. From these comparisons, choosing a different proportion SPC threshold would affect the start date for Virginia, where a threshold of 0.20 proportion SPC would start Virginia spawning on Julian day 140 instead of 143. To remain more conservative, we chose the higher proportion SPC threshold (0.25), but a change of 3 days does not significantly change the interpretation of the spawning duration for Virginia fish (spawning duration of 85 days vs 88 days).

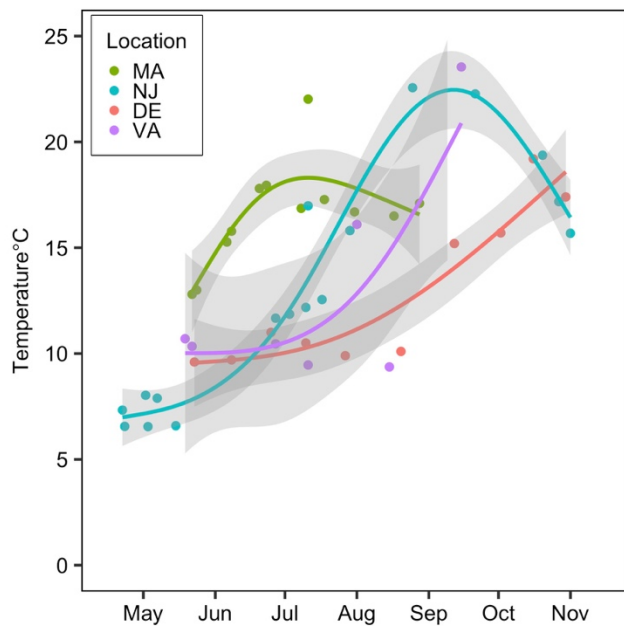


Figure S3.5 Bottom temperature throughout sampling by region

For each location, the mean temperature for each sampling day measured either from a bottom temperature logger or a handheld CTD device is shown for Virginia (purple), Delaware (red), New Jersey (blue), and Massachusetts (green). For each location, a GAM is fit to the data using the R package `ggplot`, where the solid lines are the GAM fit and the grey shading the 95% confidence intervals.

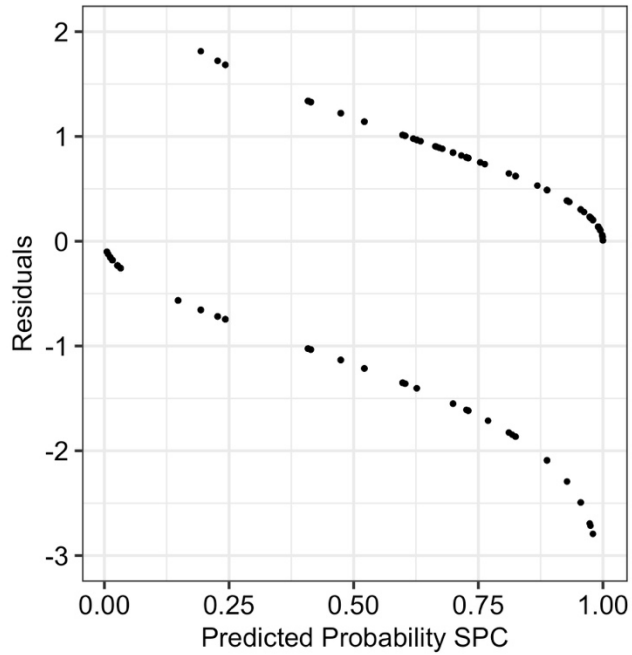


Figure S3.6 Predicted versus residuals from the best fit model for the beginning of spawning model

Because the model is a binomial fit, the predicted values are in probabilities and also show the logarithmic fits.

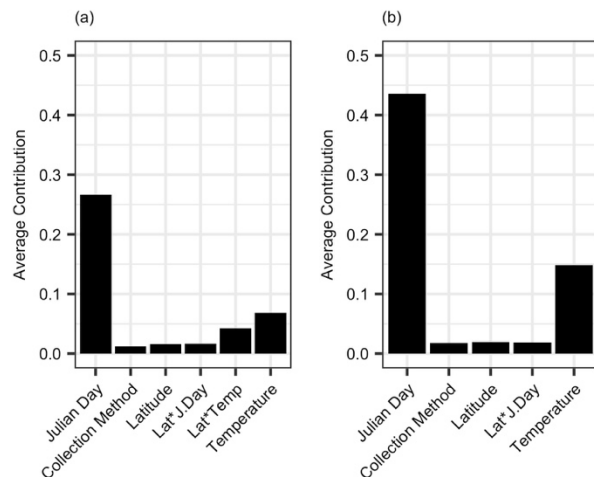


Figure S3.7 Dominance analysis for beginning and end of spawning GLMS

The results from the dominance analysis on the (a) beginning and (b) end of spawning best fit GLMs. The average contribution is derived from the McFadden R^2 values in the analysis where a higher average contribution indicates dominance over the other predictor variables. Interaction terms are denoted with a “*” between the two interacting predictors.

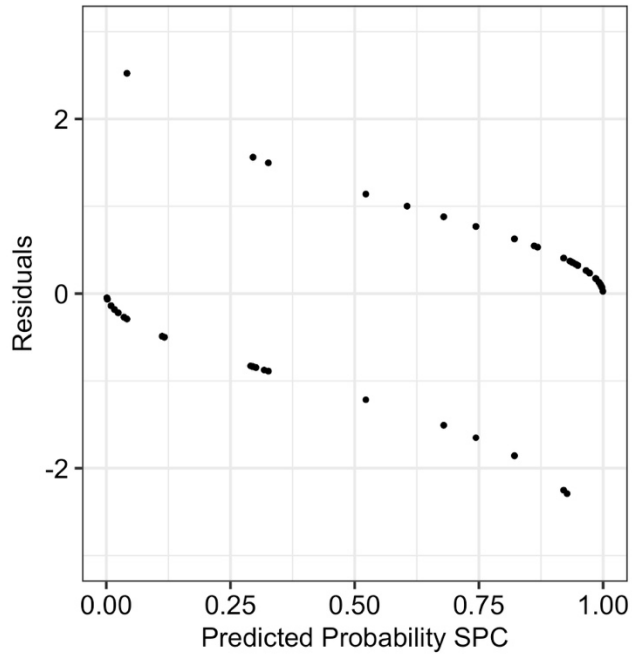


Figure S3.8 Predicted versus residuals from the best fit model for the end of spawning model

Because the model is a binomial fit, the predicted values are in probabilities and reflect the logarithmic fits.

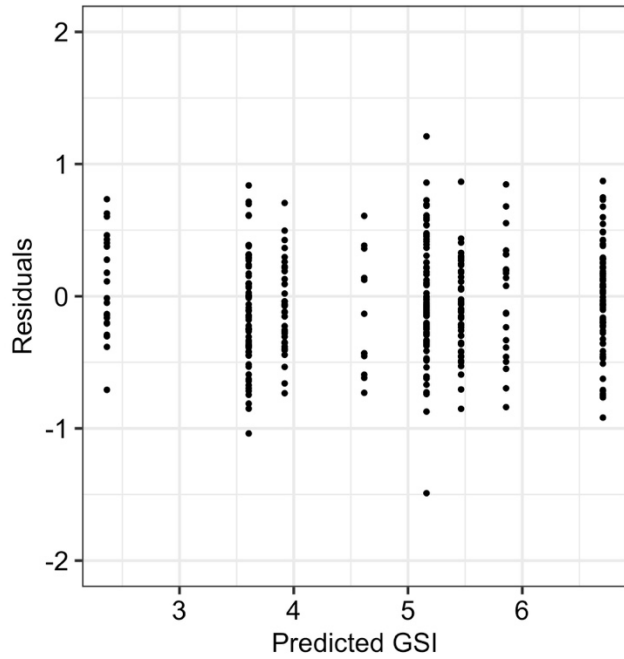


Figure S3.9 Predicted versus residuals from the best fit model for GSI

Predicted values lie within -1 to 1 and exhibit no observable pattern.

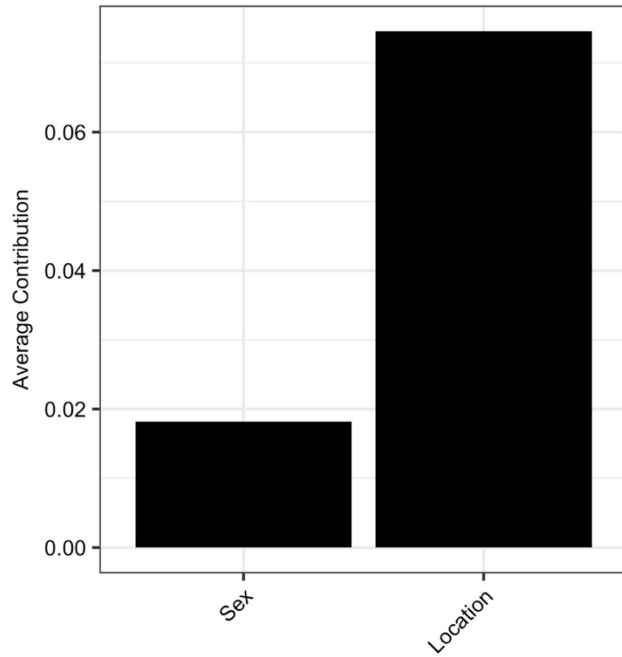


Figure S3.10 Dominance analysis on GSI best fit GLM

The average contribution is derived from the McFadden R^2 values in the analysis where a higher average contribution indicates dominance over the other predictor variables.

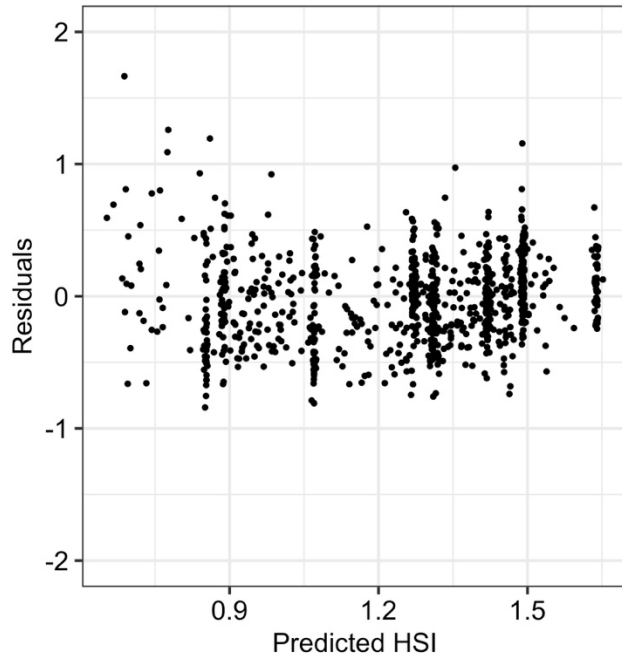


Figure S3.11 Predicted versus residuals from the best fit model for HSI

Predicted values lie within -1 to 1 and exhibit no observable pattern.

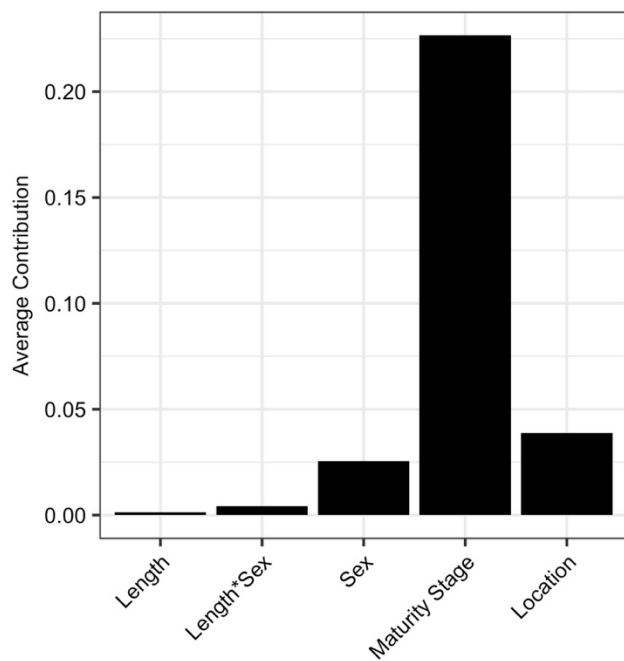


Figure S3.12 Dominance analysis on HSI best fit GLM

The average contribution is derived from the McFadden R^2 values in the analysis where a higher average contribution indicates dominance over the other predictor variables.

Interaction terms are denoted with a “*” between the two interacting predictors.

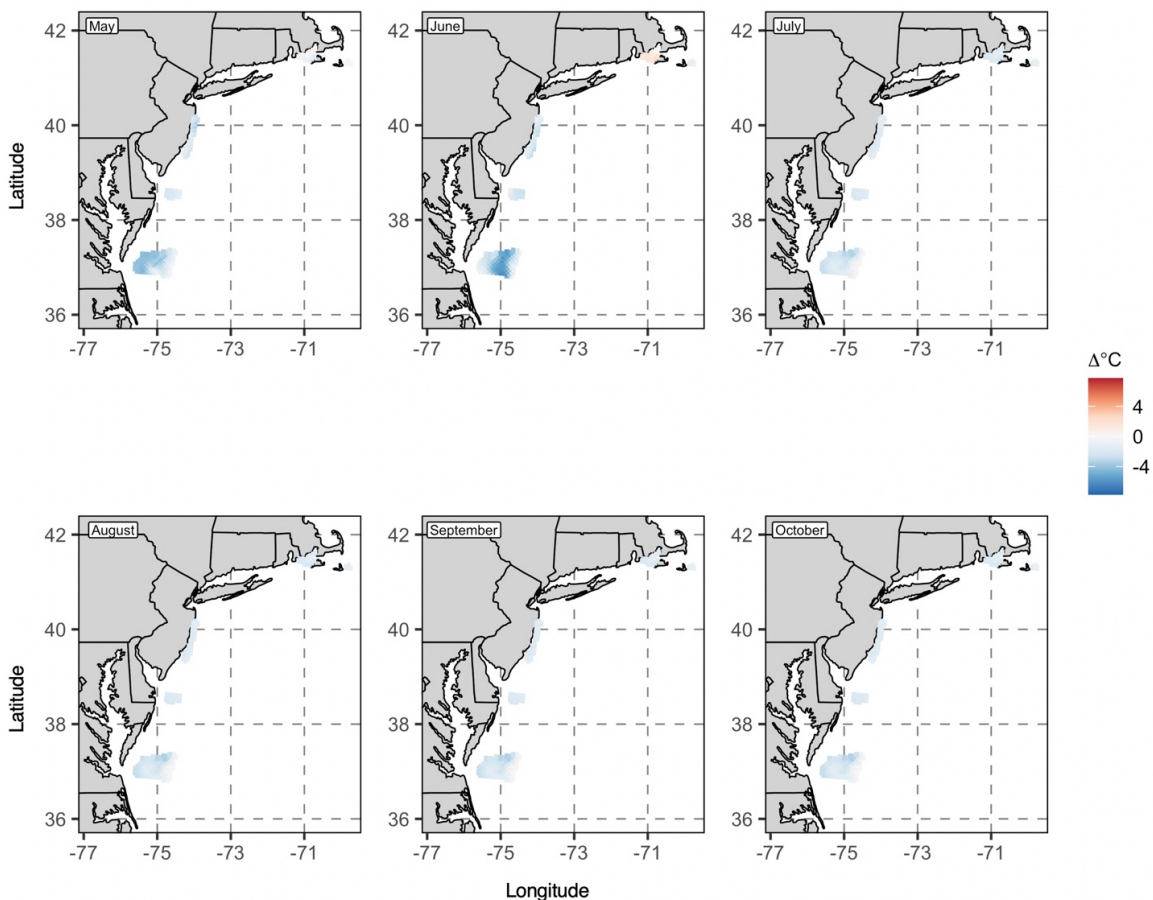


Figure S3.13 Temperature differences between 2018 and 2019 across sampling locations.

The comparison between 2018 and 2019 modeled bottom temperatures for each month of sampling is shown. The modeled bottom temperatures were retrieved from the Doppio Regional Ocean Modeling System model that provided a gridded resolution of 7x7km. For 2018, an average bottom temperature for each month was subtracted from the average bottom temperature for 2019, where blue colors indicate colder temperatures in 2018 than 2019 and red colors indicate warmer temperatures in 2018 than 2019.

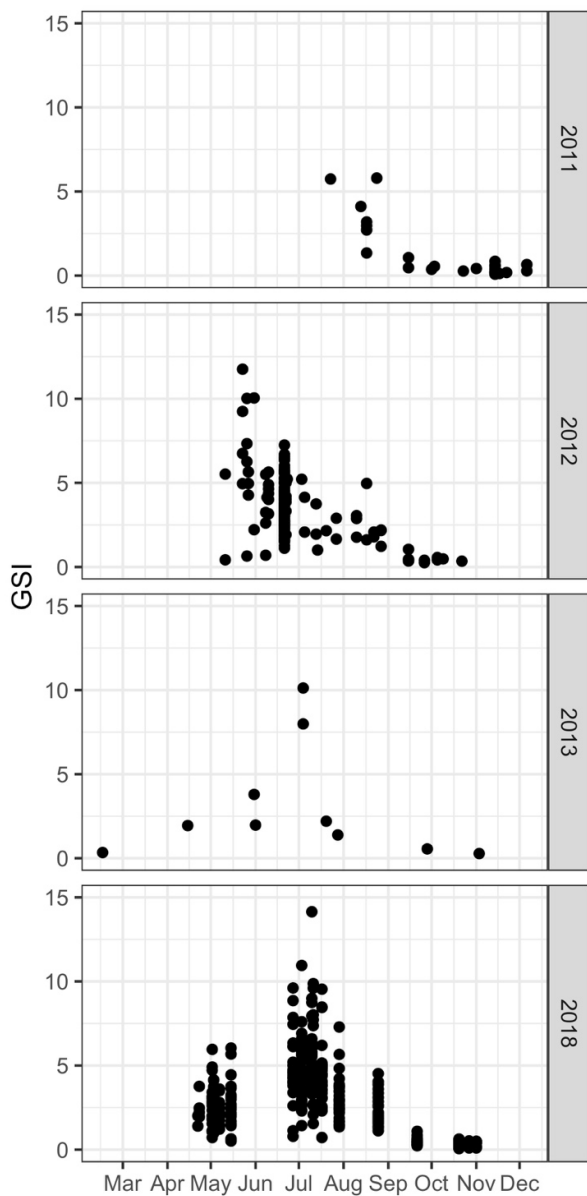


Figure S3.14 Comparison of GSI in New Jersey fish from 2011-2013

A comparison of GSI values from fish caught off the coast of New Jersey in 2011-2013 to our New Jersey fish data (2018) is provided. Data from Provost et al. (2017) provided either GSI values or a fish and gonad weight separately to allow our own calculation of GSI. For the 2018 data, fish from all maturity stages are provided because the maturity stages for the 2011-2013 were not available.

CHAPTER 4: Regional differences in energy allocation of black sea bass (*Centropristis striata*) on the US Northeast Shelf (36°N - 42°N) throughout the spawning season

4.1 ABSTRACT

Fish reproduction is energetically costly, leading to a suite of energy allocation strategies to maximize lifetime reproductive potential. Assessing energetic allocation for species that inhabit a wide distributional range can provide insight into different strategies found across individuals and populations. The Northern stock of black sea bass (*Centropristis striata*) inhabits the U.S. Northeast continental shelf from Cape Hatteras, NC to the Gulf of Maine, and spawns inshore throughout this range from April to October. To assess energy allocation toward spawning, *C. striata* were collected in four regions across this distribution and throughout their spawning season. By assessing energetic allocation (lipid, protein, total energy) in muscle, liver and gonad tissues, we identified *C. striata* as mixed breeders. This classification was chosen because they mobilized somatic energy stores towards reproductive development, but an additional energy source was needed to sustain the cumulative reproductive energy output across the spawning season. Unlike male fish, females invested more energy into liver and gonad tissues that differed regionally. For both sexes, *C. striata* in the northern portion of the distribution had higher energetic values both in the somatic stores and towards gonadal development than the fish in the southern portion of the distribution. Regional differences are relevant because although *C. striata* are managed as a unit stock, we found significant spatial variation in energetic constraints that may affect reproductive output and success (recruitment).

4.2 INTRODUCTION

Fish reproductive strategies are diverse, ranging from single to multiple breeding opportunities, oocyte development timing (synchronous, group synchronous, asynchronous), spawning pattern (total, batch), fecundity type (indeterminate, determinate), fertilization (internal, external), and embryonic development (oviparity, viviparity) (Murua & Saborido-Rey, 2003; Wootton, 1984). A myriad of reproductive strategies serve as alternative solutions to a pervasive problem of maximizing lifetime fitness through production of viable offspring while balancing the high energetic costs associated with reproduction. In some cases, the energetic cost of reproduction can lead to semelparity (Kindsvater *et al.*, 2016) or increase natural mortality in iteroparous species (Nielsen *et al.*, 2012). Adults may also forgo spawning or produce less batches of eggs if spawning conditions are poor (McBride *et al.*, 2015), a strategy typically employed in unpredictable environments to increase survival probability for the next spawning season (Finstad *et al.*, 2002). Therefore, energy allocation patterns for a particular species can provide insights into population dynamics and life history traits related to spawning that are useful to understand from both an ecological perspective and fisheries management standpoint.

Energy is supplied through the diet, and allocated towards maintenance, with any remaining surplus available for growth, storage, and reproduction (for mature individuals). Maintenance supports routine metabolic processes which include standard metabolic rates plus additional metabolism used for daily activities such as swimming and feeding (Treberg *et al.*, 2016). Growth, and subsequently larger body sizes, can be advantageous for multiple reasons including the ability to store more energy for

overwintering (Bunnell & Marschall, 2003), higher swimming efficiency (Nøttestad *et al.*, 1999), and increased fecundity (Hixon *et al.*, 2014). Surplus energy can be stored, typically in the form of lipids, within the liver or muscle tissue (Brown & Murphy, 2004), but sometimes in the viscera (Cook *et al.*, 2021) and skin (Jørgensen *et al.*, 1997). Stored lipids provide a direct source of energy that can be mobilized to other regions of the body when needed, as is done during reproductive development. Specifically for female fish, liver energy storage is important for reproductive development because vitellogenin, a lipoprotein synthesized in the liver, is mobilized towards the gonad for egg development (Hiramatsu *et al.*, 2002). Energy storage sites can be species-specific (Fiorin *et al.*, 2007), and sometimes distinctive energy allocation strategies can lead to a noticeable difference in reproductive output both in terms of egg quality and quantity (dos Santos *et al.*, 2010). Thus, energy storage allows energy acquisition (feeding) and usage (spawning) to be separated in time and/or space, which is particularly important in environments with pulsed productivity, and can be investigated through studies focused on energy storage strategies and their role in mobilization towards spawning.

The source of energy partitioned towards reproductive development varies across reproductive strategies. Fish that mobilize energy from stored reserves are classified as capital breeders while fish that supply energy through food intake are identified as income breeders; some fish utilize both strategies and are classified as mixed breeders (McBride *et al.*, 2015). Capital breeders supply a substantial percentage of their stored somatic energy towards spawning, and can lose a considerable amount of energy by the end of the spawning season (Dawson & Grimm, 1980; Jørgensen *et al.*, 1997). In many cases, the liver is used as the storage depot, and can drastically decline in both lipid

content and weight throughout spawning (Alonso-Fernández & Saborido-Rey, 2012). On the other end of the spectrum, income breeders do not utilize energy stores from liver or body reserves (Domínguez-Petit *et al.*, 2010), and their reproductive output can be affected by the food supply during the spawning season (Basilone *et al.*, 2020). Mixed breeders primarily acquire energy through their diet during the spawning season, but can supplement additional energy from body reserves when necessary, showing a slight decline in somatic stores throughout spawning (Aristizabal, 2007; Burns & Fuiman, 2020). These differing breeding strategies impose a range of energetic constraints towards reproduction.

Some fish undergo pre-spawning migrations as suitable spawning grounds may not be optimal for adults year-round, such as in cases where they are separated from feeding grounds or inhabitable for overwintering (Alexander, 1998; Buehler & Piersma, 2008). Spawning grounds may also reflect suitable habitat for larval hatching, increasing the chance of offspring survival (Jørgensen *et al.*, 2008). While ultimately advantageous, pre-spawning migrations can be energetically costly and can reduce the energy available for egg production (Hendry & Berg, 1999). In some cases, migrating fish prepare by storing more energy prior to migration (Gaillard *et al.*, 2015). Under this premise, larger fish have an advantage because of their greater energy storage capacities and higher swimming efficiencies (Jørgensen *et al.*, 2008; Slotte, 1999). Some species with an array of short to long migration distances show a spectrum of iteroparity to semelparity where fish with longer migrations can have a higher propensity towards semelparity due to the immense cost of migration and subsequent reproduction (Glebe & Leggett, 1981). Therefore, migration serves as an important life history trait that can be considered a

secondary reproductive cost and the impacts of migration distance can be explored through energy allocation dynamics.

For fish species that inhabit a wide distributional range, in addition to gradients in migration distance, differences in reproductive energy allocation and somatic energy storage can occur across depth (Hoey *et al.*, 2007), temperature (Feiner *et al.*, 2016), and/or latitudinal gradients (Mollet *et al.*, 2013). Energy allocation can also be affected by overwintering preparation, where individuals at higher latitudes with pulsed environmental productivity rapidly acquire energy reserves while fish at lower latitudes with constant productivity accumulate them more gradually (Schultz and Conover, 1997). Density dependence across a range can also influence energy allocation where fish in densely populated habitats exhibit lower reproductive investment and slower growth (Pritt *et al.*, 2020). Investigating how energy allocation differs across the wide distribution of certain fish species can provide insight into potential differences in reproductive output and recruitment success throughout a distribution.

Black sea bass (*Centropristis striata*) are an economically and ecologically important fisheries species separated as three stocks: the Gulf of Mexico stock, the Southeastern stock located from Eastern Florida to Cape Hatteras, NC, and the Northern stock located from Cape Hatteras, NC to the Gulf of Maine (Bowen & Avise, 1990; McCartney *et al.*, 2013). Between the Southeastern and Northern stock of *C. striata*, Cape Hatteras, NC is seen as a biological barrier due to the physical dynamics of the Gulf Stream (Gray & Cerame-Viuas, 1963), leading to genetic and demographic variation between the two stocks (Roy *et al.*, 2012). The Northern stock of *C. striata* (hereafter referred to as NS *C. striata*) inhabit a wide latitudinal inshore distribution, spanning ~6°

of latitude during the summer spawning season, and migrate offshore towards the southeastern continental shelf edge to overwinter (Musick & Mercer, 1977) in a narrower range of latitude. This migration pattern results in some fish migrating a farther distance than others, and because NS *C. striata* exhibit a high degree of site fidelity (Moser & Shepherd, 2008), these life history differences can persist throughout regional subgroups of NS *C. striata*. Latitudinal effects (i.e. seasonality and/or temperature) also have led to differences in the initiation, duration, and reproductive output during the spawning season (Slesinger *et al.*, 2021). NS *C. striata* are also protogynous hermaphrodites (Mercer, 1978; Wenner *et al.*, 1986), further complicating an understanding of life history variation with respect to lifetime reproductive output. The potential misspecification in stock assessment models by not accounting for within-stock life history variation of NS *C. striata* has prompted concerns. A recent stock assessment report advised that NS *C. striata* should be split into two management sub-groups at the Hudson Canyon due to differing *C. striata* life history characteristics (NEFSC, 2017).

A better understanding of the intraspecific differences of NS *C. striata* energy allocation throughout their distribution would add to existing information regarding best management practices. First, management is based on estimated biomass for state-specific quotas, and a more holistic view of *C. striata* spawning and recruitment can aid in future management decisions. Second, the US Northeast Shelf has been experiencing rapid ocean warming (Chen *et al.*, 2020; Pershing *et al.*, 2015); regional variation in energy allocation provides a base onto which the current and future effects of ocean warming can be anticipated. Third, *C. striata* centre of biomass has been shifting northward over time (Bell *et al.*, 2015; Kleisner *et al.*, 2017), which could be a response

to ocean warming in the southern portion of their range (Slesinger *et al.*, 2019) and/or increased biomass in the northern region as a result of previous fisheries management (Bell *et al.*, 2015). Heterogeneity in energy allocation may reveal that life history strategies at the expanding edge differ from those closer to the centre of biomass. Therefore, we asked, 1) are there regional differences in NS *C. striata* somatic and reproductive energetics, and 2) what are the seasonal trends in energetic usage throughout the spawning season across the entire distribution?

4.3 METHODS

Collections and sample processing of NS *C. striata* are more fully described in Slesinger *et al.*, (2021). Briefly, NS *C. striata* were collected across their distribution, from south to north, off the coasts of Virginia (VA), Delaware (DE), New Jersey (NJ), and Massachusetts (MA) using both hook and line and fish traps. Collections occurred in 2018 and 2019, and targeted the spawning season which occurs from ~April – October (Drohan *et al.*, 2007). After collection, fish were measured to obtain a length and weight, and dissected to remove the liver and gonad. For both, a wet-weight (± 0.01 g) of the entire organ was measured before processing. A section of epaxial muscle tissue ($\sim 3.35 \pm 1.163$ g) was also removed above the lateral line and underneath the first dorsal spine. For each tissue, a weighed sub-sample was preserved at -80°C for lipid extractions.

The sex and maturity stage of each fish was determined by macroscopic inspection of the gonad to link energetic analyses with the spawning condition. Maturity stages were classified as developing, spawning capable (includes ripe and ripe and running fishes), spent, and resting based on classifications from Brown-Peterson *et al.*

(2011). Because *C. striata* are protogynous hermaphrodites (Mercer, 1978), transitioning fish were identified using criteria from Klibansky and Scharf, (2015) and removed from analysis (N = 5).

4.3.2 Ethics Statement

Detailed description of fishing permits and IACUC protocol have been published in Slesinger *et al.* (2021). Slesinger performed all hook-and-line collections and euthanasia, which were done in accordance to Rutgers University IACUC Protocol (#PROTO201800054). Additional state or federal issued fishing permits can be found in Table 1 of Slesinger *et al.* (2021) (Table 3.1 in Chapter 3).

4.3.3 Lipid Extractions

A subsample of *C. striata* (281 out of 898) was selected for lipid extractions to provide ~5-8 fish per day of collection per region, covering a range of maturity stages (Table 4.1) and weights. For each fish, the total lipids were extracted from liver, gonad, and muscle tissues for a total of 843 lipid extractions. Prior to lipid extractions, a ~0.5g sample of tissue was weighed (+/- 0.001g), freeze dried to a constant dry weight, and then reweighed to calculate the percent dry-weight ($\%dry\text{-weight} = 100 * (\text{dried weight} / \text{wet weight})$). To run samples in duplicate, the dried sample was then homogenized through mechanical crushing, divided into two equal parts, and reweighed to provide a dried weight of each sub-sample. Total lipids were extracted using a modified chloroform:methanol extraction (Folch *et al.*, 1957). On each extraction day, an external standard (nonadecanoic acid, C19:0) was also ran in duplicate. For each sample, the lipid

extraction process was repeated three times to ensure high extraction efficiency. Total lipids were measured gravimetrically as the weight gain in a pre-weighed gas-chromatography vial and expressed as lipid concentration (LC; g lipid/g dry weight). If the difference in lipid concentration between samples ran in duplicate was >10%, a third sample was analysed. The mean of replicate samples for each fish was used for analyses below.

4.3.4 Estimation of Energy Densities

In order to estimate the energy density (kJ/g wet weight) of each tissue, both lipid and protein concentrations are required. Only LC and %dry-weight were only measured in the present study, but the energy density (ED) of each tissue type (muscle = MED, liver = LED, gonad = GED) was estimated with and validated using proximate composition data from the energy density values reported in Wuenschel *et al.* (2013) as follows. The %dry-weight from each sample provided the total g of dry-weight per g of wet-weight. Lipid, protein, and ash, all as g/g dry-weight, were assumed to comprise of all of the dry-weight (there is minimal energetic contribution from carbohydrates in fish; Love, 1980) and therefore add to one. Tissue-specific linear relationships between g ash/g dry-weight and g dry-weight/g wet-weight from the Wuenschel *et al.*, (2013) samples, were used to estimate g ash/g dry-weight from the g dry-weight/g wet-weight of samples in the present study. Protein (g protein/ g dry-weight) was calculated as one minus the combined g lipid/ g dry-weight and estimated g ash/g dry-weight. Next, g protein/g dry-weight was multiplied by the respective tissue g dry-weight/g wet-weight to provide g protein/g wet-weight. Finally, g lipid/g wet-weight and g protein/g wet-weight were

converted to an ED by multiplying 39.565 kJ/g wet-weight for lipid and 23.64 kJ/g wet-weight for protein (Henken *et al.*, 1986); total ED of the tissue was the sum of the lipid and protein energy densities. To validate the ED estimates to Wuenschel *et al.* (2013), a linear regression of ED ~ %dry-weight was used to assess the fit of both data sets together (Figs S4.1-S4.3). The total weight of the liver and gonad were multiplied by ED to obtain a liver total energy (LTE; kJ) and gonad total energy (GTE; kJ).

4.3.5 Data Analysis

Compositional measurements (lipid concentration [LC]; energy density [ED]; total energy [TE]) were analysed for liver and gonad tissue using generalized linear models (GLMs). Sex-specific (female, male) models were run given different energy allocation in these tissues by sex and because analysing how the energetic dynamics differed between female and male throughout spawning and region was not the purpose of this study. However, preliminary analyses showed similar values and trends in muscle measurements between female and male fish, and were therefore combined for their analysis of compositional measurements. To evaluate the importance of region for each compositional measurement, a null model with predictor variables of *weight* (continuous) and *maturity stage* (categorical with four levels) was competed against a regional model with the same predictor variables as in the null model and the addition of *region* (categorical with four levels). Bayesian Information Criterion (BIC), which provides robust hypothesis testing without overfitting, was used to evaluate whether region should be included in each model (Aho *et al.*, 2014).

An error distribution and appropriate link function was chosen for each compositional measurement to account for specific data structure (Table S4.1). Beta distribution with a logit link was used for the LC models because these values are between 0 and 1. A gamma distribution was used for both the ED and TE models because both metrics are non-zero with a right tailed distribution. The canonical inverse link was used for the ED models, and a log link was used for the TE models due to a better fit.

Generalized additive models (GAMs) were employed to further assess *C. striata* TE usage throughout the spawning season. A month integer was obtained based on collection date of the fish. Separate sex-specific GAMs were run for response variables LTE and GTE with *weight* (continuous) and *region* (factor with four levels) as parametric predictors and a smooth term of *month* with a *region* interaction as the non-linear term. For the smooth term, a thin plate spline was used. *K*, the number of knots, was selected through BIC and checked using `gam.check()` in the MGCV package in R to ensure enough knots for analysis while avoiding overfitting.

Results from these GAMs provided a continuous prediction of sex-specific LTE and GTE per region throughout the spawning season. In order to compare LTE and GTE across region, a median weight of all fish (315g) was used for predictions. The day of the start and end of spawning, which were taken from the criterion of 25% of the population being spawning capable, and peak gonadosomatic index were obtained from Slesinger *et al.* (2021). From these, the LTE and GTE were estimated for those days to provide total energy present at the start and throughout to the end of spawning. Cumulative energy present throughout spawning over the spawning duration and the energy usage per day were calculated based on the cumulative energy and spawning duration.

All data analysis was conducted using R (Version 4.0.1; R Core Team, 2019). GLMs with beta distribution were run using the package Betareg (Cribari-Neto & Zeileis, 2010), and for all, estimated marginal means were calculated using the package Emmeans (Lenth, 2020). GAMs were run using the package MGCV (Wood, 2013). Significance of a value was determined at a p-value < 0.05.

4.4 RESULTS

4.4.1 Tissue Specific Lipid and Energy

In total, 14 GLMs were analysed which included two for muscle (LC, ED), six for liver and six for gonad (sex-specific LC, ED, and TE). Out of the 14 GLMs, region was an important predictor for 10 of the models (Table 4.2). For muscle, region was important for MED but not for MLC. For female fish, region was always an important predictor while for male fish, region was an important predictor for LLC, LTE and GLC. For all model selections, Δ BIC was > 2.

Muscle GLMs combined female and male fish for analyses (Table 4.3). For MLC, region was not an important predictor. Weight was a significant predictor (p-value < 0.001), where an increase in weight conferred with an increase in MLC (Fig 4.1a), and for maturity stage, spawning capable, spent and rest categories were all significant (p-value < 0.05) indicating the change in MLC for each maturity stage was significant compared to developing fish. For MED, region was an important predictor, where NJ and MA were significantly different than VA fish (p-value < 0.001). Spawning capable and spent were significant for maturity stage (p-value < 0.05). Altogether, MLC declined throughout the spawning season (Fig 4.1b); MED closely followed, with some post

spawning recovery (Fig 4.1d). Regionally, MED was lower in the northern sampling sites including NJ and MA (Fig 4.1e).

For female fish, liver energetics were clearly affected by spawning, and region was important for all measurements (Table 4.3). For LLC, SPC and SPT fish were significantly different than developing fish (p -value < 0.05 ; Fig 4.2b), and NJ and MA were significantly different than VA (p -value < 0.01), but showed a general declining trend from south to north (Fig 4.2c). Similar to LLC, LED was significantly lower (p -value < 0.01) in NJ and MA fish compared to DE and VA fish (Fig 4.2f). For maturity stage, LED in spawning capable and spent fish was significantly lower than in developing fish (p -value < 0.01). For LTE, weight was a significant predictor (p -value < 0.001), with increasing weight leading to higher LTE (Fig 4.2g). Throughout the spawning season, there was a significant decline in LTE for spawning capable, spent, and rest from developing fish (p -value < 0.05 ; Fig 4.2h). Across region, NJ and MA were significantly different than VA (p -value < 0.01), showing a decline in LTE from south to north (Fig 4.2i). Altogether, each compositional measurement decreased throughout the spawning season with some post spawning recovery seen by a slight increase in values from spent to rest fish (Figs 4.2b,e,h), and values were generally higher in the southern locations of VA and DE (Figs 4.2c,f,i).

Male fish liver energetics differed from female fish in that specific measurements were less affected by spawning, and region was not an important predictor for LED (Table 4.3). For LLC, there were no significant differences between maturity stages throughout the spawning season (Fig 4.2b), and VA was significantly higher (p -value < 0.001) than the other regions (Fig 4.2c). Similar to LLC, there were no significant

differences in LED between maturity stages in male fish (Fig 4.2e). Parallel to female fish LTE, weight was a significant predictor (p -value < 0.001) and across region LTE was significantly different in NJ and MA fish than from VA fish (p -value < 0.01 ; Fig 4.2i). Unlike LLC and LED, LTE differed across maturity stage where spent and rest were significantly lower than developing fish (p -value < 0.05 ; Fig 4.2h). Overall, LLC and LED did not change throughout the spawning season but LTE did with a decrease from developing to rest fish. This suggests a liver size contribution to total energy levels rather than a compositional change. Region was important for male LLC mostly due to the higher values in the VA fish, but there was a general decline in LTE from south to north suggesting a size component as well (region was not an important predictor for LED).

Region was important for all gonad measurements for female fish (Table 4.3). Female GLC significantly declined in the spent and rest stages (p -value < 0.001 ; Fig 4.3b). Across region, DE and NJ were significantly different than VA (p -value < 0.05 ; Fig 4.3c). For GED across the spawning season, spawning capable, spent, and rest were significantly different than DEV for female fish (p -value < 0.001 ; Fig 4.3e), and throughout region NJ and MA were significantly different than VA (p -value < 0.05 ; Fig 4.3f). For GTE, weight was a significant predictor (p -value < 0.001) with larger fish predicted to have higher GTE (Fig 4.3g). Across the spawning season, there was a significant decline in spent and rest fish (p -value < 0.001 ; Fig 4.3h), and by region there was a significant difference in NJ and MA from VA fish (p -value < 0.01 ; Fig 4.3i). Altogether, across the spawning season, GLC, GED and GTE declined for female fish. However, between developing and spawning capable stages, there was no change in GLC, a decrease in GED and an increase in GTE. This suggests that between these two

stages, lipid concentration of dried tissue remained constant while a decline in GED could be driven by the hydration of oocytes (increasing the denominator), and an increase in GTE a result of increasing gonad size. For the regional trends, there was also a general decline in gonad energetics from south to north.

Male fish gonad energetics were generally lower than female fish and region was only important for GLC (Table 4.3), where VA was significantly lower than the other regions (p-value < 0.001; Fig 4.3c). There was no change in GLC throughout spawning (Fig 4.3b). For GED, spent and rest were significantly different than developing fish (p-value < 0.001; Fig 4.3e). Similar to female GTE, weight was a significant predictor (p-value < 0.001; Fig 4.3g) and there was a significant difference in spent and rest fish from developing fish (p-value < 0.001; Fig 4.3h). Overall across the spawning season, there was no change in GLC, an increase in GED, and a decrease in GTE.

4.4.2 Seasonal Patterns

The four seasonal GAMs (LTE, GTE for female and male fish) showed sex and regional differences in energy usage throughout the spawning season. All GAM results were predicted at the median weight (315g) of all fish in the study to allow comparisons between regions and sex. For all GAMs, weight was a significant predictor (p-value < 0.001). For LTE, the female and male GAMs explained 70.5% and 60.9% of the deviance, respectively (Table 4.4). The monthly smooth term for DE, NJ and MA were significant (p-value < 0.01) for female fish and VA and DE monthly smooth terms were significant (p-value < 0.05) for male fish. All regional EDF values were near one suggesting a linear relationship between LTE and month. For GTE, the female and male

GAMs explained 78.1% and 72% of the deviance, respectively. For both, the smooth term for month by region was significant (p -value < 0.001), and only GTE for male fish from VA and MA showed a linear relationship.

Across the spawning season GTE was higher than LTE for female fish while GTE and LTE were similar for male fish (Fig 4.4). LTE steadily declined throughout spawning, whereas GTE peaked or plateaued before declining. By incorporating the start and end of spawning days, and peak GSI day for each region from Slesinger *et al.* (2021), energy usage throughout the spawning season was assessed with respect to differing spawning season lengths between the regions. For each region, the decline in GTE occurred near or on the peak GSI day, and GTE and LTE intersected near the end of spawning (Fig 4.4). Regionally, there were higher starting GTE values in DE and VA, and lower in NJ and MA. The cumulative LTE kJ for female fish was higher in VA and DE (~3000 kJ) compared to NJ and MA (~1000 kJ). Male LTE cumulative kJ increased from north to south (Table 4.5). For GTE, cumulative kJ was highest in DE (female: ~11,800 kJ; male: ~ 3,700 kJ) and lowest in MA (female: ~1,700kJ; male: ~950kJ). While the spawning duration was longer in DE compared to MA, contributing to the higher cumulative kJ values, the kJ/day showed that the daily output of MA fish was 75% lower than DE.

4.5 DISCUSSION

We observed significant sex-specific changes in *C. striata* energetics throughout the spawning season as well as spatial variation across the Northern stock (NS) for a majority of the measures evaluated. Throughout the spawning season, liver, muscle and

gonad tissue energetic values declined, with some post spawning recovery in the liver and muscle, implying direct use of these tissues energy stores for spawning. Male fish invested less energy in reproduction than female fish, and were also compositionally different as seen by size differences of the organ primarily influencing total energetic values. Female fish were more often dissimilar across their distribution than male fish, and there was a general pattern of lower energetics in the northern sampling locations (MA, NJ) compared to the southern sampling locations (DE, VA). Notably, less energy was allocated to gonad energy in the northern sampling sites, which corroborates with the lower GSI found in Slesinger *et al.* (2021). These energetic differences are significant. For example, in order for MA and DE female fish to have the same energetic output throughout the spawning season, MA fish would need to double the DE daily output to reach that value with a shorter spawning season.

NS *C. striata* energetic allocation in body stores and towards reproduction differed significantly across their distribution, whereby higher LC, ED, and TE in muscle, liver and gonad tissues occurred in the southern fish (VA, DE) compared to the northern fish (NJ, MA). In the muscle, MLC and MED decreased throughout spawning, suggesting some use of muscle energetics towards reproduction. Regionally, MED also decreased from south to north, which could be indicative of migration effects on pre-spawning conditions (Wuenschel *et al.*, 2013), as NS *C. striata* migration distances are longer in the northern portion of the distribution. For the liver, female fish measurements all decreased throughout spawning with some post spawning recovery while male fish measurements did not change, except for LTE. Regionally, the general decline in energetics from south to north was a dominant pattern for female fish but less so in male

fish. For female fish, LLC, LED, and LTE were all higher in the southern than the northern sampling regions, which would suggest a link between higher lipid storage leading to higher LED and LTE. For the male fish, only LLC and LTE were significant for region. However, the regional effect for LLC was likely driven by the overall higher values in the VA fish compared to the rest of the fish, whereas LTE regional differences were similar to those seen in the female fish. Both female and male LTE were driven by liver size, but we suggest female livers were also compositionally different as seen by changes in LLC and LED, while male fish livers were compositionally similar as their total energetic differences were only driven by variances in liver size. Gonad energetics for female fish were similar to liver in that there was a comparable decreasing energetics trend from south to north and declines in gonad energetics throughout the spawning season. For the male fish, GLC was the only measurement where region was significant, and as in liver, this was likely driven by the differing values in VA fish compared to the rest. The increase in GED was likely compositional where post-spawning gonads contain less water decreasing the denominator, and a decrease in GTE indicates the influence of gonad size.

Seasonally, NS *C. striata* total energy in liver and gonad decreased throughout spawning and maintained the trend of higher energetics in the southern sampling locations. Female GTE was higher than LTE throughout the spawning season and intersected at the end of spawning, while male fish GTE and LTE were similar throughout the spawning season. Cumulative LTE and GTE were both higher in female fish than male fish, but the net difference was higher in cumulative GTE (e.g. net difference for DE fish between female and male was ~1000kJ for LTE and ~8000kJ for

GTE). Throughout the spawning season, the day of peak GSI coincided with the decline in GTE. Regionally, cumulative LTE and GTE was lower in the northern than the southern sampling sites for both male and female fish. This difference could be a product of the longer spawning seasons in the southern sampling locations. In order for MA fish with a shorter spawning season to match the cumulative GTE of DE fish, they would need to double their daily GTE kJ output of the DE fish (~240kJ/day). However, it should be noted that the cumulative energy metric assumes constant spawning frequency throughout the distribution, and increasing cumulative GTE could also be achieved in MA by increasing their spawning frequency. Whether this is possible given temperature regulation of oocyte development and/or liver energy storage or energy intake restraints is unknown, but warrants future investigation.

Throughout their distribution, NS *C. striata* energy allocation patterns suggest they employ a mixed breeding strategy. Prior to spawning, NS *C. striata* female fish LTE values ranged from 50-150kJ, and LLC, LED, and LTE values declined throughout the spawning season (Figs 4.2 b,e,h). For capital breeding fish such as pouting (*Trisopterus luscus*), LTE values decreased throughout spawning, like in NS *C. striata*, but pre-spawning LTE values were closer to 400kJ (Alonso-Fernández & Saborido-Rey, 2012). In contrast, LED values for European hake (*Merluccius merluccius*), an income breeder, remained constant throughout the spawning season (Domínguez-Petit *et al.*, 2010). For NS *C. striata*, Rosa *et al.* (2020) also found hepatic lipid storage mobilized towards gonad development, confirming liver and muscle energy consumption throughout the spawning season. However, starting liver energetic values for NS *C. striata* were lower than in capital breeders, suggesting NS *C. striata* are employing a mixed breeding

strategy (Aristizabal, 2007). A mixed breeding strategy is conducive to the life history of NS *C. striata* who are asynchronous multiple-batch spawners with a long spawning season spanning from April to October (Drohan *et al.*, 2007). Therefore, supplementing energy towards spawning through body stores relaxes the requirement of adequate energy intake through the diet, but also does not constrict the amount of available energy towards spawning to be determined months before spawning as *C. striata* migrate inshore.

Under the premise that NS *C. striata* are mixed breeders, the regional differences in energetic values of NS *C. striata* could be explained by different feeding conditions throughout the distribution. NS *C. striata* are generalist feeders that ingest a variety of prey consisting of crustaceans, molluscs, bivalves and zooplankton (Garrison & Link, 2000; Steimle & Figley, 1996). Food limitation may not exist during the spawning season but energetic supply could be limited by nutritional quality. For example, NS *C. striata* in the Gulf of Maine had a less varied diet and, subsequently, lower condition than fish collected in Southern New England (McMahan *et al.*, 2020). Variation in the diet or reliance on single prey items can lead to notable effects on fish nutrition. For example, documented cases of salmonids experiencing thiamine deficiencies that subsequently led to reproductive failure are likely caused by consuming a diet primarily of clupeids (Fisher *et al.*, 1996; Keinänen *et al.*, 2018). In a spawning experiment, Southern flounder (*Paralichthys lethostigma*) fed a diet with high docosahexaenoic acid (an omega-3 fatty acid) still supplemented hepatic and somatic stores towards egg production, potentially due to a lack of other essential fatty acids in the diet (Burns & Fuiman, 2020). This is notable because *C. striata* dietary lipid and fatty acid intake has been shown to affect

fertilization success and egg quality (Bentley *et al.*, 2009). Altogether, with some reliance on food supply during spawning, regional differences in diet could lead to changes in energy allocation and, subsequently, reproductive output.

A notable difference between spawning locations for NS *C. striata* is the relative distance required to migrate there from overwintering grounds located along the continental shelf edge of the southeastern portion of the US Northeast shelf (Moser & Shepherd, 2008), leading to a gradient of minimal to no migration in the south to a longer migration (~400-500km) to the north. In our study, NS *C. striata* in the northern locations began spawning at lower energy reserves, apparent in both muscle and liver tissues, which are suggested to be dominant energy stores for NS *C. striata* (La Rosa *et al.*, 2020; Wuenschel *et al.*, 2013). In preparation for pre-spawning migrations, some fish store more energy to match the energetic demands of migration, which allows fish with differing migration distances to be similar energetically upon arrival to the spawning grounds (Gaillard *et al.*, 2015; Hendry & Berg, 1999). In other cases, fish can allocate more energy towards reproduction upon arrival to the spawning grounds (Glebe & Leggett, 1981). However, in the two-year period we studied, NS *C. striata* that migrate farther arrived at the spawning grounds with lower energy reserves and were unable to recover energy stores through the diet; these fish also had lower reproductive energy. Continued monitoring for NS *C. striata* in the northern portion of their range would provide additional insight into the frequency that fish enter spawning grounds in low condition and how this may impact reproductive development.

Differences in energy allocation across the distribution and between sexes may also be influenced by the fact that *C. striata* are protogynous hermaphrodites, changing

sex from female to male. In the Southeastern (SES) stock, *C. striata* reach peak fecundity at intermediate sizes instead of the largest sizes, likely due to a change in energetic allocation towards growth prior to sex-transition (Klibansky & Scharf, 2017), which has also been found for other protogynous fish species (Gamboa-Salazar *et al.*, 2020). Peak fecundity at intermediate sizes contrasts with the typical relationship of increasing female size can lead to higher fecundity (Hixon *et al.*, 2014). Therefore, relationships between growth and reproduction may differ as fish age because these dynamics suggest that at some point, fish shift a higher proportion of energy allocation towards growth and/or storage instead of reproduction which would be advantageous after transitioning to male. The factors leading to sexual transition at the individual level are not well known but likely include size, age, energetic status, densities of males, and mating system (e.g. harem, lek, aggregation) all of which may vary across a distribution. While we did collect a few individuals that were in transition, we did not explore energetics in these fish due to small sample sizes and because energetics of transition were not a focus of this study. Further investigation of regional differences in size/age at transition, mating systems, and sex ratios is needed.

A notable trend in energetic allocation of NS *C. striata* throughout their distribution was the significantly lower somatic and reproductive energetic values in MA fish. There are several possible explanations for this result. To start, and as mentioned above, NS *C. striata* migrating to the northern portion of their distribution have a longer migration, and appear to arrive in lower energy status that cannot be recovered before spawning. MA fish also have a shorter spawning season and to match the cumulative energy output as seen in DE fish, they would need to double their daily GTE output

(assuming similar spawning frequency). Next, larger body sizes are advantageous for longer migrations both for swimming energy efficiency and capacity to store energy (Slotte, 1999). NS *C. striata* exhibit some site fidelity (Moser & Shepherd, 2008), which suggests MA fish likely return to the same spawning region the following year. Therefore, NS *C. striata* in MA would benefit by allocating some energy towards somatic growth during the summer, which could be at the cost of gonad development. Also, NS *C. striata* biomass has been increasing in the northern regions leading to higher population density in the MA region. Density dependence effects are known to affect growth and fecundity for a number of fish including the round goby (*Neogobius melanostomus*; Gutowsky and Fox, 2012; Houston *et al.*, 2014), largemouth bass (*Micropterus salmoides*; Pritt *et al.*, 2020), and European anchovy (*Engraulis encrasicolus*; Basilone *et al.*, 2020). High population density in the MA region could therefore negatively affect energy allocation and reproductive output. Finally, there could be dietary differences throughout the range as has been seen in NS *C. striata* from Southern New England and northward (McMahan *et al.*, 2020), affecting energetic intake and allocation. Altogether, the low energetic status of MA fish could be due to a combination of abiotic and biotic factors.

While there were intraspecific differences across the distribution of NS *C. striata*, their energy allocation patterns across the distribution were suitable for spawning at higher latitudes where productivity is pulsed. Specifically, NS *C. striata* utilized both endogenous and exogenous energy sources during spawning and maintained high gonad energetic output, as compared to fish with protracted spawning seasons (Alonso-Fernández & Saborido-Rey, 2012). Spawning strategies and energy allocation in NS *C.*

striata may differ from other stocks, the SES and Gulf of Mexico (GOMexS) stocks, due to differences in location and population dynamics. SES *C. striata* are non-migratory (Watanabe, 2011) and spawn from March to May with potentially a secondary spawning period in September to October (Wenner *et al.*, 1986). Notably, SES *C. striata* have lower GSI than NS *C. striata* (~2-3; Link, 1980 vs ~6-8 Slesinger *et al.*, 2021). Across the distribution of the SE stock, variation within the population also exists within size at age in males and females (McGovern *et al.*, 2002). The GOMex stock are also non-migratory and spawn from December to April (Hood *et al.* 1994). GOMexS *C. striata* grow faster and have shorter lifespans than SES and NS *C. striata* (Hood *et al.* 1994). Between the three stocks, NS *C. striata* are the only fish to seasonally migrate, which may require differing energy allocation strategies prior to and post spawning. To our knowledge, there are no studies focused on the dynamics of energy allocation throughout a spawning season of SES and GOMexS *C. striata*. However, based on previous studies, we would speculate SES and GOMexS *C. striata* are predominantly income breeders and energetic analyses would reflect maintained somatic energy stores throughout spawning. Future studies on the energetic allocation in *C. striata* throughout the entire range would provide information important for the species as a whole and add context to the results in this study.

Study limitations led to NS *C. striata* collections spanning across two sampling years, where NJ and MA were sampled in 2018 and DE and VA sampled in 2019, potentially leading to regional differences reflecting interannual variances in energetics. An in-depth discussion on this study limitation can be found in Slesinger *et al.* (2021). In short, ocean conditions were similar across the two years and the timing of peak

spawning corroborated with other studies of NS *C. striata*, but interannual differences between NS *C. striata* energetics and reproductive output could still have occurred. For the northern regions, the trend of lower energetics from south to north is reflected in a comparison between NJ and MA (i.e. see Table 4.5). For the southern regions, there was an opposite trend, but it should be noted that sampling in VA was challenging (see Slesinger *et al.* (2021) for discussion). Substantial variation in estimated annual fecundity has been documented for SES *C. striata* (Klibansky & Scharf, 2017), suggesting the species has considerable flexibility in annual energy allocation to reproduction. Time-series of fecundity and energetics data are needed to fully understand the drivers and pathways regulating reproductive potential. In the future, additional sampling can help resolve potential interannual differences in NS *C. striata* energetics. Nonetheless, these data provide a snapshot into potential energetic conditions NS *C. striata* can experience throughout their range, and may serve as window into interannual differences seen in NS *C. striata* recruitment. For example, years with strong cohorts of NS *C. striata* can arise from spatially heterogeneous production, such as the 2011 year class for which a majority of age-0 fish were from north of the Hudson Canyon, and could also have been driven by warm winter conditions of 2012 (Miller *et al.*, 2016). Therefore, recruitment success can occur unevenly throughout the range, and our data provide evidence that there are major differences in adult energetics and reproductive potential throughout the distribution. While this would not affect the current interpretation of the data, due to time constraints, we did not dissect nor measure the energetics of the viscera, another potential storage depot for *C. striata*, particularly as other sites reach capacity (Wuenschel *et al.*, 2013). While we may have overlooked a potential energy source that could differ regionally, we

found similar trends in liver, muscle, and gonad across the regions. Differences in viscera energy could explain higher gonad energetics in some of the fish; however, this information would likely be additive to liver energetics as fish with higher gonad energy typically had higher liver energy.

Overall, we found regional differences in NS *C. striata* energy allocation associated with differences seen in reproductive energy investment and output. Our data suggest that NS *C. striata* closer to the centre of their geographic range had higher energy allocation towards spawning than those from more northern locations where abundances have increased recently. While not directly tested in this study, there are multiple sources of regional differences that can give rise to the energetic dissimilarities including abiotic factors (i.e. temperature), migration distance, diet, and density dependence. That these regional drivers may affect energy allocation towards reproduction is important as NS *C. striata* are managed as one stock with regional quota differences apportioned by biomass. As ocean warming continues along the US Northeast Shelf (Chen *et al.*, 2020), and NS *C. striata* centre of biomass expands northward (Kleisner *et al.*, 2017), it is important to address the interaction between shifting biomass, where a higher proportion of fish are spawning further north along the shelf, and potential energetic limitations or benefits at that location. Ocean warming can occur at different rates throughout seasons, and the view of longer migration distances as a result of summer warming assumes a constant winter temperature. However, should there be increased winter warming opening available habitat further inshore and north, this may reduce the final migration distance, or lead to continued separation of the species which usually mix during the winter. Finally, this research is focused on a single species of fish but has implications for other

species with wide latitudinal distributions and/or pre-spawning migrations, as it is apparent that differences throughout the distribution of this fish can lead to substantial dissimilarities in energetic allocation and reproduction which should be considered for future management, especially under continued ocean warming.

4.6 ACKNOWLEDGEMENTS

We would like to acknowledge Anthony Vastano for methodology guidance; Joe Langan for statistical support; Rutgers University undergraduates Emma Huntzinger, Aviva Lerman, Karolina Zbaski, Jillian Devita, Zakqary Roy, Timothy Stolarz, Sophia Berezin, and Jacob Dale for assistance with lipid extractions; Zöe Kitchell, Lauren Cook, Jacquelyn Veatch, Zach Feiner, and Nick Battista for helpful and productive discussions; Olaf Jensen for laboratory space and equipment used during extractions; and Lora McGuinness for building and safety support, especially through the thick of COVID-19. This research was supported, in part, by the National Oceanic and Atmospheric Administration (NOAA) Office of Oceanic and Atmospheric Research (OAR), Coastal and Ocean Climate Applications (COCA) Program (NA150AR4310119).

4.7 REFERENCES

- Aho, K., Derryberry, D., & Peterson, T. (2014). Model selection for ecologists: the worldviews of AIC and BIC. *Ecology*, *95*, 631–636.
- Alexander, R. M. (1998). When is migration worthwhile for animals that walk, swim or fly? *Journal of Avian Biology*, *29*, 387–394.
- Alonso-Fernández, A., & Saborido-Rey, F. (2012). Relationship between energy allocation and reproductive strategy in *Trisopterus luscus*. *Journal of Experimental Marine Biology and Ecology*, *416–417*, 8–16.
- Aristizabal, E. O. (2007). Energy investment in the annual reproduction cycle of female red porgy, *Pagrus pagrus* (L.). *Marine Biology*, *152*, 713–724.
- Basilone, G., Ferreri, R., Barra, M., Bonanno, A., Pulizzi, M., Gargano, A., ... Aronica,

- S. (2020). Spawning ecology of the European anchovy (*Engraulis encrasicolus*) in the Strait of Sicily: Linking variations of zooplankton prey, fish density, growth, and reproduction in an upwelling system. *Progress in Oceanography*, *184*, 102330.
- Bell, R. J., Richardson, D. E., Hare, J. A., Lynch, P. D., & Fratantoni, P. S. (2015). Disentangling the effects of climate, abundance, and size on the distribution of marine fish: an example based on four stocks from the Northeast US shelf. *ICES Journal of Marine Science*, *72*, 1311–1322.
- Bentley, C. D., Watanabe, W. O., Rezek, T. C., & Seaton, P. J. (2009). Preliminary investigations on the effects of dietary lipid on the spawning performance and egg quality of black sea bass *Centropristis striata* L. *Aquaculture Research*, *40*, 1873–1883.
- Bowen, B. W., & Avise, J. C. (1990). Genetic structure of Atlantic and Gulf of Mexico populations of sea bass, menhaden, and sturgeon: Influence of zoogeographic factors and life-history patterns. *Marine Biology*, *107*, 371–381.
- Brown-Peterson, N. J., Wyanski, D. M., Saborido-Rey, F., Macewicz, B. J., & Lowerre-Barbieri, S. K. (2011). A standardized terminology for describing reproductive development in fishes. *Marine and Coastal Fisheries*, *3*, 52–70.
- Brown, M., & Murphy, B. R. (2004). Seasonal dynamics of direct and indirect condition indices in relation to energy allocation in largemouth bass *Micropterus salmoides* (Lacepede). *Ecology of Freshwater Fish*, *13*, 23–36.
- Buehler, D. M., & Piersma, T. (2008). Travelling on a budget: Predictions and ecological evidence for bottlenecks in the annual cycle of long-distance migrants. *Philosophical Transactions of the Royal Society B: Biological Sciences*, *363*, 247–266.
- Bunnell, D. B., & Marschall, E. A. (2003). Optimal energy allocation to ovaries after spawning. *Evolutionary Ecology Research*, *5*, 439–457.
- Burns, C. M., & Fuiman, L. A. (2020). Determining the position of southern flounder *Paralichthys lethostigma* on the reproductive energy allocation spectrum using an essential fatty acid as a maternal dietary biomarker. *Environmental Biology of Fishes*, *103*, 1137–1148.
- Chen, Z., Kwon, Y. O., Chen, K., Fratantoni, P., Gawarkiewicz, G., & Joyce, T. M. (2020). Long-term SST variability on the Northwest Atlantic continental shelf and slope. *Geophysical Research Letters*, *47*, 1–11.
- Cook, D., Herbert, N., & Jerrett, A. (2021). Growth and energy storage responses vary seasonally in the Australasian snapper *Chrysophrys auratus* with only modest changes in aerobic scope. *Marine Ecology Progress Series*, *659*, 199–217.
- Cribari-Neto, F., & Zeileis, A. (2010). Beta Regression in R. *Journal of Statistical Software*, *34*, 1–24.
- Dawson, A. S., & Grimm, A. S. (1980). Quantitative seasonal change in the protein, lipid and energy content of the carcass, ovaries and liver of adult female plaice, *Pleuronectes platessa*. *Journal of Fish Biology*, 493–504.
- Domínguez-Petit, R., Saborido-Rey, F., & Medina, I. (2010). Changes of proximate composition, energy storage and condition of European hake (*Merluccius merluccius*, L. 1758) through the spawning season. *Fisheries Research*, *104*, 73–82.
- Drohan, A. F., Manderson, J. P., & Packer, D. B. (2007). Essential Fish Habitat Source Document: Black Sea Bass, *Centropristis striata*, life history and habitat

- characteristics, 2nd edition. *NOAA Tech Memo NMFS NE 200*, 68 p.
- Feiner, Z. S., Wang, H. Y., Einhouse, D. W., Jackson, J. R., Rutherford, E. S., Schelb, C., ... Höök, T. O. (2016). Thermal environment and maternal effects shape egg size in a freshwater fish. *Ecosphere*, 7.
- Finstad, A. G., Berg, O. K., Langeland, A., & Lohrmann, A. (2002). Reproductive investment and energy allocation in an alpine Arctic charr, *Salvelinus alpinus*, population. *Environmental Biology of Fishes*, 65, 63–70.
- Fiorin, R., Malavasi, S., Franco, A., & Franzoi, P. (2007). Comparative energy allocation in two sympatric, closely related gobies: The black goby *Gobius niger* and the grass goby *Zosterisessor ophiocephalus*. *Journal of Fish Biology*, 70, 483–496.
- Fisher, J. P., Fitzsimons, J. D., Combs, G. F. J., & Spitsbergen, J. M. (1996). Naturally occurring thiamine deficiency causing reproductive failure in Finger Lakes Atlantic salmon and Great Lakes lake trout. *Transactions of the American Fisheries Society*, 125, 167–178.
- Folch, J., Lees, M., & Stanley, G. H. S. (1957). A simple method for the isolation and purification of total lipids from animal tissues. *Journal of Biological Chemistry*, 226, 497–509.
- Gaillard, M., Bernatchez, L., Tremblay, R., & Audet, C. (2015). Regional variation in energy storage strategies in American glass eels from Eastern Canada. *Comparative Biochemistry and Physiology -Part A : Molecular and Integrative Physiology*, 188, 87–95.
- Gamboa-Salazar, K. R., Wyanski, D. M., Buble, W. J., & Klibansky, N. (2020). Effects of age and size on spawning and egg production in gag and scamp grouper off the southeastern United States. *ICES Journal of Marine Science*, 77, 290–299.
- Garrison, L., & Link, J. S. (2000). Fishing effects on spatial distribution and trophic guild structure of the fish community in the Georges Bank region. *ICES Journal of Marine Science*, 57, 723–730.
- Glebe, B. D., & Leggett, W. C. (1981). Latitudinal Differences in Energy Allocation and Use During the Freshwater Migrations of American Shad (*Alosa sapidissima*) and Their Life History Consequences. *Canadian Journal of Fisheries and Aquatic Sciences*, 38, 806–820.
- Gray, I. E., & Cerase-Vivas, M. J. (1963). The circulation of surface waters in Raleigh Bay, North Carolina. *Limnology and Oceanography*, 8, 330–337.
- Gutowsky, L. F. G., & Fox, M. G. (2012). Intra-population variability of life-history traits and growth during range expansion of the invasive round goby, *Neogobius melanostomus*. *Fisheries Management and Ecology*, 19, 78–88.
- Hendry, A. P., & Berg, O. K. (1999). Secondary sexual characters, energy senescence, and the cost of reproduction sockeye salmon. *Canadian Journal of Zoology*, 77, 1663–1675.
- Henken, A. M., Lucas, H., Tijssen, P. A. T., & Machiels, M. A. M. (1986). A comparison between methods used to determine the energy content of feed, fish and faeces samples. *Aquaculture*, 58, 195–201.
- Hiramatsu, N., Matsubara, T., Weber, G. M., Sullivan, C. V., & Hara, A. (2002). Vitellogenesis in aquatic animals. *Fisheries*, 68, 694–699.
- Hixon, M. a, Johnson, D. W., & Sogard, S. M. (2014). Structure in Fishery Populations. *ICES Journal of Marine Science*, 71, 2171–2185.

- Hoey, J., McCormick, M. I., & Hoey, A. S. (2007). Influence of depth on sex-specific energy allocation patterns in a tropical reef fish. *Coral Reefs*, *26*, 603–613.
- Houston, B. E., Rooke, A. C., Brownscombe, J. W., & Fox, M. G. (2014). Overwinter survival, energy storage and reproductive allocation in the invasive round goby (*Neogobius melanostomus*) from a river system. *Ecology of Freshwater Fish*, *23*, 224–233.
- Jørgensen, C., Dunlop, E. S., Opdal, A. F., & Fiksen, Ø. (2008). The evolution of spawning migrations: State dependence and fishing-induced changes. *Ecology*, *89*, 3436–3448.
- Jørgensen, E. H., Johansen, S. J. S., & Jobling, M. (1997). Seasonal patterns of growth, lipid deposition and lipid depletion in anadromous Arctic charr. *Journal of Fish Biology*, *51*, 312–326.
- Keinänen, M., Käkälä, R., Ritvanen, T., Pönni, J., Harjunpää, H., Myllylä, T., & Vuorinen, P. J. (2018). Fatty acid signatures connect thiamine deficiency with the diet of the Atlantic salmon (*Salmo salar*) feeding in the Baltic Sea. *Marine Biology*, *165*, 1–17.
- Kindsvater, H. K., Braun, D. C., Otto, S. P., & Reynolds, J. D. (2016). Costs of reproduction can explain the correlated evolution of semelparity and egg size: Theory and a test with salmon. *Ecology Letters*, *19*, 687–696.
- Kleisner, K. M., Fogarty, M. J., McGee, S., Hare, J. A., Moret, S., Perretti, C. T., & Saba, V. S. (2017). Marine species distribution shifts on the U.S. Northeast Continental Shelf under continued ocean warming. *Progress in Oceanography*, *153*, 24–36.
- Klibansky, N., & Scharf, F. S. (2015). Success and failure assessing gonad maturity in sequentially hermaphroditic fishes: Comparisons between macroscopic and microscopic methods. *Journal of Fish Biology*, *87*, 930–957.
- Klibansky, N., & Scharf, F. S. (2017). Fecundity peaks prior to sex transition in a protogynous marine batch spawning fish, black sea bass (*Centropristis striata*). *ICES Journal of Marine Science*, *75*, 1042–1053.
- Lenth, R. (2020). emmeans: Estimated Marginal Means, aka Least-Squares Means. *R Package Version 1.4.7*, <https://CRAN.R-project.org/package=emmeans>.
- Link, G. W. J. (1980). Age, growth, reproduction, feeding, and ecological observations of the three species of *Centropristis* (Pisces: Serranidae) in North Carolina waters. (Doctoral thesis: University of North Carolina at Chapel Hill). Retrieved from <https://www.proquest.com/openview/0445cc5988d252d2957d7ff17da780c7/1?pq-origsite=gscholar&cbl=18750&diss=y>
- Love, R. M. (1980). *The Chemical Biology of Fishes*, vol. 2. London: Academic Press.
- McBride, R. S., Somarakis, S., Fitzhugh, G. R., Albert, A., Yaragina, N. A., Wuenschel, M. J., ... Basilone, G. (2015). Energy acquisition and allocation to egg production in relation to fish reproductive strategies. *Fish and Fisheries*, *16*, 23–57.
- McCartney, M. A., Burton, M. L., & Lima, T. G. (2013). Mitochondrial DNA differentiation between populations of black sea bass (*Centropristis striata*) across Cape Hatteras, North Carolina (USA). *Journal of Biogeography*, *40*, 1386–1398.
- McGovern, J. C., Collins, M. R., Pashuk, O., & Meister, H. S. (2002). Temporal and spatial differences in life history parameters of black sea bass in the Southeastern United States. *North American Journal of Fisheries Management*, *22*, 1151–1163.
- McMahan, M. D., Sherwood, G. D., & Grabowski, J. H. (2020). Geographic variation in

- life-history traits of black sea bass (*Centropristis striata*) during a rapid range expansion. *Frontiers in Marine Science*, 7, 567758.
- Mercer, L. P. (1978). The reproductive biology and population dynamics of black sea bass, *Centropristis striata*. (Doctoral Thesis: College of William and Mary—Virginia). Retrieved from <https://scholarworks.wm.edu/etd/1539616774/>.
- Miller, A. S., Shepherd, G. R., & Fratantoni, P. S. (2016). Offshore habitat preference of overwintering juvenile and adult black sea bass, *Centropristis striata*, and the relationship to year-class success. *PLoS ONE*, 11.
- Mollet, F. M., Engelhard, G. H., Vainikka, A., Laugen, A. T., Rijnsdorp, A. D., & Ernande, B. (2013). Spatial variation in growth, maturation schedules and reproductive investment of female sole *Solea solea* in the Northeast Atlantic. *Journal of Sea Research*, 84, 109–121.
- Moser, J., & Shepherd, G. R. (2008). Seasonal distribution and movement of black sea bass (*Centropristis striata*) in the Northwest Atlantic as determined from a mark-recapture experiment. *Journal of Northwest Atlantic Fishery Science*, 40, 17–28.
- Murua, H., & Saborido-Rey, F. (2003). Female reproductive strategies of marine fish species of the North Atlantic. *Journal of Northwest Atlantic Fishery Science*, 33, 23–31.
- Musick, J. A., & Mercer, L. P. (1977). Seasonal distribution of Black Sea Bass, *Centropristis striata*, in the Mid-Atlantic Bight with comments on ecology and fisheries of the species. *Trans. Amer. Fish. Soc.*, 106, 12–25.
- NEFSC (Northeast Fisheries Science Center). (2017). The 62nd northeast regional stock assessment workshop (62nd SAW). Ref. Doc. 17-03, NEFSC, Woods Hole, MA.
- Nielsen, J. R., Lambert, G., Bastardie, F., Sparholt, H., & Vinther, M. (2012). Do Norway pout (*Trisopterus esmarkii*) die from spawning stress? Mortality of Norway pout in relation to growth, sexual maturity, and density in the North Sea, Skagerrak, and Kattegat. *ICES Journal of Marine Science*, 69, 197–207.
- Nøttestad, L., Giske, J., Holst, J. C., & Huse, G. (1999). A length-based hypothesis for feeding migrations in pelagic fish. *Canadian Journal of Fisheries and Aquatic Sciences*, 56, 26–34.
- Pershing, A. J., Alexander, M. A., Hernandez, C. M., Kerr, L. A., Le Bris, A., Mills, K. E., ... Thomas, A. C. (2015). Slow adaptation in the face of rapid warming leads to collapse of the Gulf of Maine cod fishery. *Science*, 350, 809–812.
- Pritt, J. J., Zweifel, R. D., Tyszko, S. M., & Conroy, J. D. (2020). Variation in reproductive investment among Ohio reservoir largemouth bass populations. *Transactions of the American Fisheries Society*, 149, 552–564.
- R Core Team. (2019). R: A language and environment for statistical computing. R Foundation for Statistical Computing, Vienna, Austria. URL <https://www.R-project.org/>. 2019.
- La Rosa, G. A., Woodland, R. J., & Rowe, C. L. (2020). Carbon:nitrogen ratio as a proxy for tissue nonpolar lipid content and condition in black sea bass *Centropristis striata* along the Middle Atlantic Bight. *Marine Biology*, 167, 1–13.
- Roy, E. M., Quattro, J. M., & Greig, T. W. (2012). Genetic management of black sea bass: Influence of biogeographic barriers on population structure. *Marine and Coastal Fisheries*, 4, 391–402.
- dos Santos, R. N., Amadio, S., & Ferreira, E. J. G. (2010). Patterns of energy allocation

- to reproduction in three Amazonian fish species. *Neotropical Ichthyology*, 8, 155–161.
- Schultz, E. T., & Conover, D. O. (1997). Latitudinal differences in somatic energy storage: Adaptive responses to seasonality in an estuarine fish (Atherinidae: *Menidia menidia*). *Oecologia*, 109, 516–529.
- Slesinger, E., Andres, A., Young, R., Seibel, B., Saba, V., Phelan, B., ... Saba, G. (2019). The effect of ocean warming on black sea bass (*Centropristis striata*) aerobic scope and hypoxia tolerance. *PLoS ONE*, 14, 1–22.
- Slesinger, E., Jensen, O. P., & Saba, G. (2021). Spawning phenology of a rapidly shifting marine fish species throughout its range. *ICES Journal of Marine Science*, 78, 1010–1022.
- Slotte, A. (1999). Effects of fish length and condition on spawning migration in Norwegian spring spawning herring (*Clupea harengus* L. *Sarsia*, 84, 111–127.
- Steimle, F. W., & Figley, W. (1996). The importance of artificial reef epifauna to black sea bass diets in the Middle Atlantic Bight. *North American Journal of Fisheries Management*, 16, 433–439.
- Treberg, J. R., Killen, S. S., MacCormack, T. J., Lamarre, S. G., & Enders, E. C. (2016). Estimates of metabolic rate and major constituents of metabolic demand in fishes under field conditions: Methods, proxies, and new perspectives. *Comparative Biochemistry and Physiology -Part A : Molecular and Integrative Physiology*, 202, 10–22.
- Watanabe, W. O. (2011). Species Profile: Black Sea Bass. *SRAC Publication No. 7207*, 1–16.
- Wenner, C. A., Roumillat, W. A., & Waltz, C. W. (1986). Contributions to the life history of black sea bass, *Centropristis striata*, off the southeastern united states. *Fishery Bulletin*, 84, 723–742.
- Wood, S. (2013). Package ‘mgcv’ version 1.8-24. R. Package. 2013.
- Wootton, R. J. (1984). Introduction: tactics and strategies in fish reproduction. In G. W. Potts & R. J. Wootton (Eds.), *Fish Reproduction: strategies and tactics* (pp. 1–12). New York: Academic Press.
- Wuenschel, M. J., McBride, R. S., & Fitzhugh, G. R. (2013). Relations between total gonad energy and physiological measures of condition in the period leading up to spawning: Results of a laboratory experiment on black sea bass (*Centropristis striata*). *Fisheries Research*, 138, 110–119.

4.8 TABLES

Table 4.1 Sample sizes of fish by region, sex, and maturity stage.

N is the total number of fish per region by sex.

Region	Sex	Maturity Stage				n
		DEV	MAT	SPT	REST	
MA	F	10	23	6	5	44
	M	5	10	7	1	23
NJ	F	23	18	6	4	51
	M	13	9	5	3	30
DE	F	9	17	14	0	40
	M	7	15	17	1	40
VA	F	4	16	7	0	27
	M	8	7	11	0	26

Table 4.2 BIC values used to compete the null and regional models.

Bold values indicate the lowest BIC and the chosen model

Tissue	Sex	Model	Measurement		
			Lipid (g/g dw)	ED (kJ/g ww)	TE (kJ)
Muscle	All	Null	-1554.69	262.97	NA
		Regional	-1540.56	215.11	NA
Liver	F	Null	-225.20	652.30	1376.39
		Regional	-237.98	646.75	1364.76
	M	Null	-195.60	446.64	1006.90
		Regional	-198.83	449.71	1004.27
Gonad	F	Null	-549.70	485.49	1642.10
		Regional	-566.83	478.55	1628.76
	M	Null	-518.79	129.61	996.12
		Regional	-522.34	141.43	999.10

Table 4.3 Model results for the regional GLMs.

Model results with model coefficients and p-values; <0.05 = *, <0.01 = **, <0.001 = ***.

A - indicates region was not selected for in the specific model. The intercept is set as

DEV for maturity stage and VA for region.

Tissue	Sex	Model	n	Intercept	Weight	SPC	SPT	REST	DE	NJ	MA
Muscle	All	Lipid	281	-2.739	0.000***	-0.078*	-0.157***	-0.220**	-	-	-
		ED	281	0.194	0.000	0.005*	0.007**	-0.002	-0.003	0.012***	0.014***
Liver	F	Lipid	162	-0.524	0.000	-0.243*	-0.574***	0.012	-0.046	-0.326**	-0.660***
		ED	162	0.114	0.000	0.016**	0.017**	-0.009	0.001	0.019**	0.026***
		TE	162	3.065	0.003***	-0.212*	-0.670***	-0.404*	-0.058	-0.425***	-0.522***
	M	Lipid	119	-0.749	0.000	0.055	0.017	0.140	-0.386***	-0.452***	-0.552***
	ED	119	0.122	0.000	0.003	0.003	0.009	-	-	-	
	TE	119	2.945	0.002***	-0.214	-0.299*	-0.732**	-0.229	-0.459**	-0.540**	
Gonad	F	Lipid	162	-1.414	0.000	0.055	-0.505***	-0.912***	0.153*	-0.176**	0.006
		ED	162	0.137	0.000	0.020***	0.043***	0.062***	-0.004	0.021**	0.015*
		TE	162	3.744	0.003***	0.134	-1.742***	-2.589***	0.161	-0.456**	-0.603***
	M	Lipid	119	-1.826	0.000	0.000	0.045	-0.124	0.171***	0.174***	0.182***
	ED	119	0.275	0.000	-0.003	-0.033***	-0.069***	-	-	-	
	TE	119	3.157	0.001***	0.171	-0.992***	-2.830***	-	-	-	

Table 4.4 GAM results for each model.

Model results with the coefficients for parametric values and estimated degrees of freedom for smooth terms and whole model deviance explained. For the parametric terms, VA is the intercept.

p-values; <0.05 = *, <0.01 = **, <0.001 = ***

Model	Term	VA	DE	NJ	MA	Weight	Dev. Exp
TLE female	Coef	2.614	0.219	-0.184	-0.089	0.003***	70.5%
	EDF	1.699	1.036***	1.420***	2.483**	-	
TLE male	Coef	2.568	-0.005	-0.271	-0.117	0.002***	60.9%
	EDF	1.516***	1.000*	1.048	1.963	-	
TGE female	Coef	2.485	1.225***	0.236	-0.454	0.003***	78.1%
	EDF	3.428***	2.810***	3.843***	2.067***	-	
TGE male	Coef	2.710	0.299*	-0.297*	-0.331*	0.002***	72%
	EDF	1.000***	2.615***	3.656***	1.000***	-	

Table 4.5 Liver and gonad total energy (kJ) amounts cumulative and throughout spawning.

Liver and gonad total energy (kJ) at the start and end of spawning based on 25% spawning capable criterium in Slesinger et al. 2021. Values are estimated from the seasonal GAMs. Cumulative kJ is the total energy from start to end of spawning; spawning days = the length of the spawning season based on above criterium; kJ/day provides a crude estimate of the energy usage per day for the given tissue, sex, and region.

Tissue	Sex	Region	Start (kJ)	End (kJ)	Cumulative kJ	Spawning Days	kJ/day
Liver	F	MA	23.01	17.81	1087.06	55	19.76
		NJ	26.33	20.42	1386.40	39	35.55
		DE	44.66	26.66	3385.20	96	35.26
		VA	52.24	18.31	3100.07	88	35.23
	M	MA	19.58	13.88	857.80	55	15.60
		NJ	21.18	17.55	1156.10	39	29.64
		DE	29.25	22.12	2473.39	96	25.76
		VA	40.39	18.67	2656.71	88	30.19
Gonad	F	MA	54.02	11.48	1734.37	55	31.53
		NJ	98.40	9.50	2690.65	39	68.99
		DE	176.05	29.68	11842.56	96	123.36
		VA	116.82	23.67	6639.98	88	75.45
	M	MA	25.33	10.84	956.12	55	17.38
		NJ	35.11	7.00	1235.91	39	31.69
		DE	53.89	11.67	3727.67	96	38.83
		VA	39.11	14.50	2209.80	88	25.11

4.9 FIGURES

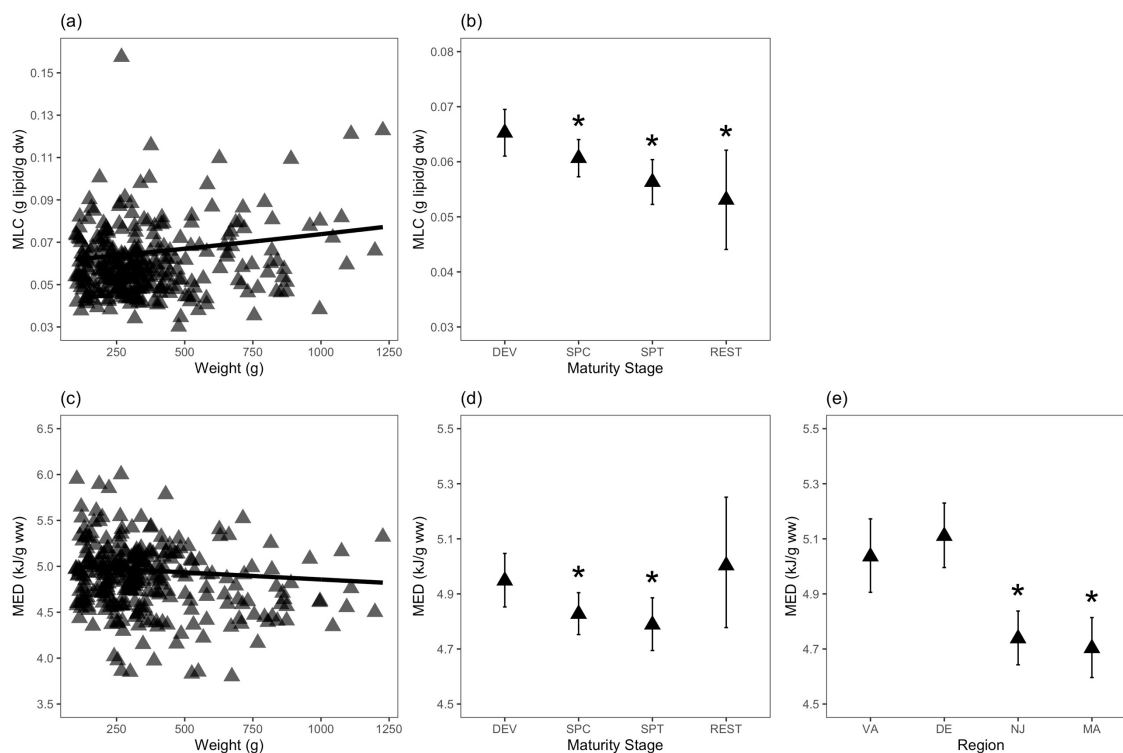


Figure 4.1 Compositional model results for muscle GLMs.

Muscle GLMs results for MLC (a-b) and MED (c-e) are shown. The model fit of weight (g) by MLC (a) and MED (c) are shown in blue with raw data points depicted in triangles. For maturity stage results (b and d) and regional results (e), the estimated marginal mean \pm standard error are plotted in triangles. For maturity stage, DEV = developing, SPC = spawning capable, SPT = spent, and REST = resting. For region, the region codes are plotted, from left to right, following the continental shelf from south to north. A * indicates a significant difference (p-value < 0.05) from the model intercepts (DEV for maturity stage and VA for region). No regional results for MLC indicate that region was not selected for in the MLC model. Female and male fish are combined in these plots.

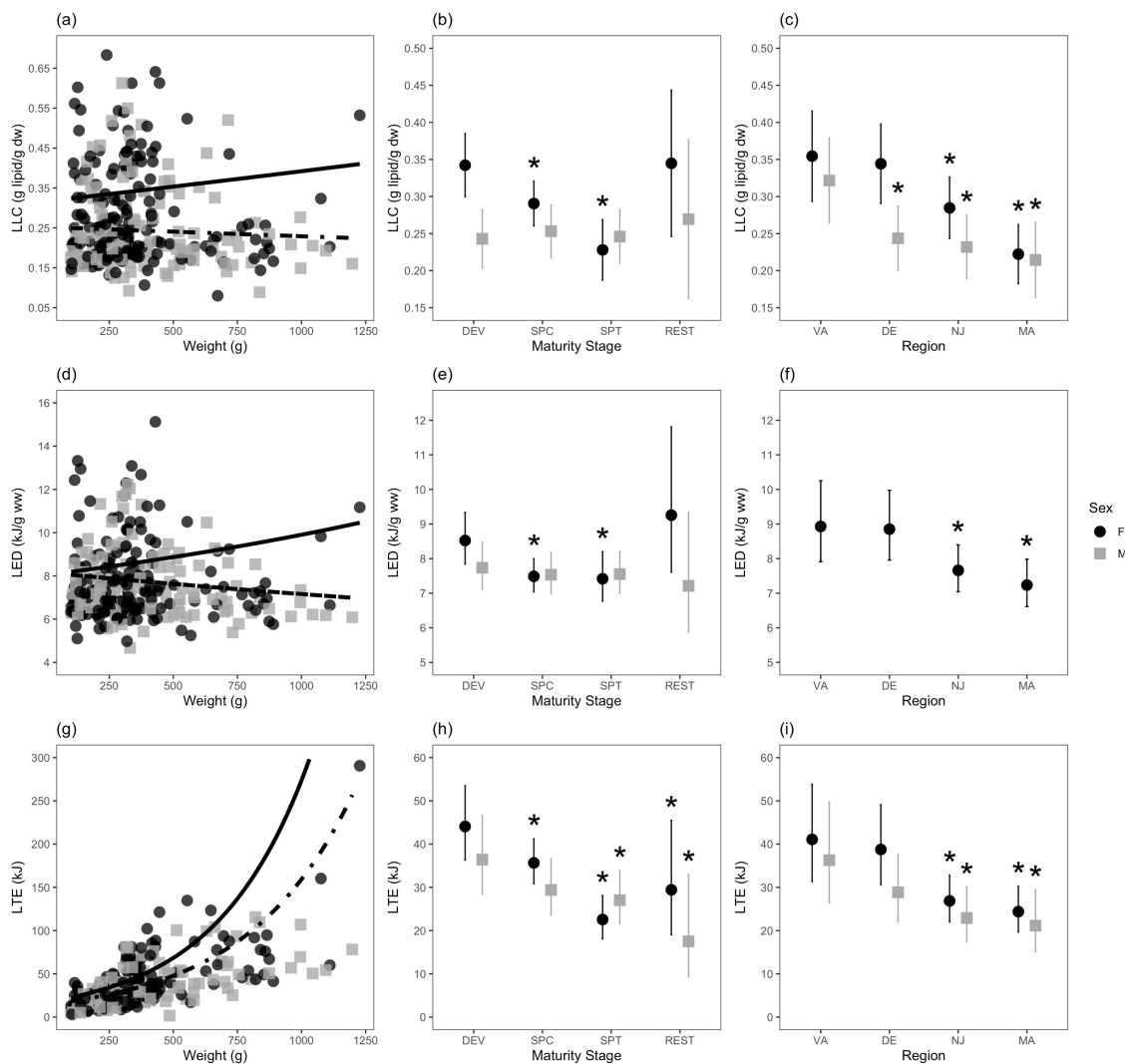


Figure 4.2 Compositional model results for liver GLMs.

Liver GLMs results for LLC (a-c), LED (d-f), and LTE (g-i) are shown. The model fit of weight (g) for LLC (a), LED (d), and LTE (g) are plotted in a solid line for female fish and dashed line for male fish. For maturity stage results (b, e, h) and regional results (c, f, i), the estimated marginal mean \pm standard error are plotted in black circles for female fish and grey squares for male fish. For maturity stage, DEV = developing, SPC = spawning capable, SPT = spent, and REST = resting. For region, the region codes are plotted, from left to right, following the continental shelf from south to north. A *

indicates a significant difference ($p\text{-value} < 0.05$) from the model intercepts (DEV for maturity stage and VA for region). Male GLMs where region was not selected are shown by an absence of regional data points plotted for male fish.

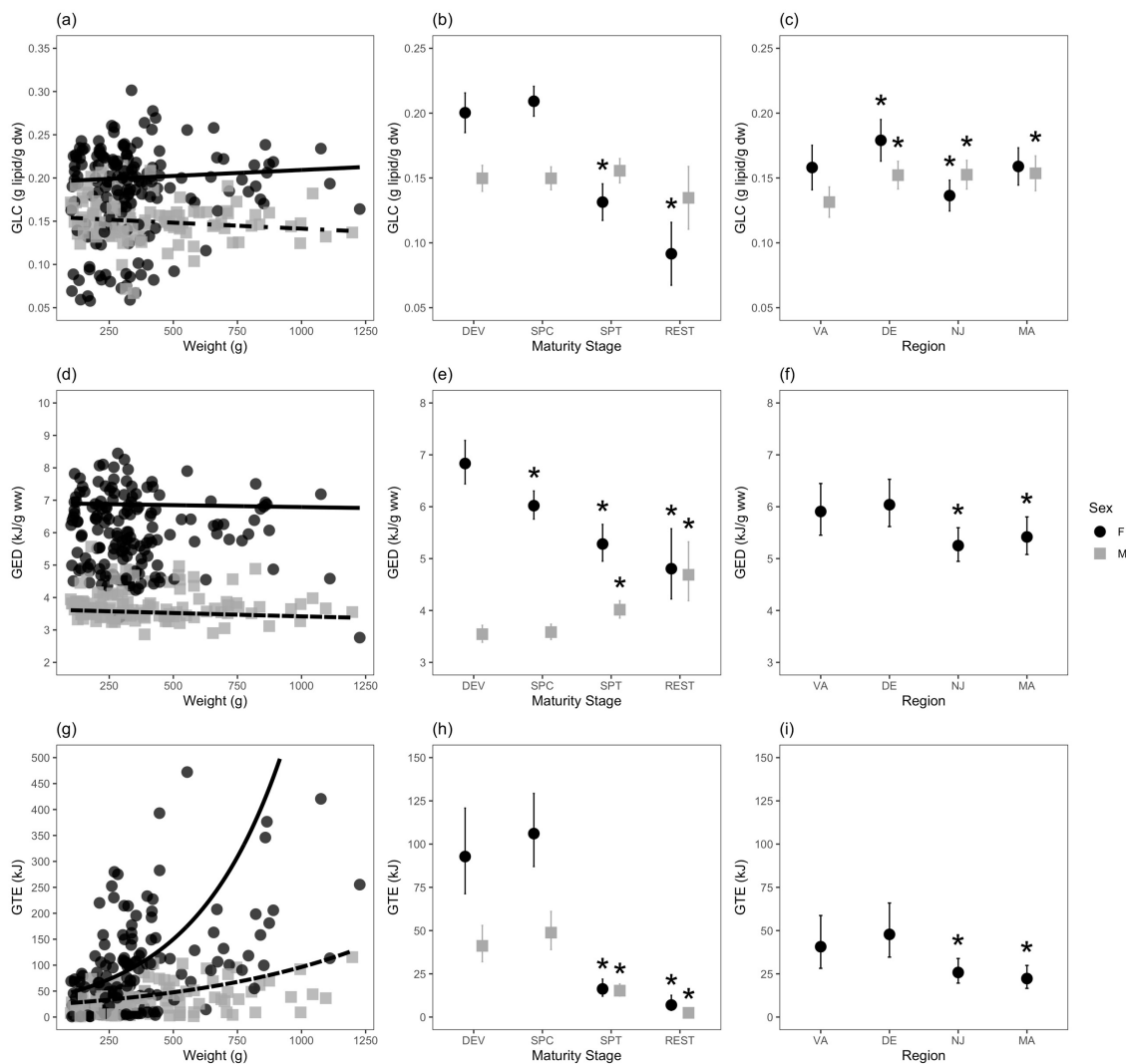


Figure 4.3 Compositional model results for gonad GLMs.

Gonad GLMs results for GLC (a-c), GED (d-f), and GTE (g-i) are shown. The model fit of weight (g) for GLC (a), GED (d), and GTE (g) are plotted in a solid line for female fish and dashed line for male fish. For maturity stage results (b, e, h) and regional results (c, f, i), the estimated marginal mean \pm standard error are plotted in black circles for female fish and grey squares for male fish. For maturity stage, DEV = developing, SPC = spawning capable, SPT = spent, and REST = resting. For region, the region codes are plotted, from left to right, following the continental shelf from south to north. A *

indicates a significant difference ($p\text{-value} < 0.05$) from the model intercepts (DEV for maturity stage and VA for region). Male GLMs where region was not selected are shown by an absence of regional data points plotted for male fish.

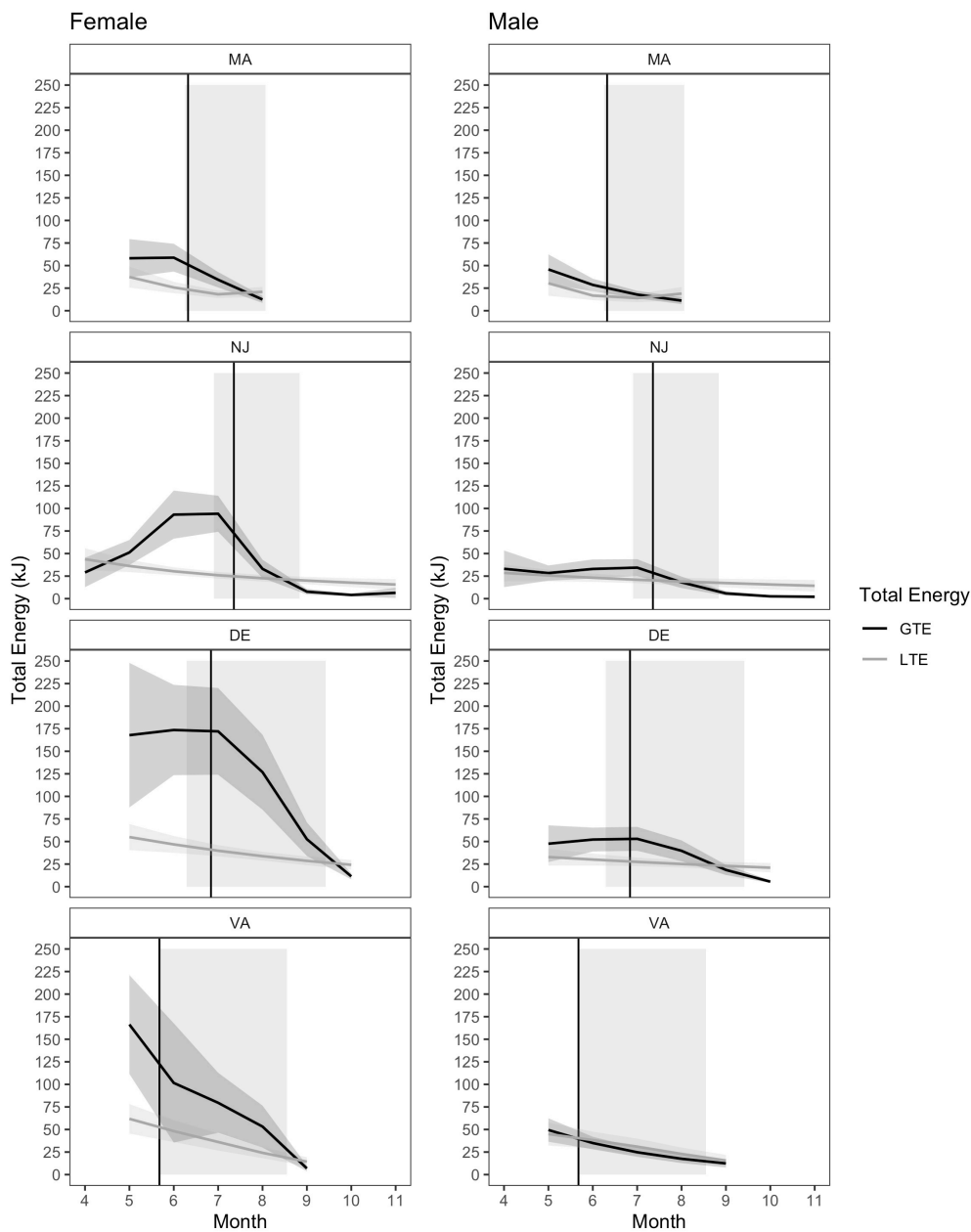


Figure 4.4 Seasonal GAM results.

Seasonal GAMs plotted by region where LTE (grey line) and GTE (black line) are shown, the shading is the 95% confidence interval, and the left column are female fish and right column are male fish. The shaded grey rectangle denotes the length of the spawning season and the solid black vertical line shows the day of peak GSI from Slesinger *et al.* 2021.

4.10 SUPPLEMENTAL INFORMATION

Table S4.1 The models used in analysis, their distribution family and link functions.

Analysis	Response variable	Model	Distribution family	Link
Compositional	LC (g lipid/g dry weight)	GLM	Beta	Logit
	ED (kJ/g wet weight)	GLM	Gamma	Inverse
	TE (kJ)	GLM	Gamma	Log
Seasonal	TLE	GAM	Gamma	Log
	TGE	GAM	Gamma	Log

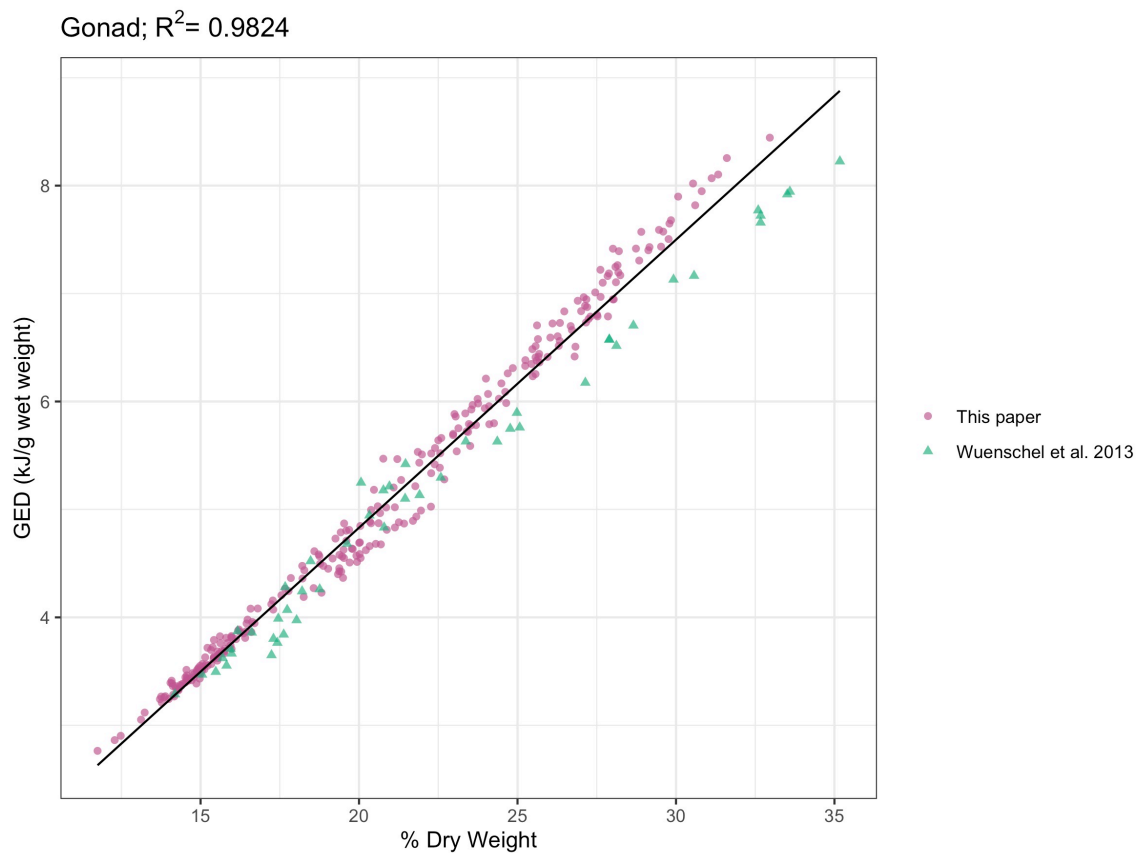


Figure S4.1 Linear trend of gonad % dry-weight and GED.

Linear trend of gonad % dry weight to GED for this paper and data from Wuenschel et al. 2013 to assess fit of our estimated ED values from those already published for *C. striata*.

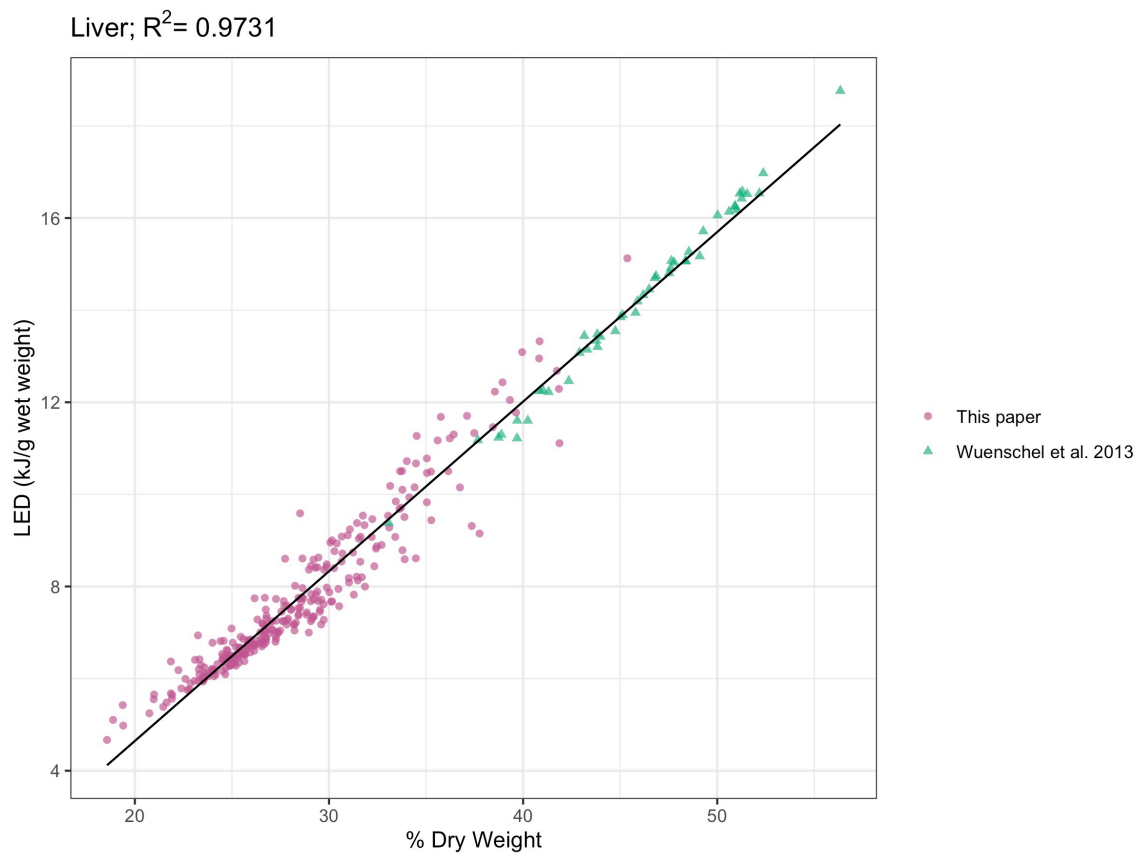


Figure S4.2 Linear trend of liver % dry-weight and LED.

Linear trend of liver % dry weight to LED for this paper and data from Wuenschel et al. 2013 to assess fit of our estimated ED values from those already published for *C. striata*.

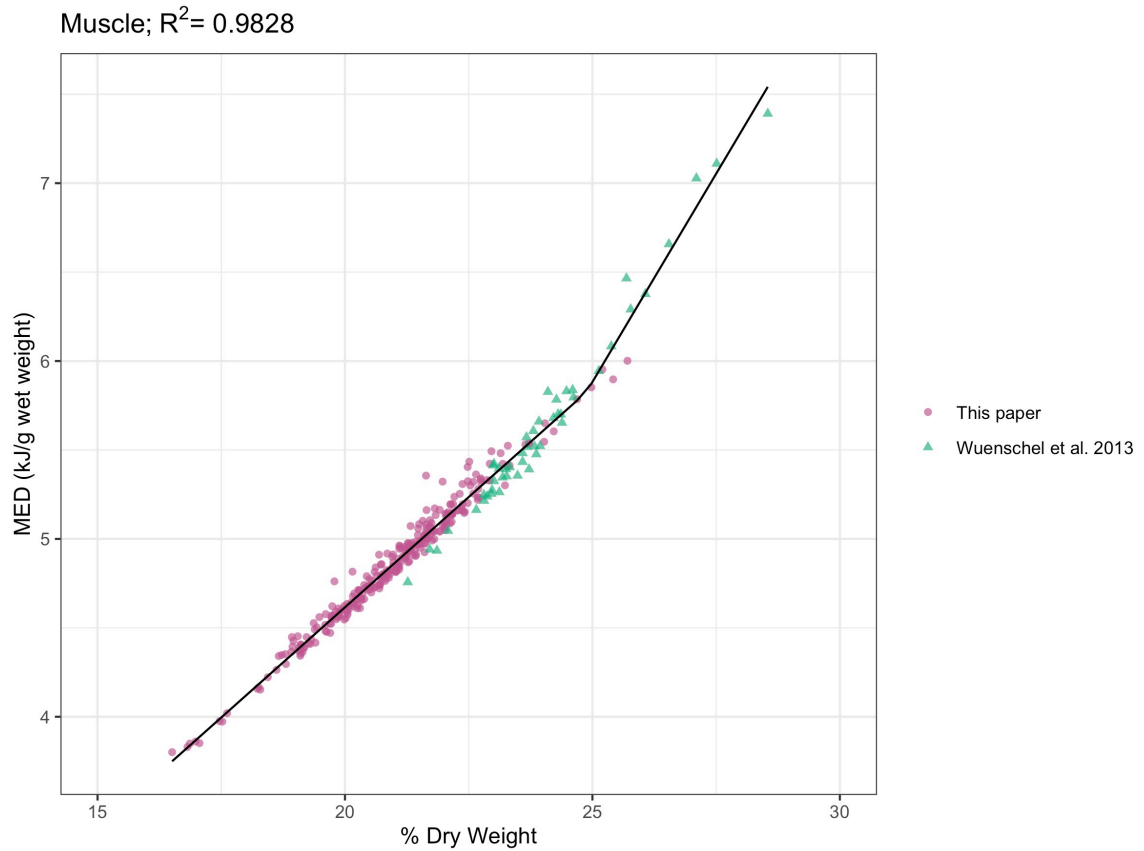


Figure S4.3 Linear trend of muscle % dry-weight and MED.

Regression of muscle % dry weight to MED, using a broken stick regression, for this paper and data from Wuenschel et al. 2013 to assess fit of our estimated ED values from those already published for *C. striata*.

CHAPTER 5: Physiologically-based assessment of historical and future changes in metabolically available habitat for US Northeast Shelf species

5.1 ABSTRACT

The US Northeast Shelf (USNES) has been experiencing rapid ocean warming, which has been touted as a major driver of shifting fish distributions throughout the shelf. Many studies link temperature to changing distributions through statistical analyses. In this study we apply species-specific physiological parameters from laboratory studies to provide a mechanistic link between this documented environmental change and organismal responses. We used the physiology-focused Metabolic Index (MI) for five USNES species (Atlantic cod, black sea bass, cunner, spiny dogfish, and summer flounder) to assess the impacts of ocean warming, providing insight into change in habitat over time and estimates of future habitat loss. Species-specific differences were used to infer the impact of various MI metrics on assessing suitable habitat and distribution shifts. From 1970 to the present, MI has been decreasing across all seasons in nearly all locations investigated. For spring and winter, this decrease may not be as problematic because a decrease in MI could also indicate that habitat is expanding for cold-intolerant species. However, for summer and fall, MI declines have and will continue to reach limiting values for all five species. Inshore/midshelf positions within the southern USNES lose the highest percentage of suitable thermal habitat, which is concerning as this coincides with spawning seasons for many fish. Overall, by using species-specific physiologically-based parameters, we were able to show the USNES has and will continue to see the loss of suitable thermal habitat.

5.2 INTRODUCTION

Anthropogenic climate change is reshaping our world. Adverse effects from climate change are becoming more frequent including catastrophic wildfires (Xu *et al.*, 2020), historic flooding (Bevacqua *et al.*, 2020), and large-scale coral reef die-offs (Ainsworth *et al.*, 2016). Within the marine environment, ocean warming has become a pervasive issue. On the first order, oceans are warming because they act as a reservoir for atmospheric warming, increasing ocean heat content (Gleckler *et al.*, 2016). Secondary factors can also contribute to continued or accelerated warming such as changes in large-scale ocean circulation patterns (Dhame *et al.*, 2020) or ocean-atmosphere climate phenomena (i.e. ENSO; Cai *et al.*, 2018). Specifically within the U.S. Northeast Shelf (USNES), which has been experiencing rapid ocean warming (Pershing *et al.*, 2015; Chen *et al.*, 2020), changes in circulation patterns between the Gulf Stream and Labrador current are notable drivers in the recent increases in temperature (Saba *et al.*, 2016; Caesar *et al.*, 2018).

Fish are ectotherms, and as such, rising ocean temperature will also increase animal body temperatures and subsequently increase metabolism and energy demands (Bennett, 1978). Warmer temperatures outside of those typically experienced by a fish can have a variety of effects with a range of severity levels. At the extremes, fish in temperatures too warm may experience higher mortality (Rodgers *et al.*, 2018) or cease feeding (Chabot *et al.*, 2016). At temperatures eliciting a less severe response, fish may experience higher metabolism which is manageable if energy demands are met through feeding (Biro *et al.*, 2007; Pörtner and Peck, 2010). If energy demands are not met, fish have to partition remaining energy stores towards metabolic maintenance, reducing

available energy for growth and reproduction (Rijnsdorp *et al.*, 2009). Temperature responses that are non-lethal but reduce life-time fitness are problematic on longer timespans as they can lead to reduced population growth. Because fish are mobile, another common response to ocean warming is migration out of suboptimal regions, leading to species distribution shifts (Pinsky *et al.*, 2013). Distribution shifts can be poleward, such as in tunas in the Western Atlantic and Eastern Pacific (Monllor-Hurtado *et al.*, 2017) and yellowfin whiting in Australia (Smith *et al.*, 2019), or deeper, like in demersal fish in the North Sea (Dulvy *et al.*, 2008). Investigating the cause and extent of species distribution shifts based on ocean warming is important for both understanding changes in ecosystems and species assemblages (Perretti *et al.*, 2017) and for avoiding future conflicts in fisheries management as fish transverse state or national boundaries (Pinsky *et al.*, 2018).

The USNES, which extends from Cape Hatteras, NC to the Gulf of Mexico, provides habitat to many ecologically and economically important marine fish species. Ocean warming along the USNES is a suggested driver of species distribution shifts, and has been reported previously (e.g. Nye *et al.*, 2009; Bell *et al.*, 2015; Kleisner *et al.*, 2017; Morley *et al.*, 2018). Notably, each of these studies focuses on distribution data from NEFSC fishery trawl surveys and the statistical relationship of abundance, biomass or presence/absence (P/A) to temperature (and sometimes additional physical parameters such as salinity or rugosity). In theory, these statistical correlations provide ranges of suitable and limiting temperatures that can be tracked over time to show recent distribution shifts and predict future impacts (Manderson *et al.*, 2011; Kohut *et al.*, 2016). However, the USNES undergoes dramatic seasonal variability that complicates the

understanding of longer climate trends in temperature (Richaud *et al.*, 2016), and can lead to highly migratory ecology. Therefore, the specific fishery data input can drastically affect estimations of thermal habitat, mostly due to the data only reflecting a snap-shot in time and space of prevailing conditions and unavoidable biases within survey designs (Nazzaro *et al.*, 2021).

Species-specific parameters derived from experiments can provide metrics that relate animal physiology to environmental temperature, and therefore provide a direct mechanistic link between temperature and impact on an organism. The Metabolic Index (MI) relates the oxygen supply of the environment to the oxygen demand of an organism and is affected by temperature through species-specific thermal sensitivities. Species-specific parameters are obtained in laboratory studies that measure P_{crit} (the minimum oxygen level required to support resting or standard metabolic rate) at a range of temperatures. From this information, MI can be calculated across a species range by obtaining *in situ* measured or modeled temperature and oxygen data. The lowest MI where species are present is defined as the MI_{crit} (Deutsch *et al.*, 2015). Usually, MI_{crit} for individual species averages around 3 indicating a limiting level for sustaining populations. For normoxic species where their $P_{c,max}$ is at an oxygen level of 21 kPa, MI is equivalent to factorial aerobic scope (maximum/standard metabolic rate; Seibel and Deutsch, 2020). Thus, the MI_{crit} translates to conditions where maximum metabolic rate capacity is at 2-5 times the standard metabolic rate, providing scope for activities beyond baseline maintenance. MI represents a metric that correlates with, and may define, distribution limits based on environmental conditions that cause MI to be at MI_{crit} or less. There is no current consensus on whether MI is the limiting agent below MI_{crit} or if MI

values above MI_{crit} provide meaningful information, especially because MI increases with decreasing temperatures without a decelerating mechanism to account for cold-intolerances. MI has successfully delineated the edges of and spatial change in habitat due to ocean warming and/or deoxygenation for fish species including Atlantic cod (Deutsch *et al.*, 2015), reef fish (Duncan *et al.*, 2020), summer flounder (Deutsch *et al.*, 2020), and Pacific anchovy (Howard *et al.*, 2020).

The purpose of this study was to investigate critical MI values for five US NES fish species (Atlantic cod, black sea bass, cunner, spiny dogfish, and summer flounder) to investigate MI critical values, changes in MI over time, and future predictions of suitable thermal habitat loss. This study focused specifically on using a physiologically-based parameter to assess the impact of ocean warming on metabolically available habitat. Fish species were selected based on those that had distribution data from fishery trawl surveys as well as parameters from laboratory physiology studies that determined P_{crit} at two or more temperatures. Cunner and Atlantic cod represented colder water species, spiny dogfish an intermediary species, and black sea bass and summer flounder represented warmer water species. In addition, these species have differing migration and seasonal habitat usage patterns, providing the opportunity to compare species-specific MI dynamics from fish with differing life histories and physiological adaptations. Altogether, this study provides an account of how MI varies across species both seasonally and throughout time, species sensitivities through MI_{crit} , and a conservative view into habitat loss into the future under continued ocean warming.

5.3 METHODS

5.3.1 Defining Strata and Regions

Temperature, oxygen, and species distribution data were initially organized at a stratum level to provide a common scale of measurement. Strata selection was first based on those designated in the NEFSC fishery trawl survey as they define distinct ecological production units, cover the domain of the USNES, and are the measurement level for the fish trawl survey data (see below). NEFSC strata were obtained from the NOAA github server (https://github.com/NOAA-EDAB/FisheryConditionLinks/tree/master/NES_BOTTOM_TRAWL_STRATA). Spatial resolutions of data sources for temperature, dissolved oxygen (DO), and species distributions were highly variable. Some smaller strata were combined to create larger sampling units to increase sample sizes of temperature and DO data within a stratum based on modifications from Walsh *et al.*, (2015) and Chen *et al.*, (2021). Specifically, smaller offshore and inshore strata were combined within the same latitudinal bands.

After strata were combined, they were further modified. First, strata were given letter codes to designate across-shelf location for inshore (I), midshelf (M) and offshore (O) regions, and number codes to designate along-shelf positions with 01-19 from south to north (Fig 5.1). Second, two NEFSC strata units spanned across (south to north) the Hudson Canyon. Due to observed differences in physical dynamics between the northern and southern flanks of the Hudson Canyon (Chant *et al.*, 2008; M05, O05, M04, and O04 in this paper; Fig. 5.1), these strata were divided accordingly, whereby the split north and south flanks were combined with their respective northern and southern counterparts.

For certain analyses (i.e. minimum MI trends) the shelf was also divided by region based on Walsh *et al.*, (2015) and Mountain, (2003). Regions included the Southern Shelf (SS), New York Bight (NYB), Southern New England (SNE), Georges Bank (GB), and Gulf of Maine (GOM). Strata were classified within these regions based on their locations (Fig S5.1).

5.3.2 Compilation of Temperature and Oxygen Data

Temperature and dissolved oxygen data, the two environmental parameter inputs for MI calculations, were mined across the USNES. Bottom temperature data were obtained from the simulations of the Northwest Atlantic Ocean in the Regional Ocean Modelling System (ROMS-NWA; Shchepetkin and McWilliams, 2005) for the period 1970-1992 and from Global Ocean Physics Reanalysis (Glorys12v1 reanalysis; Fernandez and Lellouche, 2018) for the period 1993-2019. Bottom temperature from ROMS-NWA used for the period 1970-1992 were bias-corrected because previous studies highlighted strong and consistent warm bias in bottom temperature in the cold pool region (Chen *et al.*, 2018; Chen and Curchitser, 2020). In order to bias-correct bottom temperature from ROMS-NWA, we used the monthly climatologies of observed bottom temperature from the Northwest Atlantic Ocean regional climatology (NWARC) over decadal periods from 1965 to 1994 (Seidov *et al.*, 2016a, 2016b, du Pontavice pers. comm). Bottom temperature data was available in a regular $1/10^\circ$ latitude grid and from -76.8°W to -65.5°W (longitude) and 35.5°N to 43.5°N (latitude). Based on individual cell latitude and longitude coordinates, temperature cells were assigned to specific strata and then further classified by month, season and year. Seasons were set at winter (D, J,

F), spring (M, A, M), summer (J, J, A) and fall (S, O, N). For each specific grouping, a mean temperature was calculated. The highest resolution calculation was at strata, year, and season level to make direct comparisons with the fishery data that were collected during spring and fall seasons. Using these groupings, we plotted seasonal variation in mean temperature across the USNES (Fig S5.2) and calculated the strata-based linear trend in temperature change over time (1970-2019; Fig S5.3).

Dissolved oxygen data from 1970 to 2019 across the spatial domain of the USNES were retrieved from CTD casts that were accessed through the NCEI database, MARMAP survey, and BCO-DMO database. DO units from these data sources were dissimilar, and all were converted into partial pressure (PO_2) if they were not already reported as PO_2 . Only PO_2 data that passed quality control reported in the data were used in analysis. Next, bottom PO_2 was defined as the deepest measurement from a CTD cast. In order to validate whether the deepest depth was near the bottom, the NOAA bathymetry grid was overlain on the CTD cast coordinates and depths were compared. Any casts with the deepest measurement shallower than the bottom 20% of total water column depth were removed. This allowed for a sliding scale instead of providing a strict cut off (e.g., 1m above the bottom). For example, with this metric, at a bottom depth of 5m a measurement would be at or deeper than 4m to be accepted while a bottom depth of 100m would require measurements at or deeper than 80m. If the CTD bottom depth was too shallow based on criteria above, it was removed from analyses. Next, anomalously low or high PO_2 values (those greater than 3 standard deviations away from the mean) were removed from each stratum (Montes *et al.*, 2016). This removed PO_2 values that were $<7kPa$ or $>29kPa$, which removed 129 observations or 1.7% of total PO_2 data.

The final number of PO₂ data measurements was 7,628, and compared to temperature measurements, highlighted the sparsity of PO₂ data across time and space on the USNES. The PO₂ data resolution was too limited across space and time to provide adequate coverage needed to calculate mean PO₂ at the resolution of stratum/season/year. With at least 5 measurements per strata/season/year and a total of 43 strata x 4 seasons x 49 years, ~42,000 data measurements would be needed. Fortunately, environmental change along the USNES is temperature, and not oxygen driven (Deustch *et al.* 2015) and the focus of this study is on the effects of temperature changes on species physiology, allowing us to relax the requirement for high resolution PO₂ data in the present study. Instead, we used seasonal mean PO₂ values calculated from the available data for the inputs to calculate MI (Fig S5.4) to provide annual temporal variation. PO₂ averages over region or interannual time scales was not considered due to uneven distribution of raw data within regions and decades (Fig S5.5). Our approach of utilizing the available PO₂ data provides a conservative view of PO₂ patterns over season, and highlights the need for additional, higher-resolution oxygen data for finer-scale examination.

We did not use modeled bottom ocean PO₂ because the sparsity of PO₂ observations in the USNES does not allow for model validation. Moreover, high-resolution ocean models are required for the USNES due to its high complexity in regional ocean circulation and bathymetry (Saba *et al.* 2016), and thus biogeochemical models that can resolve PO₂ at these resolutions are both not common and have yet to be validated.

5.3.3 Incorporation of Fishery Data

Fishery data were used to provide information on species distribution over space and time. Five fish species were selected for this analysis: Atlantic cod, black sea bass, cunner, spiny dogfish, and summer flounder. These species represent an array of cold and warm water species and differing seasonal migration patterns, are collected in the NEFSC trawl, and have the required physiological parameters determined from laboratory studies. Data from the NEFSC bottom trawl survey was accessed to include data from 1972-2019 and across the strata domain. Analysis for fishery data began in 1972 due to complete sampling of spring and fall seasons across strata by 1972. For each fish species and season (spring, fall), data were condensed into the modified strata. For each stratum, season and year, a presence or absence was assigned for each fish. Presence/absence data were chosen instead of biomass because MI_{crit} is defined by where fish are *not* found rather than a value to provide optimal values for habitat. These data provided regional and temporal variation in species distributions (Fig S5.6) where changes in spring and fall habitat were apparent and distribution shifts were noticeable over time.

5.3.4 Calculation of Species-Specific MI Parameters

MI was calculated for the five species by first obtaining the species-specific metabolic parameters, A_o and E_o . P_{crit} and temperature from laboratory studies (Table 5.1) were regressed as $\ln(P_{crit})$ and inverse temperature (Fig 5.2), where the intercept was A_o and the slope was E_o (Table 5.2). A_o is a measure of the physiological oxygen supply, derived from P_{crit} and standard metabolic rate. E_o is the temperature sensitivity parameter where a steeper slope (higher E_o) indicates increased temperature sensitivity. MI (ϕ) was

then calculated through Equation 1 where A_o and E_o are the species-specific terms, B^n is a mass-scaling component, K_B is the Boltzmann constant, T is temperature (K), and PO_2 is oxygen (kPa). At a given size and temperature, the equation simplifies to $PO_2:P_{crit}$, a ratio of the environmentally available oxygen to that required to sustain maintenance metabolic demand. In this study, comparisons of MI within a single season (e.g. fall) were made with constant averaged seasonal environmental PO_2 (oxygen availability) and varying MI was a product of changing fish oxygen demand through temperature.

$$\phi = A_o B^n \frac{PO_2}{e^{(-E_o/K_B T)}}$$

Equation 1

5.3.5 Determining MI_{crit} , Minimum MI Dynamics, and MI Rate of Change Over Time

After species-specific parameters were obtained, MI was calculated across all strata, years, and seasons. For temperature, the stratum-based mean was used while for PO_2 , seasonal-based mean across the entire spatial domain was used. First, we identified the MI_{crit} for each species based on methods in Deutsch *et al.* (2015). Briefly, MI_{crit} is the lowest MI value within a species distribution, or in other words, the lowest MI value encountered by a species based on where they are present. Therefore, for our species, presences were determined for each stratum, season, and year. However, a stratum/season/year presence was removed if fish were not present over 10% of the entire time series (e.g. Atlantic cod presence in strata I01 during spring would not be included if it occurred once across the 50 year time-span). This avoided spurious and rare presences to be used, but allowed for inclusion of strata where fish have recently been present (e.g.

O06 for black sea bass in fall; Fig S5.6). Within the dataset of fish presence, the lowest MI was identified as the MI_{crit} and the stratum where MI_{crit} occurred was visually assessed with presence/absence data (Fig 5.3).

The trends in annual minimum MI for each species were also investigated. Minimum MI trends can show the spatiotemporal change in the lowest MI values a species experiences with respect to their distribution, which may, but not always, reach limiting MI values (*see below MI_{crit}*). Within the presence-only data, the minimum MI for each year was determined. Next, the linear trend in minimum MI for spring and fall was calculated, and the region and shelf position where the minimum MI occurred for a specific year was identified. A decreasing trend of minimum MI over time could indicate species remaining in their habitat and experiencing warming temperatures while a constant minimum MI over time could indicate movement of fish into different regions and potentially avoiding warming regions. Therefore, species' presence/absence was also employed to identify if changes in minimum MI were due to fish changing location or whether a change in minimum MI was reflecting physical dynamics within the region.

The rate of MI change over time was analyzed by strata and season for each species. This analysis focused on a holistic view of MI change over time based on ocean warming, irrespective of fish presence or absences, and therefore could be assessed across all seasons and avoid potential distribution biases related to historic fishing pressure (Bell *et al.*, 2015; also addressed in *Discussion*). Species- and season-specific Generalized Linear Models (GLMs) were employed to obtain the trend in MI over time within each strata using Equation 2. Species and season-specific GLMs were analyzed separately instead of including one model with interactions because the significance of

differing slopes across species or season was not a focal question. Across the five fish species, the same trend (positive or negative) was found, but the magnitude of change differed based on the species-specific thermal sensitivities. Therefore, a stratum mean and standard deviation was calculated.

$$MI \sim Year * Stratum + \varepsilon_i \quad \text{Equation 2}$$

5.3.6 Prediction of Future MI and Habitat Loss

While some species may already be at their MI limits in portions of the USNES, we explored future change in suitable thermal habitat. We used species-specific MI_{crit} to predict the year for which MI_{crit} has been or will be reached. To do this, the linear MI rate of change from the species- and season-specific analyses in Equation 2 were used to predict MI up to the year 2150. For each species, the first year where MI_{crit} was reached was identified for each stratum (Table S5.1).

5.4 RESULTS

5.4.1 Species-Specific MI_{crit} and Minimum MI Dynamics

For the five USNES species, the two colder water species, Atlantic cod and cunner, had lower MI_{crit} values than black sea bass, summer flounder, and spiny dogfish (Table 5.2). For black sea bass and spiny dogfish, the strata where MI_{crit} occurred showed a decreasing trend in MI over time (Fig 5.3), potentially representing metabolic traits changing over time or that conditions in the past were not yet limiting for these fish. Regardless of mechanism, this highlights the importance of the timespan of data used for determining the MI_{crit} . For Atlantic cod, cunner, and summer flounder, the strata where

MI_{crit} occurred showed a relatively constant trend in MI over time, but for Atlantic cod and summer flounder, fish were sometimes absent even though habitat was metabolically available.

Minimum MI, the lowest MI value measured per year, during spring varied between the species. The cold water species, Atlantic cod and cunner, had more variance where minimum MI occurred, while black sea bass, spiny dogfish, and summer flounder all experienced minimum MI along the SS, likely reflecting the cold-limits of the warmer water species. For Atlantic cod, minimum MI slightly decreased over time, and occurred primarily in offshore water. This minimum was more consistently in offshore SNE prior to 2000 and then predominantly in offshore GOM (Fig 5.4). Atlantic cod presences were mostly constant throughout time in the offshore portions of GOM and SNE, indicating the changes in minimum MI were due to differences in the oceanography across the two regions. Black sea bass minimum MI remained constant over time and occurred on the SS but showed an across-shelf trend over time from offshore to midshelf/inshore (Fig 5.4), coinciding with black sea bass presence increasing further inshore across the time series. For cunner, minimum MI trends were also constant over time and the location of minimum MI was primarily offshore in SNE in the earlier part of the time series, became more frequent on GB in the later part of the time series, and had some occasional occurrences inshore NYB (Fig 5.4). When cunner were present further south, more southern locations contained the minimum MI. Spiny dogfish and summer flounder minimum MI trends were similar with a decrease over time, albeit a steeper decline for summer flounder, and a transition of minimum MI occurring offshore SS towards inshore

SS (Fig 5.4). For both, there were no clear patterns of shifting minimum MI location with a change in presence, and likely reflects warming within those strata.

During fall, all species, except for cunner, experienced a decrease in minimum MI over time (Fig 5.5). Atlantic cod minimum MI occurred either on GB or midshelf and inshore SNE. Generally, because Atlantic cod were always present on GB, minimum MI occurred in SNE when fish were present (Fig 5.5). Black sea bass minimum MI decreased, and this solely occurred in the inshore SS (with a few midshelf early cases; Fig 5.5). As black sea bass were always present in the SS, the decrease in their minimum MI was due to warming in that region. Cunner minimum MI did not change over time but the location of minimum MI did, from inshore NYB to GB (Fig 5.5). Notably, when minimum MI occurred in a more southern location (i.e. NYB), this also coincided with the only times cunner were present there throughout the time series. Spiny dogfish minimum MI also decreased throughout the time series and occurred in almost every portion of the shelf, except for in the GOM (Fig 5.5). This wide distribution of minimum MI occurrences also reflects a similar wide distribution of presences for spiny dogfish, with some overlap in recent years where spiny dogfish are found further south and inshore coinciding with minimum MI locations. Summer flounder also experienced decreasing minimum MI over time primarily occurring in inshore regions of the NYB or SNE, and sometimes GB (Fig 5.5). Generally, when minimum MI occurred further south, also coincided with the furthest south presence for southern flounder.

5.4.2 MI Rate of Change Over Time

The rate in MI change per year for each strata and season was determined for each species. The trends (i.e. negative or positive) were similar amongst all species, and therefore, a mean and standard deviation was calculated providing a general species-wide trend in MI (Fig 5.6). For each season, there was a negative change in MI over time, except for a few strata that showed increasing MI (albeit a weak trend). Notably, when the rate of MI change was farther from 0, the standard deviation increased, which reflects the differing thermal sensitivities of the species.

In winter, the rate of MI change was negative except for four strata (Fig 5.6), which is representative of cooling in those regions (Fig S5.3). Inshore, the southern strata and those off of SNE had the greatest decrease in MI over time, while for midshelf and offshore, the southern strata had the smallest decrease or slight increase in MI over time. Especially for offshore, the rate of decrease in MI over time was relatively constant north of the SS. Spring had a similar rate of MI change over time as winter (Fig 5.6), where the greatest decrease in MI in the midshelf occurred within SNE, and decreases in MI occurred offshore in the more northern regions (except for the decrease starting north of GB). However, there was a stronger latitudinal trend of greater decrease in the rate of MI change over time in the southern than northern locations. Both summer and fall exhibited similar trends with the summer revealing strong decreasing rates in MI over time (Fig 5.6). For both, inshore and midshelf strata experienced greater decreases in the rate of MI change over time in southern locations compared to northern locations. Offshore, the rate of MI change was slightly negative from O01 to O10, and then showed stronger negative trends from O11 onward. O11 to O19 represent the offshore strata of the GOM, and these

results may reflect the differing oceanographic changes occurring in the GOM and along the Middle Atlantic Bight (which comprises of regions SS, NYB, and SNE).

5.4.3 Prediction of Future MI and Habitat Loss

Species-specific MI_{crit} was used to determine the year a specific strata and season have or would reach limiting values. To do this, the MI trends from the GLMs were used to predict MI up until 2150. Summer and fall exhibited the highest number of strata reaching MI_{crit} (Fig 5.7), while winter and spring saw fairly low levels of strata loss (Fig S5.7). The actual years MI_{crit} were reached are found in Table S5.1. Notably, while the rate in MI decrease over time was greater for summer than for fall, fall still experienced more suitable thermal habitat loss due to persistently warmer temperatures during this season. For all species, suitable thermal habitat loss defined as a strata reaching MI_{crit} was primarily concentrated in southern and/or inshore portions of the USNES, although the timing of when MI_{crit} was reached differs across the species. The strata in which species' MI_{crit} was reached prior to 2000 indicate species distribution limits. Stratum I08 also showed suitable thermal habitat loss for all species over next 30-120 years. All species, except for black sea bass, also show some suitable thermal habitat loss in habitat on GB and in the southern GOM 30-150 years from now.

Atlantic cod and cunner, the colder water species, show similar suitable thermal habitat loss, with Atlantic cod experiencing greater suitable thermal habitat losses due to their increased thermal sensitivity. For Atlantic cod and cunner, fall habitat that is limited prior to 2000 indicates prior species distributions limits located in the southern and inshore portions of the USNES. Over time, there is a degree of continued suitable thermal

habitat loss further north into the NYB with Atlantic cod reaching limits sooner than cunner. Both species will experience a loss of suitable thermal habitat along GB and southern GOM, while Atlantic cod will also experience loss within SNE. Black sea bass and spiny dogfish will experience similar suitable thermal habitat loss. Mostly, these species will lose suitable thermal habitat within the southern and inshore portions of the range. However, spiny dogfish were already limited at the most southern strata inshore and midshelf, and will experience more northern habitat suitable thermal loss off the coast of New Jersey when compared to black sea bass. Summer flounder has and will continue to experience similar suitable thermal habitat loss as spiny dogfish, but has already reached limiting values in the inshore portion of the range and will experience more within GB and southern GOM.

5.5 DISCUSSION

Throughout the USNES, MI for five important fish species has been decreasing in step with continued ocean warming in the region. By only using seasonal PO_2 means, and subsequently constant oxygen supply, the differences in MI across time and space within a season provide a comparison of differing fish oxygen demand as determined by temperature and species-specific parameters. The rate of MI decrease varied across season, with declines in summer and fall seasons leading to suitable thermal habitat limitation, while the decrease in MI in the winter and spring months could indicate the opening of habitat for some species. MI varied for the five species based on their differing thermal sensitivities (E_o) and life histories (warm vs. cold water species). For most species, minimum MI locations either corresponded to timepoints when fish were

found furthest south (i.e. fish location drove trends in MI) or were a result of fish experiencing changing ocean conditions without clear movement away from those locations. Future MI habitat loss is substantial in the southern and inshore portions of the USNES for all species, with some species losing habitat along GB and southern GOM.

Our results were somewhat in agreement with two other studies focused on USNES fish (Kleisner *et al.*, 2017; Morley *et al.*, 2018). For Atlantic cod, all three studies confirmed loss of suitable thermal habitat into the future due to warming, although we found less evidence of spring warming limiting adult Atlantic cod (but see differences in life stages: Langan *et al.*, 2020). Black sea bass decrease in thermal habitat was in agreement with Kleisner *et al.* (2017), however, both studies may not have accurately portrayed the increase in thermal habitat in the spring due to warming in regions that were historically cold. Cunner loss in thermal habitat was also in agreement with Morley *et al.* (2018), while spiny dogfish and summer flounder show contrasting results. For both, Kleisner *et al.* (2017) and Morely *et al.* (2018) showed increasing suitable habitat with warming, while in this study, we showed thermal habitat loss into the future. These discrepancies could be due to differing interpretations of suitable thermal habitat, e.g. limiting habitat based on physiological parameters or loss of “optimal” habitat based on species biomass or abundance. Differences between studies provide an opportunity to approach investigations of distribution shifts with deductive reasoning and highlight the importance of using both types of studies.

5.5.2 Decreasing MI from 1970 – Present

Across all seasons, MI generally decreased over time, but summer and fall season decreases reached limiting values and experienced faster rates of decrease over time. Spring and winter decreases were more prominent in the GOM and northern portions of the USNES, while the faster summer and fall declines trended in the southern portions of the range and within inshore and midshelf locations. Summer MI for all species decreased more rapidly than fall MI, but fall MI still approached MI_{crit} more frequently due to seasonally warmer temperatures in fall.

Large fluctuations in MI were driven by USNES seasonality, creating more variance across seasons than over time within a season. The USNES experiences cold winter and spring seasons, warming in the summer which leads to stratification, and fall overturn and water column breakdown as storms pass through (Rasmussen *et al.*, 2005). For bottom temperature, fall overturn mixes cold stratified water with warm surface water, and therefore is typically the warmest season (Richaud *et al.*, 2016). However, there are shelf locations with well-mixed water columns extending warm surface waters down to the bottom (Fig S5.2). Therefore, most species on the USNES will likely only experience limiting MI values in bottom waters below seasonal stratification in the summer and fall. This suggests the use of MI may be more relevant to summer and fall species distribution than the more well mixed waters in the winter and spring. Understanding the summer and fall MI characteristics and trends is imperative as this time coincides with many fish spawning seasons, and spawning adults and embryos are the most sensitive to warming (Dahlke *et al.*, 2020).

Contrastingly, while winter and spring warming (as seen by a decrease in MI in those seasons) may not push below MI_{crit} , observed MI trends may still impact species in different ways. Some USNES species may benefit, especially those that are warmer water species living at their northern range edges (i.e black sea bass, McCartney *et al.*, 2013). Warmer winters are especially conducive towards larval survival (Hurst, 2007) and can benefit species by increasing larval recruitment (Miller *et al.*, 2016). On the other hand, warming winters may be problematic for other species, such as Atlantic cod in SNE (Langan *et al.*, 2020). However, within the framework of MI, comparing effects based on MI values well above MI_{crit} should be cautioned against, and exploring the consequences of warming in winter and spring may be better suited for another physiological metric focused on cold-intolerances.

5.5.3 Species-Specific Differences in Minimum MI and Future Habitat Loss

For the five USNES species, differences in calculated MI values were an artifact of the species-specific physiological parameters that reflected thermal sensitivity (i.e. the relative change in MI per 1°C in temperature) and life histories (cold vs. warm species). MI_{crit} values differed amongst the species where the colder water species had the lowest MI_{crit} and the warmer water species had higher MI_{crit} . All of these MI_{crit} values fell within the 2-5 MI range proposed by Deutsch *et al.* (2015, 2020), but disagreed with some of the absolute values in Deutsch *et al.* (2020). Atlantic cod and black sea bass MI_{crit} values were similar, but MI_{crit} values in this study were lower for cunner and higher for summer flounder than reported in Deutsch *et al.*, (2020) (Table 5.3). This discrepancy would overestimate future suitable thermal habitat loss for cunner and underestimate potential

suitable thermal habitat loss for summer flounder. Because E_o values were similar for all species (Table 5.3), MI_{crit} disagreement could be due to several factors. First, our distribution data focused on presences of fish at depth instead of depth-integrating presences throughout the entire water column, and may reflect only an MI_{crit} representative of the benthos. Second, the spatial domain and resolution of our data was at the strata level covering the extent of the USNES while for Deutsch *et al.*, (2020) data was analyzed at a $1^\circ \times 1^\circ$ grid and beyond the USNES. This is notable because by extending the sampling domain, clear species limits are easier to denote, while for us, we were analyzing limits within the known species distributions. Third, our oxygen measurements differed in that Deutsch *et al.*, (2020) used modeled oxygen from the World Ocean Atlas in the same $1^\circ \times 1^\circ$ grid while our oxygen was seasonally averaged across the shelf. A $1^\circ \times 1^\circ$ grid is inappropriate to use for analyses specifically assessing dynamics along the USNES due to the shape, the complex bathymetry, and oceanography of the shelf, which require finer-resolution models to resolve the biogeochemistry (Saba *et al.* 2016). While we simplified oxygen, temperature dynamics were more representative of the USNES dynamics than would have been resolved at a $1^\circ \times 1^\circ$ grid. The disagreement for cunner and summer flounder may also be due to differences in oxygen availability. However, should oxygen values have been substantially off, we would expect there to be discrepancy for all fish analyzed. Fourth, our species distribution data were from different data sources (NOAA bottom trawl survey: this study; Ocean Biodiversity Information system: Deutsch *et al.* (2020)). As the number of studies employing MI for species distribution analyses increases, assessments on

discrepancies between studies will help hone methodology, interpretation and analyses for future studies.

Habitat loss as defined by the year where a specific stratum and season reached or fell below MI_{crit} was substantial for all five species in the summer and fall seasons. Fall saw the highest extent of strata reaching MI_{crit} . While at some point all species will experience loss in suitable habitat in the inshore and southern portions of the USNES (SS and NYB), the cold water species, Atlantic cod and cunner, reached MI_{crit} there prior to 2000, indicating historic range limits. Into the future, Atlantic cod, cunner, and summer flounder will also lose suitable thermal habitat in GB and southern GOM. Inshore/midshelf suitable thermal habitat loss during summer and fall is notable as this is typically when many species reproduce and do so in these regions adjacent to nursery grounds for hatching larvae, potentially driving recent shifts in larval distributions (Walsh *et al.*, 2015). Notably, these estimates of future suitable thermal habitat loss are conservative as they extend the trend in MI change over time from 1970-2019 out unto 2150. It is possible that warming may accelerate into the future, and finer scale climate models could show accelerated suitable thermal habitat loss. Also, these projections are extensions of current trends and should not be taken as actual predictions of changing distributions of these fish. With more advanced estimations of temperature, oxygen, and species-interactions, loss in suitable thermal habitat may occur sooner and across a wider spread of the shelf (Kleisner *et al.*, 2017).

Atlantic cod minimum MI showed a decreasing trend over time for both spring and fall seasons. During spring, minimum MI occurred offshore but over time shifted regionally from SNE to the GOM, and during fall, minimum MI occurred either on GB or

SNE. For the spring, Atlantic cod presences did not change between the respective regions, indicating the decrease in MI was due to warming temperatures in those regions, but for fall, cod presence typically synced with the timing of minimum MI occurred in SNE. Across the USNES, Atlantic cod is managed as two stocks, the GOM and GB stocks, and SNE fish are managed with the GB fish, although they may be genetically different (Zemeckis *et al.*, 2014). Within this dataset, the different cod stocks were not differentiated and location of minimum MI fall differences could be an artifact of Atlantic cod stock structure. The general shift in Atlantic cod distribution has been poleward and deeper, especially as Atlantic cod are at their southern population limits in the SNE and GB (Nye *et al.*, 2009). However, recently the Atlantic cod population has been increasing in the SNE as supported by increased recruitment (Langan *et al.*, 2020). Strata where MI_{crit} has always been limiting and where future strata will become limiting support other documented studies on declines in Atlantic cod suitable thermal habitat, potentially obstructing future stock rebuilding (Pershing *et al.*, 2015).

Black sea bass minimum MI was constant over time in the spring and decreased over time in the fall. Black sea bass are a warm water species, and the Northern stock (the focus of this study) are the most northern within the full range of black sea bass (McCartney *et al.*, 2013). During spring, minimum MI consistently occurred on the offshore SS, but shifted inshore and midshelf later in the time series, which coincided with increased presence of black sea bass in those regions. We suggest this change in location of minimum MI is indicative of the opening of habitat in regions that were historically too cold. Winter and spring warming have been link to black sea bass distribution shifts in the spring (Bell *et al.*, 2015) and increased recruitment from larval

overwintering survival (Miller *et al.*, 2016), which suggests warming in these seasons may be beneficial for black sea bass. During fall, black sea bass minimum MI decreased, and this always occurred (except for 3 times) in the inshore SS where black sea bass have been present. This result is surprising and indicates that with warming, black sea bass still remain in their original distribution and as a result, MI continues to decrease. Indeed, Walsh *et al.*, (2015) showed that adult black sea bass center of biomass rate of movement was nonsignificant during fall, and perhaps extirpation of black sea bass out of warming regions has not occurred yet. In line with this result, MI_{crit} was defined from a presence that occurred relatively recently, and suggests that if MI_{crit} was calculated earlier in the time series, it would overestimate MI_{crit} today. Perhaps black sea bass were never at their MI_{crit} in the past or have undergone physiological adaptation. As such, black sea bass will likely experience the least amount of habitat loss in the summer and fall seasons compared to the other USNES species. Black sea bass thermal maximum tolerable temperature was around 24°C (Slesinger *et al.*, 2019). The only stratum in this data set whose mean temperature reached 24°C or higher was stratum I01, which started to reach this temperature in the early 2000's. Nonetheless, black sea bass distribution advancement north is apparent and important as they are already negatively impacting the American lobster fishery (McMahan and Grabowski, 2019).

Cunner minimum MI did not change over time for both spring and fall. Cunner had the lowest thermal sensitivity out of all the studied species, and as such, appears to reside in a much narrower range of MI values. However, for both seasons, minimum MI occurrences in more southern locations (inshore NYB) coincided with times when cunner were present farther south. Out of the five species studied, cunner are the only non-

targeted species by recreational and commercial fisheries, and previous attempts at describing suitable thermal habitat links have been unsuccessful (Shackell *et al.*, 2014). Due to limited interest and data availability, most distribution information has been derived from regional studies. For example, over time, cunner abundance has decreased near inshore portions of the SNE (Collie *et al.*, 2008) but has increased in parts of the GOM (Witman and Lamb, 2018); these phenomena occur a decade apart and do not explain variation in between the SNE and GOM. Cunner will experience suitable habitat loss within the inshore and midshelf portions of SS and NYB and some on GB, which may push fish further into the GOM. This result corroborates with Morley *et al.* (2018) who showed a shift in distribution poleward and habitat loss. While cunner are not a target species, changing distribution is notable due to their predation on urchins and the impacts this can have on kelp forests in the GOM (Ojeda and Dearborn, 1991).

Spiny dogfish minimum MI decreased in both spring and fall. During spring, minimum MI occurred along the SS transitioning from offshore to inshore over time, and with no change in presences, indicating a location-based decrease in MI. During fall, minimum MI occurred throughout the USNES, except for the GOM. Generally, when spiny dogfish were further south their minimum MI also occurred there. For spiny dogfish, the southern inshore and midshelf strata reached MI_{crit} prior to 2000, and in the future, will experience loss of habitat inshore and midshelf SS and NYB. This result is surprising as spiny dogfish have been touted as one of the species that will benefit by warming waters (Sagarese *et al.*, 2014; Kleisner *et al.*, 2017), and have been shown to have a southward distribution shift (Nye *et al.*, 2009). However, many studies, including this one, pool spiny dogfish into one group, even though there are differences in both

southern and northern stocks (Carlson *et al.*, 2014), leading to potential differences in thermal tolerances, and aggregations based on sex (Dell'Apa *et al.*, 2014). Understanding drivers of their distribution changes is important, especially as spiny dogfish have functionally replaced Atlantic cod trophic niche (Morgan and Sulikowski, 2015).

Summer flounder minimum MI also decreased during both spring and fall seasons. Minimum MI occurred mostly in the SS and transitioned to primarily inshore since the 1990's. There was not a change in presence during this time suggesting the decrease in MI was due to warming in the region. For fall, minimum MI occurred throughout the NYB, SNE and GB, with no relation to summer flounder presence. Summer flounder surprisingly showed loss of habitat in the inshore SS and midshelf up to Delaware prior to 2000, and future habitat loss inshore and midshelf NYB as well as into the GOM and GB. Summer flounder distribution has been shifting northward and eastward over time in both spring and fall (Bell *et al.*, 2015). Suggested drivers of this shift include bottom temperature trends (Pinsky *et al.*, 2013), climate variability with the Gulf Stream Index (O'Leary *et al.*, 2019), and fishing pressure (Bell *et al.*, 2015). However, other studies suggest the drivers remain unresolved as temperature and fishing pressure explain some but not most of the variation in the data (Perretti and Thorson, 2019). Our MI_{crit} analyses do suggest that temperature is a driver in shifting distributions (although MI_{crit} could be overestimated leading to quicker loss of suitable thermal habitat than may be experienced). Resolving the drivers and future shifts in summer flounder distribution are important because as a popular fishery species, changing distributions have already impacted fishing communities (Pinsky *et al.*, 2021).

5.5.4 Case Study: Dissolved Oxygen in the NYB

Due to limitations of dissolved oxygen measurements throughout the USNES, PO₂ used in this study was averaged by season, precluding any interannual or spatially resolved oxygen data availability for the calculation of MI. Environmental change within the USNES is primarily temperature driven (Deutsch *et al.* 2015), and this region has not experienced general declines in PO₂ (Breitburg *et al.*, 2018) and/or worsening hypoxia (Rabalais and Turner, 2019). However, this estimation of PO₂ will bias some regions where PO₂ may be lower than the seasonal estimate. Broadly, for normoxic species, a 1kPa decline in PO₂ will lead to a ~5% decrease in MI (1kPa/21kPa = 0.048; Seibel and Deutsch, 2020). Here, we investigate potential biases in MI by exploring a region that is known to experience lower PO₂ during summer and experienced a single large hypoxia event in 1976 (Falkowski *et al.*, 1980), the NYB.

The NYB is an area that has seasonal Cold Pool formation during the summer, where cold winter water advects from the north and vernal heating at the surface creates a strong stratification layer, encapsulating the cold bottom water during the summer (Houghton *et al.*, 1982; Castelao *et al.*, 2008; Chen *et al.*, 2018). The Cold Pool is an important thermal refuge for many fish species (Sullivan *et al.*, 2005), but can also experience decreasing PO₂ levels due to stratification (Kemp *et al.*, 1994) that isolates surface water oxygen sources including phytoplankton blooms and atmospheric exchange (Schofield *et al.*, 2012). Therefore, this region typically experiences lower than average bottom water PO₂ during the summer, and into the fall until Cold Pool breakdown occurs. This seasonal NYB stratification can lead to significant low oxygen events including a large hypoxia event that occurred in the summer of 1976 with region wide impacts

(NMFS, 1977; Falkowski et al. 1980). This large hypoxia event was a result of a combination of anthropogenic and natural conditions including large runoff, unusual climatological regimes (i.e. wind patterns and spring storm events), a deep thermocline, and changes in the community dynamics at the lower trophic levels (Falkowski *et al.*, 1980).

Two strata within the NYB, I04 and M04, representing inshore and midshelf portions of the NYB were considered. We focused on the summer season when water was likely stratified and well before the fall Cold Pool breakdown. MI was recalculated for each species using the raw PO₂ CTD bottom depth values during the summer season (MI_{CTD}) from the two strata and compared to the values (MI_{STUDY}) used in this study (Fig S5.8). The calculation of MI from the raw CTD data included all PO₂ measurements, including any that fell outside of the cut-off of three standard deviations away from the mean. The raw oxygen data were only available in the 1970's and 2010's and did not allow for an interannual comparison, however MI_{CTD} and MI_{STUDY} were visually assessed on a time series from 1970-2019. During the 1970's, there was high variability in PO₂ measurements, leading to variable MI_{CTD} throughout the two strata, and MI_{STUDY} was centered around the mean of M04 and higher than the mean of I04. During the 2010's, MI_{STUDY} was similar to MI_{CTD} for M04, but were much lower in I04. Lower MI_{CTD} were sometimes below MI_{crit} for all species, indicating that during low PO₂ events, some regions may have limited oxygen availability in relation to animal oxygen demand. During the 1976 hypoxia event, MI_{CTD} was usually below MI_{crit}, except for one data point for black sea bass. For the summer, there were no fishery data to compare species presence and absence with the MI values to assess MI_{crit} alongside the MI_{CTD} results.

Altogether, the influence of PO₂ on MI is nontrivial in certain regions of the USNES, may fluctuate interannually with a dependence on stratification within the system, but no obvious long-term trend in increasing or decreasing PO₂. The factors that create strong or weak stratification are outside the scope of this study, but highlights the importance for future oxygen monitoring that resolves both seasonal and regional variation. For example, the hypoxia event of 1976 severely limited MI for the five species, and was the result of multiple anthropogenic and natural causes. Understanding the drivers for hypoxia events like the one in 1976 will be important to track whether they become more frequent in shelf waters of the USNES as they can drive the loss of metabolically available habitat beyond the observed trend from increased temperature.

We recommend that future research on the USNES focus on increasing finer scale oxygen measures. Regions where oxygen has been decreasing (i.e. Pacific Ocean, Gulf of Mexico) have long-term oxygen time series for which finer scale oxygen measurements could be derived. Our analysis was limited by the lack of oxygen data and lack of validated high-resolution modeled data, and accounting for variance in oxygen supply could lead to a quicker loss in habitat (assuming much of our estimates were overestimated, i.e. NYB).

5.5.5 Considerations When Using Metabolic Index

Species-specific physiological parameters are incredible tools that can be used to investigate how changing environments may affect species distributions. Most papers focused on species distribution and temperature use statistical relationships between where fish are found and the temperatures they reside in (e.g. Kleisner *et al.*, 2016).

These studies are invaluable towards our understanding of how ocean warming will impact the USNES ecosystems as they can provide estimates of suitable thermal habitat across a range of temperatures as well as incorporate more physical features such as salinity and rugosity into their models. Only focusing on temperature can sometimes mask true vulnerability to environmental change (McHenry *et al.*, 2019), especially for some benthic organisms with a high affinity towards structure (Roberts *et al.*, 2020). However, there are pitfalls to estimating extents of habitat based on fishery data and temperature correlations (Nazzaro *et al.*, 2021), which highlights the utility of incorporating species-specific physiological metrics to mechanistically determine the effect of temperature on a species. The use of MI allows for a species-specific evaluation of metabolically available habitat and can highlight different responses of species beyond a statistical relationship of presence and absence. For example, a species may be present in a certain location for various reasons including searching for food, migrating, and spawning, and the temperature at that location in time and space may be a correlation not causation of presence. MI provides a direct physiological mechanism as to why habitat may be metabolically available or unavailable based on organismal oxygen requirements. Of course, an organism may also be absent in metabolically available habitat, and this highlights the utility of combining approaches to provide a wholistic view of species distributions.

How the species-specific metrics are defined during laboratory studies is important to consider when making comparisons across species and applying them towards describing and predicting species response to environmental change in a system. The calculation of the species-specific parameters used in the MI equation come from

studies that measure P_{crit} at multiple temperatures. The methodologies used to calculate P_{crit} can differ between studies. For Atlantic cod, black sea bass, cunner, and summer flounder, a breakpoint method of calculating P_{crit} was employed (Claireaux and Chabot, 2016) while for spiny dogfish, the alpha method was used (Seibel *et al.*, 2021). The alpha method can lead to a lower P_{crit} value on average as this method relies on the highest metabolic rate/ PO_2 data point instead of through a regression through a scatter of data points (Seibel *et al.*, 2021). Variance in MI_{crit} across species is expected, but P_{crit} values lower than measured could underestimate MI. For example, if black sea bass P_{crit} was overestimated by 0.5 or 1kPa (assuming constant change across temperature), E_o would increase respectively, and thus increase MI at each temperature (Fig S5.9). However, the variance between estimated MI decreases at warmer temperatures, which reduces the potential error at temperatures of concern in this study. Also, higher MI_{crit} values would be estimated but they may still confer with the same temperature (and just be numerically higher). Notably, other studies on MI utilize the breakpoint method (Duncan *et al.*, 2020) or estimate species-specific parameters (E_o and A_o) from relationships between temperature, PO_2 and fish abundance (Howard *et al.*, 2020). Recalculating P_{crit} for each species to compare methods (breakpoint vs alpha) is outside of the scope of this paper but we urge caution when interpreting parameters from physiology studies and how that methodology may alter respective analyses.

MI_{crit} in Deutsch *et al.* (2015) was defined as the lowest MI value where fish were present across an entire study period. For some of our fish, like black sea bass, the stratum where MI_{crit} occurred showed decreasing MI values over time, and fish were present for most of the study period. This suggests 1) the time frame to calculate MI_{crit} is

important to consider; and 2) black sea bass in the past were never at their MI_{crit} ; or 3) black sea bass have adapted physiologically to warming. Also, MI_{crit} was determined based on fish presences, which can be affected by a variety of other factors, including past fishing history. For summer flounder, past fishing pressure has been identified as a major driver of their center of biomass shift (Bell 2015). In comparison to other MI studies, some focus on a large geographic range beyond where species distribution occur to determine MI_{crit} (Deutsch *et al.*, 2015, 2020). For many species in this study, assessment beyond the distribution was not possible as southern population counterparts occupy habitat at the species southern range edge, and determining which fish are part of which population is challenging, complicating distinguishing true presence and absences at the southern range edges. Other studies, such as Howard *et al.*, (2020) and Duncan *et al.*, (2020) analyze at a finer resolution, but also do so from a region with more oxygen data coverage. Studies can also use different methods, such as using frequency distributions or machine learning algorithms with presence-absence data, to determine the MI_{crit} (Deutsch *et al.*, 2020). Differing methods and data resolution appear to be non-trivial when determining MI_{crit} and should be further explored when developing this metric.

Finally, MI is a limiting metric instead of a metric that can provide an indication of a specific temperature to describe “optimal” thermal habitat. Determining species’ range edges is difficult, and many do not exhibit clear shifting range edges that are synced with changes in temperature (Fredston *et al.*, 2021), especially for those that have warmer southern populations such as black sea bass and summer flounder.

5.5.6 Conclusions

Ocean warming along the USNES has already impacted important fish species (Kleisner *et al.*, 2017). As warming will continue into the future (Saba *et al.*, 2016), recognizing the impacts on species allows for preparation and/or mitigation of negative consequences in the fishing community (Rogers *et al.*, 2019) and on ecosystems (McMahan and Grabowski, 2019). By using a physiologically-based approach, we showed the utility of MI in estimating suitable thermal habitat for five USNES species as another methodologically approach for understanding the impacts of ocean warming on species distributions. Through MI, the loss of suitable thermal habitat was shown mechanistically rather than through correlations between temperature and species presence and absence. Continued improvements in data collection both at the physical parameter and physiology levels will benefit future studies.

5.6 ACKNOWLEDGEMENTS

We gratefully acknowledge those who engaged in productive scientific discussions about the physiology, oceanography, and interpretation of results including Alyssa Andres, Lauren Cook, Nick Battista, Jackie Veatch, Alexa Fredston, Vincent Saba, and Olaf Jensen. We also thank Sean Lucey for providing NOAA NEFSC fishery survey data, and Laura Nazzaro, Joe Caracappa, and Lori Garzio for assistance with data acquisition.

5.7 REFERENCES

- Ainsworth, T. D., Heron, S. F., Ortiz, J. C., Mumby, P. J., Grech, A., Ogawa, D., Eakin, C. M., *et al.* 2016. Climate change disables coral bleaching protection on the Great Barrier Reef. *Science*, 352: 338–342.
- Bell, R. J., Richardson, D. E., Hare, J. A., Lynch, P. D., and Fratantoni, P. S. 2015. Disentangling the effects of climate, abundance, and size on the distribution of

- marine fish: an example based on four stocks from the Northeast US shelf. *ICES Journal of Marine Science*, 72: 1311–1322.
- Bennett, A. F. 1978. Activity metabolism of the lower vertebrates. *Annual Review of Physiology*, 40: 447–469.
- Bevacqua, E., Vousdoukas, M. I., Zappa, G., Hodges, K., Shepherd, T. G., Maraun, D., Mentaschi, L., *et al.* 2020. More meteorological events that drive compound coastal flooding are projected under climate change. *Communications Earth & Environment*, 1:47: 1–11.
- Biro, P. A., Post, J. R., and Booth, D. J. 2007. Mechanisms for climate-induced mortality of fish populations in whole-lake experiments. *Proceedings of the National Academy of Sciences of the United States of America*, 104: 9715–9719.
- Breitburg, D., Levin, L. A., Oschlies, A., Grégoire, M., Chavez, F. P., Conley, D. J., Garçon, V., *et al.* 2018. Declining oxygen in the global ocean and coastal waters. *Science*, 359: 1–11.
- Caesar, L., Rahmstorf, S., Robinson, A., Feulner, G., and Saba, V. 2018. Observed fingerprint of a weakening Atlantic Ocean overturning circulation. *Nature*, 556: 191–196.
- Cai, W., Wang, G., Dewitte, B., Wu, L., Santoso, A., Takahashi, K., Yang, Y., *et al.* 2018. Increased variability of eastern Pacific El Niño under greenhouse warming. *Nature*, 564: 201–206.
- Carlson, A. E., Hoffmayer, E. R., Tribuzio, C. A., and Sulikowski, J. A. 2014. The use of satellite tags to redefine movement patterns of spiny dogfish (*Squalus acanthias*) along the U.S. east coast: Implications for fisheries management. *PLoS ONE*, 9: e103384.
- Castelao, R., Glenn, S., Schofield, O., Chant, R., Wilkin, J., and Kohut, J. 2008. Seasonal evolution of hydrographic fields in the central Middle Atlantic Bight from glider observations. *Geophysical Research Letters*, 35: 6–11.
- Chabot, D., Koenker, R., and Farrell, A. P. 2016. The measurement of specific dynamic action in fishes. *Journal of Fish Biology*, 88: 152–172.
- Chant, R. J., Wilkin, J., Zhang, W., Choi, B., Hunter, E., Castelao, R., Glenn, S., *et al.* 2008. Dispersal of the Hudson River Plume in the New York Bight. *Oceanography*, 21: 148–161.
- Chen, Z., Curchitser, E., Chant, R., and Kang, D. 2018. Seasonal Variability of the Cold Pool Over the Mid-Atlantic Bight Continental Shelf. *Journal of Geophysical Research: Oceans*, 123: 8203–8226.
- Chen, Z., Kwon, Y. O., Chen, K., Fratantoni, P., Gawarkiewicz, G., and Joyce, T. M. 2020. Long-Term SST Variability on the Northwest Atlantic Continental Shelf and Slope. *Geophysical Research Letters*, 47: 1–11.
- Chen, Z., and Curchitser, E. N. 2020. Interannual Variability of the Mid-Atlantic Bight Cold Pool. *Journal of Geophysical Research: Oceans*, 125: 1–20.
- Chen, Z., Kwon, Y. O., Chen, K., Fratantoni, P., Gawarkiewicz, G., Joyce, T. M., Miller, T. J., *et al.* 2021. Seasonal Prediction of Bottom Temperature on the Northeast U.S. Continental Shelf. *Journal of Geophysical Research: Oceans*, 126: 1–27.
- Claireaux, G., and Chabot, D. 2016. Responses by fishes to environmental hypoxia: Integration through Fry's concept of aerobic metabolic scope. *Journal of Fish Biology*, 88: 232–251.

- Collie, J. S., Wood, A. D., and Jeffries, H. P. 2008. Long-term shifts in the species composition of a coastal fish community. *Canadian Journal of Fisheries and Aquatic Sciences*, 65: 1352–1365.
- Dahlke, F., Wohlrab, S., Butzin, M., and Pörtner, H. 2020. Thermal bottlenecks in the lifecycle define climate vulnerability of fish. *Science*, In press: 65–70.
- Dell’Apa, A., Cudney-Burch, J., Kimmel, D. G., and Rulifson, R. A. 2014. Sexual Segregation of Spiny Dogfish in Fishery-Dependent Surveys in Cape Cod, Massachusetts: Potential Management Benefits. *Transactions of the American Fisheries Society*, 143: 833–844.
- Deutsch, C., Ferrel, A., Seibel, B., Portner, H. O., and Huey, R. B. 2015. Climate change tightens a metabolic constraint on marine habitats. *Science*, 348: 1132–1136.
- Deutsch, C., Penn, J. L., and Seibel, B. 2020. Metabolic trait diversity shapes marine biogeography. *Nature*, 585: 557–562. Springer US.
- Dhame, S., Taschetto, A. S., Santoso, A., and Meissner, K. J. 2020. Indian Ocean warming modulates global atmospheric circulation trends. *Climate Dynamics*, 55: 2053–2073.
- Dulvy, N. K., Rogers, S. I., Jennings, S., Stelzenmüller, V., Dye, S. R., and Skjoldal, H. R. 2008. Climate change and deepening of the North Sea fish assemblage: A biotic indicator of warming seas. *Journal of Applied Ecology*, 45: 1029–1039.
- Duncan, M. I., James, N. C., Potts, W. M., and Bates, A. E. 2020. Different drivers, common mechanism; the distribution of a reef fish is restricted by local-scale oxygen and temperature constraints on aerobic metabolism. *Conservation Physiology*, 8: 1–16.
- Falkowski, P. G., Hopkins, T. S., and Walsh, J. J. 1980. An analysis of factors affecting oxygen depletion in the New York Bight. *Journal of Marine Research*, 38: 479–506.
- Fernandez, E., and Lellouche, J. M. 2018. Product user manual for the global ocean physical reanalysis product GLORYS12V1. *Copernicus Product User Manual*, 4: 1–15.
- Fredston, A., Pinsky, M., Selden, R. L., Szuwalski, C., Thorson, J. T., Gaines, S. D., and Halpern, B. S. 2021. Range edges of North American marine species are tracking temperature over decades. *Global Change Biology*, 27: 3145–3156.
- Gleckler, P. J., Durack, P. J., Stouffer, R. J., Johnson, G. C., and Forest, C. E. 2016. Industrial-era global ocean heat uptake doubles in recent decades. *Nature Climate Change*, 6: 394–398.
- Houghton, R. W., Schlitz, R., Beardsley, R. C., Butman, B., and Chamberlin, J. L. 1982. The Middle Atlantic Bight Cold Pool: Evolution of the Temperature Structure During Summer 1979.
- Howard, E. M., Penn, J. L., Frenzel, H., Seibel, B. A., Bianchi, D., Renault, L., Kessouri, F., *et al.* 2020. Climate-driven aerobic habitat loss in the California Current System. *Science Advances*, 6: 1–12.
- Hurst, T. P. 2007. Causes and consequences of winter mortality in fishes. *Journal of Fish Biology*, 71: 315–345.
- Kemp, P. F., Falkowski, P. G., Flagg, C. N., Phoel, W. C., Smith, S. L., Wallace, D. W. R., and Wirrick, C. D. 1994. Modeling vertical oxygen and carbon flux during stratified spring and summer conditions on the continental shelf, Middle Atlantic Bight, eastern U.S.A. *Deep-Sea Research Part II*, 41: 629–655.

- Kleisner, K. M., Fogarty, M. J., McGee, S., Barnett, A., Fratantoni, P., Greene, J., Hare, J. A., *et al.* 2016. The effects of sub-regional climate velocity on the distribution and spatial extent of marine species assemblages. *PLoS ONE*, 11: 1–21.
- Kleisner, K. M., Fogarty, M. J., McGee, S., Hare, J. A., Moret, S., Perretti, C. T., and Saba, V. S. 2017. Marine species distribution shifts on the U.S. Northeast Continental Shelf under continued ocean warming. *Progress in Oceanography*, 153: 24–36.
- Kohut, J., Palamara, L., Curchitser, E., Manderson, J., and Didomenico, G. 2016. Cooperative development of dynamic habitat models informed by the Integrated Ocean Observing System (IOOS) informs fisheries management decision making in the coastal ocean. *OCEANS 2015 - MTS/IEEE Washington*: 1–8. MTS.
- Langan, J. A., McManus, M. C., Zemeckis, D. R., and Collie, J. S. 2020. Abundance and distribution of atlantic cod (*Gadus morhua*) in a Warming southern New England. *Fishery Bulletin*, 118: 145–156.
- Manderson, J., Palamara, L., Kohut, J., and Oliver, M. J. 2011. Ocean observatory data is useful for regional habitat modeling of species with different vertical habitat preferences. *Marine Ecology Progress Series*, 438: 1–17.
- McCartney, M. A., Burton, M. L., and Lima, T. G. 2013. Mitochondrial DNA differentiation between populations of black sea bass (*Centropristis striata*) across Cape Hatteras, North Carolina (USA). *Journal of Biogeography*, 40: 1386–1398.
- McHenry, J., Welch, H., Lester, S. E., and Saba, V. 2019. Projecting marine species range shifts from only temperature can mask climate vulnerability. *Global Change Biology*, 25: 4208–4221.
- McMahan, M. D., and Grabowski, J. H. 2019. Nonconsumptive effects of a range-expanding predator on juvenile lobster (*Homarus americanus*) population dynamics. *Ecosphere*, 10: e02867.
- Miller, A. S., Shepherd, G. R., and Fratantoni, P. S. 2016. Offshore habitat preference of overwintering juvenile and adult black sea bass, *Centropristis striata*, and the relationship to year-class success. *PLoS ONE*, 11.
- Monllor-Hurtado, A., Pennino, M. G., and Sanchez-Lizaso, J. L. 2017. Shift in tuna catches due to ocean warming. *PLoS ONE*, 12: 1–10.
- Montes, E., Muller-Karger, F. E., Cianca, A., Lomas, M. W., Lorenzoni, L., and Habtes, S. 2016. Decadal variability in the oxygen inventory of North Atlantic subtropical underwater captured by sustained, long-term oceanographic time series observations. *Global biogeochemical cycles*, 30: 460–478.
- Morgan, A. C., and Sulikowski, J. A. 2015. The role of spiny dogfish in the northeast United States continental shelf ecosystem: How it has changed over time and potential interspecific competition for resources. *Fisheries Research*, 167: 260–277.
- Morley, J. W., Selden, R. L., Latour, R. J., Frölicher, T. L., Seagraves, R. J., and Pinsky, M. L. 2018. Projecting shifts in thermal habitat for 686 species on the North American continental shelf. *PLoS ONE*, 13: 1–28.
- Mountain, D. G. 2003. Variability in the properties of shelf water in the Middle Atlantic Bight, 1977-1999. *Journal of Geophysical Research: Oceans*, 108: 1–11.
- Nazzaro, L., Slesinger, E., Kohut, J., Saba, G. K., and Saba, V. S. 2021. Sensitivity of marine fish thermal habitat models to fishery data sources. *Ecology and Evolution*, 11: 13001–13013.

- NOAA, N. M. F. S. 1977. Oxygen depletion and associated environmental disturbances in the Middle Atlantic Bight in 1976. Technical Service Report No 3: 471.
- Nye, J. A., Link, J. S., Hare, J. A., and Overholtz, W. J. 2009. Changing spatial distribution of fish stocks in relation to climate and population size on the Northeast United States continental shelf. *Marine Ecology Progress Series*, 393: 111–129.
- O’Leary, C. A., Miller, T. J., Thorson, J. T., and Nye, J. A. 2019. Understanding historical summer flounder (*Paralichthys dentatus*) abundance patterns through the incorporation of oceanography-dependent vital rates in Bayesian hierarchical models Cecilia. *Can. J. Fish. Aquat. Sci.*, 76: 1275–1294.
- Ojeda, P. F., and Dearborn, J. H. 1991. Feeding ecology of benthic mobile predators: experimental analyses of their influence in rocky subtidal communities of the Gulf of Maine. *Journal of Experimental Marine Biology and Ecology*, 149: 13–44.
- Perretti, C. T., Fogarty, M. J., Friedland, K. D., Hare, J. A., Lucey, S. M., McBride, R. S., Miller, T. J., *et al.* 2017. Regime shifts in fish recruitment on the Northeast US Continental Shelf. *Marine Ecology Progress Series*, 574: 1–11.
- Perretti, C. T., and Thorson, J. T. 2019. Spatio-temporal dynamics of summer flounder (*Paralichthys dentatus*) on the Northeast US shelf. *Fisheries Research*, 215: 62–68.
- Pershing, A. J., Alexander, M. A., Hernandez, C. M., Kerr, L. A., Le Bris, A., Mills, K. E., Nye, J. A., *et al.* 2015. Slow adaptation in the face of rapid warming leads to collapse of the Gulf of Maine cod fishery. *Science*, 350: 809–812.
- Pinsky, M. L., Worm, B., Fogarty, M. J., Sarmiento, J. L., and Levin, S. A. 2013. Marine taxa track local climate velocities. *Science*, 341: 1239–1242.
- Pinsky, M. L., Reygondeau, G., Caddell, R., Palacios-Abrantes, J., Spijkers, J., and Cheung, W. W. L. 2018. Preparing ocean governance for species on the move. *Science*, 360: 1189–1192.
- Pinsky, M. L., Fenichel, E., Fogarty, M., Levin, S., McCay, B., St. Martin, K., Selden, R. L., *et al.* 2021. Fish and fisheries in hot water: What is happening and how do we adapt? *Population Ecology*, 63: 17–26.
- Pörtner, H. O., and Peck, M. A. 2010. Climate change effects on fishes and fisheries: Towards a cause-and-effect understanding. *Journal of Fish Biology*, 77: 1745–1779.
- Rabalais, N. N., and Turner, R. E. 2019. Gulf of Mexico Hypoxia: Past, Present, and Future. *Limnology and Oceanography Bulletin*, 28: 117–124.
- Rasmussen, L. L., Gawarkiewicz, G., Owens, W. B., and Lozier, M. S. 2005. Slope water, gulf stream, and seasonal influences on southern Mid-Atlantic Bight circulation during the fall-winter transition. *Journal of Geophysical Research C: Oceans*, 110: 1–16.
- Richaud, B., Kwon, Y. O., Joyce, T. M., Fratantoni, P. S., and Lentz, S. J. 2016. Surface and bottom temperature and salinity climatology along the continental shelf off the Canadian and U.S. East Coasts. *Continental Shelf Research*, 124: 165–181. Elsevier.
- Rijnsdorp, A. D., Peck, M. A., Engelhard, G. H., Möllmann, C., and Pinnegar, J. K. 2009. Resolving the effect of climate change on fish populations. *ICES Journal of Marine Science*, 66: 1570–1583.
- Roberts, S. M., Boustany, A. M., and Halpin, P. N. 2020. Substrate-dependent fish have shifted less in distribution under climate change. *Communications Biology*, 3: 1–7.
- Rodgers, G. G., Donelson, J. M., McCormick, M. I., and Munday, P. L. 2018. In hot water: sustained ocean warming reduces survival of a low-latitude coral reef fish.

- Marine Biology, 165: 1–10.
- Rogers, L. A., Griffin, R., Young, T., Fuller, E., St. Martin, K., and Pinsky, M. L. 2019. Shifting habitats expose fishing communities to risk under climate change. *Nature Climate Change*, 9: 512–516.
- Saba, V. S., Griffies, S. M., Anderson, W. G., Winton, M., Alexander, M. A., Delworth, T. L., Hare, J. A., *et al.* 2016. Enhanced warming of the Northwest Atlantic Ocean under climate change. *Journal of Geophysical Research: Oceans*, 120: 1–15.
- Sagarese, S. R., Frisk, M. G., Cerrato, R. M., Sosebee, K. A., Musick, J. A., and Rago, P. J. 2014. Application of generalized additive models to examine ontogenetic and seasonal distributions of spiny dogfish (*Squalus acanthias*) in the Northeast (US) shelf large marine ecosystem. *Canadian Journal of Fisheries and Aquatic Sciences*, 71: 847–877.
- Schofield, O., Roarty, H., Saba, G. K., Xu, Y., Kohut, J., Glenn, S., Manderson, J., *et al.* 2012. Phytoplankton dynamics and bottom water oxygen during a large bloom in the summer of 2011. *Oceans, 2012, IEEE*: 1–6.
- Seibel, B. A., and Deutsch, C. 2020. Oxygen supply capacity in animals evolves to meet maximum demand at the current oxygen partial pressure regardless of size or temperature. *Journal of Experimental Biology*, 223: jeb210492.
- Seibel, B. A., Andres, A., Birk, M. A., Burns, A. L., Shaw, C. T., Timpe, A. W., and Welsh, C. J. 2021. Oxygen supply capacity breathes new life into critical oxygen partial pressure (Pcrit). *Journal of Experimental Biology*, 224: 1–12.
- Seidov, D., Baranova, O. K., Johnson, D. R., Boyer, T. ., Mishonov, A. V., and A.R., P. 2016a. Northwest Atlantic Regional Climatology (NCEI Accession 0155889). NOAA National Centers for Environmental Information, <https://ww>: Accessed 25 March 2021.
- Seidov, D., Baranova, O. K., Boyer, T., Cross, S. L., Mishonov, A. V., and Parsons, A. R. 2016b. Northwest Atlantic regional ocean climatology. U.S. Department of Commerce, National Oceanic and Atmospheric Administration, National Environmental Satellite, Data, Information Service, National Centers for Environmental Information.
- Shackell, N. L., Ricard, D., and Stortini, C. 2014. Thermal habitat index of many Northwest Atlantic temperate species stays neutral under warming projected for 2030 but changes radically by 2060. *PLoS ONE*, 9.
- Shchepetkin, A. F., and McWilliams, J. C. 2005. The regional oceanic modeling system (ROMS): A split-explicit, free-surface, topography-following-coordinate oceanic model. *Ocean Modelling*, 9: 347–404.
- Slesinger, E., Andres, A., Young, R., Seibel, B., Saba, V., Phelan, B., Rosendale, J., *et al.* 2019. The effect of ocean warming on black sea bass (*Centropristis striata*) aerobic scope and hypoxia tolerance. *PLoS ONE*, 14: 1–22.
- Smith, K. A., Dowling, C. E., and Brown, J. 2019. Simmered then boiled: Multi-decadal poleward shift in distribution by a temperate fish accelerates during marine heatwave. *Frontiers in Marine Science*, 6: 1–16.
- Sullivan, M. C., Cowen, R. K., and Steves, B. P. 2005. Evidence for atmosphere-ocean forcing of yellowtail flounder (*Limanda ferruginea*) recruitment in the Middle Atlantic Bight. *Fisheries Oceanography*, 14: 386–399.
- Walsh, H. J., Richardson, D. E., Marancik, K. E., and Hare, J. A. 2015. Long-term

- changes in the distributions of larval and adult fish in the northeast U.S. shelf ecosystem. *PLoS ONE*, 10: 1–31.
- Witman, J. D., and Lamb, R. W. 2018. Persistent differences between coastal and offshore kelp forest communities in a warming Gulf of Maine. *PLoS ONE*, 13: 1–32.
- Xu, R., Yu, P., Abramson, M. J., Johnston, F. H., Samet, J. M., Bell, M. L., Haines, A., *et al.* 2020. Wildfires, Global Climate Change, and Human Health. *The New England Journal of Medicine*, 383: 2173–2181.
- Zemeckis, D. R., Martins, D., Kerr, L. A., and Cadrin, S. X. 2014. Stock identification of Atlantic cod (*Gadus morhua*) in US waters: an interdisciplinary approach. *ICES Journal of Marine Science*, 71: 1490–1506.

5.8 TABLES

Table 5.1 Species information used in this study.

Summer flounder was the only fish with multiple studies, and summer flounder and cunner were the only fish with 2 temperature bins.

Species Name	Common Name	Temperature (°C)	Critical PO ₂ (kPa)	Citation
<i>Centropristis striata</i>	Black sea bass	12	4.13	Slesinger et al. 2019
		17	4.48	
		22	4.58	
		27	6.64	
		30	7.95	
<i>Gadus morhua</i>	Atlantic cod	5	3.49	Schurmann & Steffensen 1997
		10	4.91	
		15	6.42	
<i>Paralichthys dentatus</i>	Summer flounder	22	5.67	Caposella et al 2012
		30	8.19	
		22	5.60	Schwieterman et al. 2019
		30	8.00	
<i>Squalus acanthias</i>	Spiny dogfish	10	3.33	Andres et al. in prep
		13	3.24	
		17	3.9	
		21	4.37	
		23	4.42	
<i>Tautoglabrus adspersus</i>	Cunner	1	3.58	Corkum & Gamperl 2009
		8	4.53	

Table 5.2 Species-specific parameters.

The species-specific parameters defined from the linear regressions (E_o and A_o), and respective MI_{crit} and maximum MI values (to provide a range of MI conditions experienced).

Species	E_o	A_o	MI_{crit}	Max MI
Atlantic cod	0.42	6.68E-07	2.66	7.20
Black sea bass	0.27	4.77E-04	3.13	7.00
Cunner	0.22	2.20E-03	2.95	5.16
Spiny dogfish	0.19	1.44E-02	4.28	7.53
Summer flounder	0.35	1.96E-05	4.03	8.89

Table 5.3 Comparison of species parameters between this study and Deutsch et al. 2020

Comparison of species E_o and MI_{crit} between this study (top value for each species) and Deutsch *et al.*, (2020) (bottom value for each species). Same study indicates if values were used from the same original study. * we used two studies and a calculated mean, one of which was the same as in Deutsch *et al.*, (2020).

Species	E_o	MI_{crit}	Same study
Atlantic cod	0.42	2.66	no
	0.35	2.4	
Black sea bass	0.27	3.13	yes
	0.23	3.27-3.29	
Cunner	0.22	2.95	yes
	0.24	3.33-3.45	
Summer flounder	0.35	4.03	yes*
	0.35	2.97-3.35	

5.9 FIGURES

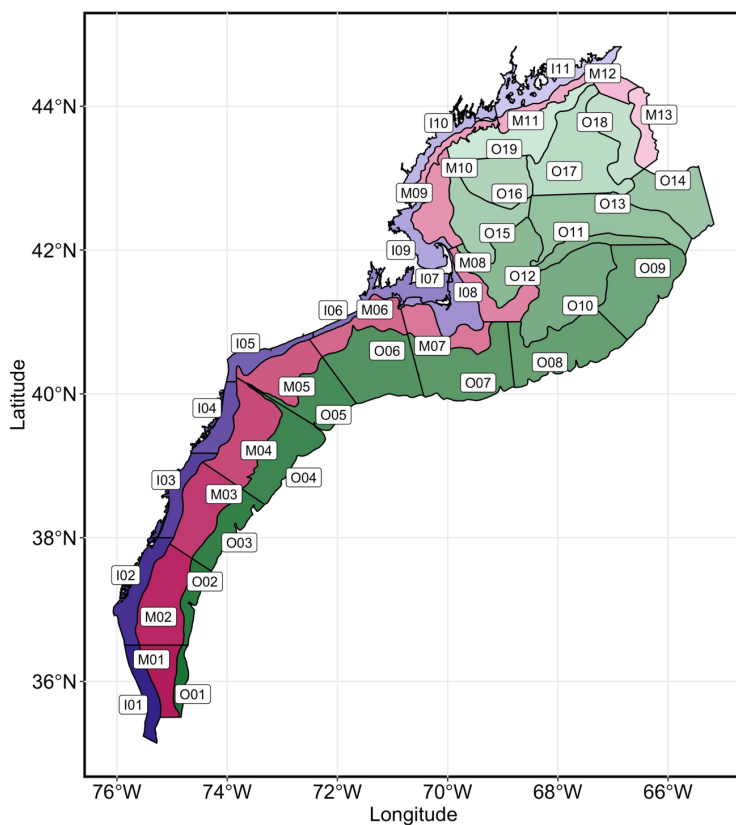


Figure 5.1 Strata defined for this study.

Letter codes indicate across-shelf position (I = Inshore, M = Midshelf, O = Offshore) and number codes indicate along-shelf position from lower numbers in the south and higher in the north. The coloration of offshore (green), midshelf (magenta), and inshore (purple) is used throughout this paper and shading designates the gradient from south to north.

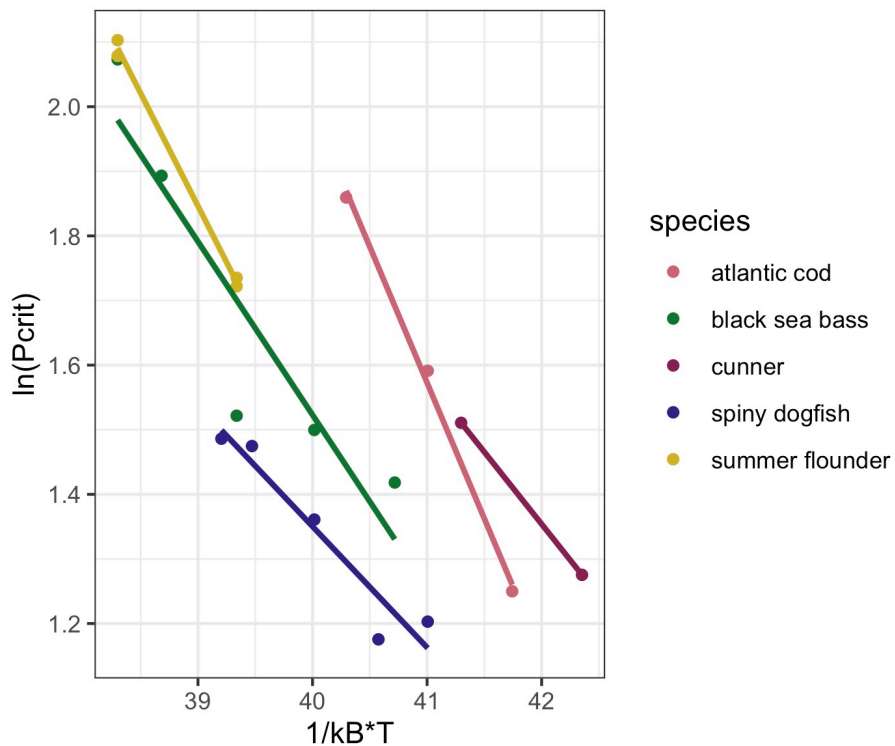


Figure 5.2 Regression of $\ln(P_{crit})$ and inverse temperature for each species.

The distinction between cold and warm water species is shown where cod and cunner are further to the right (inverse temperature) compared to summer flounder and black sea bass. The slope of the line (E_o) indicates the thermal sensitivity of the fish, whereby a steeper slope indicates higher temperature sensitivity.

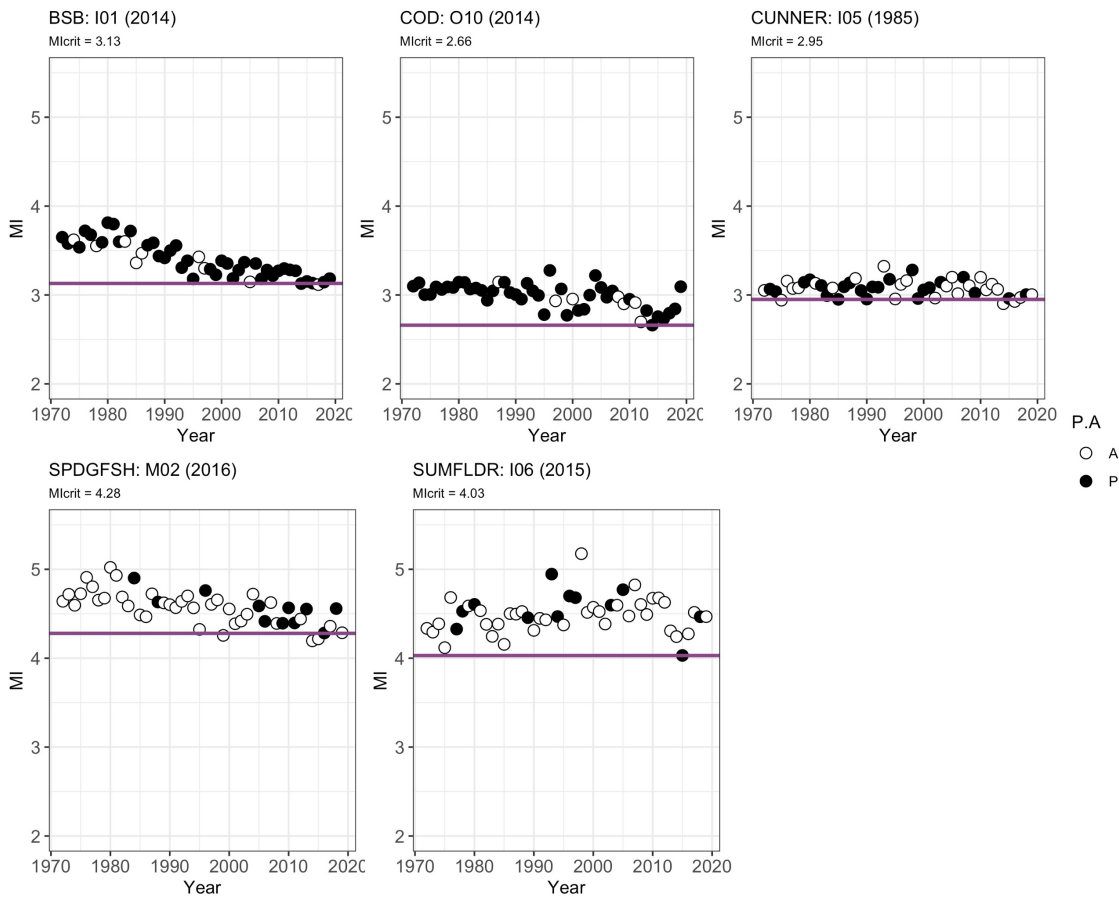


Figure 5.3 MI_{crit} values and evaluation for each species

For the stratum in which MI_{crit} occurred, the MI for each species across time is plotted with presence (P; black dots) and absence (A; white dots). The year within the plot title indicates the year that MI_{crit} was identified. The purple line denotes the MI_{crit} . Each panel includes data from fall, the season MI_{crit} occurred. The decreasing or stable trend in MI over time highlights climatological trends within the respective stratum (i.e. during fall, warming in I01 and constant temperatures in I05).

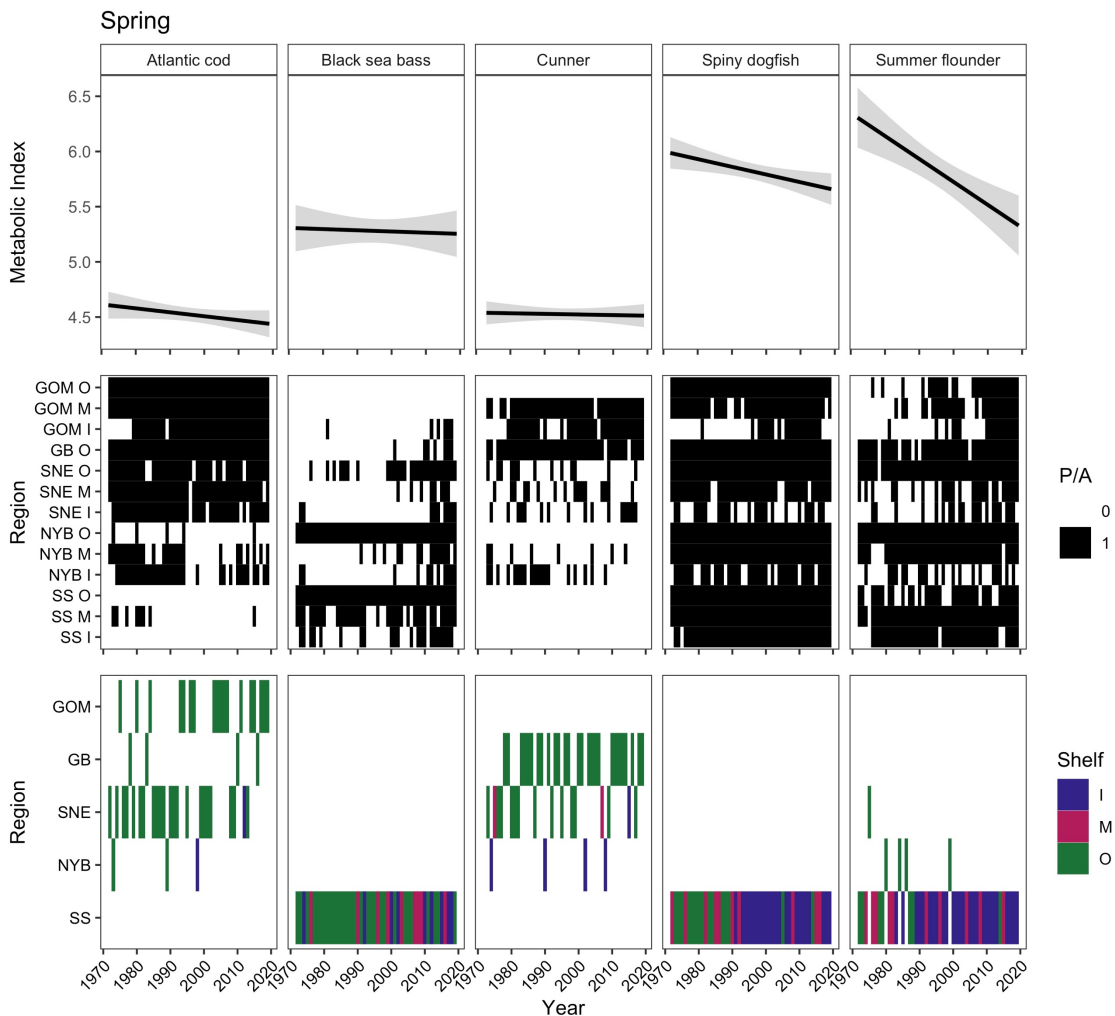


Figure 5.4 Minimum MI trends in spring.

The assessment of minimum MI overtime in spring. The top row shows the general linear trend in minimum MI overtime for each species. The middle row shows the presence(black)/absence(white) for each species across time by respective region and shelf location. The bottom row shows the region and shelf (inshore = purple; midshelf = magenta; offshore = green) where the minimum MI occurred for that particular year.

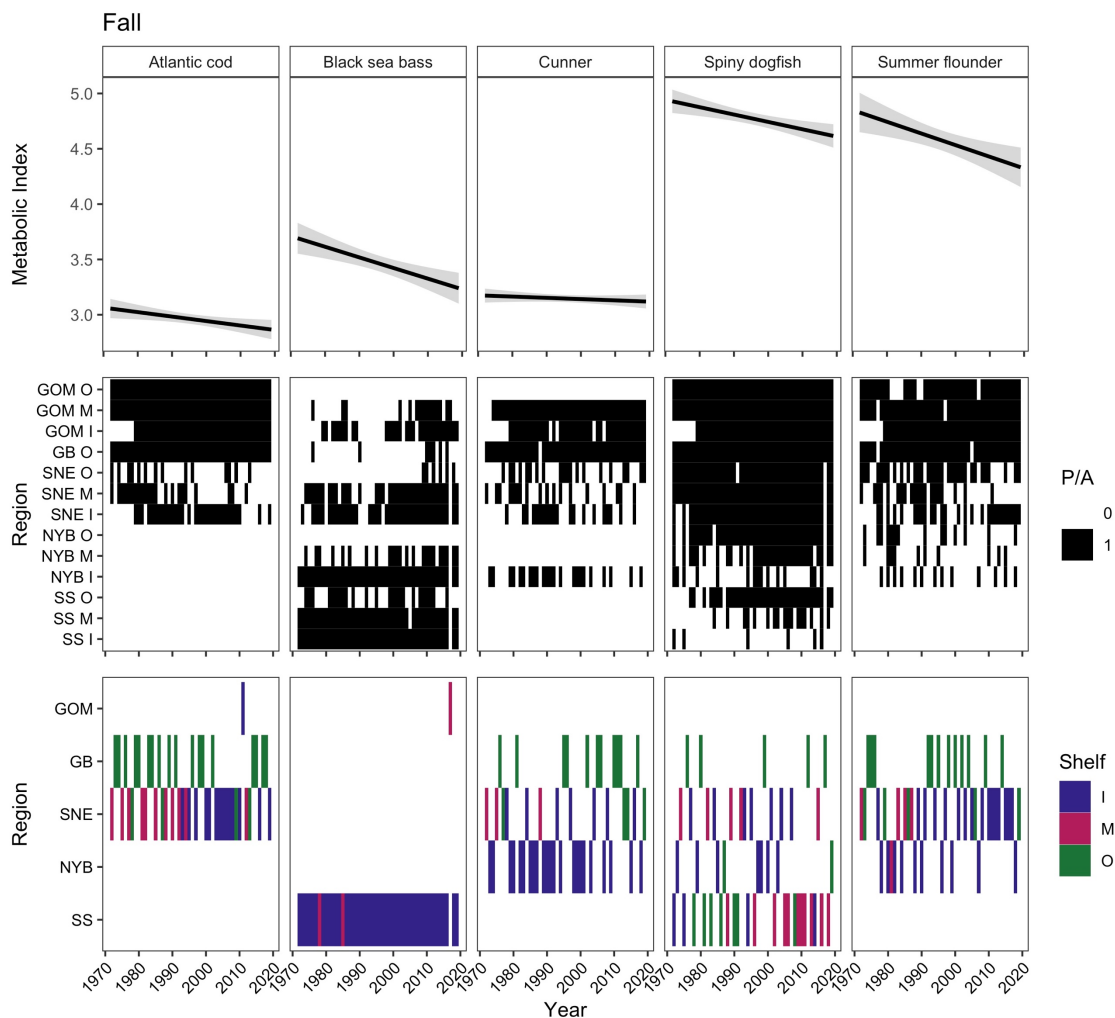


Figure 5.5 Minimum MI trends in fall.

The assessment of minimum MI overtime in fall. The top row shows the general linear trend in minimum MI overtime for each species. The middle row shows the presence(black)/absence(white) for each species across time by respective region and shelf location. The bottom row shows the region and shelf (inshore = purple; midshelf = magenta; offshore = green) where the minimum MI occurred for that particular year. Note, there was minimal sampling for black sea bass in 2017, leading to error in the

location of minimum MI location (midshelf GOM) as this was the only location black sea bass were identified in that year.

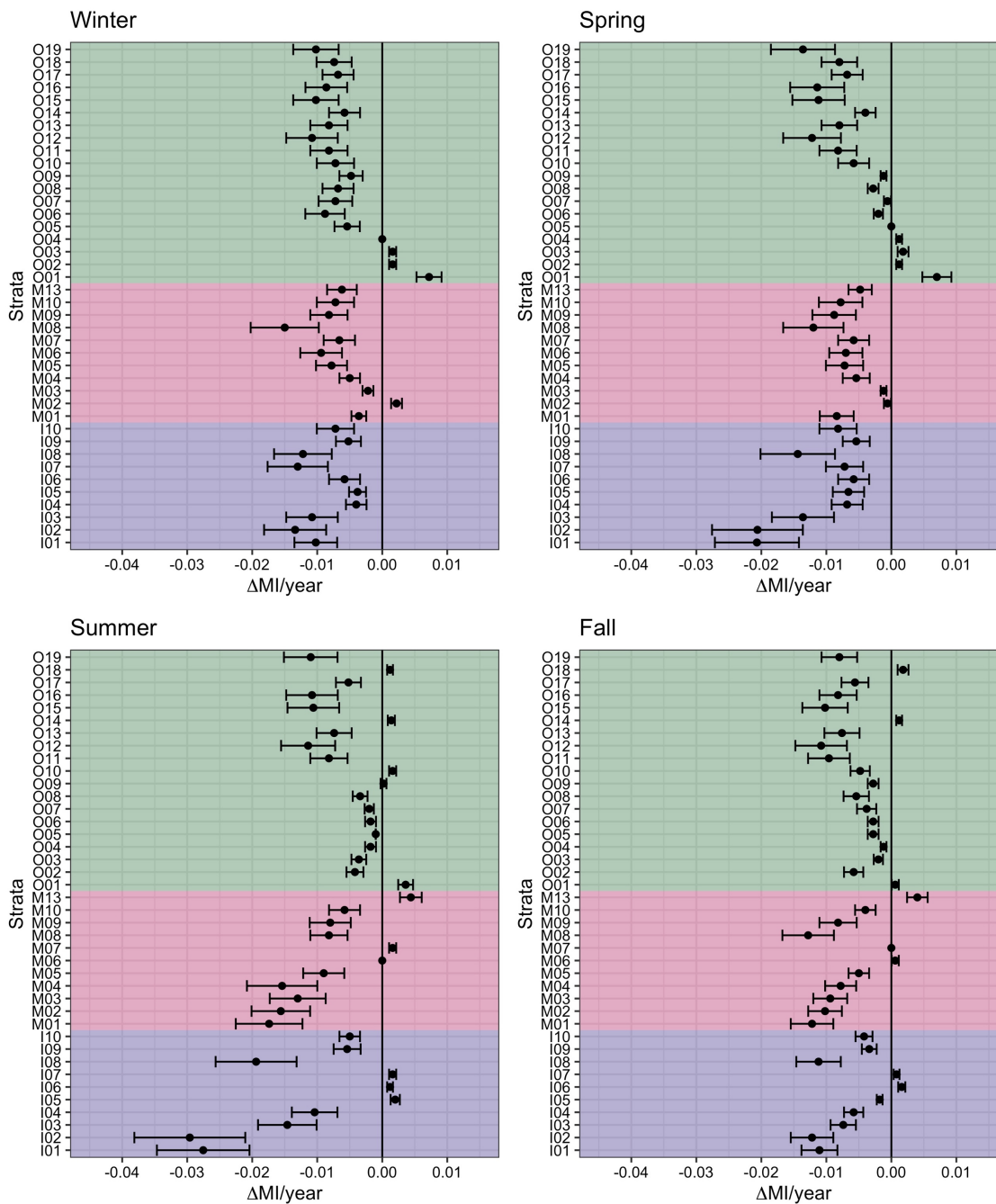


Figure 5.6 MI trends over time per stratum.

The general trend of MI over time for species combined with mean and standard deviation plotted for each strata. Strata are ordered by shelf position and from south to north. The line indicates no change in MI. As the rate of MI change increases, the

standard deviation also increases exemplifying the differences in thermal sensitivities in the five species.

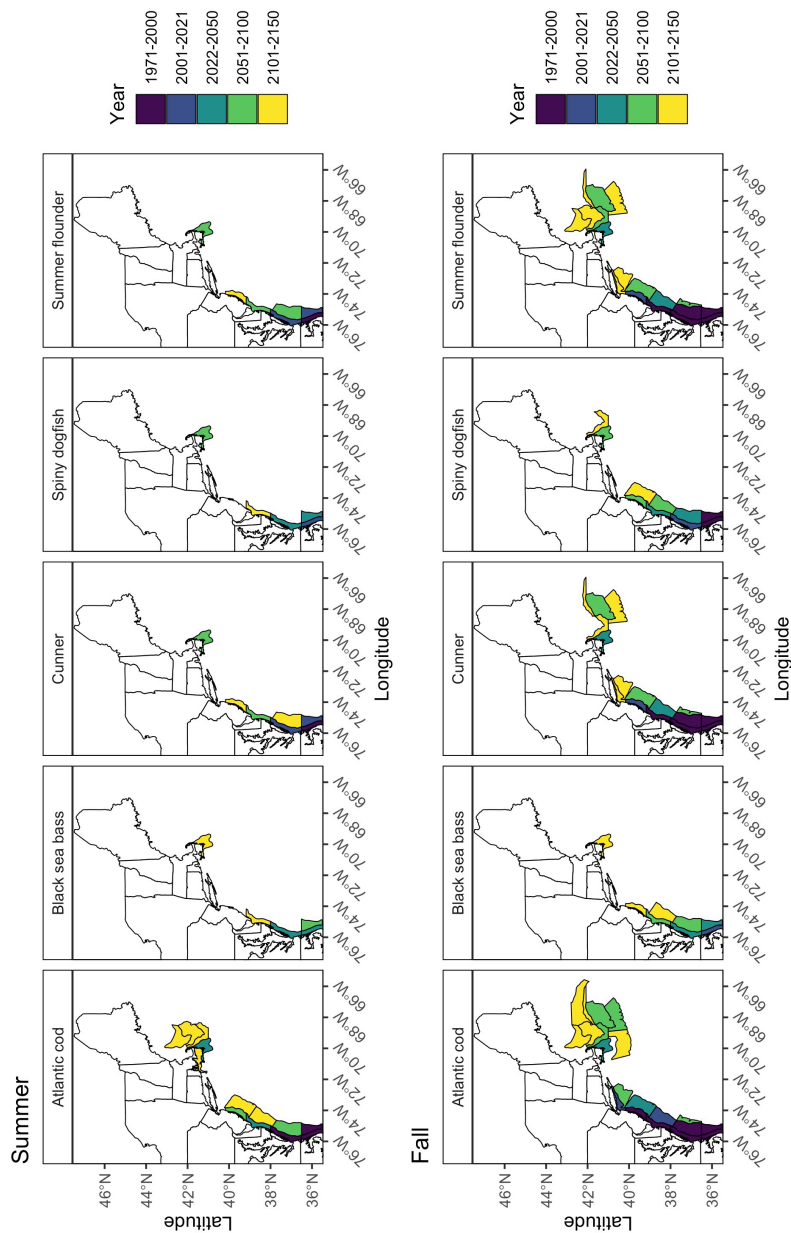


Figure 5.7 MI_{crit} values for summer and fall.

The binned year range that MI_{crit} was or will be reached for each species is shown by stratum for fall and summer. The MI_{crit} year was binned into 5 time periods: 1971-2000, 2000 to present, present to 2050, 2050 to 2100 and 2100 to 2150. The actual year MI_{crit} is reached can be found in SI Table 1. Locations where MI_{crit} were reached prior to the present, and especially those prior to 2000, indicate range limits for those species.

5.10 SUPPLEMENTAL INFORMATION

Table S5.1 Year when MI_{crit} is reached.

The year MI_{crit} has been or will be reached for each species separated by season. Bsb = black sea bass, cod = Atlantic cod, cnr = cunner, spdg = spiny dogfish, and sumf = summer flounder.

	Winter					Spring				
	bsb	cod	cnr	spdg	sumf	bsb	cod	cnr	spdg	sumf
I01		2041	2055	2078	2052	2117	2055	2080	2108	2068
I02	2117	2066	2079	2102	2076	2143	2084	2109	2137	2097
I03		2147								
I08		2135								
M01	2131	2038	2063	2102	2056		2090	2131		2112
M08		2139								
O12		2135								
O15		2137								
O16		2148								
O19		2138								

	Summer					Fall				
	bsb	cod	cnr	spdg	sumf	bsb	cod	cnr	spdg	sumf
I01	2022	1970	1980	2002	1979	2010	1970	1970	1988	1970
I02	2045	1995	2006	2028	2005	2020	1973	1980	2000	1981
I03	2127	2039	2063	2102	2056	2059	1980	1992	2027	1993
I04		2092	2134		2121	2120	1983	2007	2067	2007
I05							2005	2082		2072
I06							2053			2133
I07		2115					2030	2082		2069
I08	2118	2044	2067	2100	2059	2086	2017	2033	2063	2030
I10							2147			
M01	2073	1983	2003		2001	2035	1970	1970	1999	1970
M02		2069	2103		2098	2117	1970	1990	2054	1992
M03		2150					2026	2056	2118	2053
M04		2147					2038	2066	2118	2060
M05							2064	2101		2091

M06							2096			2144
M07							2127			
M08		2134					2083	2111		2101
O06							2126			
O07							2122			
O08							2095	2140		2134
O10							2061	2117		2105
O11							2122			2146
O12		2142					2123			2143
O13							2141			
O15		2136					2123			2143
O16							2136			
O19							2125			2146

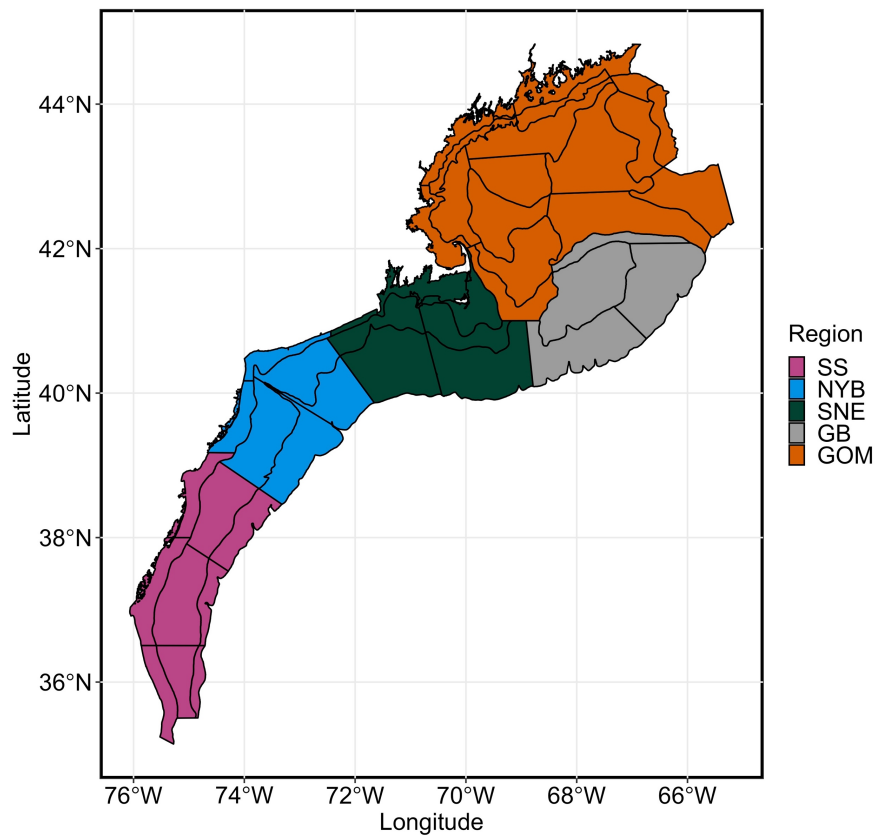


Figure S5.1 Defined regions across USNES.

Regions identified with strata outlines indicating which stratum are within each region.

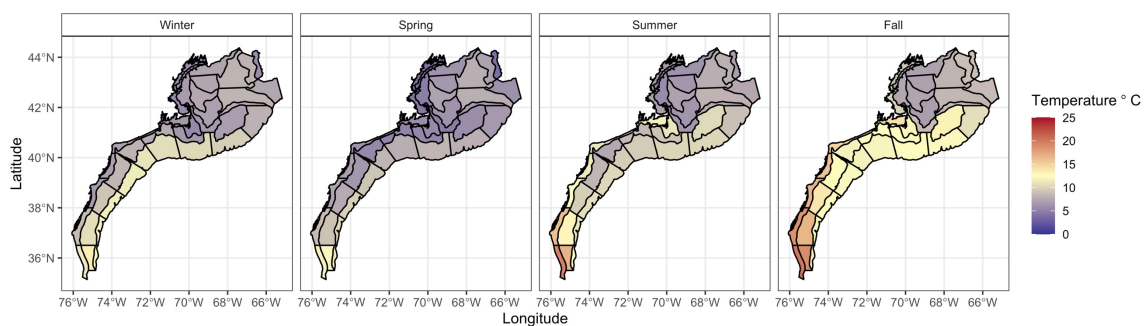


Figure S5.2 Temperature throughout each season across USNES.

Strata-based mean seasonal bottom temperature (1970-2019). This resolution still provides distinct features of the USNES: 1) warming in fall that starts in the southern inshore portion of the shelf during summer, 2) cooler midshelf summer strata when compared to inshore and offshore reflecting the ‘Cold Pool’, and 3) the warmer offshore strata in winter and spring representing the thermally suitable ocean conditions that many fish migrate to for overwintering.

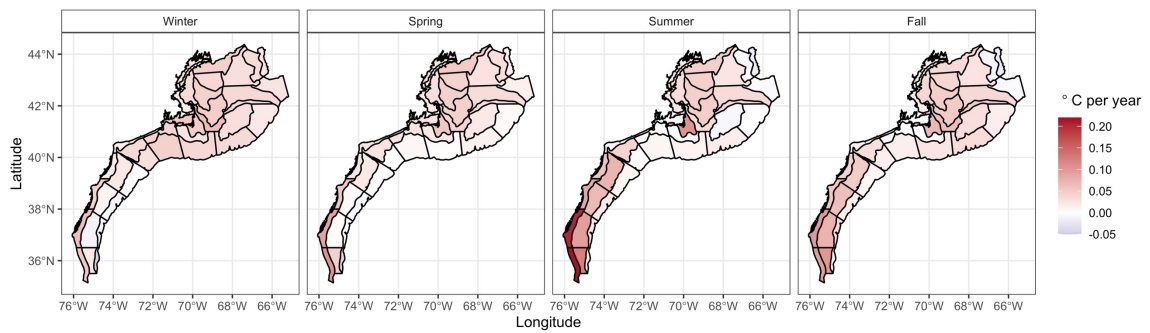


Figure S5.3 Temperature trends over time per stratum.

Strata-based temperature change over time (1970-2019) based on the linear trend in seasonal-based mean temperature from 1970-2019. Warm colors indicate positive slope (increasing temperature) and cool colors indicate negative slopes (decreasing temperature). Strata that depict cooling for winter: M02, O01, O02, O03, O04; spring: O01, O02, O03, O04, O05; Summer: I05, I06, I07, M07, M13, O01, O09, O10, O014, O15; and fall: I06, I07, M06, M07, M13, O01, O14, O18.

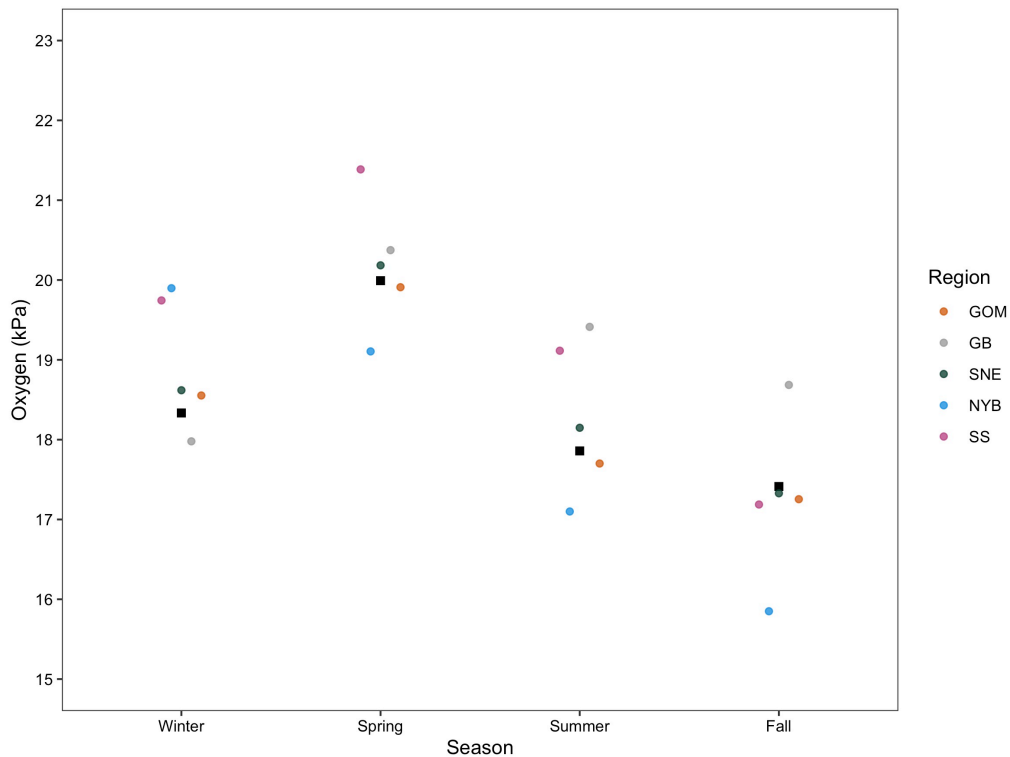
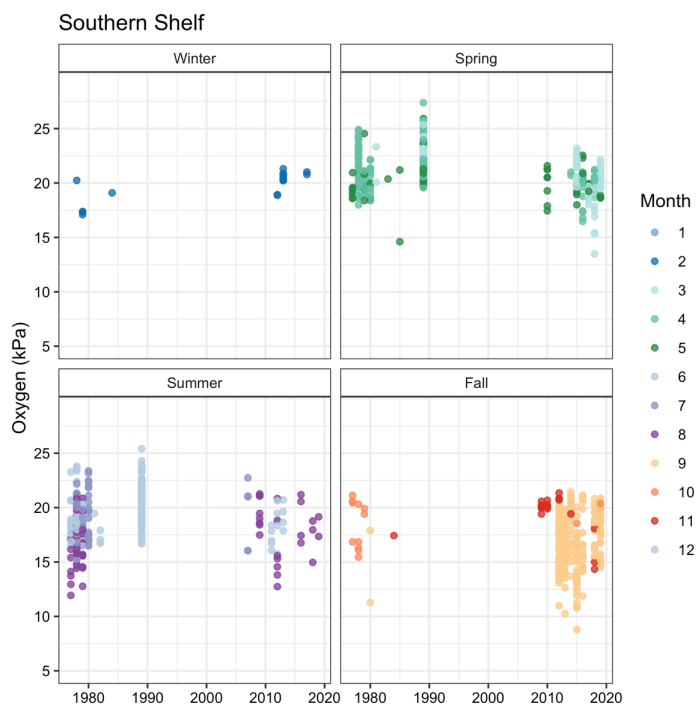


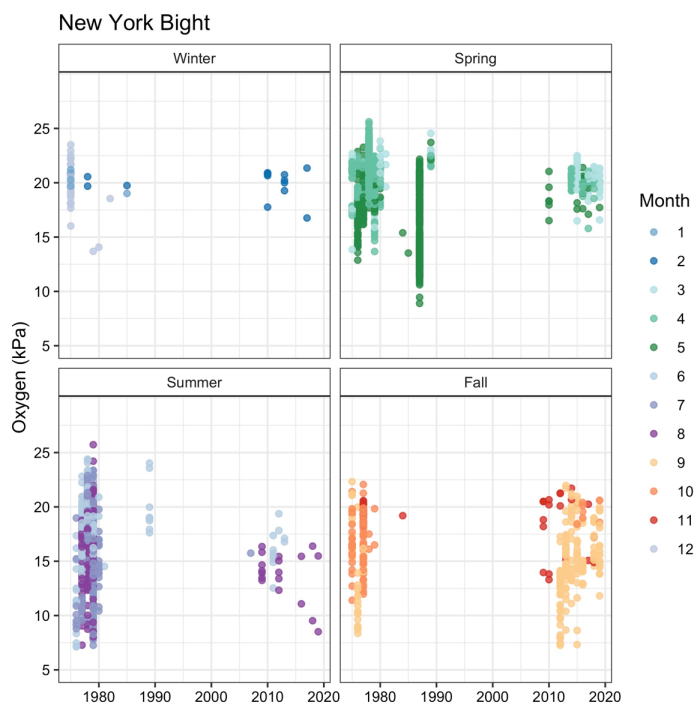
Figure S5.4 Mean oxygen (kPa) values per season.

Mean oxygen values for each season (black squares) shows higher oxygen values in the colder seasons and lower oxygen in the warmer seasons. While not used in this study, the variation with the regional means is shown by their respective colors. Seasonal trends by region are constant but the seasonal mean can bias regional oxygen measurements by ~2kPa.

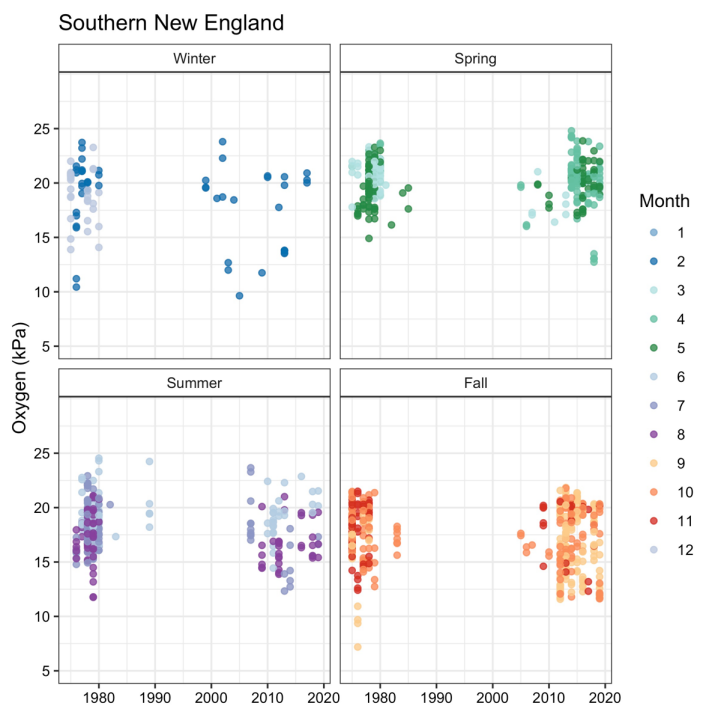
(a)



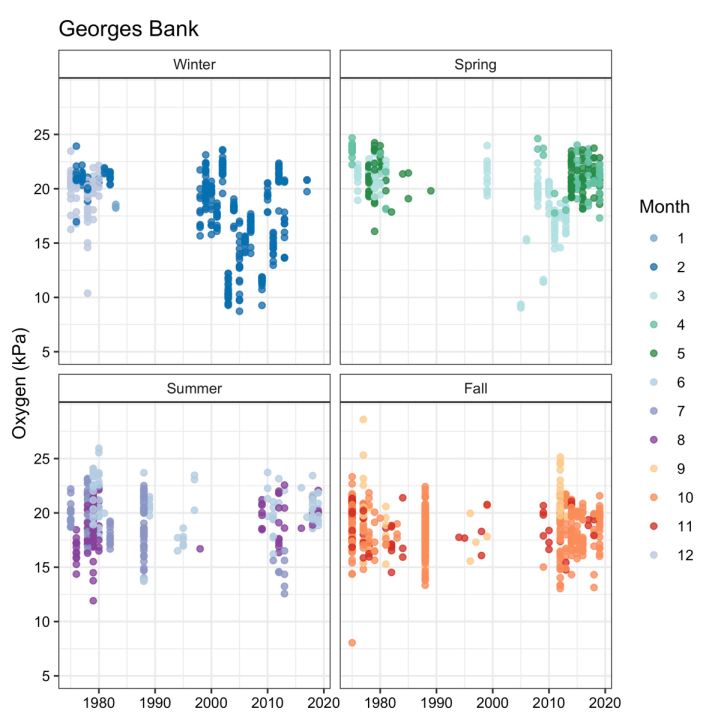
(b)



(c)



(d)



(e)

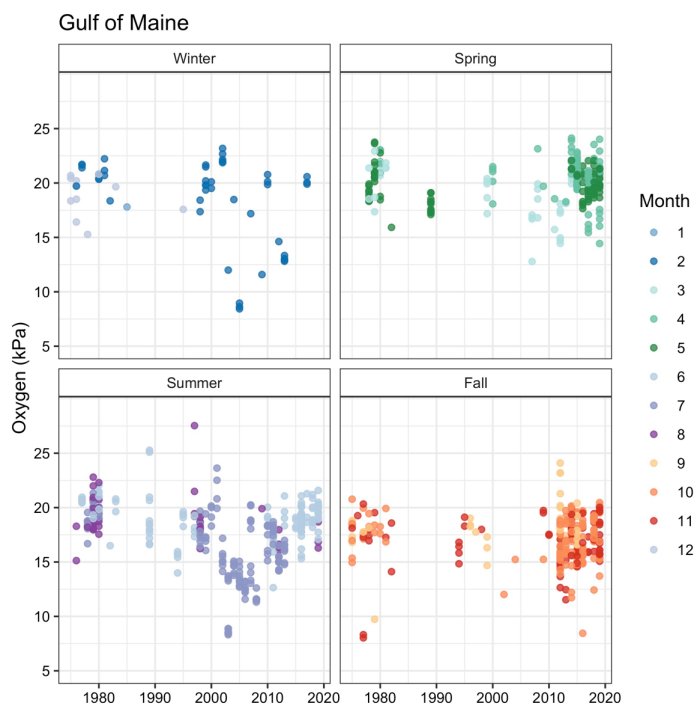
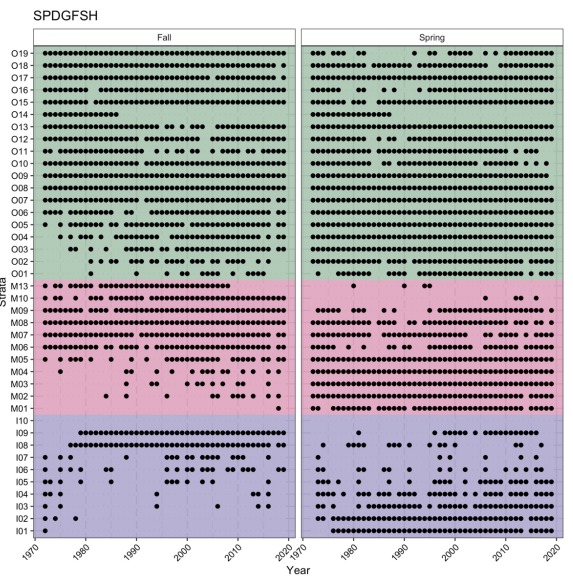
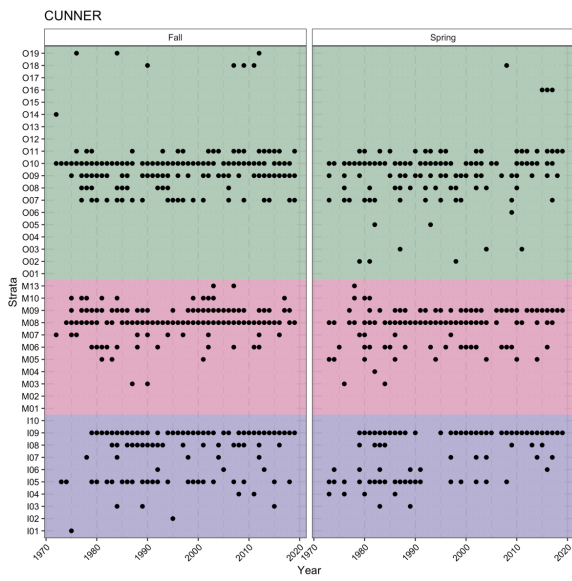
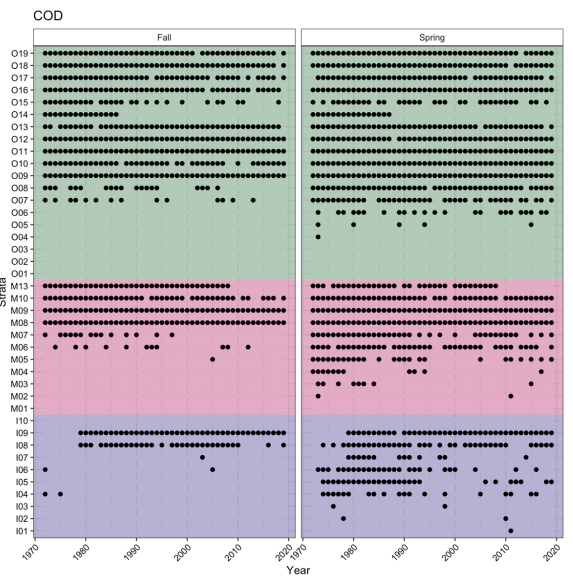
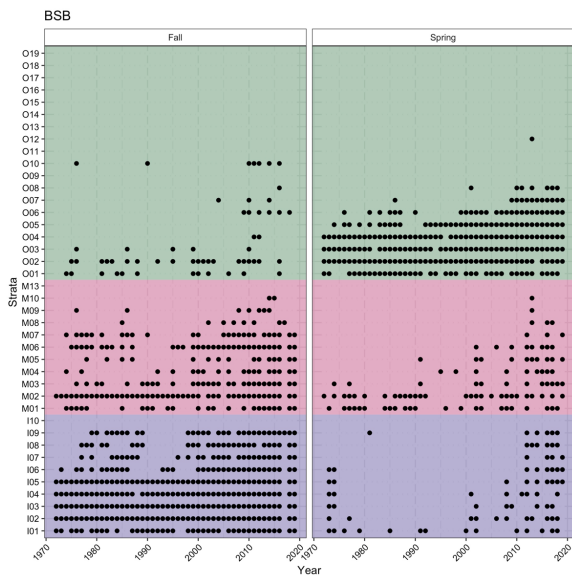


Figure S5.5 Raw oxygen (kPa) values for each region and season.

Oxygen distribution across entire sampling time period designated by month and season for Southern Shelf (a), New York Bight (b), Southern New England (c), Georges Bank (d), and Gulf of Maine (e).



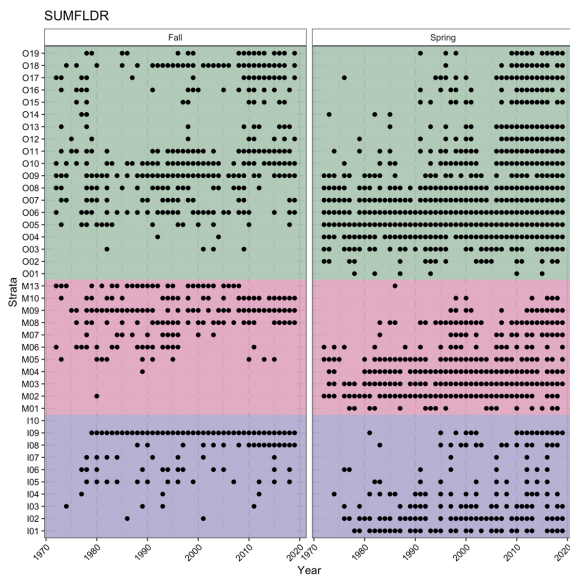


Figure S5.6 Species presences across year, season, and stratum.

Season, for these analyses, includes only Fall and Spring. Shelf region is color coded for inshore = purple, midshelf = pink, offshore = green. Strata are also organized from south to north (down to up) within each shelf stratum (refer to map in Fig. 5.1).

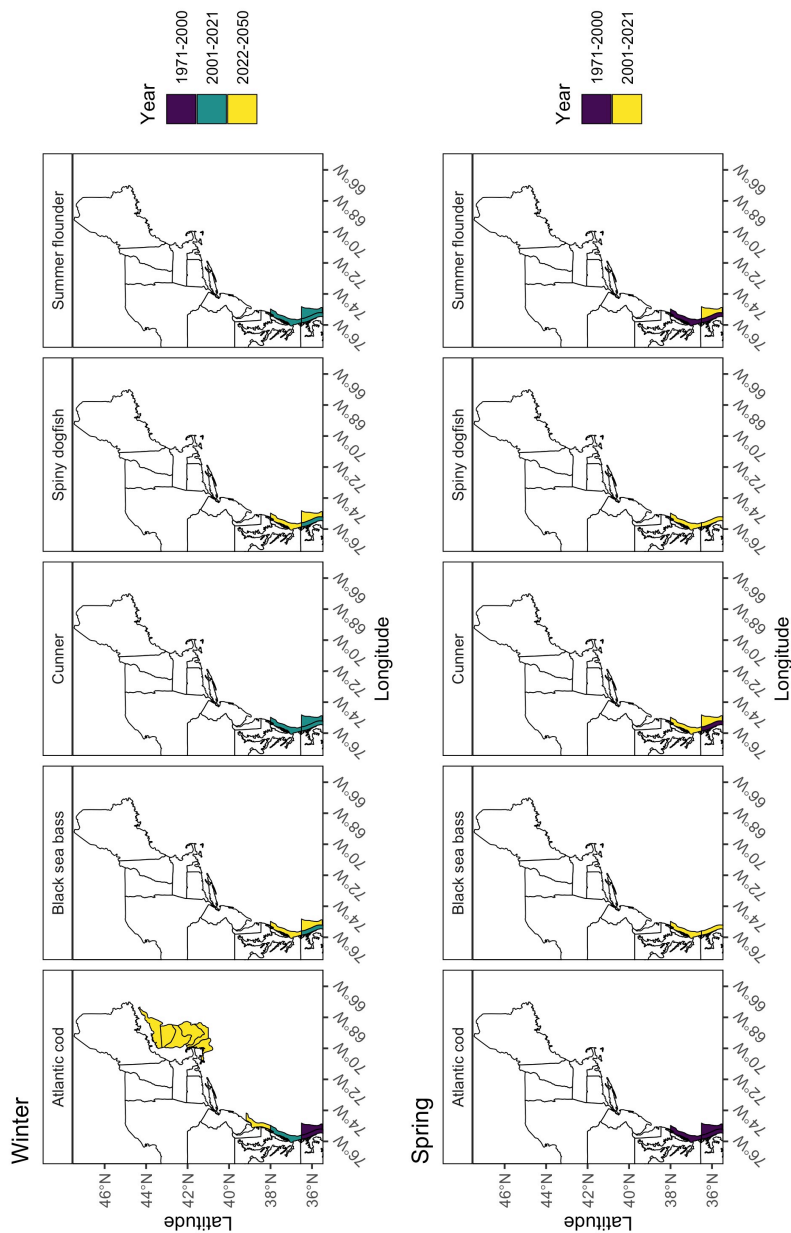


Figure S5.7 MI_{crit} values for winter and spring.

The binned year range that MI_{crit} was or will be reached for each species is shown by stratum for winter and spring. The MI_{crit} year was binned into 5 time periods: 1971-2000, 2000 to present, present to 2050, 2050 to 2100 and 2100 to 2150. The actual year MI_{crit} is reached can be found in SI Table 1. Locations where MI_{crit} were reached prior to the present, and especially those prior to 2000, indicate range limits for those species.

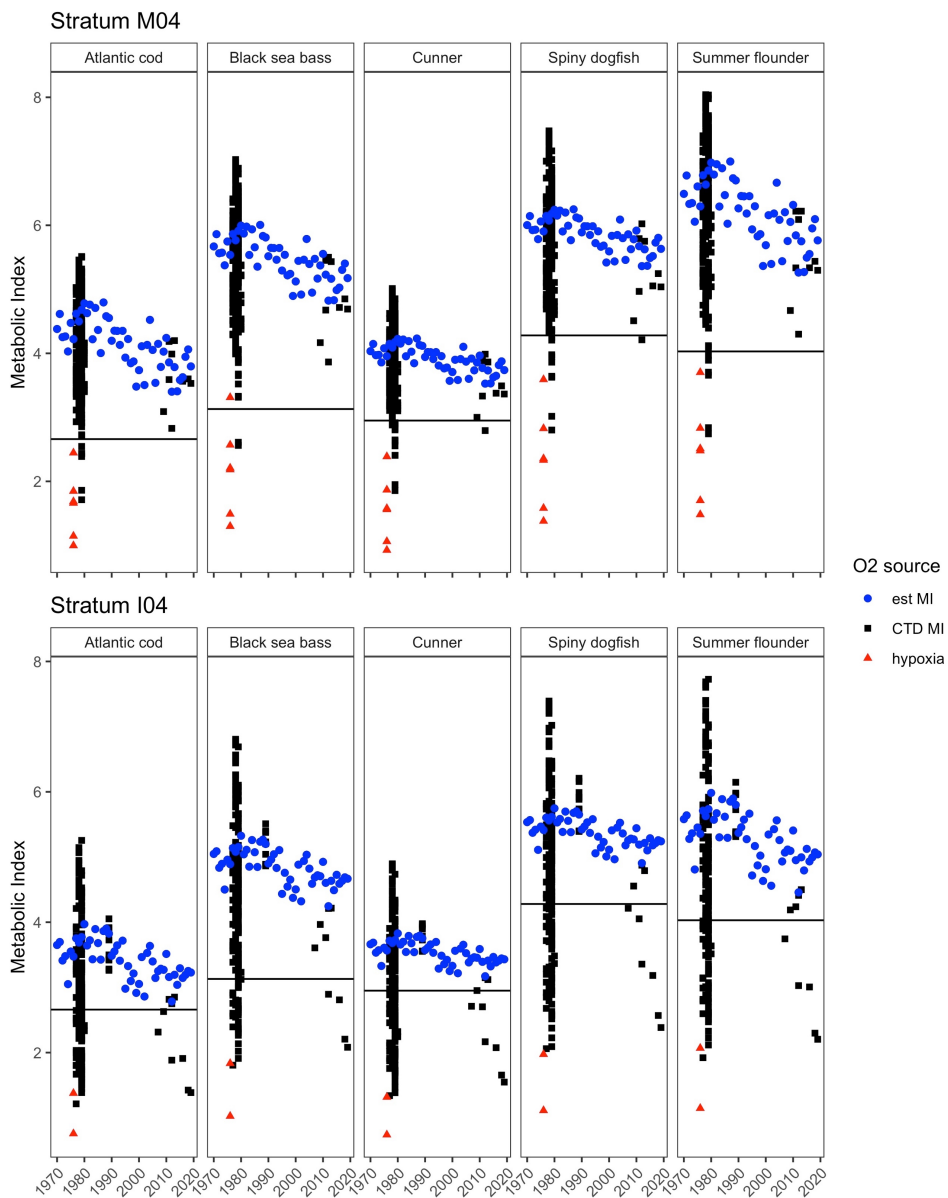


Figure S5.8 Case study of oxygen in NYB.

Comparison of differing MI values based on estimated MI from seasonal oxygen used in this study (blue circle), MI calculated from raw CTD values (black square), and MI calculated from raw CTD values during the 1976 hypoxia event (red triangle). The black horizontal line depicts the MI_{crit} defined in this study.

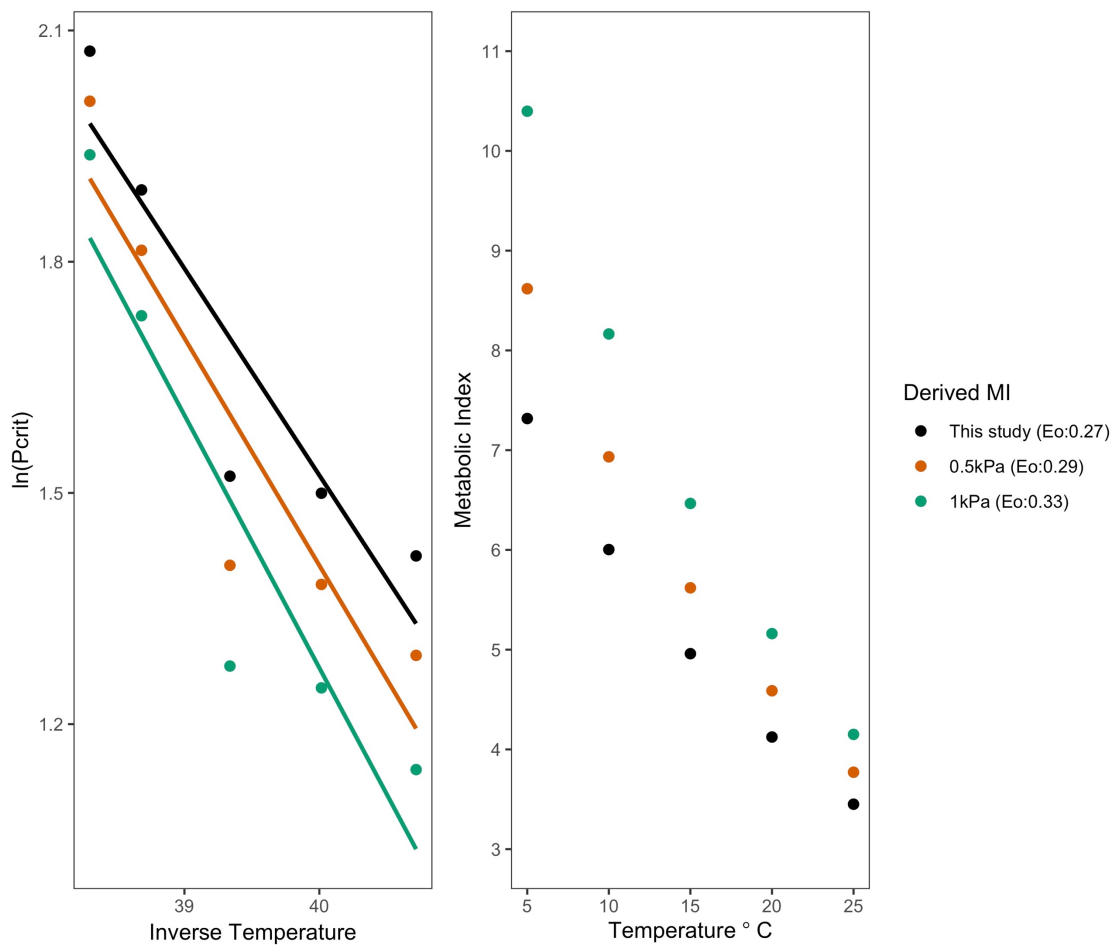


Figure S5.9 Comparison of MI parameters with differing error in P_{crit} .

Comparison of linear regression of P_{crit} and temperature and metabolic index across temperature for differing P_{crit} values for black sea bass including those used in this study (black), a decrease in 0.5kPa for P_{crit} (orange), and a decrease in 1kPa for P_{crit} (green).

CHAPTER 6: Conclusions

Ocean warming continues to impact marine ecosystems, including the US Northeast Shelf (USNES). The implications of ocean warming can range from physiological impacts on individual species to shifts in species assemblages within ecosystems. Such effects at individual to ecosystem levels can impact fisheries in a variety of ways including modifications to fishers' target species to changes in fisheries management focused on distribution or life history parameters. In order to be proactive towards the current and future effects of ocean warming on fish species, the effects of ocean warming at the individual level need to be understood first. Chapters 2 and 5 explored the physiological effects of ocean warming on black sea bass and thermal habitat changes in black sea bass and four other important USNES species, respectively. Also, as species biomass changes throughout a distribution the impacts of intraspecific differences throughout the distribution also need to be investigated. Chapters 3 and 4 investigated the intraspecific differences in black sea bass throughout their distribution within the context of the recent center of biomass shift.

Studying the effects of ocean warming through physiology-based laboratory experiments allows for mechanistic hypotheses to be tested. Chapter 2 investigated the effects of ocean warming on black sea bass by measuring various whole-animal responses to a range of temperatures that included current and future bottom ocean temperatures. A chronic exposure to projected warm bottom temperature (30°C) was also included. I found black sea bass "optimal" temperature to be ~24°C based on the temperature where aerobic scope was highest, but suggested this temperature was likely a maximum tolerable temperature. This designation was chosen because black sea bass

Metabolic Index neared 3 at 24°C, which is seen as a population limiting level (Deutsch *et al.*, 2015). In addition, black sea bass were unable to acclimate to a month-long 30°C exposure as seen by a significant drop in their aerobic scope. Finally, I found that black sea bass were likely oxygen demand limited instead of oxygen supply limited based on comparisons between the acute and chronic 30°C treatment groups. At the acute exposure to 30°C, both standard and maximum metabolic rates increased and hypoxia tolerance decreased. For the chronic 30°C exposure experiment, black sea bass standard metabolic rates and hypoxia tolerance remained the same as at the acute 30°C group, but maximum metabolic rate decreased. This suggests that black sea bass were able to maintain their oxygen supply capacity but their oxygen demand decreased (i.e. the decrease in MMR). As the southern portion of their distribution has currently been reaching 24°C or higher in the summer and fall months, I propose that part of black sea bass shift in biomass is due to the warming in the southern portion of the range to temperatures.

Providing empirical evidence of how ocean warming may affect black sea bass helps to explain the current shifts in biomass that have been documented on the USNES. When determining the effects of shifting biomass, it is also important to understand the intraspecific differences throughout the distribution and how that may affect the population into the future. For example, if the center of biomass is increasing in a region that sees lower recruitment and reproductive output, the long-term effects could result in a decline in the population. Chapters 3 and 4 focused on disentangling the intraspecific differences in black sea bass throughout their distribution during the spawning season. From field collections of black sea bass throughout their distribution and the spawning season, Chapter 3 focused on spawning phenology and output while Chapter 4 focused on

energy allocation with respect to spawning. Black sea bass exhibited significant intraspecific differences in their spawning dynamics and energy allocation. Spawning duration increased from north to south, which was expected with latitudinal trends and increasing summer seasons. However, reproductive output was lower in the northern regions which was unexpected as population spawning at higher latitudes with shorter spawning seasons will usually have higher reproductive output to compensate for the shorter spawning season (Kokita, 2004). Black sea bass energetic allocation also differed across the distribution and results paralleled to those found in Chapter 3. Specifically, energetic allocation towards reproductive development decreased from south to north. The northern regions also had lower pre-spawning energetics in their somatic stores, and this could be due to a suite of factors. These results suggest that black sea bass in their current higher center of biomass region experience lower energetic statuses and reproductive output which may impact population dynamics into the future if recruitment decreases in that region.

Information about past, present and future changes in thermal habitat can provide more insight into species responses to ocean warming. Studies have already focused on the relationship between ocean warming and distribution (e.g. Kleisner *et al.*, 2017), but many of these studies use statistical correlation between temperature and species distribution. In Chapter 5, I used information from laboratory physiology studies on five fish species of the USNES to determine their Metabolic Index (MI) and assess how MI has changed over time, the MI limits (MI_{crit}) of the species, and future loss in habitat based on MI_{crit} . Across the USNES and each season, MI decreased over time. For winter and spring, a decrease in MI was less concerning because values already started high due

to cold temperatures. However, for summer and fall, the decrease in MI reached some MI_{crit} limits for the species studied. I found that MI_{crit} was lower for the cold water species than the warm water species and that the range of MI reflected either species experiencing decreasing MI or similar MI by moving to different regions. Future loss in habitat due to portions of the USNES reaching MI_{crit} values or less is significant for each species, especially in the southern and inshore portions of the USNES for most, and across the entirety of the USNES for Atlantic cod. Overall, by using physiological parameters to determine suitable thermal habitat, I was able to show the impacts of ocean warming on five USNES species and provide a modest prediction of future habitat loss into the future.

Black sea bass overall seem to tolerate warm temperatures up to 24°C and are unable to acclimate to temperatures above 30°C. Under future ocean warming scenarios, the southern portion of black sea bass range may reach 30°C in the next 70 years (Saba *et al.*, 2016) and the results from Chapter 5 corroborate with this result. However, warming along the USNES is occurring across all seasons and black sea bass may also benefit from ocean warming in certain portions of the year. In the cold months across winter and spring, black sea bass overwinter at the continental shelf break in the southeastern portion of the shelf because temperature is more stable and inshore temperatures become too cold. As these seasons warm, black sea bass habitat may expand allowing fish to remain closer inshore, eliminating the need for a lengthy cross- or along-shelf migration. This dynamic has already been suggested for black sea bass larval survival and a potential cause of good recruitment years, as the number of fish reaching age 1 seems to be tethered to winter survival (Miller *et al.*, 2016). Therefore, the impacts of ocean warming

should be viewed holistically as there may be multiple outcomes that may or may not act synergistically.

A major result of this dissertation was the significant intraspecific variation in population dynamics of black sea bass throughout their distribution. Variation in reproduction, energetics, and recruitment can affect the population size in respective regions because black sea bass exhibit site fidelity (Moser and Shepherd, 2008). In other words, if a region produces a high number of recruits, those fish will likely return to that region year after year increasing the local population size during the inshore months. However, if a portion of the region is not conducive to high recruitment (as was seen in the northern sampling portion), which currently coincides with the higher center of biomass, then this could have negative implications on black sea bass. This is particularly pertinent because part of the northern region increase in biomass may be due to a large cohort in 2011 that was predominantly from fish in the north (Miller *et al.*, 2016). The 2011 year class will age out soon, and monitoring the biomass in the northern region will expose how closely regional population dynamics are affected by interannual recruitment success. Regional intraspecific differences is important for fisheries management, especially on the USNES where the regulations that differ across states are based on population dynamics and biomass. Current allocation changes to the commercial black sea bass fishery (ASMFC, 2021) reflect management recognizing the shift in the center of biomass. However, without an understanding of the full implications of a shift in biomass, then changes in management may not benefit the population. Fish population dynamics are inherently stochastic and hard to predict, but results from this dissertation

show that even in areas where there is a high biomass, black sea bass may be experiencing lower reproductive output and recruitment, at least in some years.

Across multiple species of fish, ocean warming also seems to affect the distribution of thermal habitat. For cold water species, such as cunner and Atlantic cod, habitat throughout the USNES may become unsuitable in the summer and fall months, while for warmer water species such as black sea bass, summer flounder, and spiny dogfish, mostly inshore and southern areas may become unsuitable. However, the effects fisheries management can have on population dynamics should also be addressed in the context of understanding changes in distributions. While MI_{crit} was estimated using presence/absence fish distribution data, predicted future habitat loss was solely based on physiological and physical oceanography parameters and when they reached MI_{crit} . In reality, fisheries management will also play a role in dictating the change in fish distributions as has been seen before for species such as summer flounder (Bell *et al.*, 2015).

The results presented in this dissertation fill important research gaps by providing new information about black sea bass life history dynamics in the context of ocean warming and distribution shifts. In addition, this dissertation provides the first account of using physiological parameters measured in the lab to measure change in the thermal habitat of fish species of the USNES. Recommendations from this dissertation for black sea bass are as follows:

- 1) **Further physiological parameters should be measured related to warming.** Aerobic scope was used to provide an optimal temperature for black sea bass, but this metric did not perform well and instead provided us

with an estimation of a maximum tolerable temperature. The Metabolic Index was useful but is more suited towards providing conditions that lead to limiting habitat where MI_{crit} is reached. Therefore, further physiological studies could provide finer-scale information about the impacts of warming on black sea bass, providing a more representative thermal optimum used for habitat modeling studies. Also, physiology experiments were run on fish collected off of the coast of New Jersey. Measuring these physiological parameters in other black sea bass throughout the Northern stock range, as well as within other stocks, would provide additional insight into thermal tolerances and preferences.

- 2) **Additional focus on cold limits on black sea bass.** In certain seasons, ocean warming will be problematic for black sea bass. However, in other seasons ocean warming may open available habitat by increasing temperatures warmer than black sea bass cold thermal limits. Future work should also focus on this dynamic of ocean warming as winter survival can change the amount of larval recruitment and may benefit the northern locations where those larvae typically have longer migrations and potentially a higher mortality rate than other larvae in the southern portion.
- 3) **Monitoring of life history traits related to reproduction and recruitment throughout the entire distribution is needed.** My dissertation research only provided a snapshot into what may be variable interannual trends. Additional years of sampling can place this dissertation's results into context of where energetic and reproductive parameters lie within the potential range of

conditions. For example, if the results in the northern region are representative of a “bad” year, additional years of sampling would provide context to how parameters change if conditions are better and/or a frequency of how often these “bad” years occur. Overtime, this information can be accompanied with measurements of annual recruitment to link together potential warning signs of bad recruitment years.

- 4) **Additional studies on the Southeastern and Gulf of Mexico stocks.** The scope of this dissertation was only on the Northern stock of black sea bass, and while they are considered genetically distinct, additional information from the other stocks of black sea bass would provide relevant information such as their acclimation or adaptation potentials. Specifically, black sea bass are a Serranid, a tropical reef fish family, and the Northern stock represents the most northern individuals in this family. Therefore, black sea bass in the Northern stock may possess adaptations or acclimation potentials from their evolutionary history. Studying the two other more southern and non-migratory stocks could illuminate potential adaptive capacities.

6.2 REFERENCES

- Atlantic States Marine Fisheries Commission (ASMFC). 2021. Addendum XXXIII to the summer flounder, scup, and black sea bass fishery management plan. Black sea bass commercial allocation. 1–15 pp.
- Bell, R. J., Richardson, D. E., Hare, J. A., Lynch, P. D., and Fratantoni, P. S. 2015. Disentangling the effects of climate, abundance, and size on the distribution of marine fish: an example based on four stocks from the Northeast US shelf. *ICES Journal of Marine Science*, 72: 1311–1322.
- Deutsch, C., Ferrel, A., Seibel, B., Portner, H. O., and Huey, R. B. 2015. Climate change tightens a metabolic constraint on marine habitats. *Science*, 348: 1132–1136.
- Kleisner, K. M., Fogarty, M. J., McGee, S., Hare, J. A., Moret, S., Perretti, C. T., and

- Saba, V. S. 2017. Marine species distribution shifts on the U.S. Northeast Continental Shelf under continued ocean warming. *Progress in Oceanography*, 153: 24–36.
- Kokita, T. 2004. Latitudinal compensation in female reproductive rate of a geographically widespread reef fish. *Environmental Biology of Fishes*, 71: 213–224.
- Miller, A. S., Shepherd, G. R., and Fratantoni, P. S. 2016. Offshore habitat preference of overwintering juvenile and adult black sea bass, *Centropristis striata*, and the relationship to year-class success. *PLoS ONE*, 11.
- Moser, J., and Shepherd, G. R. 2008. Seasonal distribution and movement of black sea bass (*Centropristis striata*) in the Northwest Atlantic as determined from a mark-recapture experiment. *Journal of Northwest Atlantic Fishery Science*, 40: 17–28.
- Saba, V. S., Griffies, S. M., Anderson, W. G., Winton, M., Alexander, M. A., Delworth, T. L., Hare, J. A., *et al.* 2016. Enhanced warming of the Northwest Atlantic Ocean under climate change. *Journal of Geophysical Research: Oceans*, 120: 1–15.